Imperial College London

Institute of Clinical Sciences

Temporal Control Principles in Cell Cycle Regulation

Ana Rita Carvalho Araújo

January 2018

Submitted in part fulfilment of the requirements for the degree of

Doctor of Philosophy of Imperial College London

Declaration

I certify that the work presented in this thesis is my own, and that any work carried out by others has been properly acknowledged and appropriately referenced in the text and here:

— Dr Lendert Gelens (KU Leven) generated the two ODE models described in this thesis: an ODE model that predicts that positive feedback brings about modularity in mitosis (chapter 3) and an ODE model that predicts that the strength of Cdk1-APC feedback controls the refractory period (chapter 4).

Ana Rita Carvalho Araújo

The copyright of this thesis rests with the author and is made available under a Creative Commons Attribution Non-Commercial No Derivatives licence. Researchers are free to copy, distribute or transmit the thesis on the condition that they attribute it, that they do not use it for commercial purposes and that they do not alter, transform or build upon it. For any reuse or redistribution, researchers must make clear to others the licence terms of this work.

There is something irreversible about acquiring knowledge; and the simulation of the search for it differs in a most profound way from the reality.

J. Robert Oppenheimer, 1947

Abstract

Cell division is characterized by a sequence of events by which a cell gives rise to two daughter cells. In order to maintain the integrity of the genome, cell growth, chromosome duplication and chromosome segregation must be coordinated in a manner that ensures the faithful transmission of hereditary information from one generation to the next. Mis-segregation of chromosomes, chromosomal abnormalities and de-regulation of cell division timing are well known hallmarks of cancer. Even though the molecular machinery that drives cell division is the same in all tissues cell cycle duration in mammalian cells varies for different cell types: embryonic cells divide faster than differentiated cells, for example. In addition, classical experiments have highlighted a high level of variability in cell cycle duration even within the same cell type. Understanding temporal control of cell division and, in particular, how the same cell cycle regulators control differences in cell cycle length is a fundamental question in cell and developmental biology. To address this question, a multidisciplinary approach combining live cell imaging of human cells and mathematical modelling was used. It was found that duration of mitosis is strictly dependent on feedback regulation networks that control mitotic entry. Positive feedback within these networks ensures that mitosis is short and temporally insulated from upstream cell cycle events. Modulation of regulatory feedbacks was also found to allow fine-tuning of cell division frequency, showing once more the importance of feedback control in temporal regulation of cell division. The work presented in this thesis suggests that understanding cell cycle dynamics at a single cell level provides a powerful way to derive control principles in cell cycle regulation. Moreover, combining experimental approaches with computational analysis allows a quantitative understanding of temporal control in cell division at a single cell level. This is likely to lead to transformative insights into cell cycle in health and disease states.

Acknowledgements

I would like to thank Silvia who hosted me in her lab and accepted to guide me through this lifetime journey. Under her supervision, I discovered a new way of doing science that is innovative, interdisciplinary, accurate, creative, independent and how important it is to communicate it. I definitely changed the way I do and think about science and value a lot more basic biology and the impact that this type of research has in systems-level. Your support, dedication and patience were very important during these three years and there are not enough words to describe how thankful I am that our lives crossed back in Portugal in April 2014. One more time, thank you for your everyday enthusiasm and for always pushing me and challenge me to do everything even better.

I would like to thank my thesis examiners who accepted to evaluate this work, Dr Enrique Martinez-Perez and Dr Peter Thorpe who reviewed this manuscript. Thanks also to my mentors, Professor David Rueda and Dr Tobias Warnecke, for their advice and discussions during these three years.

Everything that I learned during these years was possible because of all the amazing people that are or have been working in the quantitative cell biology group. Thank you, Chiara, Borzo, Sheriff and Adrienne for always helping me from day one, for all the patience, friendship, help, companionship and motivation shared. Also thank you to Chryssa for sharing a lot of knowledge about handling hESC besides all the joy and laughs in tissue culture. A special thank goes to Alix that was essential to get me settled when I arrived in a new country and for sharing all the moments of this journey with me. I also would like to thank Helen, for always being willing to help us and saying some Portuguese words once in a while.

Thanks to all the MRC-LMS institute members that make it a great place to work due to the stimulating scientific environment and all friendly gets together. Special thanks go to the

FACS facility, James and Thomas, that were patient enough to sort my never-ending cell lines. I am also very thankful to share these PhD years with my MRC-LMS student cohort. You made everything go smoothly when I moved here and it was always refreshing to see friendly faces in the corridor. Theresa and Marta, thank you for all your friendly advices and becoming part of my life.

To GABBA community for all the support during these PhD years. It is a great pleasure to be part of this community and be able to share my research every December with such exciting scientists. Thank you Fundação para a Ciência e a Tecnologia (FCT) for funding the work presented in this thesis and I hope you continue to support this amazing PhD program. A massive thank goes to "the Portuguese gang" – Delfim, Elsa and Raquel. Thank you for all the fun, laughs, advice and time shared. Your support was essential to keep going during these years and all the scientific conversations with you were always very inspiring. Raquel, thank you for being such a great friend with always time to support me and guide me in less better days, as well as in all goings to the ballet and for being such an amazing cooker. Obrigada aos três!

Finalmente, mas não menos importante quero agradecer aos meus queridos pais, Olga e Manuel, e à minha maninha, Marta, por serem a melhor família que alguém pode desejar ter. Pais, vocês são o exemplo de que tudo é possível e a vocês agradeço toda a ajuda, força e amor que me deram durante toda a minha vida, mas especialmente durante estes três anos. Maninha, obrigada por seres muitas vezes a mana mais velha e me ajudares a ver que tudo na vida tem um lado positivo. Um obrigada também aos meus avós Maria Ana e António por toda a ajuda e à minha avó Adélia por ser uma força da natureza. Tia Fátima e tio Zé obrigada por toda a preocupação e por terem sempre uma palavra amiga a dizer. Apesar de todo o trabalho e falta de sol, a parte mais difícil deste doutoramento foi estar longe de vocês.

Thank you! Obrigada!

Contents

Declaration **3**

Abstract **9**

Acknowledgements **11**

List of Figures **21**

List of Tables **27**

Abbreviations **29**

1. Introduction **35**

1.1. Historical cell cycle overview **35**

1.2. Models for temporal control of cell division **38**

1.2.1. Checkpoint Control 40

1.2.2. Cyclin specificity 42

1.2.3. The quantitative model for cell cycle progression 45

1.2.4. The kinase-phosphatase ratio model 48

1.3. Temporal control of interphase **50**

1.3.1. APC-Cdh1 maintains low levels of Cdk1 activity during G1-phase 50

1.3.2. Commitment to a new cell division cycle – progression through G1/S/G2 .. 52

1.4. Temporal progression through mitosis 55

1.4.1. Mitotic entry 56

1.4.1.1. Phosphorylation of Tyrosine 15 inactivates Cdk1 activity 56

1.4.1.2. Cdk1 activity promotes dephosphorylation of Tyrosine 15 57

1.4.2. Spindle assembly checkpoint (SAC) drives metaphase to anaphase transition 60

1.4.3. Mitotic exit 61

1.5. Embryonic, normal and cancer cells have different division cycles 63

1.6. Systems-levels feedback control 66

1.6.1. Negative feedback loops 66

1.6.2. Positive feedback loops 68

1.6.3. Interlinked feedback regulation 71

1.7. Studying cell cycle dynamics – from classical to novel tools 73

1.8. Aims and outline of this thesis 75

2. Methods 77

2.1. Cell Lines 77

2.1.1. Growth medium of different cell lines 79

2.1.2. Maintaining, freezing and thawing cell lines 80

2.1.2.1. Somatic and cancer cell lines 80

2.1.2.2. Human embryonic stem cells (hESC) 80

2.1.2.3. Mouse embryonic stem cells (mESC) 81

2.2. Biosensors, shRNA, cell transfection and establishment of stable cell lines....81

2.2.1. Transient transfection of cells 82

2.2.2. Lentiviral production for lentiviral based infections..... 82

2.2.3. Lenti-viral based infection of cells..... 83

2.2.4. Fluorescence Activating Cell Sorting (FACS)..... 83

2.2.5. shRNAs used in this study..... 84

2.2.6. Stable cell lines made in this study 85

2.3. Inhibitors and small molecules 87

2.4. Microscopy..... 87

2.4.1. Live cell imaging..... 87

2.4.2. Immunofluorescence..... 89

2.4.3. EdU labelling and detection..... 91

2.5. Data analysis 91

2.5.1. Software and statistical analysis used 91

2.5.2. Analysis of cell cycle dynamics 91

2.5.2.1. Measuring cell cycle dynamics usign Cdt1-venus, H2B-Turquoise, PCNA-mCherry sensors..... 92

2.5.2.2. Measuring cell cycle dynamics using Dnmt1-CFP, DNA Ligase-YFP and H2B-mCherry sensors..... 93

2.5.2.3. Measuring dynamics of mitosis and Cdk1 activity using Cyclin B1-YFP, H2B-Turquoise, NLS-mCherry sensors..... 94

2.5.3. Immunofluorescence analysis..... 95

2.5.4. Curve fitting 95

2.5.5. Cell cycle trajectory analysis 95

2.6. Cloning and Molecular Biology 96

2.6.1. Classical restriction-enzyme based cloning 96

2.6.1.1. Polymerase chain reaction (PCR) 96

2.6.1.2. Restriction digest of vector and plasmid DNA 97

2.6.1.3. Purification of gel bands from agarose gel 97

2.6.1.4. Ligation reaction of vector and DNA fragments 97

2.6.2. Gibson Isothermal Assembly based cloning 98

2.6.3. Transformation of *E.coli* cells 99

2.6.4. Isolation of plasmid DNA 99

2.6.5. RT-qPCR 99

2.7. ODE model of temporal control of mitosis 100

3. Temporal Insulation of Mitosis 109

3.1. Summary 109

3.2. Aims 110

3.3. Mitosis is short, constant and independent of cell cycle length 110

3.3.1. Timing of mitosis is short and kept constant in different cell lines 110

3.3.2. Duration of mitosis does not correlate with cell cycle length 113

3.3.3. Temperature does not influence the lack of correlation between time of mitosis and cell cycle length 115

3.4. Perturbing Spindle Assembly Checkpoint (SAC) does not make mitosis dependent on cell cycle length 116

3.5. Positive feedback keeps mitosis temporally insulated from variability of early cell cycle events 120

3.5.1. Experimental design to test the role of positive feedback in the temporal modularity of mitosis 121

3.5.2. Switch-like activation of Cdk1 is compromised when positive feedback is perturbed 122

3.5.3. Perturbing positive feedback makes mitosis variable 124

3.5.4. Positive feedback keeps mitotic events synchronised 124

3.5.5. Positive feedback ensures that duration of mitosis is coupled with mitotic entry 126

3.5.6. When positive feedback is compromised, duration of mitosis becomes coupled with upstream cell cycle events 127

3.5.7. Positive feedback and not SAC affects temporal insulation of mitosis 128

3.5.7.1. SAC has no effect on the variability of mitosis duration and synchronicity of mitotic events in the presence of Wee1 inhibitor 129

3.5.7.2. SAC does not contribute to temporal insulation of mitosis 133

3.5.8. Breaking Cdk1 activation and spatial positive feedbacks couple duration of mitosis to earlier cell cycle events 135

3.5.9. Compromising positive feedback compromises cell viability 140

3.6. Mitotic phosphatases role on temporal modularity of mitosis 142

3.7. ODE model predicts positive feedback brings about temporal modularity in mitosis 148

3.8. Highlights from investigating temporal control of mitosis 155

4. Temporal Control of Interphase 157

4.1. Summary 157

4.2. Aims 158

4.3. Cells can respond to a mitotic trigger anytime during the cell cycle 158

4.3.1. Wee1 inhibition promotes cell division and acts as a mitotic trigger 159

4.3.2. Cells in G1-phase try to replicate DNA before entering in mitosis prematurely 160

4.4. A refractory period after mitosis renders cells unable to undergo a second mitotic division 162

4.5. ODE model predicts that the strength of Cdk1-APC feedback controls the refractory period 164

4.6. Human embryonic stem cells do not have a refractory period..... 167

4.6.1. hESC have shorter cell division cycles 167

4.6.2. hESC express very low levels of Cdh1 168

4.6.3. Mitotic cyclins are highly expressed in hESC..... 169

4.6.4. hESC respond immediately to a mitotic trigger..... 171

4.7. Refractory period can be re-established in hESC 172

4.7.1. Ectopic expression of Cdh1 in hESC by a doxycycline-based inducible system 172

4.7.2. Over-expression of Cdh1 reduces the levels of mitotic cyclins in hESC 174

4.7.3. Over-expression of Cdh1 makes G1-phase and cell cycle length longer in hESC..... 176

4.7.4. Over-expression of Cdh1 delays the response of hESC to a mitotic trigger . 177

4.8. Refractory period can be shortened in somatic cells..... 179

4.8.1. Knocking down of Cdh1 shortens the length of G1-phase and cell cycle length in somatic cells 180

4.8.2. Downregulation of Cdh1 makes somatic cells respond faster to mitotic trigger 182

4.9. Molecular characterisation of refractory period 184

4.10. Major highlights of temporal control of interphase 191

5. Cell Cycle Dynamics in Single Cells: a preliminary comparative study …. 193

5.1. Summary 193

5.2. Aims 194

5.3. Different cell lines have different cell cycle dynamics 194

5.4. Comparing cell cycle dynamics in normal cells vs. paired cancer cells 198

5.4.1. A pair of normal vs. cancerous cells behave differently throughout the different cell cycle phases 199

5.4.2. Interdependency of different cell cycle phases time is different in normal and cancer cells 200

5.5. Major highlights of cell cycle dynamics in single cells 202

6. Discussion 203

6.1. Feedback regulation is important for temporal control of cell division 203

6.2. Monitoring cell cycle dynamics in single cells as a way to derive regulatory principles in cell division 215

7. Final conclusions 221

8. Future directions 223

9. References 225

10. Appendices 255

10.1. Appendix A – Publication: Positive Feedback Keeps Duration of Mitosis Temporally Insulated from Upstream Cell-Cycle Events 255

List of Figures

Figure 1.1. The cell cycle 36

Figure 1.2. Schematic showing differences in cell cycle length of various human cell types 39

Figure 1.3. Checkpoint controls can arrest passage through the cell cycle 41

Figure 1.4. Expression of cyclins through the cell cycle 44

Figure 1.5. The quantitative model that drives orderly cell cycle progression 47

Figure 1.6. The ratio between phosphorylation and dephosphorylation events are responsible for ordering cell cycle progression 49

Figure 1.7. APC/C activity is controlled through the regulated binding of two co-activators – Cdc20 and Cdh1 51

Figure 1.8. Stages of mitosis in a vertebrate cell 55

Figure 1.9. Mitotic entry is regulated by positive feedback control 58

Figure 1.10. Mitotic checkpoint complex avoids APC/C activation before satisfaction of SAC requirements 60

Figure 1.11. Mitotic phosphorylations need to be removed in order to finish mitosis 62

Figure 1.12. Embryonic vs. somatic cell cycle 64

Figure 1.13. Positive and negative feedback motifs 66

Figure 1.14. Examples of bistability in cell cycle regulation 69

Figure 1.15. Interlinked feedback control is widely use in cell cycle regulation 72

Figure 2.1. Pipeline for the quantitative analysis of live-cell imaging experiments used in this study 88

Figure 2.2. Cell cycle dynamics measured in MCF10A with the biosensors Cdt1-venus, H2B-Turquoise, PCNA-mCherry 92

Figure 2.3. Cell cycle dynamics measured in MCF10A with the biosensors Dnmt1-CFP, DNA-ligase-YFP and H2B-mCherry 93

Figure 2.4. Mitosis dynamics measured in MCF10A with the biosensors Cyclin B1-YFP, H2B-Turquoise, NLS-mCherry 94

Figure 2.5. Building an ODE model to predict modularity in mitosis 105

Figure 3.1. Cell cycle dynamics in MCF10A, RPE and Hela cells 111

Figure 3.2. Duration of mitosis is short and constant across different cell lines 112

Figure 3.3. Duration of mitosis does not correlate with cell cycle length in single cells 114

Figure 3.4. Duration of mitosis is constant in temperature-driven changes of cell cycle length 115

Figure 3.5. Mean expression of Mad2 in MCF10A, RPE and Hela cells stably expressing shMad2 and PCNA-mCherry 117

Figure 3.6. Duration of G1-phase and mitosis measured in the presence and partial absence of SAC 118

Figure 3.7. Perturbing SAC does not affect temporal insulation of mitosis 119

Figure 3.8. Schematic of the experimental design to test wheter positive feedback keeps duration of mitosis constant and uncoupled from previous cell cycle events 121

Figure 3.9. Breaking positive feedback results in a graded Cdk1 activation 123

Figure 3.10. Perturbing positive feedback results in a longer and more variable duration of mitosis....124

Figure 3.11. Positive feedback keeps early and late mitotic events in sync....125

Figure 3.12. Perturbing positive feedback makes duration of mitosis correlate with when cells enter mitosis....126

Figure 3.13. Positive feedback keeps mitosis temporally insulated from upstream cell cycle events....128

Figure 3.14. Mean expression of Mad2 in MCF10A, RPE and Hela cells stably expressing shMad2 and NLS-mCherry....129

Figure 3.15. Absence of SAC does not make duration of mitosis variable....130

Figure 3.16. SAC has no role in keeping mitotic events synchronized. All cell lines stably expressed NLS-mCherry....132

Figure 3.17. SAC inhibition alone cannot uncouple timing of mitotic entry and duration of mitosis....134

Figure 3.18. SAC does not contribute to duration of mitosis being temporally insulated from duration of upstream cell-cycle events....135

Figure 3.19. Cdk1AF expression makes duration of mitosis longer, more variable, and dependent on time of mitotic entry....137

Figure 3.20. Cdc25-CD expression makes mitotic duration coupled with mitotic entry....138

Figure 3.21. Leptomycin B treatment makes duration of mitosis longer and more variable....139

Figure 3.22. Perturbing positive feedback compromises the cell viability....141

Figure 3.23. PP1 specific inhibitor makes cells arrest at mitosis....143

Figure 3.24. Mean expression of PP1 isoforms and PP2A in MCF10A cells stably expressing shPP1 isoforms or shPP2A and NLS-mCherry....144

Figure 3.25. Perturbing mitotic phosphatases does not make duration of mitosis more variable and coupled with cell cycle length.....145

Figure 3.26. Absence of mitotic phosphatases alone does not make duration of mitosis coupled with mitotic entry.....147

Figure 3.27. ODE model predicts that the double-negative feedback loop involving APC-cdc20 and Mad2-cdc20 gives rise to bistability.....151

Figure 3.28. ODE modelling predicts that positive feedback promotes temporal modularity in mitosis.....152

Figure 3.29. Histograms showing duration of mitosis in the absence and presence of Mad2 and with or without positive feedback.....153

Figure 3.30. Histograms showing duration of mitosis in the absence and presence of Reversine and with or without positive feedback.....154

Figure 4.1. Schematic of the experimental design to understand if cells can be pushed into mitosis at any time during the cell cycle.....158

Figure 4.2. Mitotic trigger promotes premature divisions in the majority of cells.....160

Figure 4.3. When stimulated with a mitotic trigger, cells try to replicate DNA while entering mitosis.....161

Figure 4.4. Somatic cells have a refractory period after mitosis where they are immune to mitotic triggers.....163

Figure 4.5. ODE model predicts that the strength of Cdk1-APC feedback controls the refractory period.....166

Figure 4.6. After 3 days of differentiation with BMP4, hESC almost double their cell cycle length.....168

Figure 4.7. Contrary to differentiated cells, hESC express very low levels of APC-Cdh1 169

Figure 4.8. hESC express very high levels of Cyclin B1 and Cyclin A2 comparatively to differentiated cells.....170

Figure 4.9. hESC enter into mitosis immediately after treatment with Wee1 inhibitor 171

Figure 4.10. Ectopic expression of Cdh1 in hESC can be induced with doxycycline.... 172

Figure 4.11. Ectopic expression of Cdh1 in hESC is time and dose dependent 173

Figure 4.12. Over-expression of Cdh1 in hESC decreases levels of Cyclin B1 and Cyclin A2 175

Figure 4.13. G1-phase and cell cycle length increase in hESC over-expressing Cdh1 .. 176

Figure 4.14. Refractory period can be re-established in hESC by over-expressing Cdh1 178

Figure 4.15. Relative expression of Cdh1 mRNA in Hela, MCF10A, and RPE stably expressing shCdh1 and Cdt1-mcherry and H2B-YFP 179

Figure 4.16. Downregulation of Cdh1 in somatic cells decreases duration of G1-phase and cell cycle length 181

Figure 4.17. Downregulation of Cdh1 decreases response time to a mitotic trigger in somatic cells 183

Figure 4.18. Cell cycle trajectory of G1-phase regulators in Hela cells 187

Figure 4.19. Cell cycle trajectory of G1-phase regulators in MCF10A cells 188

Figure 4.20. Cell cycle trajectory of G1-phase regulators in RPE cells 189

Figure 4.21. Cell cycle trajectory of G1-phase regulators in hESC cells 190

Figure 5.1. Cell cycle dynamics of three somatic cell lines measured with two different sets of cell cycle biosensors 195

Figure 5.2. A different set of cell cycle biosensors also show that duration of interphase correlates with cell cycle length 197

Figure 5.3. Time of different cell cycle phases in paired normal vs. cancer cell lines ... 199

Figure 5.4. G1-phase is inversely correlated with S-phase and G2-phase in normal cells but not in cancer cells 201

Figure 6.1. Duration of mitosis as well as the overall cell cycle length scales well with chromosome number 204

Figure 6.2. Positive feedback keeps duration of mitosis temporally insulated from upstream cell cycle events 208

Figure 6.3. Cdk1:APC-Cdh1 feedback strength modulates the length of refractory period. 213

Figure 6.4. 3D representation of duration of G1-, S- and G2-phases of MCF10A and MCF7 cells 218

List of Tables

Table 1.1 Negative feedbacks in the cell cycle. 67

Table 1.2. Positive feedbacks and double negative feedback loops in the cell cycle..... 70

Table 2.1. List of all cell lines used in this thesis. 77

Table 2.2. DNA constructs used in this thesis..... 82

Table 2.3. shRNA used to downregulate cell cycle genes. 84

Table 2.4. Stable cell lines made and used in this thesis..... 85

Table 2.5. Inhibitors and small molecules used in this thesis. 87

Table 2.6: List of primary and secondary antibodies used 89

Table 2.7: Primers used for qPCR. 100

Abbreviations

APC/C	Anaphase promoting complex/Cyclosome
ATP	Adenosine triphosphate
au	Arbitrary units
BMP4	Bone morphogenetic protein 4
bp	Base pair
BrdU	5-bromo-2'-deoxyuridine
BSA	Bovine serum albumin
Bub3	Budding uninhibited by benzimidazole 3
BubR1	Budding uninhibited by benzimidazole-related 1
CAK	Cdk-Activating Kinase
Cdc	Cell division cycle
Cdc25-CD	Cdc25 catalytic dead
Cdh1/Fzr1	Cdc20 related 1/Fizzy-realted protein
Cdk	Cyclin-dependent kinase
Cdk1AF	Cdk1 T14A, Y15F mutation
cDNA	Complementary DNA
CFP	Cyan fluorescent protein
CKI	Cyclin-dependent kinase inhibitor
Cln	Budding yeast cyclin
CuSO4	Copper(II) sulfate

DAPI	4',6-diamidino-2-phenylindole
dH_2O	Distillate water
DMEM	Dulbecco's modified Eagle's medium
DMSO	Dimethyl sulfoxide
DNA	Deoxyribonucleic acid
DNA Lig	DNA Ligase I
Dnmt1	DNA (cytosine-5)-methyltransferase 1
dNTPs	Deoxynucleotide (dNTP) solution mix
DOX	Doxycycline
EdU	5-Ethynyl-2´-deoxyuridine
EGF	Epidermal growth factor
eIF2α	Eukaryotic initiation factor 2 α
em	Emission wavelength
ES	Embryonic stem cell
EV	(sh)Empty vector
ex	Excitation wavelength
FACS	Fluorescence activated cell sorting
FEAR	Cdc Fourteen Early Anaphase Release
FRET	Förster/fluorescence resonance energy transfer
G1/2	Gap phase 1/2
GFP	Green fluorescent protein
GUSB	Glucuronidase beta
h	hour(s)
H2B	Histone H2B
hESC	Human embryonic stem cells
iCdh1	Doxycycline inducible Cdh1
iRNA	Interference RNA
kb	kilobase
LED	Light-emitting diode
M	Mitosis

m	Slope of the trend line
M-phase	Mitosis
MAD	Mean absolute deviation
Mad2	Mitotic arrest deficient 2 protein
MAPK	mitogen activated protein kinase
MCC	Mitotic checkpoint complex
mCherry	Monomeric red fluorescent protein
MEK	mitogen activated protein kinase kinase
MEN	Mitotic Exit Network
mESC	Mouse embryonic stem cell
min	minute(s)
mL	millilitre
mM	milliMolar
MPF	M-phase promoting factor
mir	Micro RNA
ms	Miliseconds
NEB	Nuclear envelope breakdown
NER	Nuclear envelope reformation
nm	nanoMeter
OA	Okadaic acid
ODE	Ordinary differential equation
Orc	Origin recognition complex
p-	phosphorylated
PAX2	Paired box gene 2
PBS	Phosphate buffered saline
PCNA	Proliferating cell nuclear antigen
PCR	Polymerase chain reaction
PEI	Polyethylenimine
Pfu	DNA polymerase
Plk	Polo-like kinase 1

pmol	picoMolar
PP	Protein phosphatase
PP1	Protein phosphatase 1
PP2	Protein phosphatase 2
qPCR	Quantitative polymerase chain reaction
r	Person correlation coefficient
R^2	Coefficient of determination
Rb	Retinoblastoma protein
RNA	Ribonucleic acid
rpm	Revolutions per minute
RT	Reverse transcriptase
S	Serine
SAC	Spindle assembly checkpoint
SAC inh	Spindle assembly checkpoint inhibitor - reversine
SCF	Skp, Cullin, F-box containing complex
SCR	(shRNA)Scramble
Ser	Serine
shRNA	Short hairpin RNA
T	Threonine
TAE	Tris-acetate-EDTA buffer
Thr	Threonine
TRI	Trizol
U	Enzyme unit
V	volt
VSVG	Vesicular stomatitis Indiana virus G protein
Wee1 inh	Wee1 inhibitor - PD0166285
WT	Wild type
Y	Tyrosine
YFP	Yellow fluorescent protein
μL	microLitre

μm	microMetre
μM	microMolar

1. Introduction

1.1. Historical cell cycle overview

Cells are the basic structural, functional and biological units of all living organisms. They were discovered by Robert Hooke in 1665 and the cell theory that states that all living organisms are composed of one or more cells was first developed in 1839 by Matthias Jakob Schleiden and Theodor Schwann. All new cells originate by the division of existing cells and all cells are believed to descend from a single ancestral cell that lived 3 to 4 billion years ago. The evolution of all cells and organisms until today was dependent on the successful transmission of genetic information during cell division.

Cell division is fundamental to the maintenance and development of life on Earth as we know it. In single-cell organisms, cell division is coupled with reproduction since it gives rise to a whole new organism. In multicellular organisms, cell division of a single cell gives rise to different communities of cells that are the founders of the different tissues. In adult organisms, cell division maintains the integrity of tissues, replacing cells that die or are lost due to environmental damage (Baserga, 1985; Prescott, 1976). Since cell division and reproduction is so important for the maintenance of life it is important to have a detailed and complete understanding how this process occurs.

The division of a cell can be simplified by dividing the process into a series of ordered events: duplication of cell contents and equal distribution of the contents into two daughter cells. These highly regulated series of events that lead to reproduction of eukaryotic cells is called cell cycle (Figure 1.1). The first part of the cell cycle, called interphase, is when all the cell components are duplicated, which results in a gradual doubling of cell size until the end of the phase. However, chromosomes must be duplicated only once per cycle during DNA synthesis phase (S-phase). The equal segregation of chromosomes as well as the distribution of duplicated cell components into two daughter cells occurs during mitosis, which is

followed by the physical cell division – cytokinesis. All these events repeat with a period time required to double the cytoplasmic mass and many other cellular components (Novak and Tyson, 2003). In somatic cells, S-phase and mitosis each occur after a gap phase - G1-phase and G2-phase, respectively - when little or no change is observed in terms of cytoplasm volume (Truman et al., 2001). G1-phase and G2-phase provide extra time for cellular growth and replication of organelles, and is also the time when some checkpoints take place.

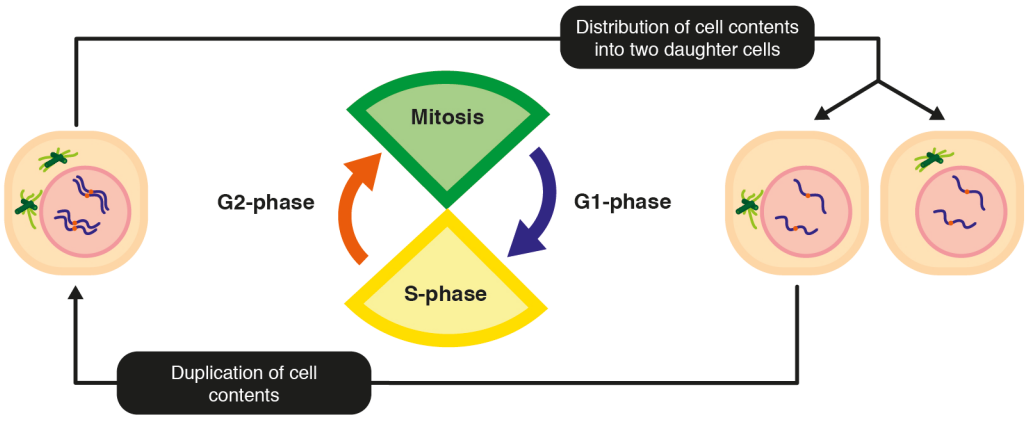


Figure 1.1. The cell cycle. Cell division begins with duplication of cell's components, followed by components equally divided between two daughter cells.

The fidelity of cell division depends on regulatory mechanisms that ensure that the events of cell cycle occur in an ordered manner. This is achieved by a complex regulatory network known as the cell cycle control system, which controls the timing and coordination of all cell cycle events. Moreover, the order and progression of cell cycle events is conditioned by the dependency of one event on another and by feedback from the cell cycle machinery into the control system. If the control system detects an issue in the completion of a certain cell cycle event it will delay progression through cell cycle by delaying the initiation of the later events until the problem is solved.

The eukaryotic cell cycle is driven by cyclin dependent kinases (Cdks) that bind and are regulated by cyclins. Budding yeast (*Saccharomyces cerevisiae*) and fission yeast (*Schizosaccharomyces pombe*) are model organisms that were crucial to many of the first studies of cell cycle regulation. Both have a single Cdk – Cdc28 and Cdc2, respectively - that were identified in the early 70s in mutant allele screens (Hartwell et al., 1970; 1973; Nurse, 1975; Nurse et al., 1976). Cdks are serine/threonine kinases that depend on direct binding to their regulatory subunit – a cyclin protein – in order to become active. Although the number of Cdk homologues has increased during evolution, Cdk-cyclin complexes are conserved across all eukaryotes from yeast to human (Cao et al., 2014). This universality was first demonstrated in late 80s, when the human Cdk1 was shown to be able to complement the fission yeast Cdc2 (Lee and Nurse, 1987; Nurse, 1990). Additionally, it was discovered that the Cdk-cyclin complex was the mysterious M-phase promoting complex (MPF) discovered in 1971 in *Xenopus laevis*, which had been shown to peak in mitosis and being able to initiate nuclear division when transplanted from an egg into an oocyte (Dunphy et al., 1988; Labbe et al., 1989; Lohka and Maller, 1988; Masui and Markert, 1971; Wasserman and Smith, 1978). The cell cycle control network in vertebrates is more complex than in yeast cells and involves multiple Cdks and Cyclins that contribute to orderly progression through the different cell cycle phases (Malumbres et al., 2009; Santamaría et al., 2007; Satyanarayana and Kaldis, 2009). Transitions through the cell cycle are ordered, unidirectional and therefore require a close regulation of the cell cycle machinery both in time and space.

Diverse eukaryotic systems – from unicellular yeast, to *Drosophila*, egg extracts from *Xenopus laevis*, and mammalian cell lines – were used to conduct studies on regulation of cell division. This allowed to access the conservation and variation in the mechanisms of cell cycle regulation across evolution and have a wide understanding of this process, fundamental for all eukaryotes. In this thesis, human cell lines were used as a model to investigate the role that time plays during cell division. Adding on previous knowledge, it was aimed to provide new contributions to the field of temporal control of cell cycle.

1.2. Models for temporal control of cell division

The fundamental mechanisms that regulate cell cycle are conserved across evolution from yeast to humans (Morgan, 2007). In multicellular organisms, the components of the cell cycle are essentially the same in all tissues. However, within the same organism the length of the cell cycle varies (Figure 1.2). Early divisions during embryogenesis happen every 4.4 hours and some post-mitotic cells like neutrons stay all their lives in a non-dividing state (Capra, 1996; Wong et al., 2010). How different cell types have such different temporal dynamics in the cell cycle remains unknown. Even within the same population of cells there is some variability. Variability in cell division has been a subject of interest for many years (Al-Dewachi et al., 1979; Atay and Skotheim, 2014; Kempe et al., 2015; Kiviet et al., 2014; Lord and Wheals, 1981; Morris et al., 1979; Shields, 1977). Recently, it was shown that pairs of cousins' cells have more similar cell cycle dynamics than mother and daughter cells, suggesting that within the same population of cells there is variability in progression through the cell cycle (Sandler et al., 2015). This might be explained by the influence of external factors present in the local environment at the time of beginning the new cell cycle (Sandler et al., 2015). Recent studies showed that the time of cell cycle might be related to a particular cellular function. Primary murine resting B cells, when stimulated in culture, take on average 35 hours to complete a first division followed by up to five short division cycles that take an average of 9 hours, after which cells die by apoptosis (Hawkins et al., 2009). This observed pattern of rapid division followed by complete cessation reproduces what happens when a B cell is exposed to an antigen *in vivo*; first their population needs to expand, then division ceases because there are sufficient cells to fight the infection. So, when stimulated by an antigen, B cells population follow a pattern of population growth, cessation and finally cell death (Hawkins et al., 2009; Turner et al., 2008). Temporal control of cell cycle was also shown to be important for the function of differentiated T cells. Naïve T cells have a short cell cycle length, but once they encounter an antigen their cell cycle time gradually increases as they become differentiated cells (Kinjyo et al., 2015; Marchingo et al., 2014). Moreover, the precise duration of the first two divisions in early embryonic development is important for the successful implantation and survival of *in vitro* fertilised embryos (Wong et al., 2010).

In early embryos, such as *Xenopus laevis* and *Drosophila* embryos, egg fertilization triggers a rapid and remarkably synchronous series of cell divisions. Cell growth usually does not occur during these first and early divisions, and G1- and G2-phase are minimal or non-existent. It is thought that the goal of this initial stage of embryogenesis is to rapidly duplicate and distribute the genome in order to generate enough critical mass needed for the self-organization into the correct structures to form an embryo (Turner et al., 2014; van den Brink et al., 2014). On the other hand, somatic cells have usually much longer cell cycles. Mitosis and cytokinesis occur in rapid succession before entering the next G1-phase. When a cell enters interphase of the next cell cycle everything happens in a much more passed way, and

gap phases are highly important to maintain the integrity of the new daughter cells that are going to be generated. Unlike embryonic stem cells, somatic cells are considered to prioritise maintaining genome integrity and mass, in order to not disrupt the tissue integrity. This shows that embryonic and somatic cells have different temporal dynamics during cell cycle and different biological aims when they divide.

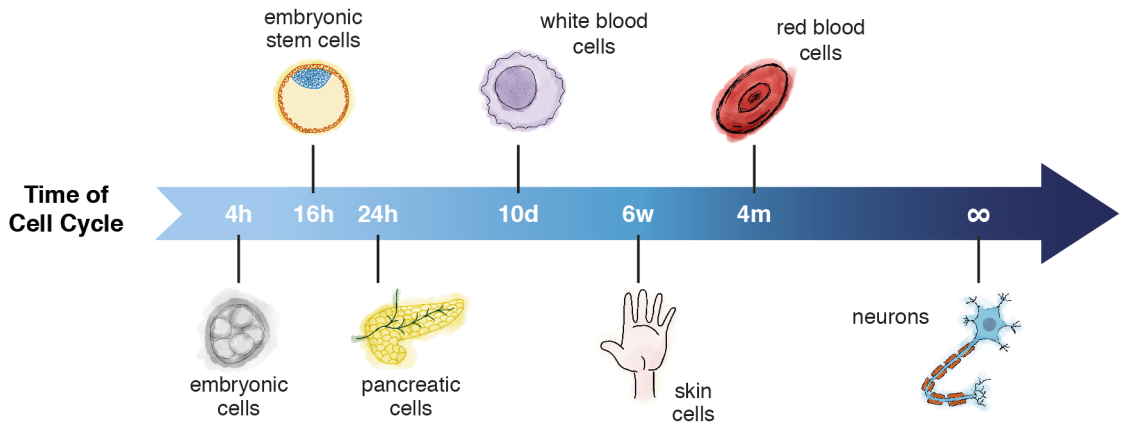


Figure 1.2. Schematic showing differences in cell cycle length of various human cell types (Calder et al., 2013; Capra, 1996; Wong et al., 2010). (Not in scale)

From these examples, it is clear that cell cycle duration not only varies between cell types, but can be altered as cell function changes. Thus, the question is – How is time controlled during cell cycle? Over the years different models, which are not mutually exclusive, have tried to explain the ordering of cell cycle events and implicitly time control during it:

i) Checkpoints or surveillance mechanisms – late events only take place if earlier events are successfully completed by the action of checkpoints (Hartwell and Weinert, 1989; Weinert and Hartwell, 1988);
ii) Cyclin specificity – ordered progression through cell cycle is possible because different Cyclins are expressed at different time during cell cycle and 'team up' with cyclin dependent kinases (Cdks) at different cell cycle phases (Amon et al., 1993; Minshull et al., 1990; Murray and Kirschner, 1989; Surana et al., 1991);
iii) The quantitative model – the increase of Cdk activity during cell cycle triggers different cell cycle phases; low levels of Cdk activity trigger S-phase and high levels of Cdk activity will trigger mitotic entry (Coudreuse and Nurse, 2010; Stern and Nurse, 1996; Swaffer et al., 2016);
iv) Kinase-phosphatase ratio model – the sequential phosphorylation or dephosphorylation events are consequences of cell cycle substrates responding to distinct thresholds of the ratio of Cdks to Cdk-counteracting phosphatases (Bouchoux and Uhlmann, 2011; Queralt and Uhlmann, 2008; Visintin et al., 1998; Wolf et al., 2006).

1.2.1. Checkpoint Control

Hartnell and Weinert were the first to propose a model to understand the ordering of cell cycle events (Hartwell and Weinert, 1989). They introduced the "checkpoint" concept, which postulates that a cell will check at particular times during the cell cycle to determine whether an earlier event has been properly finished before proceeding to the next cell cycle event. For this reason, ordering of the cell cycle events is enforced by checkpoints or surveillance mechanisms (Figure 1.3).

The first checkpoint is called Start or the G1/S checkpoint, and it ensures that the environment is favourable for proliferation and the cell genome is ready to replicate. It is called the 'restriction point' in mammalian cells (Hartwell et al., 1974; Pardee, 1974; Zetterberg and Larsson, 1985). If there are appropriate nutrients source, extracellular

mitogens are presents and their internal program permits, cells then pass the G1-phase checkpoint and commit to DNA replication. Then S-phase Cyclins bind to Cdks to form active complexes that phosphorylate proteins involved with the initiation of DNA replication, centrosome duplication, and other early cell cycle events.

The next check point occurs at the boundary between G2-phase and mitosis and is usually called the 'replication checkpoint'. In yeast, mammalian cells, *Aspergillus*, and other eukaryotic organisms, arrest of S-phase happens if specific inhibitors or replication enzymes are inactivated, preventing entry into mitosis. This checkpoint monitors whether the DNA is fully replicated and undamaged before undergoing chromosome condensation and nuclear division (Bartek and Lukas, 2001; Bartek et al., 2004; Hartwell, 1978; Michael et al., 2000). If everything is ready to enter into mitosis, mitotic Cyclins form complexes with Cdks and phosphorylate proteins that promote the assembly of the mitotic spindle, thereby pushing cells to metaphase.

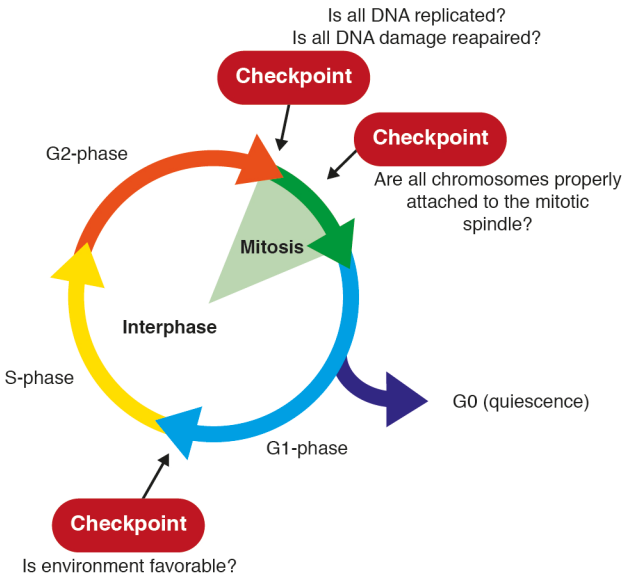


Figure 1.3. Checkpoint controls can arrest passage through the cell cycle. Three major checkpoints impose order and unidirectionality of cell cycle progression. In G1-phase the cell checks if the environment is favourable, in G2-phase the cells checks if all the DNA is replicated and repaired before enter mitosis and at metaphase the cell checks if all the chromosomes as perfectly aligned at metaphase plate and all kinetochores attached to the mitotic spindle.

It is precisely at this point in the cell cycle – metaphase – that the last checkpoint occurs. It is commonly called the 'spindle assembly checkpoint' (SAC) or mitotic checkpoint, and it controls the transition from metaphase to anaphase. It ensures that sister chromatids only separate when all the chromosomes are aligned in the metaphase plate and attached to the mitotic spindle via the kinetochores (Hoyt et al., 1991; Li and Murray, 1991; Santaguida and Musacchio, 2009). A single chromosome that is not properly attached to the mitotic spindle delays progression to anaphase until the lagging chromosome arrives at the metaphase plate (Rieder et al., 1995). When all the requirements of this checkpoint are met, Cdk-cyclin complexes stimulate the activation of anaphase-promoting complex (APC/C) that triggers destruction of Cyclins and sister-chromatid separation and segregation, finishing one cell cycle with the cytokinesis of the two new born cells (Chang and Barford, 2014; Primorac and Musacchio, 2013).

1.2.2. Cyclin specificity

The first cyclin was identified in sea urchins as a protein with oscillating expression levels that peak during the mitosis of each cell cycle (Evans et al., 1983). Studies in different organisms showed that there are different types of Cyclins, which have different substrate specificity to Cdks (Miller and Cross, 2001). Cyclins are a broad family of proteins that share weak homology in their amino acid sequence apart from the primary structure called 'cyclin box', which contributes to Cdk association (Andrews and Measday, 1998; Kobayashi et al., 1992; Noble et al., 1997). Cyclins are synthesized and activated in a cell cycle-dependent manner and transcriptional and post-translational modifications are the major mechanisms involved in the regulation of their levels (Amon et al., 1993) (Figure 1.4). Cyclins can be divided into four different classes, based on the timing of their expression and their function in the cell cycle: G1-phase Cyclins regulate cell cycle entry and G1/S Cyclins, S-phase Cyclins and mitotic Cyclins regulate entry into their respective phases (Morgan, 2007).

Type D-cyclins (D1, D2 and D3) are expressed early in the cell cycle, and are commonly named G1-phase Cyclins (Cln3 in budding yeast). Unlike most of the other cyclins, D-cyclins levels do not oscillate, but increase gradually throughout the cell cycle in response to cell growth and external stimuli (Böhmer et al., 1996). D-cyclins activate Cdk4 and Cdk6, consequently committing the cell to a round of DNA replication and physical division into two daughter cells. The central function of Cdk-cyclin D complexes is to regulate members of Retinoblastoma (Rb) family (Sherr and McCormick, 2002). pRb factors act as a braking

mechanism to induce cells to exit the cell cycle. pRb negatively regulates G1-phase progression by repressing E2F transcription factors that promote DNA replication. Another important role of Rb is to repress the transcription of Cyclin E, which suggests that Cyclin D's essential role might be inducing Cyclin E expression and progression into S-phase (Lukas et al., 1997). Moreover, Cdk4-cyclin D complexes are able to sequester $p27^{Kip1}$ and $p21^{Cip1}$ inhibitors promoting Cdk2-cyclin E activation and progression to S-phase (Sherr and McCormick, 2002).

In late G1-phase, Cdk2-cyclin E complexes levels peak, making Cyclin E (Cln1 and Cln2 in budding yeast) the G1/S boundary Cyclin. Cyclin E levels oscillate during cell cycle, peaking at late G1 and being destroyed in early S-phase. The Cdk2-cyclin E complex further phosphorylates pRB in order to activate more E2F, that in turn activates Cyclin E expression (Bertoli et al., 2013; Johnson and Skotheim, 2013). This regulatory relationship constitutes a positive feedback mechanism that makes sure that Cdk2 kinase levels are high at the onset of S-phase. Cyclin E has also been presumed to trigger DNA replication by leading Cdk2 to phosphorylate proteins that regulate chromosomal origins of replication and activate DNA polymerases. After S-phase initiation, Cdk2 phosphorylates Cyclin E, targeting it for degradation by SCF complex (Dulić et al., 1992; Hwang and Clurman, 2005; Koff et al., 1992; Won and Reed, 1996).

The rise of G1/S phase Cyclins is escorted by the appearance of S-phase Cyclins – Cyclin A in vertebrates and Clb5 and Clb6 in budding yeast. Two A-type Cyclin genes have been identified – A1 and A2. When Cyclin E is targeted for degradation, Cyclin A binds to Cdk2 in order to further promote DNA replication and at the same time prevent assembly of new replication complexes. Cyclin A can bind both to Cdk2 and Cdk1 and its levels increase throughout S-phase, peaking at G2-phase and early mitosis (Bertoli et al., 2013; Pines and Hunter, 1991; 1992). Cdk1-Cyclin A complexes weaken the Wee1/Myt1 negative feedback at mitotic entry that is essential to inactivate Cdk1-cyclin B1 complexes before cells are ready to go into mitosis. As the Wee1/Myt1 negative feedback is weaken, Cyclin B1 can be activated (Deibler and Kirschner, 2010). Quantitative live cell imaging in human cells showed that cyclin A levels begin to decline shortly after nuclear envelope breakdown (Elzen and Pines, 2001; Geley et al., 2001).

Levels of the mitotic Cyclin – Cyclin B (Clb1, 2, 3, and 4 in budding yeast) – rise during late S-phase and G2-phase as the cell approaches mitosis and peaks at metaphase (Murray and Kirschner, 1989; Solomon et al., 1990). Mammalian cells have three B-type Cyclins; Cyclins B1, B2, and B3, but only Cyclin B1 is essential for mouse development (Brandeis et al., 1998; Strauss et al., 2018). Cyclin B1 binds to Cdk1 and this complex drives cells into mitosis and promotes the majority of mitotic events, from assembly of mitotic spindles to chromosome condensation and nuclear envelope breakdown. To be able to exit mitosis, cells need to

degrade Cyclin B1 by APC in order to inactivate Cdk1 (Hershko et al., 1994; Irniger et al., 1995; King et al., 1995).

Although different cyclins are important at different phases of the cell cycle and it is their oscillatory expression that helps organize ordering and timing during cell cycle phase transitions, numerous cyclins can be deleted with only mild consequences on organismal development. For example, although Cyclin A1 knockout mice are viable, males are sterile (Liu et al., 1998). Cyclin A2 is expressed early in development and in adult tissues, and mice lacking this protein die as early embryos (Murphy et al., 1997). Moreover, E-type cyclins are not essential for continuous cell cycling observed in a developing embryo (Geng et al., 2003). Only the major cyclin B1 is essential for early embryonic cell divisions, and hence the mouse knockout is embryonic lethal (Brandeis et al., 1998; Strauss et al., 2018). These evidences suggest that there is some level of redundancy between the different Cyclins.

The cyclin specificity model has been challenged by Paul Nurse's lab, where a fission yeast mutant line with minimal Cdk1-cyclin B network was able to run the whole cell cycle, pointing to another possible model to control time during cell division – the quantitative model (Coudreuse and Nurse, 2010).

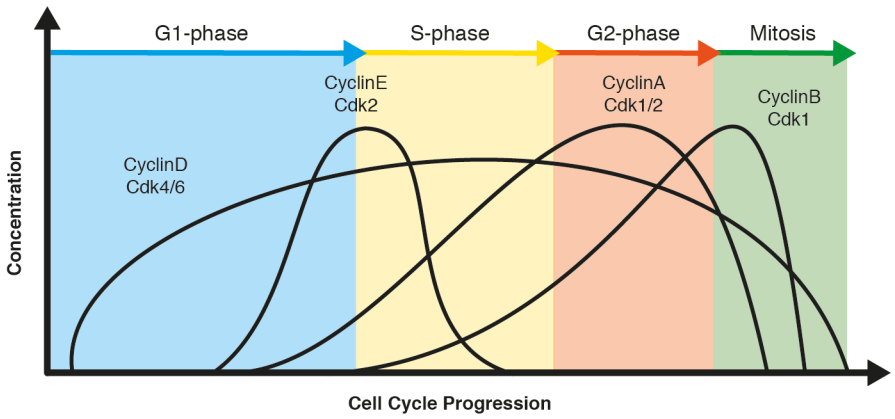


Figure 1.4. Expression of cyclins through the cell cycle. Different cyclins are expressed at different times during the cell cycle. They team up with different cyclin dependent kinases and this drives the different cell cycle phases. Cdk4 and Cdk6 bind to D-type cyclins in order to regulate events in early G1-phase; Cyclin E binds to Cdk2 and triggers DNA replication at the beginning of S-phase; Cdk2-cyclin A and Cdk1-cyclin A regulate completion of S-phase; and Cdk1-cyclin B1 drive mitotic entry.

1.2.3. The quantitative model for cell cycle progression

Cdks are the master regulators of cell cycle and different Cdks regulate cell cycle progression in higher eukaryotes. Their activities oscillate during the cell cycle because they depend on the levels of their regulatory subunits - Cyclins – which provide substrate specificity and activate the kinase (Alberts et al., 2013; Morgan, 2007; Sanchez and Dylancht, 2005). Cdks are proline-directed serine/threonine phosphatases, which target the Cdk consensus site motif S/TP(xR/K) (Holmes and Solomon, 1996). In fission and budding yeast, the same catalytic subunit - Cdc2 and Cdc28, respectively - promotes entry into S-phase and also mitosis (Nurse and Bissett, 1981; Piggott et al., 1982). Vertebrates encode a variety of different Cdk units – Cdk1, Cdk2, Cdk3, Cdk4 and Cdk6 – that will associate with the cyclins that are present at the respective cell cycle stage (Draetta et al., 1987; Hartwell et al., 1970; 1973; Lee and Nurse, 1987; Malumbres and Barbacid, 2005; Nasmyth and Reed, 1980; Russell and Nurse, 1986; Satyanarayana and Kaldis, 2009).

The ablation of all the interphase Cdks – Cdk4, Cdk6 and Cdk2 – has little or no effect on the cell cycle progression, allowing embryos to undergo organogenesis and develop until midgestation (Santamaría et al., 2007). However, mice lacking Cdk1 have impaired cell division during early stages of embryonic development, suggesting that the major mitotic regulator – Cdk1 – can compensate for interphase Cdks (Santamaría et al., 2007). Cdk1 can substitute for all the other Cdks, which means that one Cdk subunit is sufficient to keep order in cell cycle progression. In response to antiproliferative signals, members from Cip/Kip or Ink protein families will inhibit Cdks and promote cell cycle arrest. In addition to regulation by families of inhibitors, Cdks are also tightly regulated by phosphorylation and proteolysis of their regulatory partner cyclins (Frescas and Pagano, 2008; King et al., 1995; Nagahama et al., 2000; Sherr and Roberts, 1999; Vodermaier, 2004).

The previous section described the specificity of activity of particular Cdk-cyclin complexes, however the functions of cyclins are rather redundant. In animal cells, Cdk1 is the only essential Cdk and Cyclin A2 and Cyclin B1 that promote S-phase and mitosis, respectively, are the essential Cyclins (Brandeis et al., 1998; Liu et al., 1998; Pagliuca et al., 2011; Santamaría et al., 2007). In budding yeast, deletion of all Cyclin B types is usually not viable, but can be rescued by the ectopic expression of a single mitotic cyclin (Schwob et al., 1994). Specific substrates for Cdk1-cyclin B1 and Cdk2-Cyclin E were identified in *Xenopus leavis*, however, *in vitro* studies revealed that 90% of the substrates were phosphorylated with similar affinity by both kinases. Moreover, *in silico* analysis was not able to find any defining factor between both groups of substrates (Errico et al., 2010). Although cell cycle-specific substrates of different Cdk-cyclin complexes were recently defined, the previous identification of a range of substrates interacting only with one Cdk-cyclin complex might be due to the fact that each specific type of complex is present at differing times and intracellular localisations during the cell cycle (Pagliuca et al., 2011).

In 1996, Stern and Nurse proposed a quantitative model for the Cdc2 (the *S. pombe* homologue of Cdk1) control of S-phase and mitosis in fission yeast. They claimed that different levels of Cdc2 activity was sufficient to regulate cell cycle progression (Figure 1.5). According to this model, during G1-phase when Cdk activity is absent, DNA-replication would not initiate because replication regions are silenced. Low levels of Cdk activity early in the cell cycle would then initiate S-phase and maintenance of these levels would prevent cells from re-initiating DNA replication. A further increase in Cdk levels would then trigger mitotic entry. The quantitative model predicts that oscillations in Cdk activity below and above this S-phase threshold allows for rounds of re-replication without overriding mitosis (Stern and Nurse, 1996).

Later in 2010, Coudreuse and Nurse corroborated this model using a fission yeast mutant line that can proliferate with a minimal Cdk control network (Coudreuse and Nurse, 2010). This consists of a genetically engineered Cdk-cyclin chimera composed of a fusion of the Cdk Cdc2 and the mitotic Cyclin B-type Cdc13 (expressed under the Cdc13 promoter) and a mutation rendering Cdc2 sensitive to chemical inhibition by the ATP analogue 1-NMPP1 (Coudreuse and Nurse, 2010). The complex Cdc13-Cdc2 undergoes cell-cycle-regulated synthesis and destruction even without the tyrosine phosphorylation control module. Increasing concentration of Cdc13-Cdc2 over the cell cycle can initiate both S-phase and mitosis. Cycles of low, intermediate and high Cdk activity created by treatment with a chemical Cdk inhibitor are sufficient to drive S-phase and mitosis sequentially, suggesting that a lower threshold of Cdk activity may be required for S-phase in comparison to mitosis. A single Cdk-cyclin complex was able to substitute for the four Cdk-cyclin complexes acting during mitotic cell cycle. From these results, the ordering of cell cycle progression can be achieved with a single oscillating source of Cdk activity. Also in 2010, Gavet and Pines showed that increasing levels of Cdk1-cyclin B1 activity can coordinate events in prophase, constituting the first demonstration in mammalian cells that cell cycle events can be coordinated by changing thresholds of a single Cdk1-cylin B1 complex (Gavet and Pines, 2010).

It was shown in budding yeast that a quantitative model for ordering mitotic events also support the theory of a quantitative model for cell cycle progression. Titration of Cdc28-Clb2 levels showed that sequential mitotic events require increasing concentrations of this complex in order to initiate. This supports the idea that different thresholds of Cdc28-Clb2 activity are required for spindle formation and elongation in metaphase and anaphase, respectively (Oikonomou and Cross, 2011). It was also shown in somatic cells that low levels of Cdk1 activity (if Cdc25 is inhibited) maintain cells in G2-phase indefinitely, whereas high levels of Cyclin B1 cause a dramatic increase in Cdk1 activity mediated by Cdc25 (Deibler and Kirschner, 2010). Moreover, dephosphorylation of Cdk1 Y15 is a gradual process starting before nuclear envelope breakdown and continuing through prometaphase, while the cells experience cellular changes that require active Cdk1 (Lindqvist et al., 2007). In addition,

mitotic exit depends on the fast decrease of Cdk1 activity that results in part of Cyclin B1 degradation by APC/C (Sullivan and Morgan, 2007; Wäsch and Cross, 2002). Enough evidence was already presented suggesting that indeed different thresholds of Cdk1 activity can drive the overall cell division cycle, supporting the idea that Cdk1 might act as a biochemical oscillator (Stern and Nurse, 1996).

The quantitative model is centred on Cdk activity but every kinase activity is counteracted by phosphatases. Indeed, PP1 and PP2A phosphatases have been described to play a crucial role in the cell cycle progression by dephosphorylating Cdks substrates (Castilho et al., 2009; Dohadwala et al., 1994; Kwon et al., 1997; Mochida et al., 2009; Wu et al., 2009). This leads to the next proposed model that suggests that is the ratio between Cdks activity and counteracting phosphatases activity that promote the timely ordered progression of cell cycle.

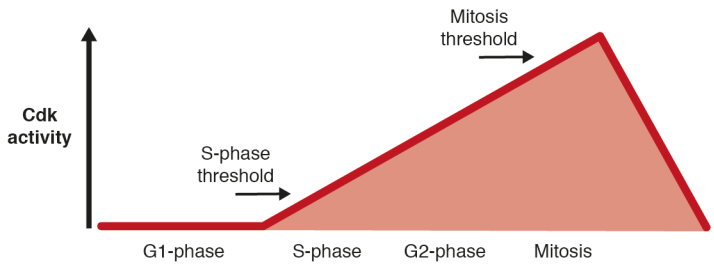


Figure 1.5. The quantitative model that drives orderly cell cycle progression. Oscillations in Cdk activity are sufficient to drive cell cycle progression in an orderly manner. Cdk is inactive during G1-phase; low levels of Cdk activity set the S-phase threshold which drives DNA replication; high levels of Cdk trigger mitotic entry and chromosomes segregation.

1.2.4. The kinase-phosphatase ratio model

Cdks are active kinases so it has been suggested over the past decade that their counteracting phosphatases would have a role in driving cell cycle progression. Cdc14 is a proline-directed Serine/threonine phosphatase and was identified as a cell cycle regulator, since mutants arrested in late anaphase (Culotti and Hartwell, 1971). It was suggested to be the major Cdk-counteracting phosphatase in budding yeast because it is required for execution of many mitotic events and for triggering of mitotic exit by directly dephosphorylating Cdk substrates (Chen et al., 2001; Gray et al., 2003; Visintin et al., 1998).

This ratio between Cdk activity and counteracting phosphatase activity determines the average duration between when a Cdk substrate is phosphorylated by Cdk and when it is correspondingly dephosphorylated by a phosphatase. So, the average phosphorylation state of a substrate population is determined by the ratio of the relative rates of phosphorylation (by Cdk) and dephosphorylation (by phosphatase) (Figure 1.6). Since this ratio changes over progression of mitosis, substrates will be in their dephosphorylated state once they approach mitotic exit (Uhlmann et al., 2011). Bouchoux and colleagues showed that each Cdk substrate responds to an individual activity ratio threshold depending on its respective affinity as a substrate for the Cdk and for the phosphatase (Bouchoux and Uhlmann, 2011). They showed in budding yeast that low levels of Cdc14 dephosphorylate Fin1 (NEK2 in humans) in early anaphase to promote spindle elongation. On the other hand, Orc6 is only dephosphorylated when Cdc14 activity levels are high at the same time that Cdk activity drops. Substrates respond differently to the decreasing ratio between Cdk and Cdc14 during mitotic exit, resulting in the temporal ordering of substrate dephosphorylation and the respective mitotic exit events. This shows that Cdk-counteracting phosphatases are an important factor in establishing thresholds of Cdk activity for phosphorylation of S-phase and mitosis substrates.

Despite the important role of Cdc14 in controlling ordering of cell cycle events by counteracting Cdk activity in budding yeast, this is not conserved in higher eukaryotes (Mocciaro and Schiebel, 2010). Although both human Cdc14 orthologues – hCdc14A and hCdc14B – can rescue Clp1-deficient fission yeast strains (orthologue of Cdc14), depletion of both paralogs in cells showed no obvious growth or mitotic defects (Berdougo et al., 2008; Mocciaro et al., 2010; Vázquez-Novelle et al., 2005).

It is known that phosphatases from PP1 and PP2A families contribute to the reversal of mitotic phosphorylations, but a specific mitotic phosphoprotein has not yet been definitively assigned in higher eukaryotes. PP1 has been identified as one of the major enzymes that dephosphorylate proteins that have been phosphorylated by Cdk in *Xenopus laevis* extracts (Wu et al., 2009). PP2A is also a strong candidate because it has been shown to be crucial for the entry and exit from mitosis in *Xenopus laevis* extracts. The depletion of PP2A and its

subunit B55 causes premature mitotic entry when Cdk activity is low, due to hyperphosphorylation of Cdk substrates. These cells then consequently fail to exit mitosis (Castilho et al., 2009; Mochida et al., 2009). PP2A is involved in a feed forward regulation loop that contributes to bistability at mitotic entry: as Cdk activity levels rise, MASTL (Greatwall kinase) inhibits PP2A, which slows the dephosphorylation of Wee1 and Cdc25 that induce Cdk1 activation at mitotic entry, allowing more activation of Cdk and consequently inactivation of PP2A-B55 (Yu et al., 2006; Zhao et al., 2008). However, depletion of MASTL in *Xenopus laevis* extracts is not sufficient to increase the dephosphorylation rate of all model Cdk substrates and Cdk inactivation can drive mitotic exit when PP2A is depleted (Castilho et al., 2009; Mochida et al., 2009). Therefore, different phosphatases might operate at the same time to reverse all the mitotic phosphorylations made by Cdk.

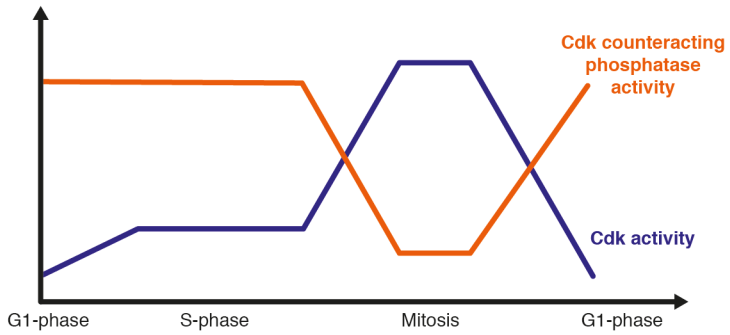


Figure 1.6. The ratio between phosphorylation and dephosphorylation events are responsible for ordering cell cycle progression. In G1-phase Cdk activity is minimal and reaches low levels in S-phase that are sufficient to phosphorylate S-phase substrates even in the presence of high levels of the Cdk-counteracting phosphatases. Phosphorylation of mitotic substrates require high levels of Cdk activity and downregulation of phosphatases (adapted from (Uhlmann et al., 2011)).

1.3. Temporal control of interphase

Interphase is the period in which cells are not dividing. It includes three distinctive parts: G1-phase, S-phase and G2-phase. G1-phase follows mitosis and it is the period that cells have to synthesize its structural proteins and enzymes essential to perform their function. During S-phase the genetic material is faithfully copied. At last, in G2-phase, cells prepare for mitosis and repair any DNA damage that might have occurred during replication.

1.3.1. APC-Cdh1 maintains low levels of Cdk1 activity during G1-phase

Decrease of Cdk1 activity in late anaphase leads to a continuous dephosphorylation and hence partial activation of Cdh1 (Crasta et al., 2008; Peters, 2006). Cdh1 is further activated when it is released from the inhibition of Mad2 and replaces cdc20 in APC/C activation site (Jaspersen et al., 1999; Kramer et al., 2000; Listovsky and Sale, 2013; Zachariae et al., 1998) (Figure 1.7.). This results in further inactivation of Cdk1 during late mitosis, and also targets Plk1, Aurora kinases and Cdc20 for destruction by APC-Cdh1 (Floyd et al., 2008; Kramer et al., 2000; Lindon and Pines, 2004). After mitotic exit, the major function of APC-Cdh1 is to keep S-phase and mitotic Cyclin levels low until a cell commits to a new division cycle. Low Cdk activity levels are maintained by degradation of Cyclins, Cdc25, and two components of the SCF complex (Skp2 and Cks1). Degradation of Skp2 and Cks1 in turn inhibits the degradation of Cyclin dependent kinase inhibitors (CKIs) – $p27^{Kip1}$ and $p21^{Cip1}$ (Bornstein et al., 2003; Carrano et al., 1999; Kamura et al., 2003). A positive feedback loop involving the Cdk inhibitor Sic1 ($p27^{Kip1}$ in mammalian cells) seems to be required to maintain low levels of Cdk activity and prevent re-synthesis of Cyclins, suggesting that the unidirectionality of mitotic exit is not only due to Cyclin degradation but also due to feedback regulation required to maintain the cell cycle in a new stable state (López-Avilés et al., 2009). Thus, G0/G1 is maintained by a cooperation between APC-Cdh1 and CKIs. Cycling cells activate APC-Cdh1 at the end of mitosis and quiescent cells maintain active APC-Cdh1 to prevent re-entry into the cell cycle (Eguren et al., 2011). In addition, cells lacking Cdh1 have a shortened G1-phase, accumulate DNA damage and undergo apoptosis (Peters, 2006). Another critical target of APC-Cdh1 is the transcription factor E2F1 that is targeted for degradation until the G1/S-phase transition is definitive (Budhavarapu et al., 2012). E2F1 promotes transcription of S-phase genes once it is released from complex with pRB (DeGregori et al., 1995).

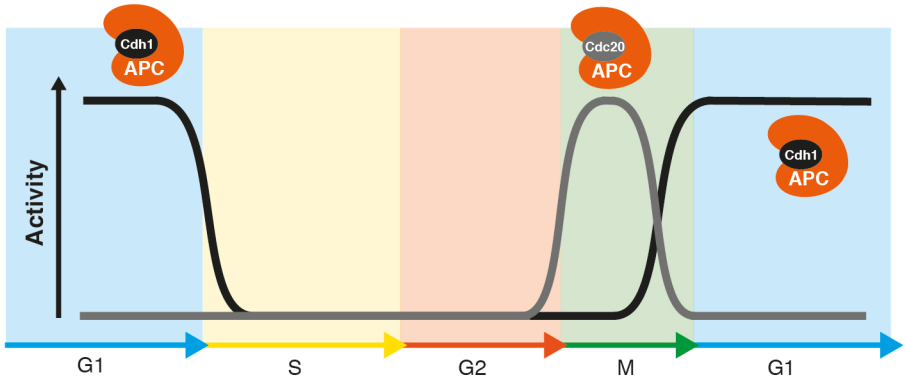


Figure 1.7. APC/C activity is controlled through the regulated binding of two co-activators – Cdc20 and Cdh1. APC/C is inactive in S-phase partially due to low-levels of Cdh1 and Cdc20. In G2-phase, Cdh1 and Cdc20 accumulate, but APC-Cdh1 remains inactive until late mitosis due to inhibition by the protein Emi1 and phosphorylation by Cdks. After SAC requirements are satisfied, APC-cdc20 begins the metaphase to anaphase transition by targeting securing for degradation, allowing sister chromatids to separate, before targeting mitotic cyclins for degradation. Subsequently, during anaphase, dephosphorylation of Cdh1 allows formation of APC-Cdh1, which continues to ubiquitinate mitotic cyclins along with new targets including Cdc20, driving cells out of mitosis into G1-phase. APC-Cdh1 activity persists throughout G1-phase until Cdh1 is inactivated at the G1/S transition.

APC-Cdh1 activity needs to be reduced in a regulated manner in order to allow cells to begin DNA replication. However, this should only happen when the cell has assembled its origins of replication and committed to another round of cell division. There are several mechanisms which allow the cell to completely ablate APC-Cdh1 activity in late G1-phase – these include a combination of inhibitors binding to APC-Cdh1 and phosphorylation by Cdk-cyclin complexes. Cdh1 mediates its own degradation by ubiquitination of UBCH10, forming a negative feedback mechanism that will eventually destroy APC-Cdh1 activity (Rape and Kirschner, 2004; Rape et al., 2006). As Cdk1 and Cdk2 activity levels rise from the G1/S transition through to anaphase, Cdh1 is phosphorylated which blocks its interaction and binding to APC/C (Kramer et al., 2000; Lukas et al., 1999; Zachariae et al., 1998). In addition, phosphorylated Cdh1 is targeted for degradation by SCF ligase which limits APC-Cdh1 activity (Benmaamar and Pagano, 2005). Finally, in late G1-phase, E2F1 activates the

transcription of Emi1 that binds as a pseudo substrate to APC/C. This inhibits the binding of Cdh1 during interphase and Cdc20 during S-phase and G2-phase (Chang et al., 2015; Grosskortenhaus and Sprenger, 2002; Hsu et al., 2002; Reimann et al., 2001). Knocking down Emi1 in human cells showed a delay in the inactivation rate of APC-Cdh1, suggesting that Emi1 accelerates the APC-Cdh1 degradation (Barr et al., 2016; Cappell et al., 2016). Subcellular localization of Cdh1 is also an important component of regulation of APC-Cdh1 activity. During G1-phase Cdh1 is nuclear, but it migrates to the cytosol between S-phase and anaphase (Jaquenoud et al., 2002; Zhou et al., 2003). The nuclear export of Cdh1 and subsequent redistribution to the cytosol is promoted by Cdk phosphorylation, sequestering Cdh1 from both APC/C and nuclear targets and reducing the efficiency of APC-Cdh1.

Several APC/C and Cdh1 components are highly expressed in post-mitotic neurons (Almeida et al., 2005; Gieffers et al., 1999). In addition to their roles in the cell cycle, Cdh1 acts as a regulator of axonal growth and patterning during brain development (Konishi et al., 2004; Lasorella et al., 2006; Stegmüller et al., 2006) and Cdc20 regulates dendrite morphogenesis (Kim et al., 2009). Cdh1 knockdown by iRNA resulted in longer axons and disrupted axonal patterning (Konishi et al., 2004). Complete depletion of Cdh1 in cultured post-mitotic neurons lead to a re-entry into S-phase and increased levels of Cyclin B1 followed by apoptotic cell death (Almeida et al., 2005; Liu and Greene, 2001). All these observations point to the importance of regulating APC-Cdh1 activity in maintaining cell identity and integrity.

1.3.2. Commitment to a new cell division cycle – progression through G1/S/G2

After mitosis, cells can either enter a quiescent state (G0) or commit to a new round of divisions and progress through G1-phase. This 'commitment point' is known as the 'restriction point' in animal cells and 'start' in yeast and is defined as the point after which a cell irreversibly commits to enter and progress through a new cell division cycle. Similar to the Start checkpoint in budding yeast (Pardee, 1974), at the restriction point mammalian cells check for nutrient availability. The existence of this commitment point was further supported by the work of Zetterberg and Larson (Zetterberg and Larsson, 1985), that described a point in early G1-phase after which cells were able to complete their cell cycle independently of the presence or absence of growth factors. It has been proposed that two, instead of one, independent checkpoints exist during G1-phase. The first one consists of the sensing of the

appropriate growth factor signals via the Ras/Raf/MAPK/Cyclin D pathway, and the second occurs later and checks for nutrient availability via the mTORC1 pathway that ultimately leads to the activation of Cdk2-cyclin E (Foster et al., 2010).

An important step of the G1/S transition is the activation of transcription by the E2F transcription factor family. This activation creates an all-or-none switch that results in the commitment to replicate DNA and enter a new round of cell division (Doncic et al., 2015; Skotheim et al., 2008). During early G1-phase, the transcriptional repressors Rb, p107, and p130 – also known as pocket proteins – are bound to E2F transcription factors in order to repress them and avoid premature transcription of S-phase activators (Ginsberg et al., 1994; Graña et al., 1998; Hatakeyama and Weinberg, 1995; Helin et al., 1993; Wirt and Sage, 2010). The association of Rb with E2F is dependent on the hypo-phosphorylation of Rb, which is mediated by Cdk4/6-cyclin D. This regulation makes E2F repression dependent on Cdk4/6-cyclin D activity, so rising Cdk4/6-cyclin D activity allows the initial activation of G1/S-phase transcription factors (Harbour et al., 1999). Cyclin E is one of the first genes to be transcribed (Eser et al., 2011), but the Cdk inhibitor $p27^{Kip1}$ suppresses Cdk2-cyclinE and interacts with Cdk4/6-cyclin D. Another member of the CKIs, $p21^{Cip1}$ also inhibits the activity of Cdk2, binding Cyclin E or Cyclin A through a conserved motif at the N-terminal, impairing the interaction between the kinase and its activator (Abbas and Dutta, 2009; Chen et al., 1996; Harper et al., 1993; 1995; Mandal et al., 1998). Sequestration of $p27^{Kip1}$ by Cdk4/6-cyclin D allows more activation of Cdk2-cyclin E (González et al., 2003). As levels of Cdk2-cyclin E activity start to rise, $p27^{Kip1}$ is phosphorylated on T187, targeting it for ubiquitination and degradation by the proteasome and making Cdk4/6-cyclin D sequestration of $p27^{Kip1}$ dispensable (Montagnoli et al., 1999; Sutterlüty et al., 1999; Tsvetkov et al., 1999). Cdk2-cyclin E complexes create a positive feedback loop whereby Cdk2-cyclin E suppresses Rb, releasing E2F from inhibition which in turn will increase the transcription of Cyclin E and lead to a quicker accumulation of active Cdk2-cyclin E complexes. This will lead the cell to committee irreversibly to a new division cycle (Skotheim et al., 2008). The G1/S transition occurs in a switch-like manner via a network that involves Cdk2-Cyclin E (Barr et al., 2016; Bertoli et al., 2013; Cappell et al., 2016) and several experimental results suggest that this transition depends on cell growth or cell size.

Further phosphorylation of Rb generates a hyper-phosphorylated Rb protein that is inactive, which releases E2F transcription factors and allows the transcription of genes needed for progression into S-phase, including Emi1 and Cyclin A (Chen et al., 1989; Ezhevsky et al., 2001; Hsu et al., 2002). However, Rb is not typically degraded after inactivation but persists until mitosis, when it is dephosphorylated by PP1 to enter the following G1-phase (Kolupaeva and Janssens, 2013). E2F1 also promotes the transcription of ORC1, Cdc6, Cdt1 and all MCM subunits that are important for the assembly of pre-replication complexes (Bosco et al., 2001; Ohtani et al., 1998; Yan et al., 1998; Yoshida and Inoue, 2004).

Cyclin A levels remain low until late G1-phase due to ubiquitination by APC-Cdh1 and subsequent degradation (Geley et al., 2001; Lukas et al., 1999; Sørensen et al., 2001). However, prior to S-phase initiation, APC-Cdh1 is inactivated and releases Cyclin A from its inhibition (Hsu et al., 2002). Cdk2-cyclin A is required to initiate DNA synthesis, prevent re-replication, and to enter into mitosis (Coverley et al., 2002; Woo and Poon, 2003). Thus, tight regulation of Cyclin E and Cyclin A results in a coordinated cell cycle progression (Havens et al., 2006). E2F-mediated transcription needs to be inactivated during S-phase, and this seems to be another role of Cdk2. It was shown that E2F1 is phosphorylated by Cdk2-cyclin A, thereby promoting its dissociation from DNA and down-regulation of E2F1 target genes (Dynlacht et al., 1994; Krek et al., 1994; Xu et al., 1994). This creates a negative feedback loop, since the Cyclin A gene is a direct target of E2F1. E2F1 is also stabilized during S-phase and G2-phase by the ubiquitin ligase regulatory SCF complex, since the E2F target gene Skp2 is a regulatory subunit of SCF. This constitutes another negative feedback loop (Campanero and Flemington, 1997; Hateboer et al., 1996; Marti et al., 1999). In order to avoid re-replication during S-phase, G2-phase, and mitosis, it is important to prevent the re-establishment of pre-replication complexes. This is accomplished through multiple redundant mechanisms: Cdc6 is phosphorylated on S54 that results on its nuclear export (Jiang et al., 1999; Petersen et al., 1999; Saha et al., 1998); Orc1 is phosphorylated by Cdk2-cyclin A and Cdk1-cyclin A and binds to the SCF-Skp2 complex in order to be destroyed (Fujita et al., 2002; Méndez et al., 2002); MCM subunits are also phosphorylated by Cdks and targeted for degradation (Fujita et al., 1998; Hendrickson et al., 1996); Geminin binds to and inhibits Cdt1 (Lee et al., 2004; Tada et al., 2001; Wohlschlegel et al., 2000). Cdt1 can also be phosphorylated by Cdk2-cyclin A and Cdk1-cyclin A, which results in Cdt1 binding to the SCF-Skp2 ubiquitin ligase complex and its subsequent rapid degradation at the G1/S transition (Li et al., 2003; Liu et al., 2004; Nishitani et al., 2004; Sugimoto et al., 2004; Takeda et al., 2005).

When cells successfully transit to S-phase, the DNA is replicated in order to have two copies that will be later divided into the two daughter cells. After the precise and accurate DNA replication, the cells enter in G2-phase. During this last phase of interphase, cells grow and activate protein synthesis in order to prepare for mitosis. In G2-phase there is a DNA damage checkpoint or usually called 'replication checkpoint' (Bartek et al., 2004; Hartwell, 1978; Michael et al., 2000). In response to DNA damage, Chk1/2 proteins will be activated by ATM/ATR-mediated phosphorylation (Liu et al., 2000; Matsuoka et al., 1998). Activated Chk1 will in turn inhibit Cdc25, consequently inhibiting Cdk1 (Furnari et al., 1997; Uto et al., 2004). Therefore, cells will arrest in G2-phase before entering into mitosis (Mailand et al., 2002).

1.4. Temporal progression through mitosis

In mammalian cells, mitosis is the most dramatic event in a cell division cycle, whereby cells undergo both biochemical and morphological changes in a small fraction of a typically long cell cycle (Morgan 2007). Mitosis can be divided into two steps: karyokinesis, which is nuclear division, followed by cytoplasmic division which is called cytokinesis. The first step can be divided in five phases: prophase, prometaphase, metaphase, anaphase, and telophase. During prophase, the chromatin condenses into defined chromosomes; nuclear envelope breakdown marks the beginning of prometaphase; at metaphase chromosomes start to align along the metaphase plate and are attached to mitotic spindles by their kinetochores; at anaphase onset, the sister chromatids separate and start to migrate to the poles; and at telophase the chromosomes arrive at the poles, the nuclear envelope starts to reform and the chromatin begins the process of de-condensation. At this point the cell is ready to begin cytokinesis, which involves the constriction of an actomyosin contractile ring (in animal cells) (reviewed by (Tanaka, 2001)) (Figure 1.8).

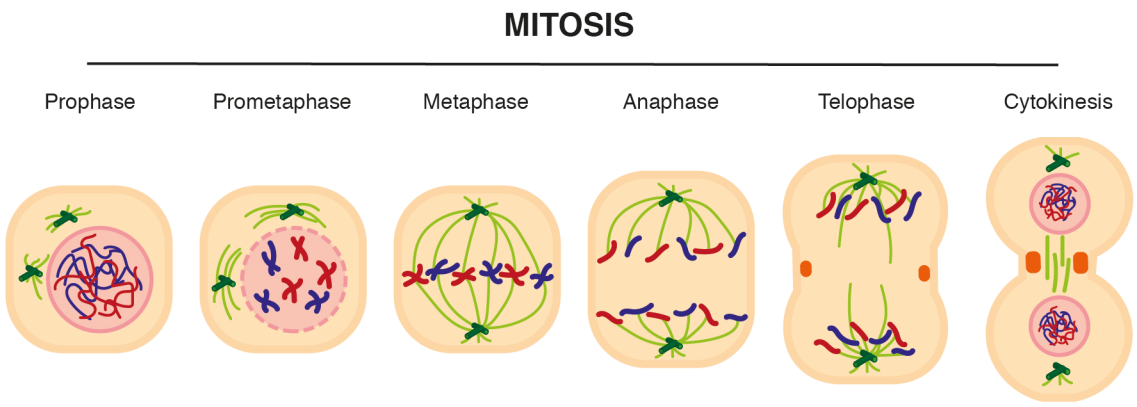


Figure 1.8. Stages of mitosis in a vertebrate cell. In vertebrate cells, six different stages can be distinguished: prophase where sister chromatids condense and the mitotic spindle starts to form; prometaphase where nuclear envelope starts to fragment; metaphase when chromosomes attached to the mitotic spindle align at the metaphase plate; anaphase when the sister chromatids separate; telophase when the chromosomes arrive to the poles and the contractile ring starts to form; and finally cytokinesis where the contractile ring creates the cleavage furrow and the nuclear envelope starts to reform.

Mitotic entry and mitotic exit are both all-or-none transitions that, once triggered, start a series of sequential events to take the cells towards metaphase or G1-phase, respectively. At the heart of mitotic regulation is the complex Cdk1-cyclinB1. In order to enter mitosis, three pre-requisites are required: synthesis and accumulation of Cyclin B1, activation of Cdk1 by CAK (Cdk activating kinase), and inactivation of Wee1. To finish mitosis Cyclin B1 is targeted for degradation by APC/C which inactivates Cdk1. Once new Cyclin B1 is synthesized it binds to Cdk1, and at the same time Cdk1 is inactivated by phosphorylation of residues T14/Y15 by Wee1/Myt1. Mitosis is thought to be driven by two different switches: the first one pushes cells into mitosis by controlling kinase activity, and the second triggers mitotic exit by controlling Cdk1-counteracting phosphatases (Mochida et al., 2016) (Figure 1.9).

1.4.1. Mitotic entry

In the early 70s, Masui and colleagues discovered that the maturation promoting factor (MPF) is responsible for triggering meiotic maturation in *Xenopus laevis* eggs. It took almost 20 years to discover that this factor corresponds to the Cdk1-cyclin B1 complex (Labbe et al., 1989; Lohka et al., 1988; Masui and Markert, 1971; Wasserman and Masui, 1976). It has been suggested that regulating the levels and activity of the Cdk1-cyclin B1 complex is key to control the order and progression of mitosis events (Gavet and Pines, 2010; Lindqvist et al., 2007).

1.4.1.1. Phosphorylation of Tyrosine 15 inactivates Cdk1 activity

Cdk1 activity is regulated at different levels, but controlling Cdk1 activity starts with the transcription and synthesis of its activator subunit – Cyclin B1. As new Cyclin B1 is synthesized, new complexes of Cdk1-cyclin B1 are formed but they are maintained in an inactive form by the activity of inhibitory kinases. Wee1 kinase catalyses an inhibitory phosphorylation of Cdk1 Y15, preventing the appropriate alignment of bound ATP transfer to the substrate peptide (Nurse, 1975; Russell and Nurse, 1987; Welburn et al., 2007). A second kinase, Myt1, is able to phosphorylate both T14 and Y15 of Cdk1 B1 (Kornbluth et al., 1994; Lundgren et al., 1991; Mueller et al., 1995a; 1995b; Watanabe et al., 1995). During

interphase, these two kinases have different intracellular localizations: Wee1 is nuclear and Myt1 is membrane-associated with Golgi and endoplasmic reticulum membrane (Booher et al., 1997; Liu et al., 1997; McGowan and Russell, 1993; Mueller et al., 1995b). When cells are ready to divide the regulatory proteins that trigger mitosis are thought to first activate Cdk1 at the centrosomes, initiating a self-amplifying wave of Cdk1 activation through the cytoplasm and into the nucleus (Jackman et al., 2003; Krämer et al., 2004). This mechanism ensures that early mitotic events are coordinated throughout the cell. Loss of Myt1 activity would be expected to disrupt this coordination by allowing premature activation of Cdk1 in the cytoplasmic compartment, even if Wee1 can still protect the nucleus from active Cdk1. So far, it is known that *Wee1* knockout mice are embryonic lethal, and siRNA against Wee1 in human cells causes critical mitotic phenotypes, but much less is known about depletion phenotypes of Myt1 (Neumann et al., 2010; Tominaga et al., 2006). Cdk1 Y15 needs to be dephosphorylated in order for active Cdk1-Cyclin B1 complexes to promote mitotic entry (Dunphy and Kumagai, 1991; Gautier and Maller, 1991; Gould and Nurse, 1989; Kumagai and Dunphy, 1992; Strausfeld et al., 1991).

1.4.1.2. Cdk1 activity promotes dephosphorylation of Tyrosine 15

In order to be active, Cdk1 needs to be phosphorylated at T161. This is catalysed by Cdk-activating kinase (CAK), which in mammalian cells corresponds to Cdk7 complexed with Cyclin H (Draetta, 1993; Fisher and Morgan, 1994; Mäkelä et al., 1994). In addition, in order to make active Cdk1-cyclin B1 complexes, the inhibitory phosphate groups on Cdk1 B1 T14/Y15 residues need to be removed. This is accomplished by Cdc25 phosphatases, which can dephosphorylate both residues in late G2-phase (Boutros et al., 2006). In humans, three different isoforms of the Cdc25 exist – CDC25A, CDC25B and CDC25C. The resulting three Cdc25 protein isoforms act at different times during cell cycle. It was demonstrated Cdc25B and Cdc25C are predominantly active during G2/M transition, while Cdc25A has a major role during interphase (Chen et al., 2001; Ferguson et al., 2005). While Cdc25A-null mice are lethal during the pre-implantation period, Cdc25B-null mice and Cdc25C-null mice are viable (Chen et al., 2001; Lincoln et al., 2002; Ray et al., 2007). Moreover, double deletion of Cdc25B and Cdc25C does not affect mouse development, suggesting that Cdc25A can step in and compensate for the absence of Cdc25B and Cdc25C (Ferguson et al., 2005). These studies showed that different Cdc25 phosphatases have different functionalities throughout development.

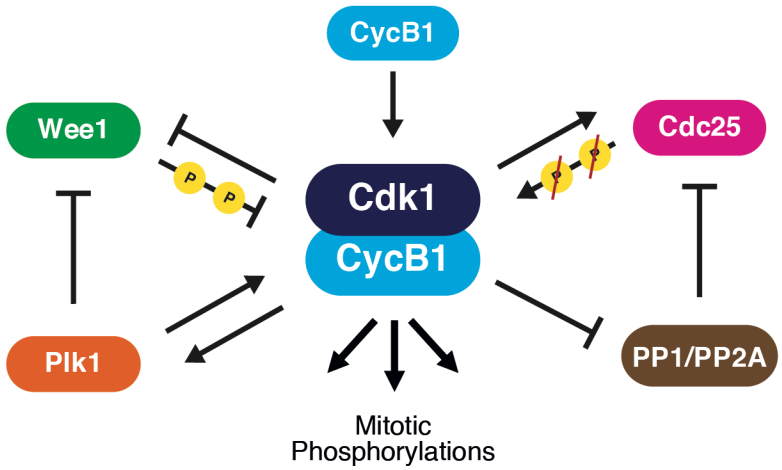


Figure 1.9. Mitotic entry is regulated by positive feedback control. Wiring diagram showing a simplified Cdk1 regulatory network, including positive and negative feedback loops.

Wee1 and Cdc25 regulate Cdk1 activity and are in turn regulated by Cdk1 through a double negative feedback loop, in which Cdk1 phosphorylates and inactivates Wee1, and a positive feedback loop, in which Cdk1 phosphorylates and activates Cdc25 (Hoffmann et al., 1993; Kumagai and Dunphy, 1992; Lu et al., 2012; McGowan and Russell, 1995; Mueller et al., 1995a; Okamoto and Sagata, 2007) (Figure 1.9). Due to feedback regulation, Wee1 and Cdc25 phosphorylation has been shown to be ultrasensitive as a function of Cdk1 activity (Kim and Ferrell, 2007; Trunnell et al., 2011).

The activation of Cdc25 and inactivation of Wee1 by positive feedback results in an explosive activation of Cdk1. In order to become active, Cdc25 needs to be released from 14-3-3 proteins by Cdk2 and Plk1 activities (Elia et al., 2003b; Kumagai et al., 1998; Margolis et al., 2003). This will initiate a positive feedback loop whereby Cdk1 further activates Cdc25 that in turn will activate more Cdk1-cyclin B1 complexes by dephosphorylating of Cdk1 T14 and Y15 (Hoffmann et al., 1993; Izumi and Maller, 1993; Izumi et al., 1992; Kumagai and Dunphy, 1992). This relatively slow dynamic of Cdk1 activation triggers nuclear translocation of Cdk1-Cyclin B1 complexes, which is itself subjected to positive feedback – nuclear Cdk1-cyclin B1 complexes promote the translocation of more Cdk1-cyclin B1 complexes to the

nucleus. The nuclear import of Cdk1-cyclin B1 complexes is promoted by the phosphorylation of serine residues in Cyclin B1, that at the same time will inhibit nuclear export (Santos et al., 2012). This positive feedback is aborted in Cyclin B1 molecules with all five mitotic phosphorylation sites mutated to alanines, which also delays the timing of the nuclear re-localisation of Cyclin B1 to coincide with, not precede, nuclear envelope breaks down (NEB) (Santos et al., 2012). Regardless of the exact mechanism of nuclear import control, the nuclear exclusion of Cyclin B1 that occurs during interphase prevents premature mitotic entry in higher eukaryotes, suggesting that one of the functions of Cdk1-Cyclin B1 is to spatially control the co-localisation of Cdk1 and its substrates (Moore et al., 2003).

Wee1 kinase is silenced by phosphorylation-dependent degradation at the G2/M transition (Michael and Newport, 1998). Wee1 and Cdk1 are also involved in a positive – or double negative – feedback loop, where Wee1 inhibits Cdk1 activation and vice versa (McGowan and Russell, 1995; Mueller et al., 1995a; Tang et al., 1993). As more Cdk1-cyclin B1 complexes become active at mitotic entry due to activation of Cdc25, more Wee1 is repressed by Cdk1. It is this regulation involving double positive feedback loops that include Wee1-Cdk1-Cdc25 which makes the activation of Cdk1 switch-like and mitotic entry an irreversible decision (Novak and Tyson, 1993a; Pomerening et al., 2003; Sha et al., 2003).

Different thresholds of Cdk1 activity drive different mitotic events; the levels of Cdk1-cyclin B1 activity required to enter mitosis are lower than the levels required for mitotic progression, which suggests that a gradual increase in Cdk1-cyclin B1 activity is critical to coordinate mitotic progression after centrosome separation (Lindqvist et al., 2007). This view is in agreement with the quantitative model of temporal regulation of cell division described in section 1.2.3. In 2010, Gavet and Pines developed a FRET probe for Cdk1 in human cells and found that the initial activation of Cdk1-cyclin B1 happens 20 to 25 minutes before nuclear envelope break down (NEB) (Gavet and Pines, 2010). The earliest substrates of the Cdk1-cyclin B1 complex are involved in cytoskeletal reorganization, which enables the cells to become round during prophase. However, this initial small increase in Cdk1-cyclin B1 activation is reversible before NEB in prometaphase (Matsusaka and Pines, 2004; Potapova et al., 2011; Rieder and Cole, 1998). Thus, increasing levels of Cdk1-cyclin B1 activity coordinate events during prophase (Gavet and Pines, 2010). Cdk1-cyclin B1 activity levels progressively increase throughout prophase before finally reaching full activation - cells that reach this activity threshold undergo further progression into mitosis, characterised by NEB and other mitotic rearrangements. Therefore, different mitotic events are thought to be organised temporally by different Cdk1-cylin B1 activity thresholds.

1.4.2. Spindle assembly checkpoint (SAC) drives metaphase to anaphase transition

High levels of Cdk1-cyclin B1 activity drive mitotic progression until the boundary of anaphase (Morgan, 2007; Wurzenberger and Gerlich, 2011). Late stages of mitosis require Cdk1-cyclin B1 inactivation by the APC/C complex (Sullivan and Morgan, 2007; Wäsch and Cross, 2002). APC/C is kept inactive by the spindle assembly checkpoint (SAC) machinery until all the chromosomes are perfectly attached to the spindle microtubules and aligned along the metaphase plate (Musacchio and Salmon, 2007; Spencer and Hieter, 1992; Wang and Burke, 1995).

During prometaphase, all SAC proteins are recruited to kinetochores including Mad1, Mps1 and Mad2 (Famulski and Chan, 2007; Howell et al., 2004; Jablonski et al., 1998; Johnson et al., 2004). Spindle assembly checkpoint signalling acts like a rheostat – it has different strengths depending on the severity of the conditions that generate the signal (Collin et al., 2013; Santaguida et al., 2011). The strength of SAC depends on the number of unattached chromosomes or improperly attached kinetochores, and will determine the rate at which the mitotic checkpoint complex (MCC) assembles. The more severe the condition that triggers the signal to activate SAC, the more robust the SAC response will be (Dick and Gerlich, 2013).

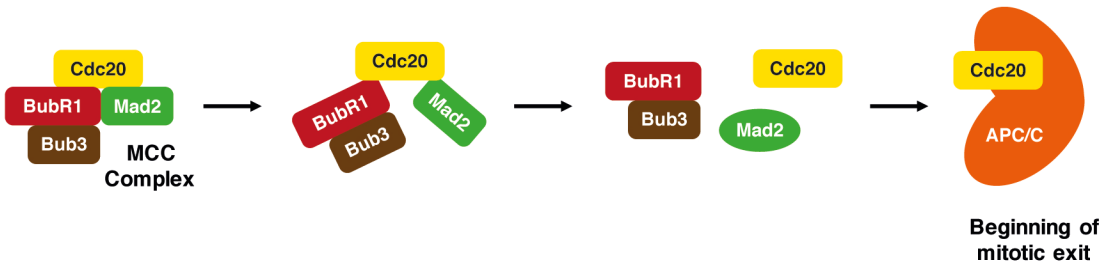


Figure 1.10. Mitotic checkpoint complex avoids APC/C activation before satisfaction of SAC requirements. When spindle assembly checkpoint machinery is turned off, MCC complex is dissembled, releasing Cdc20 that is going to bind to APC/C in order to activate it and start mitotic exit.

Aurora B is a well-known regulator of the SAC which promotes the correct kinetochore-microtubule attachment (Carmena et al., 2012). Mps1 is recruited to kinetochores by Aurora B in order to create docking sites for the hierarchical recruitment of the additional SAC proteins including Bub3, Bub1, Bubr1, Mad1, Mad2, and Cdc20 and hence to assemble the MCC complex (Diaz-Martinez et al., 2015; Lischetti et al., 2014; London and Biggins, 2014; Moyle et al., 2014). If Mps1 is not recruited to the kinetochores, SAC requirements are not satisfied and mitotic exit is delayed (Ito et al., 2012; Jelluma et al., 2010). After Mad1 is recruited, it binds to unattached kinetochores and recruits Mad2, thereby inducing a conformational change in Mad2 from an 'open' to a 'closed' form (Luo et al., 2000; 2002). In the closed form, Mad2 prevents activation of the APC/C complex by sequestering Cdc20, which is the APC/C activator (Fang et al., 1998) (Figure 1.10). Once all SAC requirements are met, the checkpoint signalling is turned off and the cells progress to mitotic exit (Fang et al., 1998; Hardwick et al., 2000; Sczaniecka et al., 2008).

1.4.3. Mitotic exit

After satisfaction of SAC requirements, cells start exiting from mitosis. This is the time where chromosomes segregate, cytokinesis happens, and the nuclear envelope reassembles. These sequentially ordered series of events are triggered by Cdk1 inactivation and the removal of Cdk1-dependent mitotic phosphorylations. However, mitotic exit is not a reverse reaction of mitotic entry. It is a linear progression into a new cell division cycle (Hégarat et al., 2016).

Once SAC requirements are fulfilled, Mad2 releases Cdc20 that will bind and activate APC/C in order to initiate mitotic exit (Foster and Morgan, 2012; Izawa and Pines, 2012; Nilsson et al., 2008; Reddy et al., 2007) (Figure 1.10). The APC-cdc20 complex is very important for securin degradation. This will release the protease separase, allowing the cleavage of cohesion 1 which holds two sister chromatids together. This event will initiate chromosome segregation (Nasmyth, 2001). APC-cdc20 complexes also play an important role in Cdk1 inactivation and subsequent exit from mitosis (Murray and Kirschner, 1989). High levels of Cdk1-Cyclin B1 complexes will activate more APC-cdc20 complexes that in turn target Cyclin B1 for degradation, thereby inactivating Cdk1 (Figure **1.11**). This feedback regulation makes the activation of APC-cdc20 occur in a switch-like manner (Yang and Ferrell, 2013; Yang et al., 2009a). Low levels of active Cdk1 allow Cdc20 to be replaced in the complex by another activator of APC/C – Cdh1. By replacing Cdc20 for Cdh1, the substrate

specificity of APC/C reduces, in order to maintain its activity throughout the subsequent G1-phase (Floyd et al., 2008; Lindon and Pines, 2004; Peters, 2006; Stewart and Fang, 2005).

It has been shown that Cyclin B1 destruction and inactivation of Cdk1 is not enough to finish mitosis (Skoufias et al., 2007). Cdk1-dependent phosphorylation of substrates also needs to be reversed, since Cdk1 activity prevents the return to G1-phase. For that reason, Cdk1 counteracting phosphatases need to be reactivated in order for the cell to progress through mitotic exit (Chen et al., 2007; Murray et al., 1989; Parry and O'Farrell, 2001; Yamano et al., 1996).

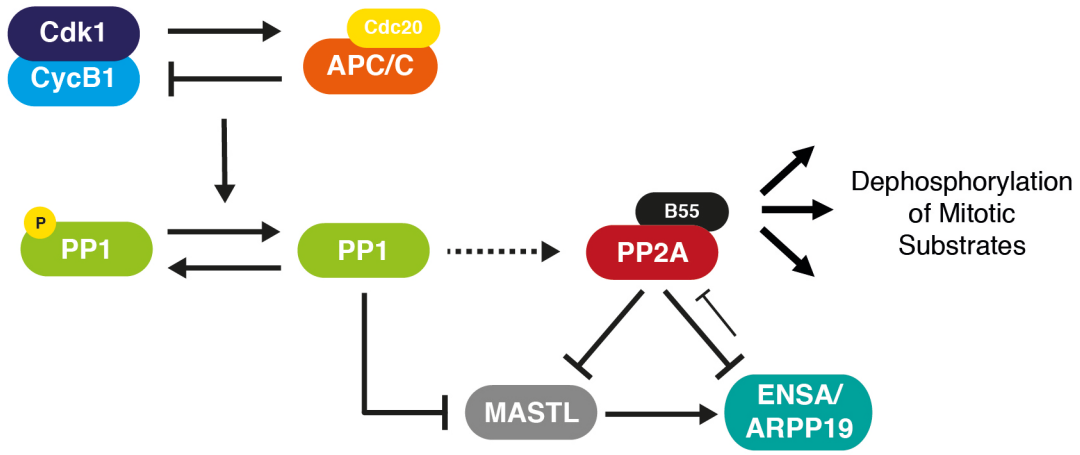


Figure 1.11. Mitotic phosphorylations need to be removed in order to finish mitosis. After satisfaction of SAC requirements, APC/C is activated by high levels of Cdk1 activity and in turn will target Cyclin B1 for degradation. Cdk1 activity starts to decrease, releasing PP1 from its inhibitory phosphorylation. PP1 can autodesphosphorylate itself and inactivate MASTL, allowing PP2A-B55 to inhibit its inhibitors ENSA and ARPP19 and hence reactivate itself. PP1 may also contribute to direct activation of PP2A-B55 but this is still not confirmed in mammalian cells

In higher eukaryotes, this role seems to be carried out mainly by PP1 and PP2A-B55 phosphatases, although other phosphatases might also be involved. In budding yeast, Cdc14 is sequestered in the nucleolus through inhibitory binding to Net1 (Shou et al., 1999; Traverso et al., 2001; Visintin et al., 1999). Cdc14 is activated and released from the nucleolus after phosphorylation of Net1 by Cdk and Polo kinase (Azzam et al., 2004; Shou et al., 2002; Yoshida and Toh-e, 2002).

PP1 is thought to be the trigger to initiate dephosphorylation of Cdk1 substrates in higher eukaryotes. Cdk1 inhibits PP1 by phosphorylation at T320 (Dohadwala et al., 1994; Kwon et al., 1997). The drop in Cdk1 activity levels during mitosis are sufficient to allow PP1 auto-dephosphorylation of T320. This activates PP1, which then inactivates MASTL by dephosphorylation. Inactivating MASTL, stops the activation of PP2A-B55 inhibitors – ARPP19 and ENSA. As PP2A-B55 is released from its inhibitors, it further dephosphorylates its inhibitors – ARPP19 and ENSA – and reactivate itself (Heim et al., 2015; Ma et al., 2016; Rogers et al., 2016) (Figure **1.11**). The importance of this signalling cascade is further supported by the observation that depletion of PP2A-B55*δ* in *Xenopus* egg extracts prevent them from exiting mitosis and at the same time, depletion of MASTL causes mitotic exit to occur. This indicates that the ratio of kinase/phosphatase activity is important to drive exit from mitosis (Mochida et al., 2009; Vigneron et al., 2009). This system causes PP2A-B55 activity to rise exponentially at the same time that Cdk1 activity drops, which allows the cells to rapidly dephosphorylate mitotic substrates and enter G1-phase.

1.5. Embryonic, normal and cancer cells have different division cycles

The cell cycle structure in normal (healthy) and cancer cells is very similar and includes four different cell cycle phases: G1-phase, S-phase, G2-phase, and mitosis. However, pluripotent cells in the epiblast lack a fully formed G1-phase and G2-phase, spending 60% of their cell cycle duration in S-phase (Faast et al., 2004; Savatier et al., 1994; Stead et al., 2002). Embryonic stem cells (ESC) have a very similar cell cycle structure, spending 65% of their cell division cycle in S-phase and only 15% in G1-phase (Becker et al., 2006) (Figure 1.12). During differentiation, embryonic stem cells gained a lengthened G1-phase and their cell cycle length increased to more than 16 hours, similar to that of somatic cells.

In somatic cells, the G1/S checkpoint needs to be overcome in order to progress to S-phase. After the G1/S checkpoint, the cell cycle becomes independent of external growth factors. A marker for this stage is the inactivation of Rb by hyper-phosphorylation and the consequent release of E2F factors. This is not the case in embryonic stem cells. Pluripotent stem cells lack the typical E2F/pRB-mediated transition in late G1-phase (Fluckiger et al., 2006). In embryonic stem cells, Rb is constitutively in a hyper-phosphorylated state due to high levels of Cdk-cyclin activity – this prevents Rb binding to E2F factors in order to inhibit them (Conklin and Sage, 2009; He et al., 2009). This leads to a short transition through G1-phase. In cancer cells, Rb function is often defective which results in E2F-dependent G1/S gene expression even in the absence of mitogens (Harbour and Dean, 2000; Malumbres and Barbacid, 2001).

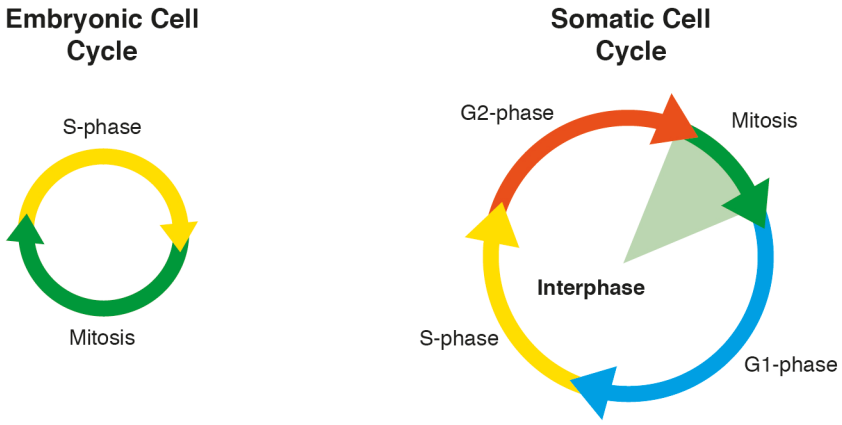


Figure 1.12. Embryonic vs. somatic cell cycle. The same cell cycle machinery is present in embryonic and somatic cells; however, their cell cycle structure is completely different. ES cells spend 65% of their cell cycle time in s-phase and have very short G1-phases. In somatic cells, as well as in cancer cells, the cell cycle is divided in four different and well-defined phases: G1-phse, S-phase, G2-phase and mitosis.

To progress through G1-phase and initiate DNA replication, the activity of Cdks is highly regulated by two different families of inhibitors in somatic cells: INK4 proteins (Chan et al., 1995; Guan et al., 1994; Hannon and Beach, 1994; Hirai et al., 1995; Serrano et al., 1993), and the Cip/Kip family that includes p21 and p27 (Dulić et al., 1994; el-Deiry et al., 1993; Gu et al., 1993; Harper et al., 1993; Malumbres and Barbacid, 2005; Noda et al., 1994; Polyak et al., 1994a; 1994b; Toyoshima and Hunter, 1994; Xiong et al., 1993). INK4 proteins are specific for the Cdk4 subfamily and distort the Cyclin interface and the ATP-binding pocket, thereby preventing Cdk4 activation (Jeffrey et al., 2000). Members of the Cip/Kip family bind both Cdk and Cyclin subunits individually, which inhibits the formation of Cdk-cyclin complexes (Pavletich, 1999). However, in embryonic stem cells, Cdk inhibitors are absent or very weakly expressed - this is directly linked with the high and constant levels of Cyclins throughout the cell cycle in these cells (He et al., 2009; Kapinas et al., 2013; Koledova et al., 2010). Inactivation of Cdk inhibitors is also a common event in tumorigenesis. Releasing the brakes of cell cycle progression - INK4 proteins, p21 and p27 – leads to deregulation of Cdk activity and further tumour development (Malumbres and Barbacid, 2009; Ortega et al., 2002).

Contrary to somatic cells, human and mouse embryonic stem cells (mESC) have a remarkable tolerance for mitotic failure-induced polyploidy, a condition that is hardly observed in mammalian somatic cells (Mantel et al., 2007). Experimentally pre-formed and isolated polyploid/aneuploid embryonic stem cells initiated caspase-dependent apoptosis, indicating that switching from pluripotency to lineage specification activated cell-death checkpoint-coupling programs that were previously silenced (Mantel et al., 2007). In somatic cells, the SAC is highly regulated and ensures the proper segregation of sister chromatids by inhibiting the metaphase-anaphase transition until all chromosomes are properly attached to the mitotic spindle (Hoyt et al., 1991; Li and Murray, 1991; Santaguida and Musacchio, 2009). Cancer cells can also overcome the spindle assembly checkpoint. Chromosomally unstable tumours are enriched in centrosomal and mitotic genes in their expression signatures, as well as altered SAC regulators. Centrosome amplification may lead to the formation of aberrant mitotic spindles with multiple poles that result in abnormal cell divisions and aneuploidy in cancer cells (Duensing et al., 2006; Hanashiro et al., 2008).

Although the cell cycle machinery is the same in different cell types, the expression levels of the different players and interaction between them change the structure and progression of different cell division cycles. The study of how these molecular factors are altered in individual cell types can potentially provide more insight into control of different cell division cycles.

1.6. Systems-levels feedback control

The cell cycle is an ordered and unidirectional sequence of events that allows cells to replicate their DNA and physically divide into two daughter cells. For this reason, the cell cycle machinery is heavily regulated as described in section 1.2. Feedback loops also play an important role in coordination of the different cell cycle phases, adding an extra layer of control to the cell cycle network (Pomerening, 2009). There are three recurrent motifs involved in cell cycle regulation: negative feedback loops, positive feedback loops and reciprocal regulation (Ferrell, 2013) (Figure 1.13).

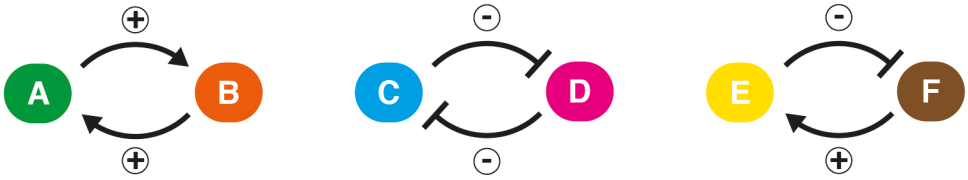


Figure 1.13. Positive and negative feedback motifs. There is a positive feedback loop between A and B; C and D have a double negative (= positive) feedback and E and F correspond to a negative feedback loop. + and – represent the active and inhibitory effect, respectively.

1.6.1. Negative feedback loops

In a negative feedback loop the output represses the input of the system. This allows stabilisation of the system by quickly approaching a new steady state. This kind of regulation is very useful in homeostatic systems, since a single negative-feedback loop will often produce a stable, auto-regulatory and adaptive response. This was shown to be the case for the first time using a gene circuit that consisted of a regulator and a transcriptional repressor module in *Escherichia coli (E. coli)*. This work showed that a single negative-feedback loop was enough for the circuit to gain stability (Becskei and Serrano, 2000). However, if the negative feedback is very strong, it destabilises the system and generates limited cycle oscillations. Elowitz and Leibler engineered a triple-negative feedback circuit also in *E. coli* that consisted of *tet* repressor (TetR) repressing lambda repressor (λcI) and a GFP reporter,

λcI repressing *lac* repressor (LacI), and LacI repressing TetR – this kind of 3-gene inter-regulatory network is commonly known as 'repressilator' (Elowitz and Leibler, 2000). This work showed that by expressing this triple-negative feedback loop, the system was able to exhibit oscillatory GFP fluorescence. However, these oscillations were noisy and varied from cell to cell (Elowitz and Leibler, 2000).

A well-known example of negative feedback in cell cycle has Cdk1-cyclin B1 and APC-cdc20 as players. Cdk1-cyclin B1 activity drives cells into mitosis but also activates APC-cdc20 in a switch-like manner in order to finish mitosis. Once activated, APC-cdc20 feeds back on Cdk1-cyclin B1 by targeting Cyclin B1 for degradation, thereby inactivating Cdk1 and driving cells out of mitosis (Glotzer et al., 1991; Pines, 2011; Yang and Ferrell, 2013). Negative feedback control is present in different transition during a cell division cycle as listed in Table 1.1.

Table 1.1 Negative feedbacks in the cell cycle.

NEGATIVE FEEDBACK LOOP	CELL CYCLE TRANSITION	REFERENCE
Small cell size → G1-phase delay cell → growth	G1 → S	(Di Talia et al., 2009)
MBF → YOX, NRM1 ⊣ MBF	G1 → S	(Aligianni et al., 2009)
E2F → mir449 ⊣ Cdk2,4,6 → E2F	G1 → S	(Yang et al., 2009a)
E2F1 → E2F7/8 ⊣ E2F1	G1 → S	(Li et al., 2008)
Unoccupied kinetochore → activation SAC → mitosis arrest	Metaphase → Anaphase	(Pines, 2011)
Cdk1 → APC-cdc20 ⊣ Cdk1	M → G1	(Jaspersen et al., 1999)

1.6.2. Positive feedback loops

Positive feedback loops can behave in different ways and have been shown to bring about signal amplification, sustained responses, and rapid switching of activities in time and space, since the output of a system has a positive effect on its own input. Often, positive feedback regulation gives rise to bistability. A system is called bistable if it has two stable steady states. To have a bistable response a number of elements are needed: some sort of feedback, either positive or double-negative; some type of non-linearity within the feedback circuit (ultrasensitivity); and the feedback loop must be properly balanced (Ferrell, 2000; Hasty et al., 2001; Laurent and Kellershohn, 1999; Smolen et al., 2000). The cell cycle can be viewed as a bistable switch where the cells transit between two stable states – interphase and mitosis (Cross et al., 2002; Novak and Tyson, 1993a; 1993b; Pomerening et al., 2003).

Division, differentiation, and death are the three major choices that cells face during their lives. Once all the conditions are met for a cell to initiate one of the choices, it often means an irreversible decision. Cell cycle regulation is very well-known system where positive feedback control is crucial to make the transition from interphase to mitosis (and vice versa) an irreversible decision. The onset of mitosis depends on the switch-like activation of Cdk1. Since Cdk1 activates its own activator, Cdc25, and inhibits its own inhibitor, Wee1 (Hoffmann et al., 1993; Kumagai and Dunphy, 1992; Mueller et al., 1995a; Solomon et al., 1990), it creates a bistable trigger that leads to an explosive activation of Cdk1 at beginning of mitosis (Novak and Tyson, 1993a; 1993b). These characteristics also make the system hysteretic (Pomerening et al., 2003; Sha et al., 2003). This is very important to make the G2-phase to mitosis transition irreversible. The same should be true for the transition from mitosis to G1-phase - in late anaphase, APC/C shifts its co-activator Cdc20 by Cdh1, which is an inhibitor of Cdk1. On the other hand, Cdk1 also inhibits Cdh1. So, Cdk1 ⊣ APC-Cdh1 ⊣ Cdk1 is a double-negative feedback loop that locks cells into interphase, making it impossible for cells in G1-phase to return to a mitotic state (Jaspersen et al., 1999; Novak et al., 2007; Sigl et al., 2009).

Bistable systems are also characterized by an abrupt transition from a low to high steady state after the activation signal reaches a certain threshold. All bistable systems are expected to display some degree of hysteresis, that is the ability to produce different steady-state signal (Ferrell, 2002; Ferrell and Xiong, 2001) (Figure 1.14.A). This means that it is more difficult to change the system from one state to the other than it is to maintain the system in one of the two states possible. Bistability and hysteresis have been shown to be important in mitotic entry. For example, the positive feedback between Cdk1 and Cdc25 generates some hysteresis (Figure 1.14.A).

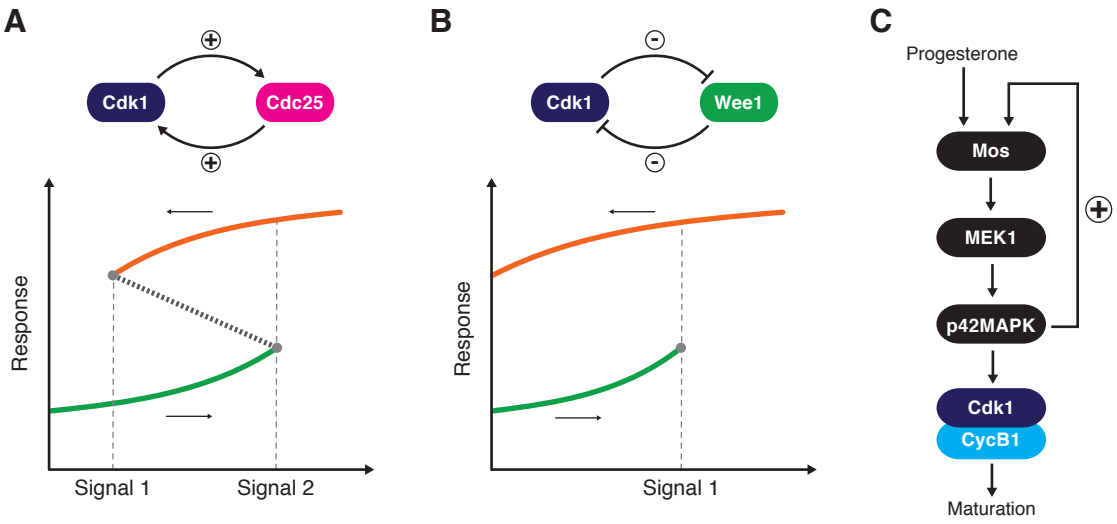


Figure 1.14. Examples of bistability in cell cycle regulation. A. Positive feedback between Cdk1 and Cdc25 gives rise to a hysteric system. Schematic representation of hysteresis – when the signal intensity is less than signal 1 or greater than signal 2, there is only one stable steady-state. When the signal intensity is in the interval between signal 1 and signal 2, two stable steady states co-exist. **B.** Double negative feedback between Cdk1 and Wee1 gives rise to irreversibility. Schematic representation of irreversibility – when the system is exposed to signal 1, it abruptly transits from low to high response level state. However, when the signal intensity shifts back from high to low, the system stays in the high response level state. **C.** A naturally occurring bistable irreversible system in *Xenopus laevis* oocytes. In response to progesterone, Mos accumulate and activates MEK1 that will then activate p42MAPK. Activation of p42MAPK stimulates more activation of Mos, activating the pathway even more. At some levels, the oocyte must convert a graded, reversible triggering stimulus – progesterone- into an all-or-none, irreversible commitment to maturation.

Table 1.2. Positive feedbacks and double negative feedback loops in the cell cycle.

POSITIVE FEEDBACK LOOP	CELL CYCLE TRANSITION	REFERENCE
Cdk2-cyclin E ⊣ p27 ⊣ Cdk2-cyclin E	G1 → S	(Sheaff et al., 1997; Vlach et al., 1997)
Cdk2-cyclin E ⊣ Rb ⊣ E2F → Cdk2-cyclin E	G1 → S	(Yao et al., 2008)
Cdc28-clb2 ⊣ Sic1 ⊣ Cdc28-clb2	G1 → S	(Nash et al., 2001; Schwob et al., 1994; Verma et al., 1997)
Cdc28-clb1/2 ⊣ Whi5 ⊣ Cdc28-clb1/2	G1 → S	(Costanzo et al., 2004; de Bruin et al., 2004; Doncic et al., 2011)
Cdc28-clb1/2 → SBF/MBF → Cdc28-clb1/2	G1 → S	(Cross et al., 1994; Skotheim et al., 2008; Wijnen et al., 2002)
Cdk1-cyclin B1 ⊣ PP1 ⊣ Cdc25 → Cdk1-cyclin B1	G2 → M	(Wu et al., 2009)
Cdk1-cyclin B1 → Cdc25 → Cdk1-cyclin B1	G2 → M	(Hoffmann et al., 1993; Kumagai and Dunphy, 1992; Solomon et al., 1990)
Cdk1-cyclin B1 ⊣ Wee1 ⊣ Cdk1-cyclin B1	G2 → M	(McGowan and Russell, 1995; Mueller et al., 1995a; Sha et al., 2003; Xiong and Ferrell, 2003)
Cdk1-cyclin B1 ⊣ Myt1 ⊣ Cdk1-cyclin B1	G2 → M	(Booher et al., 1997; Fattaey and Booher, 1997; Mueller et al., 1995b)
p-Cyclin B1 → nuclear translocation Cdk1-cyclin B1 → p-Cyclin B1	G2 → M	(Santos et al., 2012)
Plk1 ⊣ Wee1 ⊣ Cdk1-Cyclin B1 → Plk1	G2 → M	(Watanabe et al., 1995)
Plk1 → Cdk1-cyclin B1 → Plk1	G2 → M	(Abrieu et al., 1998; Elia et al., 2003a; Kumagai and Dunphy, 1996; Lobjois et al., 2009)
Cdk1-cyclin B1 ⊣ PP2A-B55 ⊣ Cdc25 → Cdk1-cyclin B1	G2 → M	(Forester et al., 2007)
Cdk1-cyclin B1 ⊣ APC-Cdh1 ⊣ Cdk1-cyclin B1	M → G1	(Zachariae et al., 1998)
Inhibitor ⊣ 1 PP1 ⊣ Inhibitor 1	M → G1	(Dohadwala et al., 1994; Kwon et al., 1997)
Securin ⊣ Separase → Cdc14 ⊣ Securin	M → G1	(Holt et al., 2008)

Irreversibility is an extreme demonstration of hysteresis and it implies that after stimulus has been removed, the system will be 'trapped' in the activated state and unable to return to basal levels of activity (Ferrell, 2002; Guidi and Goldbeter, 1997; 1998) (Figure 1.14.B). For example, at mitotic entry, the double negative feedback loop between Cdk1 and Wee1 makes entry into mitosis and irreversible decision (Figure 1.14.B). An irreversible cell fate decision is a well-documented example of an irreversible bistable-switch. For example, the maturation of *Xenopus* oocytes is controlled by a protein kinase cascade (Mos-MEK-MAPK cascade) after activation by the hormone progesterone (Figure 1.14.C). The oocyte maturation is an all-or-none response since oocytes either mature or don't. At the same time this process is irreversible since if oocytes do commit to maturation, they cannot de-differentiate even if the progesterone stimulus is removed. Thus, at some point during the signal transduction process, the oocyte converts a graded, reversible, triggering stimulus into an all-or-none and irreversible cell fate decision (Ferrell, 1999; Ferrell and Machleder, 1998).

Positive feedback and double negative feedback loops are a recurrent motif in cell cycle regulation as described in Table 1.2. Positive feedback has also been shown to be important for keeping synchronicity between events, both in interphase and mitosis. Georgi and colleagues showed that the lag time between phosphorylation of Cdc25 and phosphorylation of Cdc27 in *Xenopus* oocyte extracts is the same regardless of how long the extracts stayed in interphase (Georgi et al., 2002). In budding yeast, it was also shown that the positive feedback between Cln1/2–Cdk1 and the transcriptional regulators Whi5 and SBF/MBF is essential for synchronous expression of the G1/S regulon (Skotheim et al., 2008). Positive feedback between Cdc14 and securin helps to make the separation of sister chromatids at the end of mitosis happen in unison. If this feedback mechanism is lost, sister-chromatid separation does not occur as synchronously (Holt et al., 2008).

1.6.3. Interlinked feedback regulation

As listed in Table 1.1 and Table 1.2, negative and positive feedback loops regulate cell division in an interlinked way (Figure 1.15). For example, a negative feedback loop can oscillate easily in the presence of a bistable trigger. Cdk1 activation is embedded in positive feedback control that adds a time delay in order to destabilize the steady state of the whole system and helps the negative feedback loop of Cdk1-APC to promote oscillations (Ferrell et al., 2011; Novak and Tyson, 2008; Pomerening, 2008; Pomerening et al., 2005).

Bistability can make a negative feedback loop to oscillate in a more spikier way, and in return, a negative feedback loop can give a reset mechanism to a bistable switch (Ferrell, 2013). A bistable switch can also allow an oscillator to be more tunable (Tsai et al., 2008). The phosphorylation state of Cdk1 substrates is a good example of reciprocal regulation. When Cdk1 is activated it regulates its substrate phosphorylation in two ways: an increase in Cdk1 activity will increase the rate of substrate phosphorylation and decrease the rate of substrate de-phosphorylation, since Cdk1 inhibits its counteracting phosphatase. This behaviour makes the system ultrasensitive, which means that small changes in Cdk1 activity will cause large changes in the substrate phosphorylation (Ferrell, 2013; Ferrell and Xiong, 2001; Tyson and Othmer, 1978).

Using several feedback loops together allows oscillations to occur easily and in a larger parameter/space and Cdk1 activity to be ultrasensitive. Feedback regulation allows for cells to safeguard that a lot of conditions need to be met for a cell to divide. Therefore, sophisticated feedback regulation ensures fidelity and reliability in cell cycle progression.

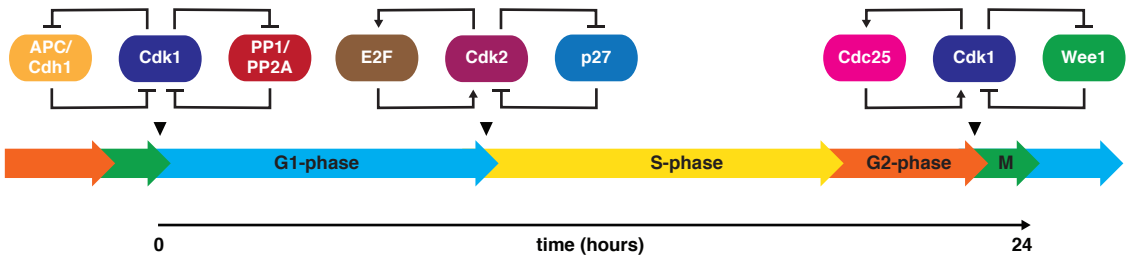


Figure 1.15. Interlinked feedback control is widely use in cell cycle regulation. Combination of multiple feedback loops safe-guards the important passage between different cell cycle phases. At mitosis to G1 transition, Cdk1 is embedded in 2 double-negative feedback loops: Cdk1 ⊣ APC-Cdh1 ⊣ Cdk1 and Cdk1 ⊣ PP1/PP2A ⊣ Cdk1. At the G1/S transition, Cdk2 is embedded in a double-negative feedback loop and a positive feedback look – Cdk2 ⊣ p27 ⊣ Cdk2 and Cdk2 → E2F → Cdk2, respectively. At G2/M transition, Cdk1 activation depends on a double negative feedback loop and a positive feedback loop – Cdk1 ⊣ Wee1 ⊣ Cdk1 and Cdk1 → Cdc25 → Cdk1. Black arrows show at which transition between cell cycle phases the feedback network is taking place.

1.7. Studying cell cycle dynamics – from classical to novel tools

In the early 70's, application of genetics coupled with molecular biology allowed effective cell cycle studies in yeast, leading to the discovery of important cell cycle genes that were then physiologically characterized and used for subsequent biochemical analysis (Hartwell et al., 1973; Nasmyth and Reed, 1980). After a decade, cell extracts and genes derived from *Xenopus laevis* or sea urchin oocytes started to be used as *in vitro* systems to study cell cycle (Lohka and Masui, 1983). In these systems, it was possible to deplete and purify crucial cell cycle components which also allowed for more precise biochemical analysis. These approaches allowed the identification of important players in the cell cycle that were later shown to be highly conserved between eukaryotic species (recently reviewd in (Cross et al., 2011; Harashima et al., 2013)).

The techniques used to study the cell cycle and associated events remained unchanged for years. Analysis of cell cycle dynamics at single cell resolution was limited to static, fixed-tissue methods including flow cytometry (Smith et al., 2000), BrdU or thymidine incorporation, and staining for cell cycle markers such as Ki67, PCNA, or phosphor-H3 (Humbert et al., 1990; Nowakowski et al., 1989). These methods are invasive and require a lot of cell manipulation, such as cell permeabilisation, fixation with aggressive chemicals, and the use of intercalating DNA stains that prevent study of temporal dynamics. This type of approaches shows a snapshot of the cell cycle at a specific time but does not provide temporal information about cell cycle dynamics. Moreover, the majority of high throughput screens provided data for an averaged cell population where information about the variability between cells was discarded. Conversely, single cell analysis by flow cytometry or microscopy provides information about cellular heterogeneity, but does not provide insight into cell dynamics. Synchronizing the cell cycle of a population of cells allows for monitoring of dynamics, but is still an artificial approach which may not reflect true *in vivo* behaviour since cells need to be chemically perturbed. For years, the variability between cells of the same population has been overlooked – this includes the cell cycle status which might have, in many cases, contributed to variability in experimental results.

The need for more accurate, non-invasive methodology for monitoring of cell cycle dynamics in individual cells was growing in the cell cycle field. The transition from mitosis to G1-phase was easily live-monitored in cultured cells due to distinct morphological changes, however transition between G1-phase and S-phase was difficult to observe in live cells. In 1997, Cardoso and colleagues showed that DNA Ligase I fused with GFP was linked with DNA replication sites during S-phase. DNA Ligase I-GFP was shown to be a unique S-phase marker that allowed monitoring of cell cycle progression in living cells, due to its cellular redistribution during different cell cycle phases (Cardoso et al., 1997). Observation of S-phase and the transition to G2-phase in live cells with PCNA-fused GFP was described in

2000 (Leonhardt et al., 2000). PCNA fused with different fluorescent proteins was used to monitor DNA replication and repair in live cells, and was shown to be an accurate, non-toxic marker of S-phase in chimera embryos (Essers et al., 2005; Kisielewska et al., 2005; Sporbert et al., 2005). In 2005, the combination of Dnmt1 fused with GFP and DNA Ligase I fused with RFP was identified to allow for direct discrimination of all cell cycle phases in live cells (Easwaran et al., 2005). However, since 2008, the FUCCI (Fluorescent Ubiquitination-based Cell Cycle Indicator) technology revolutionised the analysis of cell cycle dynamics in single cells by live-cell imaging (Sakaue-Sawano et al., 2008a). The FUCCI system uses two components of DNA replication control machinery in higher eukaryotes that have opposing effects on DNA replication. The relative abundance of Cdt1 and Geminin proteins oscillate during the cell cycle in an inverse pattern (Arias and Walter, 2007); Cdt1 levels peak in G1-phase and decline sharply after the initiation of S-phase (Li et al., 2003; Nishitani et al., 2004). On the other hand, Geminin levels are high during S-phase and G2-phase and very low during late mitosis and G1-phase (McGarry and Kirschner, 1998).

Since its original design of a two-plasmid expression system of truncated Geminin (1-110) fused with mAG (monomeric Azami-Green) and truncated Cdt1 (30-120) fused with mKO2 (monomeric Kusabira-Orange), the FUCCI system has undergone some modifications. These include altering the fluorescent proteins attached to Geminin and Cdt1 (Sakaue-Sawano and Miyawaki, 2014; Sakaue-Sawano et al., 2008b), using a single plasmid system (Ridenour et al., 2012), inducing different cellular localisations of the Cdt1 reporter (Sakaue-Sawano et al., 2008b), and the design of new FUCCI reporters based on zebrafish, mouse and fly versions of Cdt1 and Geminin (Abe et al., 2013; Sugiyama et al., 2009; Zielke et al., 2014). In 2016, FUCCI 4 was released with the aim of enabling the observation of the four cell cycle phases in a snapshot image of a population, as well as the duration of cell cycle phases in live cell imaging (Bajar et al., 2016). The original FUCCI system has a fluorescence 'gap' in early G1-phase that generates three problems: with a fluorescence gap, it is difficult to continuously track cells; it is very difficult to distinguish non-fluorescent early G1-phase cells from non-transfected cells; due to short G1-phases in embryonic cells the fluorescence of Cdt1 was easily missed. Recently, in 2017 a new improvement of the original FUCCI, called FUCCI(CA), was released (Sakaue-Sawano et al., 2017). FUCCI(CA) fully labels G1-phase with clear distinction from neighbouring phases and allows us to distinguish between S-phase and G2-phase. This new FUCCI monitors the balance between CUL4-Ddb1 and APC-Cdh1 E3 ligase activities, as opposed to the original FUCCI that monitors the balance between SCF-Skp2 and APC-Cdh1 E3 ligase activities – now called FUCCI(SCA). Besides allowing us to measure all the different cell cycle phases, FUCCI(CA) and FUCCI(SCA) do not perturb the cell cycle regulation of the transduced cells. However, FUCCI(CA) still has some limitations – the S/G2 boundary is less distinct than the G1/S boundary, and Cdt1 signal may be misinformed in the presence of DNA damage – so it cannot fully replace FUCCI(SA) (Sakaue-Sawano et al., 2017).

In addition to the considerable improvements in methodology for measuring cell cycle dynamics, tools to study cell cycle regulation have also improved in the last few years. In 2010, Gavet and Pines developed a Cdk1 FRET-based activity sensor and found that Cdk1-cyclin B1 activation happens before NEB (Gavet and Pines, 2010). In 2013, Spencer and colleagues established a Cdk2 reporter based on the fact that Cdk2 activity levels after mitosis can predict whether a specific cell will proliferate or leave the cell cycle and enter into quiescence (Spencer et al., 2013). Live-cell reporters of p27 and Cdk2 have also shown that cell cycle bistability between G1-phase and S-phase emerges from a double-negative feedback loop between p27 and Cdk2 (Barr et al., 2016). These studies show that studying dynamics of signalling in single cells over time can allow for the discovery of new regulation networks, paving the way for exciting new discoveries that will improve our understanding of the cell cycle.

1.8. Aims and outline of this thesis

The aim of the PhD work presented in this thesis was to further understand how time controls cell division using live-cell imaging of single cells. With the revolution of cell cycle biosensors field, different sets of biosensors were designed and used to quantitatively measure the cell cycle dynamics in human cell lines with different charateristics. The main aims of this thesis were:

1. Develop quantitative tools to measure cell cycle dynamics in single cells.
2. Combine mathematical modelling with experimental measurements of cell cycle dynamics in single cells.
3. Understand the molecular mechanism keeping time of mitosis short and constant.
4. Investigate which is the molecular mechanism keeping cells away from mitosis during long hours in interphase.
5. Is the cell cycle dynamics different (or similar) in normal and cancer cells?
6. Understand the role of feedback regulation in temporal control of cell division.

These questions were answered using a combination of quantitative measurements of cell cycle dynamics in single cells and mathematical analysis to infer about regulatory mechanisms of cell cycle in cell with different characteristics – embryonic stem cells, normal cells and cancer cells.

In chapter 3 of this thesis it was unveiled that the molecular mechanism that keeps time of mitosis short, constant and uncoupled from time of interphase across different cell types is positive feedback regulation that drives cells into mitosis. The observations presented in this chapter suggest a new role for positive feedback, keeping events insulated in time.

In chapter 4 it was revealed that when free cycling cells are stimulated with a mitotic trigger not all cells responded to it. There is a refractory period of about five hours after mitosis, where cells are immune to stimuli to go into mitosis. The molecular mechanism that controls the refractory period was found to be feedback control. The feedback strength between Cdk1 and APC controls the time of refractory period in different cells. Somatic cells have a refractory period and the Cdk1:APC-Cdh1 feedback is strong, but human embryonic stem cells do have a very weak Cdk1:APC-Cdh1 feedback and no refractory period was observed. By modulating the strength of Cdk1:APC-Cdh1 feedback is possible to drive different cell division cycles.

In chapter 5 it is presented preliminary data where the cell cycle dynamics of normal and cancer cells is compared. And indeed, the cell cycle dynamics between normal and cancer cells are different which suggests that further analysis might allow to infer regulatory principles important to drive the cell cycle in different cell types and might allow the establish of hallmarks of malignancy.

Finally, in chapter 6 and 7, the three different questions are discussed and final conclusions are derived showing the implications of the new findings in deepening the current knowledge in cell cycle dynamics and controlling of time during cell division.

2. Methods

2.1. Cell Lines

A plethora of different cell lines stably expressing cell cycle biosensors were used in this thesis: normal immortalized somatic cell lines MCF10A and RPE; cancer cell lines MCF7 and RPE-HPV; Hela cancer cell line; human embryonic stem cell line H9 (hESC) and mouse embryonic stem cell line R1 (mESC). Every experiment in this thesis was carried out in at least two different cell lines. The lines used in this study are listed in table 2.1.

Table 2.1. List of all cell lines used in this thesis.

Name	Source	Cat no.	Species	Cell Type	Tissue	Disease
H9	WiCell	WA09	Human	embryonic stem cell	inner cell mass	none
HEK 293T	ATCC	CRL-3216	Human	epithelial	embryonic kidney	none
Hela	ATCC	CCL-2	Human	epithelial	cervix	adeno carcinoma
MCF10A	ATCC	CRL-10317	Human	epithelial	breast	fibrocystic disease
MCF7	ATCC	HTB-22	Human	epithelial	breast	adeno carcinoma
R1	ATCC	SCRC-1011	Mouse	embryonic stem cell	inner cell mass	none
RPE	ATCC	CRL-2302	Human	epithelial	retina	none
RPE-HPV	ATCC	CRL-2502	Human	HPV-16 transfected	retina	HPV-16 transfected

RPE is a spontaneously immortalized human epithelial cell line which evolved from a human cell line that was derived from a primary RPE culture derived by Amy Aotaki-Keen in 1986 (Dunn et al., 1996). The RPE cell line retains key characteristics of RPE – in particular, it exhibits the basic phenotype common to all epithelia-forming stable monolayers that exhibit morphological and functional polarity, and also expresses the RPE-specific markers CRALBP and RPE-65. This cell line has been widely used to identify genes and signaling pathways that regulate cell growth and differentiation (Alizadeh et al., 2001; Zhang et al., 2003). This cell line is diploid with stable 46 chromosomes (source ATCC and (Dunn et al., 1996)).

MCF10A is a non-tumorigenic human mammary epithelial cell line that arose spontaneously and was isolated in 1990 (Soule et al., 1990). Cells have an aneuploidy of 48 chromosomes (source: ATCC) and were recently shown to be a trustworthy model for normal human mammary epithelial cells (Qu et al., 2015). These cells are unable to enter into senescence because of various known molecular characteristics, which include a depletion of the chromosomal locus containing the p16 and p14ARF genes (Soule et al., 1990).

Hela cells are human epithelial cells derived from an adenocarcinoma. Hela cells contain human papilloma virus 18 (HPV-18), have low expression of p53 and normal levels of pRB (source: ATCC). Hela cells have substantial aneuploidy with an average number of 82 chromosomes (range 70 to 164, source: ATCC). Despite having been widely used to understand cell physiology, signaling, and cell cycle, due to their aberrant number of chromosomes, Hela cells may not be an ideal system to study cell growth and cell cycle progression. They were nevertheless used to be able to compare the work presented here with previous studies of mammalian cell cycle, which utilized Hela cells.

MCF7 was first isolated in 1970 and established in 1973 (Soule et al., 1973). It is a widely used breast cancer cell line (Baguley and Leung, 2011) and has been the most frequently used cancer line to produce practical knowledge for clinical applications (Sweeney et al., 2012). These cells present an extensive aneuploidy with an average number of 82 chromosomes (range 66 to 87, source ATCC).

The RPE-HPV transformed cell line was derived from the RPE cell line by transfection with DH5-HPV-16. Human papilloma virus (HPV) 16, when expressed in immortalized keratinocytes, induces formation of bi-nucleated cells which is a common characteristic of precancerous cervical lesions (Hu et al., 2009). Like the RPE line, this cell line is diploid and expresses the RPE-specific markers CRALBP and RPE-65.

H9 is a human embryonic stem cell line derived in 1998 from donated human embryos produced by *in vitro* fertilization (Thomson et al., 1998). The cell line was derived from blastocyst stage cells, so the cells are no longer totipotent but are still pluripotent and can

give rise to all somatic tissues in the body. Among the different human embryonic stem cell lines, H9 and its clonal derivatives have been the most used in published research (Guhr et al., 2006). This cell line has a normal karyotype with 46 stable chromosomes.

R1 is a mouse (*Mus musculus*) embryonic cell line derived from the inner cell mass of a male E3.5 blastocyst. This cell line is germline competent and retains the totipotency of the original cell line (Nagy et al., 1993). These cells demonstrate stable embryonic stem cell characteristics in long-term culture with 2i LIF or serum LIF culture conditions, with cell doubling times of around 15 and 13 hours respectively (Tamm et al., 2013).

With the diversity of characteristics inherent in these model cell lines, we were able to infer whether various regulatory mechanisms in cell cycle dynamics are conserved or non-conserved between different cell types.

2.1.1. Growth medium of different cell lines

All cell lines were routinely tested for mycoplasma and were cultured at 37ºC and 5%CO_2 with the corresponding growth conditions:

- MCF10A were cultured in DMEM/F12 (1:1) (Gibco) supplemented with 5% horse serum (LifeTechnologies), EGF (20ng/mL) (PeproTech EC Ltd), Hydrocortizone (0.5mg/mL) (Sigma), Cholera Toxin (100ng/mL) (Sigma), Insulin (10µg/mL) (Sigma), penicillin (100U/mL), streptomycin (100µg/mL) and glutamine (4mM) (Invitrogen).
- MCF7 were cultured in MEM (Gibco) supplemented with 10% fetal bovine serum (Gibco), 1% non-essential amino acids (Gibco), 1% sodium pyruvate (Gibco), penicillin (100U/mL), streptomycin (100µg/mL) and glutamine (4mM) (Invitrogen).
- RPE and RPE-HPV were cultured in DMEM/F12 (1:1) (Gibco) supplemented with 10% fetal bovine serum (Gibco), penicillin (100U/mL), streptomycin (100µg/mL) and glutamine (4mM) (Invitrogen).
- Hela and HEK 293T were cultured in DMEM (Gibco) supplemented with 10% fetal bovine serum (Gibco), penicillin (100U/mL), streptomycin (100µg/mL) and glutamine (4mM) (Invitrogen).
- H9 (hESC) were cultured on matrigel(Corning)-coated plates using mTeSR1 medium (StemCell Technologies) supplemented with penicillin (100U/mL) and streptomycin (100µg/mL). BMP4 was used at a concentration of 50ng/mL for 3 days, in order to differentiate hESC towards a mesoderm lineage.

- R1 (mESC) were cultured on gelatin-coated dishes in Knockout™ MEM (Life Technologies), 10% FBS (Gibco), 2-Mercaptoethanol (50μM), MEM non-essential amino acids and LIF recombinant mouse protein (10ng/ml).

2.1.2. Maintaining, freezing and thawing cell lines

2.1.2.1. Somatic and cancer cell lines

Cells in culture were routinely split 1:5 every 2-3 days. Confluent cells were washed with PBS and detached by incubating for 1 minute with trypsin. To freeze cells, fresh media was added to the cells and then they were centrifuged at 1000 rpm for 5 minutes. The pellet was carefully re-suspended in 1mL of "freezing medium" corresponding to each cell line:

- MCF10A: 10% DMSO and 20% horse serum in complete growth media
- MCF7: 5% DMSO in complete growth media
- RPE and RPE-HPV: 5% DMSO in complete growth media
- Hela: 5% DMSO in complete growth media

The cell suspension was then transferred to a cryotube vial and kept at -80ºC using a freezing box filled with isopropanol. After 24 hours, the cryotube vial was transferred to a liquid nitrogen tank and stored for future use. To thaw cells, a frozen vial kept in liquid nitrogen was incubated in a water bath at 37ºC for a maximum of 2 minutes. Immediately after thawing the cell suspension was transferred into a culture dish containing growth medium. The medium was substituted next day after complete attachment of the cells in order to remove any DMSO that might have remained in the medium.

2.1.2.2. Human embryonic stem cells (hESC)

H9 human embryonic stem cells were routinely cultured in feeder-free conditions on matrigel (BD Biosciences) coated plates (usually 6-well plates). Cells were cultured using mTeSR1 (Stem Cell Technologies) and split 1:2 or 1:3 every 3-4 days. Cultures with a confluency of 80-90% were washed with PBS and incubated with gentle dissociation buffer (Stem Cell Technologies) for a maximum of 3 minutes at room temperature. The dissociation buffer was then carefully aspirated and fresh mTeSR1 medium was added to the cells. The

cells were gently dislodged with the help of a cell lifter and transferred to a new well as small colonies.

hESC were frozen with mFreSR (Stem Cell Technologies). Firstly, cells were washed twice with PBS and then 1mL of mTeSR1 was added to each well. Cells were then gently scraped with a cell lifter, taking care to break up colonies as little as possible. The suspension was then centrifuged at 1000 rpm for 5 minutes. The pellet was re-suspended in 1mL of mFreSR, added to the tube drop-wise. The mixture was then transferred to a cryotube and quickly placed into an isopropanol-containing freezing box, which was kept at -80ºC for a maximum of 24 hours after which the cryotubes were transferred and stored in a liquid nitrogen tank. To thaw hESC, a frozen vial was placed in the water bath at 37ºC for no more than 2 minutes. The suspension was transferred to a 15mL tube and 2mL of fresh mTeSR1 was added drop-wise. Cells were centrifuged at 1000 rpm for 5 minutes, and then the pellet was re-suspended very gently in 1mL of mTeSR1 and plated onto a matrigel-coated dish.

2.1.2.3. Mouse embryonic stem cells (mESC)

Mouse embryonic cells were routinely cultured in feeder-free conditions on gelatine, and split 1:5 every 2-3 days. Confluent cells were washed with PBS and detached by incubating for 1 minute with trypsin at 37ºC. To freeze cells, fresh media was added to the cells and then they were centrifuged at 1000 rpm for 5 minutes. The pellet was carefully re-suspended in 1mL of cold Freeze mix (90%FBS and 10%DMSO) and transferred to a cryotube vial and kept at -80ºC using a freezing box filled with isopropanol. After 24 hours, the cryotube vial was transferred to liquid nitrogen tank and stored for future use. To thaw cells, a frozen vial kept in liquid nitrogen was placed in the water bath at 37ºC for 1-2 minutes. The suspension was transferred to a 15mL tube and 2mL of fresh culture media was added drop-wise. Cells were centrifuged at 1000 rpm for 5 minutes and then the pellet was re-suspended very gently in 1mL of mTeSR1 and plated onto a gelatine-coated dish.

2.2. Biosensors, shRNA, cell transfection and establishment of stable cell lines

Lentiviral infection was used to make stable lines expressing cell cycle biosensors, and transient transfection of some DNA constructs was used to perturb mitotic entry. All the different constructs used in this study are listed in table 2.2.

Table 2.2. DNA constructs used in this thesis.

Biosensor	Vector	Template/Gene	Label/Tag	Source
Cdt1-venus	pCSII-EF1α	Cdt1 (Fucci) (Sakaue-Sawano et al., 2008a)	Venus	QCB Lab
Cdt1-mCherry	pCSII-EF1α	Cdt1 (Fucci) (Sakaue-Sawano et al., 2008a)	mCherry	QCB Lab
PCNA-mCherry	pCSII-EF1α	PCNA (Sporbert et al., 2005)	mCherry	QCB Lab
Dmnt1-CFP	pCSII-EF1α	DNA Dnmt1 (Easwaran et al., 2005)	CFP	This thesis
DNA-Ligase-YFP	pCSII-EF1α	DNA ligase (Easwaran et al., 2005)	YFP	This thesis
H2B-mCherry	pCSII-EF1α	H2B (Santos et al., 2012)	mCherry	QCB Lab
H2B-Turquoise	pCSII-EF1α	H2B (Santos et al., 2012)	Turquoise	QCB Lab
NLS-mCherry	pCSII-EF1α	FKBP2 (Santos et al., 2012)	mCherry	QCB Lab
CyclinB1-YFP	pCSII-EF1α	CyclinB1 (Santos et al., 2012)	YFP	QCB Lab
Cdk1-WT	pEGFP-C1	Cdk1 (Santos et al., 2012)	mCherry	QCB Lab
Cdk1AF-mCherry	pTRE-tight	Cdk1AF (Santos et al., 2012)	mCherry	QCB Lab
Cdc25-WT	pmCherry-C1	Cdc25 (Santos et al., 2012)	mCherry	QCB Lab
Cdc25-CD (C377S)	pmCherry-C1	Cdc25 (Santos et al., 2012)	mCherry	QCB Lab
iCFP-Fzr1	pLVX-TetOne-Puro	Cdh1/Fzr1	Cerulean	This thesis

2.2.1. Transient transfection of cells

cDNA of inducible Cdk1AF-mCherry and its control Cdk1-wt as well as Cdc25C-CD and its control Cdc25-wt were cloned into correspondent lentiviral vector and used to transiently transfect Hela and MCF10A cells. Hela cells were transiently transfected using the cDNA of interest and Fugene6 (Roche) according to the manufacturer's instruction. Electroporation was used to transiently transfect MCF10A using the Neon Transfection System by two electroporation pulses of 25ms each set at 1150V.

2.2.2. Lentiviral production for lentiviral based infections

The DNA sequence of interest was cloned into the lentiviral vector pCSII-EF1α and lentivirus production was carried out in HEK 293T cells. Lentivirus assembly vectors (PAX2 and VSV-G), Polyethylenimine (PEI) and the pCSII-EF1α expression vector were mixed in Optimem and the reaction incubated for 30 minutes at room temperature (PEI (μg):DNA/PAX2/VSVG (μg) ratio should be 3 : 1, DNA: PAX2 viral packaging : VSV-G viral envelope ratio should be 5 : 2 : 1). The mixture was then added drop-wise to HEK 293T cells with 6mL of normal growth media (identical to media used for culturing Hela cells) and the cells were allowed to incubate for 48 hours. Virus-containing media was collected twice - 48 and 72 hours after transfection - to get a good titre of virus. To collect virus, media was removed from HEK 293T cells and spun down at 2400 rpm for 5 minutes. The virus-containing supernatant was aliquoted in 1mL vials and snap-frozen using liquid nitrogen before storage at -80ºC.

2.2.3. Lenti-viral based infection of cells

H9, Hela, MCF10A, MCF7, RPE, RPE-HPV and R1 cells were infected overnight using a range of 8-12μg of polybrene per mL of virus-containing media used. The next morning, cells were washed with PBS twice and fresh media was added to the cells. After three to four days of infection, cells were either sorted for the lowest expression levels to avoid artefacts of overexpression, using Becton Dickinson FACS Aria III or selected using antibiotics.

Cells transduced with constructs that contained a puromycin selection cassette were selected with this antibiotic. All cells lines were selected with 2μg/mL of puromycin, with the exception of MCF10A which was selected with a concentration of 10μg/mL, and H9 which was selected with a concentration of 1μg/mL.

Inducible expression constructs were activated using doxycycline at a concentration of 1μg/mL in Hela and MCF10A cells and a range of 1-10μg/mL in H9 cells.

2.2.4. Fluorescence Activating Cell Sorting (FACS)

To prepare cells for FACS, cells were detached with trypsin or gentle dissociation buffer (only used for H9) and added to 3mL of media. The suspension was centrifuged at 1000 rpm for 5 minutes. The pellet of Hela, MCF10A, MCF7, RPE, RPE-HPV or R1 cells was then re-suspended in 1mL of cold PBS with 1%BSA and the suspension was filtered using a 75μm cell strainer. The pellet of H9 cells was re-suspended in 1mL of room temperature PBS with 1%BSA and the suspension was filtered using a 40μm cell strainer. After FACS, cells were centrifuged at 1000 rpm for 5 minutes and the pellet re-suspended in fresh media and plated in the corresponding culture dish. ROCK inhibitor (Sigma Y-27632) at a concentration 10μM was added to H9 cells at the same time of plating to help attachment.

2.2.5. shRNAs used in this study

All the shRNA clones in this study are from GIPZ Lentiviral shRNA Pool (Dharmacon, Thermo Scientific) and are listed in Table 2.3. The shRNA clones were transfected into HEK 293T cells to produce virus, which were then used to transduce MCF10, RPE and Hela cells. Transduced cells were selected with puromycin.

To build stable MCF10A, RPE and Hela cell lines with impaired spindle assembly checkpoint, a set of two shRNA specific to Mad2 were used. shRNAs were also used to decrease the expression levels of Cdh1 in MCF10A, RPE and Hela cells. MCF10A stable lines with decreased expression levels of PP1A, PP1B, PP1C and PP2A were also made. A pool of four different clones expressing shRNAs specific for each PP1 gene were used, and a pool of three different shRNA sequences were used to downregulate PP2A. shEmpty Vector and shScramble vectors were used as controls for experiments using shMad2, shCdh1 and shPP.

Table 2.3. shRNA used to downregulate cell cycle genes.

Gene	Clone/Cat no.	Sequence 5′→3′
Cdh1	V3LHS_637363	TGCTGTTGACAGTGAGCGAAGGGAAGAAGCTGTCCATGTTTAGTGAAGC CACAGATGTAAACATGGACAGCTTCTTCCCTGTGCCTACTGCCTCGGA
	V3LHS_637367	TGCTGTTGACAGTGAGCGAACGGCTACTCACAGAACCAGATAGTGAAGC CACAGATGTATCTGGTTCTGTGAGTAGCCGTGTGCCTACTGCCTCGGA
Mad2	V3LHS_327851	TGCTGTTGACAGTGAGCGCCTGGTTGTAGTTATCTCAAATTAGTGAAGCC ACAGATGTAATTTGAGATAACTACAACCAGTTGCCTACTGCCTCGGA
	V3LHS_403761	TGCTGTTGACAGTGAGCGCATGGATATTTGTACTGTTTAATAGTGAAGCC ACAGATGTATTAAACAGTACAAATATCCATTTGCCTACTGCCTCGGA
PP1A	V2LHS_262414	TGCTGTTGACAGTGAGCGACGCATCTATGGTTTCTACGATTAGTGAAGCC ACAGATGTAATCGTAGAAACCATAGATGCGGTGCCTACTGCCTCGGA
	V3LHS_635636	TGCTGTTGACAGTGAGCGACGCGGCCATAGTGGACGAAAATAGTGAAGC CACAGATGTATTTTCGTCCACTATGGCCGCGATGCCTACTGCCTCGGA
	V3LHS_635634	TGCTGTTGACAGTGAGCGACGCGGCCATAGTGGACGAAAATAGTGAAGC CACAGATGTATTTTCGTCCACTATGGCCGCGATGCCTACTGCCTCGGA
	V3LHS_635635	TGCTGTTGACAGTGAGCGACAGCGAGAAGCTCAACCTGGATAGTGAAGC CACAGATGTATCCAGGTTGAGCTTCTCGCTGTTGCCTACTGCCTCGGA
PP1B	V3LHS_393264	TGCTGTTGACAGTGAGCGAATGAATGCAAACGAAGATTTATAGTGAAGC CACAGATGTATAAATCTTCGTTTGCATTCATCTGCCTACTGCCTCGGA
	V3LHS_413510	TGCTGTTGACAGTGAGCGCAAGGACATACTTCATAATATATAGTGAAGCC ACAGATGTATATATTATGAAGTATGTCCTTATGCCTACTGCCTCGGA
	V3LHS_393266	TGCTGTTGACAGTGAGCGATACGAGGATGTCGTCCAGGAATAGTGAAGC CACAGATGTATTCCTGGACGACATCCTCGTACTGCCTACTGCCTCGGA
	V3LHS_393263	TGCTGTTGACAGTGAGCGACAGGAAAGATTGTGCAGATGATAGTGAAGC CACAGATGTATCATCTGCACAATCTTTCCTGGTGCCTACTGCCTCGGA
PP1C	V3LHS_395264	TGCTGTTGACAGTGAGCGCAAGCATGATTTGGATCTTATATAGTGAAGCC ACAGATGTATATAAGATCCAAATCATGCTTATGCCTACTGCCTCGGA
	V3LHS_395262	TGCTGTTGACAGTGAGCGAATGAGTGTGGATGAAACACTATAGTGAAGC CACAGATGTATAGTGTTTCATCCACACTCATCTGCCTACTGCCTCGGA
	V3LHS_395266	TGCTGTTGACAGTGAGCGAGTGGTTGAAGATGGATATGAATAGTGAAGC CACAGATGTATTCATATCCATCTTCAACCACCTGCCTACTGCCTCGGA
	V2LHS_170308	TGCTGTTGACAGTGAGCGCCCAGCTTCAGGAGAATGAAATTAGTGAAGC CACAGATGTAATTTCATTCTCCTGAAGCTGGATGCCTACTGCCTCGGA
PP2A	V3LHS_403290	TGCTGTTGACAGTGAGCGCCAGGAAATGATTGGAATAGAATAGTGAAGC CACAGATGTATTCTATTCCAATCATTTCCTGTTGCCTACTGCCTCGGA
	V3LHS_403288	TGCTGTTGACAGTGAGCGCGAGGTTGTCTGTAGTATTTAATAGTGAAGCC ACAGATGTATTAAATACTACAGACAACCTCATGCCTACTGCCTCGGA
	V3LHS_324709	TGCTGTTGACAGTGAGCGACAGGGACTACTTGACCGTCAATAGTGAAGC CACAGATGTATTGACGGTCAAGTAGTCCCTGGTGCCTACTGCCTCGGA
Scramble	—	TGCTGTTGACAGTGAGCGATCTCGCTTGGGCGAGAGTAAGTAGTGAAGC CACAGATGTACTTACTCTCGCCCAAGCGAGAGTGCCTACTGCCTC GGA

2.2.6. Stable cell lines made in this study

Stable H9, Hela, MCF10A, MCF7, RPE, RPE-HPV and R1 cell lines were made with different sets of sensors and shRNA expression constructs in order to perform all the experiments presented in this study. The list of all the cell lines used and made can be accessed in Table 2.4.

Table 2.4. Stable cell lines made and used in this thesis.

Cell Line	Biosensors
RPE	Cdt1-mCherry, H2B-YFP
	Cdt1-mCherry, H2B-YFP, shCdh1-GFP
	Cdt1-mCherry, H2B-YFP, shScramble-GFP
	Cdt1-venus, H2B-Turquoise, PCNA-mCherry
	CyclinB1-YFP, H2B-Turquoise
	CyclinB1-YFP, H2B-Turquoise, NLS-mCherry
	Dnmt1-CFP, DNA-ligase-YFP, H2B-mCherry
	NLS-mCherry
	NLS-mCherry, shCdh1-GFP
	NLS-mCherry, shEmptyVector-GFP
	NLS-mCherry, shMad2-GFP
	NLS-mCherry, shScramble-GFP
	PCNA-mCherry, shEmptyVector-GFP
	PCNA-mCherry, shMad2-GFP
	PCNA-mCherry, shScramble-GFP
MCF10A	Cdt1-mCherry, H2B-YFP
	Cdt1-mCherry, H2B-YFP, shCdh1-GFP
	Cdt1-mCherry, H2B-YFP, shScramble-GFP
	Cdt1-venus, H2B-Turquoise, PCNA-mCherry
	CyclinB1-YFP, H2B-CFP
	CyclinB1-YFP, H2B-Turquoise, NLS-mCherry
	Dnmt1-CFP, DNA-ligase-YFP, H2B-mCherry
	NLS-mCherry
	NLS-mCherry, shCdh1-GFP
	NLS-mCherry, shEmptyVector-GFP
	NLS-mCherry, shMad2-GFP
	NLS-mCherry, shPP1A-GFP
	NLS-mCherry, shPP1A-GFP, shPP1B-GFP
	NLS-mCherry, shPP1A-GFP, shPP1B-GFP, shPP1C-GFP
	NLS-mCherry, shPP1B-GFP
	NLS-mCherry, shPP1C-GFP
	NLS-mCherry, shPP2A-GFP
	NLS-mCherry, shScramble-GFP
	PCNA-mCherry, shEmptyVector-GFP
	PCNA-mCherry, shMad2-GFP
	PCNA-mCherry, shScramble-GFP
Hela	Cdt1-mCherry, H2B-YFP
	Cdt1-mCherry, H2B-YFP, shCdh1-GFP
	Cdt1-mCherry, H2B-YFP, shScramble-GFP
	Cdt1-venus, H2B-Turquoise, PCNA-mCherry
	CyclinB1-YFP, H2B-CFP
	CyclinB1-YFP, H2B-Turquoise, NLS-mCherry
	Dnmt1-CFP, DNA-ligase-YFP, H2B-mCherry
	NLS-mCherry
	NLS-mCherry, shCdh1-GFP

	NLS-mCherry, shEmptyVector-GFP
	NLS-mCherry, shMad2-GFP
	NLS-mCherry, shScramble-GFP
	PCNA-mCherry, shEmptyVector-GFP
	PCNA-mCherry, shMad2-GFP
	PCNA-mCherry, shScramble-GFP
MCF7	Cdt1-venus, H2B-Turquoise, PCNA-mCherry
	Dnmt1-CFP, DNA-ligase-YFP, H2B-mCherry
	NLS-mCherry
RPE-HPV	Cdt1-venus, H2B-Turquoise, PCNA-mCherry
	Dnmt1-CFP, DNA-ligase-YFP, H2B-mCherry
	NLS-mCherry
H9	Cdt1-venus, NLS-mCherry
	Cdt1-venus, NLS-mCherry, iCdh1-Cerulean
R1	H2B-GFP

2.3. Inhibitors and small molecules

In this study, a variety of inhibitors were used to perturb the normal cell cycle dynamics including mitotic entry, progression through mitosis, mitotic exit, and nuclear export (Table 2.5).

Table 2.5. Inhibitors and small molecules used in this thesis.

Name	Source	Cat no.	Concentration	Use
BMP4	Life Technologies	PHC9534	50ng/mL	Differentiation of hESC
Doxycycline	Sigma	D9891	1-10μg/mL	Induction of constructs
EdU	Thermo Fisher	A10044	10μM/mL	Measure de novo DNA synthesis
Leptomycin B	Sigma	L2913	100ng/mL	Blocking of nuclear export
Puromycin	Thermo Fisher	A1113803	1-10μg/mL	Selection of transduced cells
Reversine	Sigma	R3904	1μM/mL	Inhibition of Spindle Assembly Checkpoint
Tautomycin	Enzo Life Sciences	ALX-380-041-C025	10μM/mL	Inhibition of PP1
Wee1 Inhibitor	Sigma	PD166285	0.5-2μM/mL	Inhibition of Wee1 and Myt1

2.4. Microscopy

2.4.1. Live cell imaging

Live cell imaging was performed on either the ScanR, a fully motorized and automated inverted epifluorescence microscope system IX83 (Olympus) combined with CellVivo (Olympus), or on an IncuCyte Zoom (Essen BioScience), both of which are equipped with temperature, humidity, and CO_2 controls maintain integrity of the sample.

ScanR images were typically acquired with a 20x plan (UCPLFLN) fluorescence objective (NA 0.7) and a sCMOS (Orca Flash 4.0, Hamamatsu) camera. LED-based illumination (SpectraX LED, Lumenco) was used for excitation. Excitation (ex) and emission (em) filters were as follows: DAPI ex: 391/20nm, em: 440/521/607/700nm; CFP ex: 438/24nm, em: 460-510nm, GFP/Alexa-488 ex: 474/27nm, em: 440/521/607/700nm; YFP ex: 509/22nm, em: 515-560nm, mCherry ex: 554/23nm, em: 440/521/607/700nm and Alexa-647 ex: 650/13nm, em: 690/50nm. IncuCyte Zoom images were acquired with a 20x plan fluorescence objectives and a CCD camera. Fluorescence excitation (ex) and emission (em) filters were as follows: Green channel ex: 440-480nm, em: 504-544nm; Red channel ex: 565-605nm, em: 625-705nm.

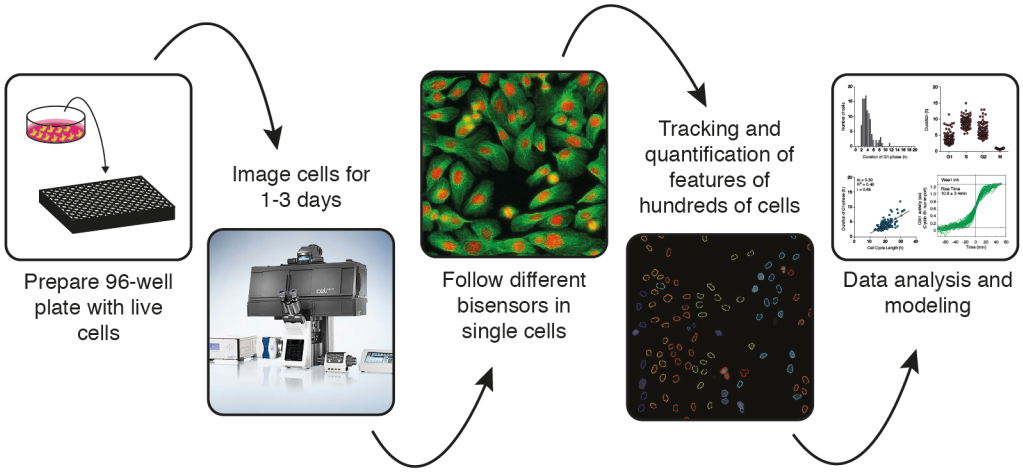


Figure 2.1. Pipeline for the quantitative analysis of live-cell imaging experiments used in this study. Seed cells in a 96-well plate 24 hours before starting the experiment. Image the cells for at least two consecutive division cycles in order to follow different biosensors and measure cell cycle dynamics using either manual or automatic image analysis to track and quantify features of hundreds of cells and perform statistical analysis.

For live cell imaging experiments, cells were plated at different confluencies in 96-well plates (Greiner Bio-One Ltd) or 96-well IncuCyte ImageLock plates on the day before the experiment, to avoid induced synchronicity of the cell cycle after splitting. A typical experiment to follow cell cycle dynamics would monitor cells from 48 to 72 hours with images taken every 10 minutes (Figure 2.1.). In experiments where the temperature was changed, cells were imaged for 16 hours at 37ºC after which the temperature was shift to either 34ºC or 40ºC for further 48 hours. To test the effect of frame frequency in mitosis duration measurements, cells were imaged every 2, 5 and 10 minutes for 24 hours.

In experiments where positive feedback at mitotic entry was perturbed using a Wee1 inhibitor only and DMSO as control, cells were imaged for 5 hours after adding the inhibitor with images taken every 3-5 minutes. When other inhibitors were combined in the same experiment – Reversine or Leptomycin B – cells were incubated for 30 minutes with these inhibitors before adding Wee1 inhibitor.

Tautomycin was added to cells 1 hour before starting the imaging. Cells were imaged for 5 hours after adding tautomycin with images taken every 4 minutes.

2.4.2. Immunofluorescence

Cells were washed twice with PBS before being fixed using 4% paraformaldehyde in PBS for 10 minutes at room temperature or 100% methanol for 15 minutes at -20ºC. Cells were washed 3 times for 5 minutes with PBS before permeabilization. PBS with 0.3% Triton X-100 at room temperature was used to permeabilize the cells for 10 minutes. Cells were then washed 3 times with PBS and incubated with blocking buffer containing 10% fetal bovine serum and 3% bovine serum albumin in PBS for 1 hour at room temperature. Cells were incubated with primary antibodies (listed in Table 2.6) at 4ºC overnight in blocking buffer. After being washed 3 times with 0.3% Tween in PBS, cells were incubated with secondary antibodies in blocking buffer for 1 hour at room temperature. Nuclei were stained using DAPI 0.5μg/mL. After staining, cells were imaged in ScanR using DAPI channel (ex: 391/20nm, em: 440/521/607/700nm), GFP/Alexa-488 channel (ex: 474/27nm, em: 440/521/607/700nm) and Alexa-647 channel (ex: 650/13nm, em: 690/50nm).

Table 2.6: List of primary and secondary antibodies used. *Fixation with Methanol

Primary Antibodies				
Name	**Source**	**Cat no.**	**Species**	**Dilution**
cdc2 (POF1)	CST	9116	Mouse	1:50
Cdc6 (pS54)	ABCAM	ab75809	Rabbit	1:100
Cdk2	ABCAM	ab32147	Rabbit	1:200
Cdt1	ABCAM	ab202067	Rabbit	1:100
Cyclin A	Santa Cruz	sc-751	Rabbit	1:100
Cyclin B1 (GNS1)*	Santa Cruz	sc-245	Mouse	1:100
Cyclin D1	Santa Cruz	sc-20044	Mouse	1:50
Cyclin E1	Santa Cruz	sc-247	Mouse	1:50
Cyclin E1 (pT77)	ABCAM	ab124696	Rabbit	1:100
Cyclin E2	ABCAM	ab40890	Rabbit	1:100
CyclinD1 (pT286)	CST	3300	Rabbit	1:2000
E2F1	ABCAM	ab179445	Rabbit	1:100
E2F1 (pS337)*	Santa Cruz	sc-130188	Rabbit	1:50
Emi1	Santa Cruz	sc-365212	Mouse	1:50
FZR1 (Cdh1)*	ABCAM	ab89535	Mouse	1:100
MAD2	BD-Biosciences	610678	Mouse	1:100
p21	CST	2947	Rabbit	1:200
p21 (pT145)	ABCAM	ab47300	Rabbit	1:500
p27 Kip1	CST	3686	Rabbit	1:1600
p27 Kip1 (pT187)*	ABCAM	ab75908	Rabbit	1:50
PP1*	Santa Cruz	sc-7482	Mouse	1:50
PP2A B subunit	CST	2290	Rabbit	1:50
Rb (pS780)	CST	8180T	Rabbit	1:400
Rb (pS807/811)	CST	8516	Rabbit	1:1600
Secondary Antibodies				
Name	**Source**	**Cat no.**	**Dye**	**Dilution**
Goat anti-mouse IgG	Life Technologies	A11001	Alexa 488	1:200
Goat anti-rabbit IgG	Life Technologies	A11008	Alexa 488	1:200
Goat anti-mouse IgG	Life Technologies	A21235	Alexa 647	1:200
Goat anti-rabbit IgG	Life Technologies	A21244	Alexa 647	1:200

2.4.3. EdU labelling and detection

EdU was added to cells at a concentration of 10μL/mL and cells were imaged in ScanR for 5 hours with images taken every 4 minutes. Cells were then washed twice with PBS before being fixed using 4% paraformaldehyde in PBS for 15 minutes at room temperature. Cells were washed 3 times with before permeabilization using PBS with 0.1% Triton X-100 for 15 minutes at room temperature. Cells were then washed 3 times with PBS and incubated with a reaction cocktail containing Tris pH 8.5 100nM and 50mM ascorbic acid, 4% CuSO4, 0.25% Pacific Blue Alexa and 10% of Buffer Additive for 30 minutes at room temperature to detect EdU. After removing the reaction cocktail, cells were washed once with 0.3% Tween in PBS for 10 minutes and 2 times with PBS for 5 minutes each. Cells were then re-imaged in ScanR using DAPI channel (ex: 391/20nm, em: 440/521/607/700nm).

2.5. Data analysis

2.5.1. Software and statistical analysis used

Automated-image analysis was done with scripts written in Matlab (Mathworks), Fiji (NIH) and ScanR Analysis software or Cell Profiler (Figure 2.1). It was not assumed that the data would follow a normal distribution, so Mann-Whitney and Kolmogrov-Smirnov tests were used to estimate p values and were calculated in Prism7. Trend lines (m), coefficient of determination (R^2), Pearson correlation coefficient (r) were calculated using Prism7 and Excel. Mean absolute deviations (MAD) were calculated at http://www.alcula.com/ calculators/statistics/ mean-absolute-deviation.

2.5.2. Analysis of cell cycle dynamics

In order to measure cell cycle dynamics in single cells, stable MCF10A, RPE, MCF7, RPE-HPV and Hela cell lines were made with two different sets of sensors in order to ensure that artefacts were not being measured, at least two biosensors were used at the same time to measure dynamics of each cell cycle phase. In this way, measuring the length of each cell cycle phase relies on different reports and it is possible to have a more accurate measurement. The cells were imaged for 48 to 72 hours in order to follow two consecutive divisions and analysed manually with Fiji software. A set of sensors was also developed to measure Cdk1 activity and monitor dynamics of mitosis.

2.5.2.1. Measuring cell cycle dynamics usign Cdt1-venus, H2B-Turquoise, PCNA-mCherry sensors

A truncated Cdt1 (30-120aa) was used to measure G1-phase length (Sakaue-Sawano et al., 2008a). Cdt1 is expressed during G1-phase and is quickly degraded at the G1/S phase transition. At the beginning of S phase PCNA starts to speckle and the speckles disappear at the beginning of G2 phase (Sporbert et al., 2005). When nuclear envelope breaks down (NEB), PCNA goes to the cytoplasm and the chromosomes are marked with H2B. H2B is used to facilitate automatic tracking of cells (Figure 2.2). The appearance and disappearance of PCNA speckles measurements are fairly subjective, but the same criteria were used for all the experiments shown in this thesis.

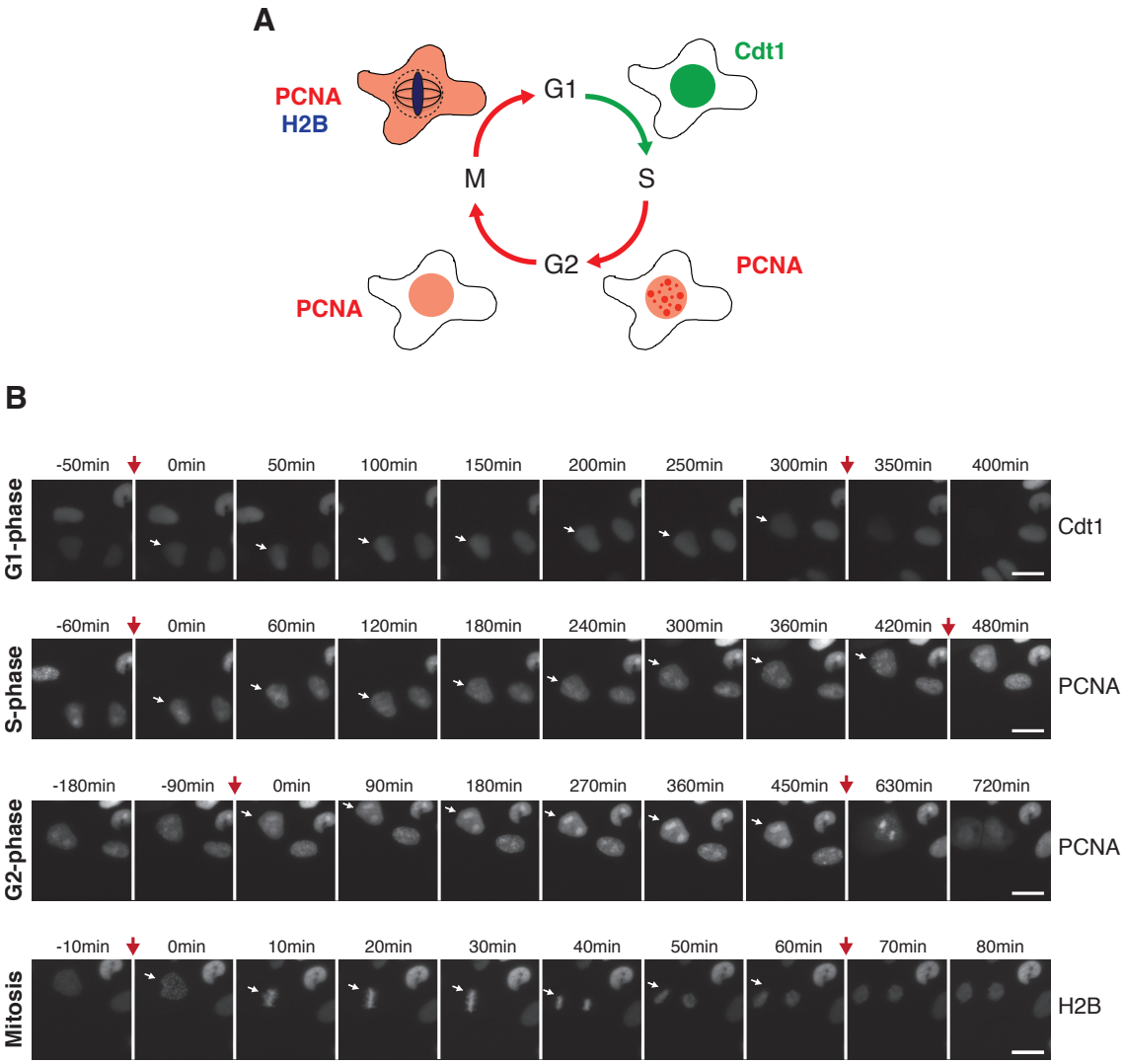


Figure 2.2. Cell cycle dynamics measured in MCF10A with the biosensors Cdt1-venus, H2B-Turquoise, PCNA-mCherry. A. Schematic of the appearance of the different biosensors proteins during cell cycle and the correspondent colour. **B.** Representative images showing how G1-, S-, G2-phase and Mitosis dynamics were measured in single cells with cell cycle biosensors. Red arrows mark the beginning and the end of the different phases. White arrows mark the cell that was followed. Scale bar 10μm.

2.5.2.2. Measuring cell cycle dynamics using Dnmt1-CFP, DNA Ligase-YFP and H2B-mCherry sensors

Dnmt1 and DNA Ligase have a nuclear localization during G1-phase and they start to speckle during S phase (Easwaran et al., 2005). When cells transit to G2-phase, DNA ligase stops speckling and Dnmt1 continues to speckle till the end of G2-phase. With nuclear envelope break down in the beginning of mitosis, Dnmt1 and DNA ligase go to the cytoplasm and the chromosomes are marked with H2B. H2B is also used to facilitate automatic tracking of cells (Figure 2.3).

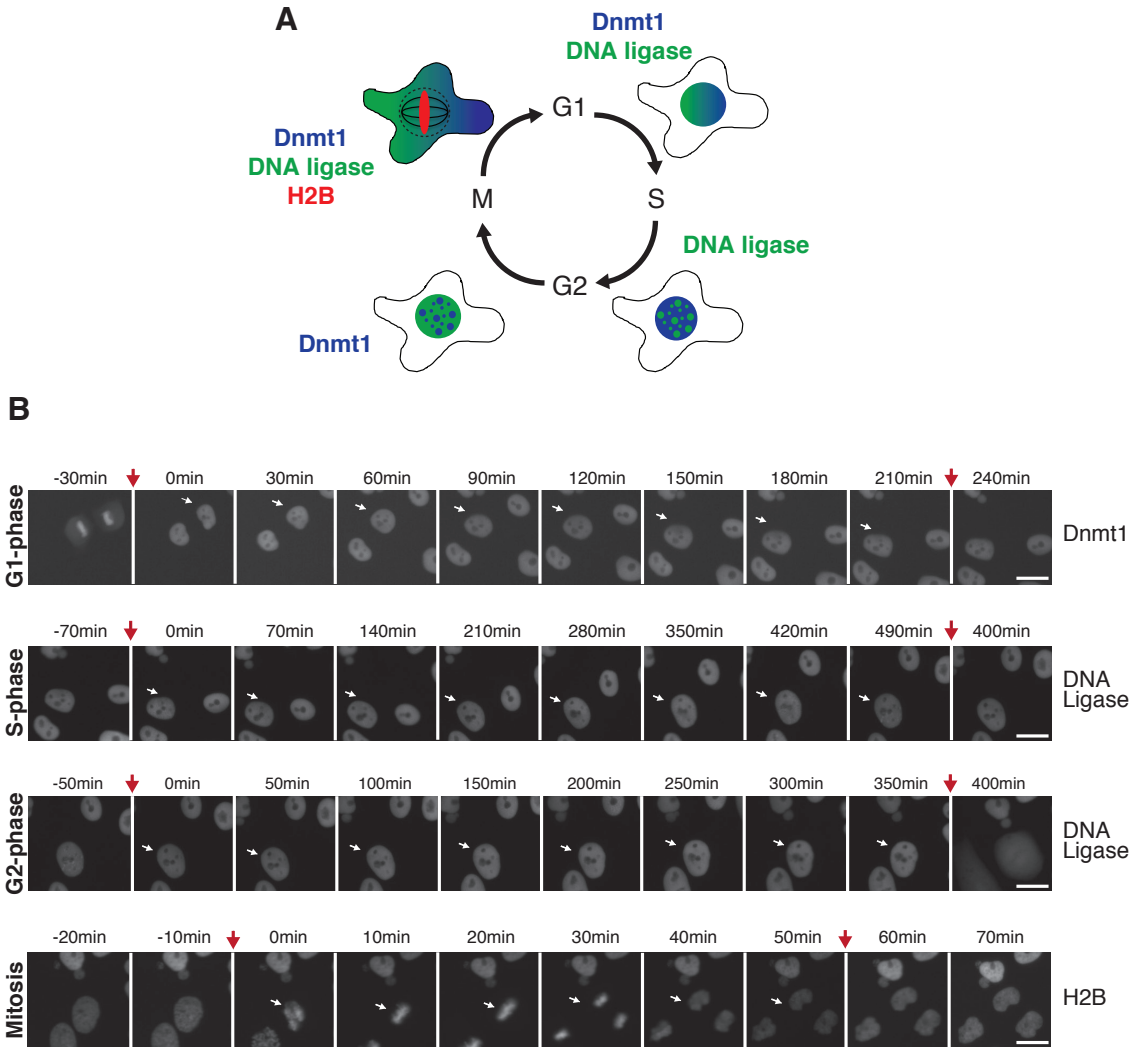


Figure 2.3. Cell cycle dynamics measured in MCF10A with the biosensors Dnmt1-CFP, DNA-ligase-YFP and H2B-mCherry. A. Schematic of the appearance of the different biosensors proteins during cell cycle and the correspondent colour. **B.** Representative images showing how G1-, S-, G2-phase and Mitosis dynamics were measured in single cells with cell cycle biosensors. Red arrows mark the beginning and the end of the different phases. White arrows mark the cell that was followed. Scale bar 10μm.

2.5.2.3. Measuring dynamics of mitosis and Cdk1 activity using Cyclin B1-YFP, H2B-Turquoise, NLS-mCherry sensors

To measure Cdk1 activity and duration of mitosis, another combination of biosensors was used in MCF10A, RPE, and Hela cell lines composed of cyclinB1-YFP, H2B-CFP and NLS-mCherry (Figure 2.4.A). H2B is used to facilitate automatic tracking of cells. Cdk1 activity was measured by measuring changes in CyclinB1 localization.

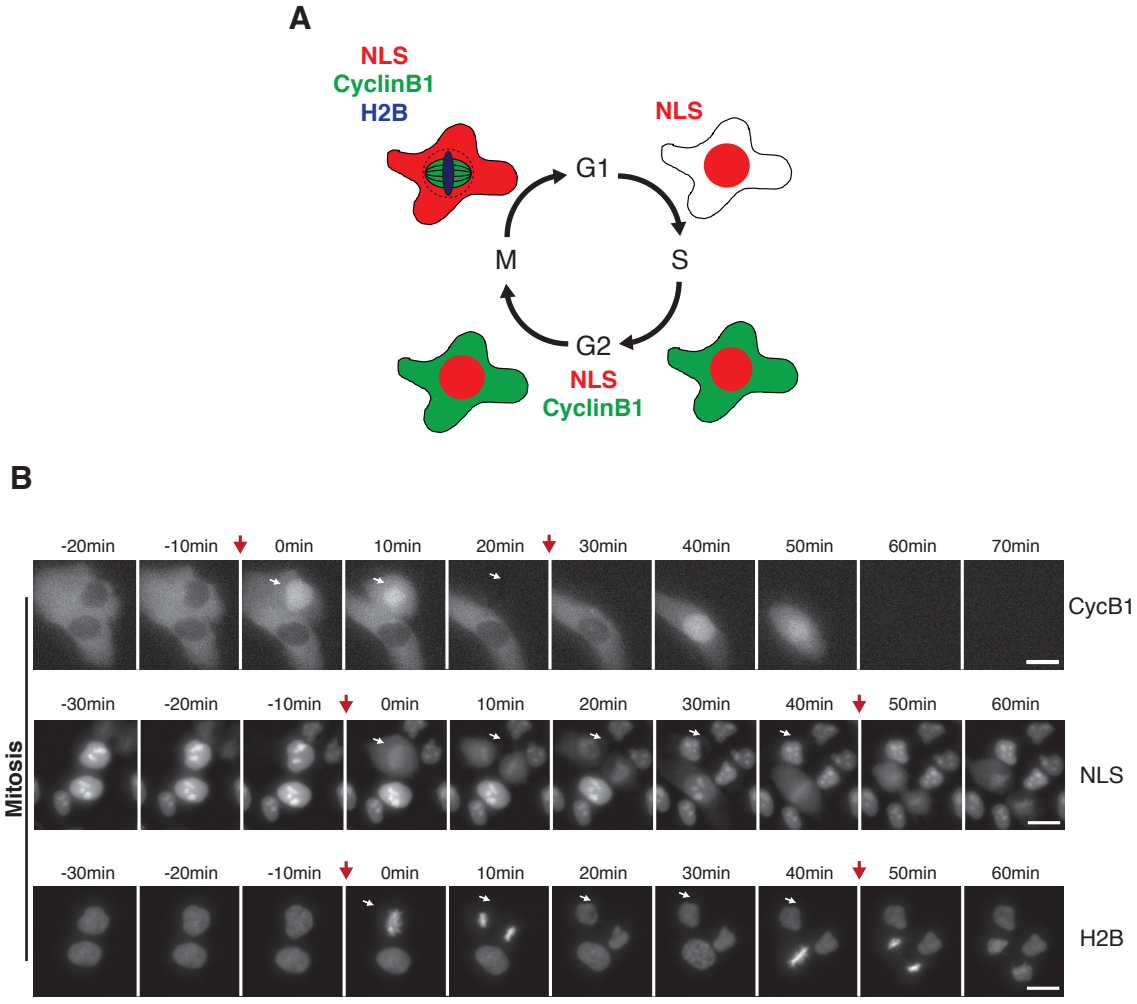


Figure 2.4. Mitosis dynamics measured in MCF10A with the biosensors Cyclin B1-YFP, H2B-Turquoise, NLS-mCherry. A. Schematic of the appearance of the different biosensors proteins during cell cycle and the correspondent colour. **B.** Representative images showing how duration of mitosis was measure using CyclinB1, NLS and H2B biosensors. Red arrows mark the beginning and the end of the mitosis measured with the different biosensors. White arrows mark the cell that was followed. Scale bar 10μm.

When Cdk1 is inactive, CyclinB1 is in the cytoplasm and when the Cdk1 becomes active at onset of mitosis, CyclinB1 migrates to the nucleus (Santos et al., 2012). Therefore, nuclear translocation of cyclinB1 was used as a proxy for Cdk1 activity. To measure duration of mitosis, a Nuclear Localization Signal (NLS) fused with mCherry was used. The sensor is nuclear during interphase and when the nuclear envelope breaks down it becomes cytoplasmic, allowing us to observe nuclear envelope break down and nuclear envelope reformation (Figure 2.4.B).

2.5.3. Immunofluorescence analysis

Cell profiler or the ScanR Analysis software was used to analyse immunofluorescence data from fixed cells. DAPI staining was used to identify cells and make the nuclear masks. When appropriated, a ring around the nuclear mask was used to measure cytoplasmic signal in order to measure nuclear/cytoplasmic ratio. Mean intensities were used to measure the expression/activity of the protein being tested within masks.

2.5.4. Curve fitting

To quantitatively measure Cdk1 activity, time courses of individual cells were fitted to the logistic equation $y=a+b/1+e-(t-t0/\tau)$ and were scaled to their fitted maximum and minimum values (b and a, respectively) and half-maximal times (t0). The rise times (τ) were calculated from the curve fits for all cells and are expressed as means ± standard deviation.

2.5.5. Cell cycle trajectory analysis

Quantifying dynamics of cell cycle progression requires imaging of fluorescent tagged biosensors in live cells. However, in the absence of endogenous cell cycle reporters, dynamic data can be estimated from static data using antibodies that recognize endogenous proteins or protein states (e.g. phosphorylation states). To estimate the dynamics of a particular cell cycle regulatory factor from static data, it was adapted the analysis described by Gut and

colleagues, and hESC and differentiated cells (MCF10A, RPE and Hela cells) were stained with DAPI and antibodies against the respective cell cycle regulator (either against an active phosphorylated form or total protein) (Gut et al., 2015). Nuclear size increases during cell cycle progression and DNA content increases as the cell progress through S-phase - this can be reflected as an increase in DAPI intensity. Therefore, measurements of the nuclear size and total DAPI intensity in each nucleus were combined to reconstruct the cell cycle time. DAPI images were segmented to generate nuclear masks for single cells. Nuclear masks were then used to quantify the total intensity of DAPI and mean intensity of cell cycle regulators immunostained in each cell. The distribution of total DAPI intensity and nuclear size of the population of single cells were normalised between 0 and 1. The normalised nuclear size and the total DAPI intensity for each cell was weighted at a ratio of 1:3 and averaged to obtain a trajectory score. The trajectory score vector was then sorted in ascending order to represent the progression in the cell cycle and therefore the index of the sorted order represents the cell cycle time.

2.6. Cloning and Molecular Biology

2.6.1. Classical restriction-enzyme based cloning

2.6.1.1. Polymerase chain reaction (PCR)

Polymerase chain reaction (PCR) was used to selectively amplify particular DNA fragments. A reaction mixture usually contained a final volume of 50µL consisting of:

- 5µL of Pfu high fidelity buffer (10x) 5µL
- 2.5U Pfu
- 1µL of 10mM dNTPs
- 100ng template DNA
- 25pmol Primer 5′ (sense)
- 25pmol Primer 3′ (anti-sense)
- top up to 50µL with dH_2O

A typical temperature program would start with 1 cycle of 2 minutes denaturation at 95ºC; 30 cycles of 30 seconds denaturation at 95ºC, 45 seconds at annealing temperature (ideal for each pair of primers), 90 seconds of elongation at 72ºC; and finally, 1 cycle of further extension for 10 minutes at 72ºC. 5µL of PCR reaction was run on an agarose gel to see single bands with the right size and products were purified with Qiagen PCR purification kit.

2.6.1.2. Restriction digest of vector and plasmid DNA

Typically, 5μg of vector and 10μg of the insert were digested using 2 restriction enzymes. 10U of each enzyme were mixed with buffer compatible with both enzymes, 2μL of 10mg/ml BSA and topped up with dH_2O to the final volume of 20μL. The mixture was incubated at 37ºC for 3 hours and then the enzymes were heat inactivated at 65ºC for 10 minutes. In the case of cleavage of plasmid DNA that was destined for subsequent ligation with insert fragment, the restricted DNA was 5′ dephosphorylated with a unit of Shrimps alkaline phosphatase for 1 hour at 37ºC in order to prevent re-ligation of incompletely digested DNA.

2.6.1.3. Purification of gel bands from agarose gel

1% (w/v) of agarose was added to 1x TAE (Tris Acetate EDTA) buffer and microwaved until agarose powder was dissolved. After cooling down, 1μg/mL ethidium bromide was added to agarose and transferred to a gel support. After the gel was solidified, 20μL of DNA digestion and dephosphorylation reactions (produced in 2.6.1.2) was loaded onto the gel using 6x DNA loading buffer and 1Kb ladder (New England Biolabs) for DNA size quantification. DNA gel bands were then excised from the gel and purified using Qiagen Gel Extraction Kit according to manufacturer's instructions.

50x TAE buffer was prepared in water accordingly:

- 2M Tris/acetate
- 50mM EDTA
- pH 8.5

2.6.1.4. Ligation reaction of vector and DNA fragments

To insert the DNA fragment of interest into the digested vector backbone a ratio of 1:6-1:10 vector to insert was used. Cut and dephosphorylated plasmid vector was mixed with DNA insert in 4μL of 5x T4 DNA Ligation Buffer (Invitrogen), 1μL of T4 DNA Ligase (Invitrogen) and H_2O for a final volume of 20μL. The mixture was incubated overnight at 16ºC and subsequently transformed into bacteria.

2.6.2. Gibson Isothermal Assembly based cloning

In order to make an inducible Cdh1 construct, pLVX-TetOne-Puro (Clontech) was cut with AgeI/BamHI and mCerulean tagged Cdh1 was amplified by PCR such that there was 30bp of overlapping sequence with the backbone. The two DNA fragments were purified and used to perform the Gibson Isothermal assembly cloning (Gibson et al., 2009). For a final volume of 5μL, equimolar amounts of DNA fragments were calculated based on the (bp) and concentration (ng/mL). After, the combined DNA was added to 15μL of isothermal assembly master mix and incubated for 1 hour at 50ºC. The reaction mix was then purified using Qiagen QIAquick PCR Purification Kit according to the manufacturer's instructions and used to transform *E. coli* Dh5α (see section 2.6.3.).

A final isothermal assembly reaction (total volume 20 uL) contained:

- 5 uL mixed DNA fragments
- 0.08 U of T5 Exonuclease
- 0.5 U of Phusion High Fidelity DNA Polymerase
- 80 U of Taq DNA Ligase
- 4 μL of 5x Reaction Buffer

5x Reaction Buffer was prepared in water accordingly:

- 500mM of Tris HCl pH 7.5
- 50mM of MgCl2
- 1mM of dGTP
- 1mM of dATP
- 1mM of dTTP
- 1mM of dCTP
- 50mM of DTT
- 5mM of NAD+
- 250 mg/mL of PEG-8000

2.6.3. Transformation of *E.coli* cells

E. coli DH5α (Sigma) chemically competent cells were used for transformation of all DNA constructs used in this study. Competent cells were thawed on ice for 30 minutes, after which 0.5μg of plasmid DNA of interest was added and incubated on ice for a further 20 minutes. In order to facilitate the uptake of plasmid DNA by the cells, they were subject to a heat-shock for 45 seconds at 42ºC in a water bath and subsequent incubation on ice for 2 minutes. After this, 250μL of room temperature S.O.C. Medium was added to the cells and the mixture was incubated for an hour in a horizontal shaker at 37ºC. The bacteria were then carefully spread on the appropriate antibiotic-containing LB agar plates (100μg/mL ampicillin or 50μg/mL kanamycin) and incubated overnight at 37ºC.

2.6.4. Isolation of plasmid DNA

Bacteria colonies were picked and incubated for 8 to 10 hours in 5mL of LB medium containing the corresponding antibiotic (100μg/mL ampicillin or 50μg/mL kanamycin) in a horizontal shaker at 37ºC. Bacterial cultures were then transferred to 200mL flasks of LB media toped up with fresh antibiotic and incubated overnight at 37ºC in a shaker. Cells were then pelleted by centrifugation at 4000 rpm for 15 minutes at 4ºC. To prepare large quantities of highly concentrated plasmid DNA, the HiSpeed-Plasmid Maxi Kit (Qiagen) was used according to the manufacturer's instructions. DNA concentration was determined using a Nanodrop spectrometer (Fisher Scientific).

2.6.5. RT-qPCR

Total RNA was extracted using TRI reagent (Life Technologies) and MaXtract High Density tubes (Qiagen) according to the manufacturer's instructions. RNA purity and quantity was assessed using a Nanodrop Spectrometer (Fisher Scientific). An absorbance ratio of 1.8-2 for A260/A280 was considered suitable for further analysis. Possible contaminating DNA was removed by treatment with DNase, and cDNA was prepared from 1μg of RNA using QuantiTect Reverse Transcription Kit (Qiagen) according to the manufacturer's instructions. qRT-PCR was performed on a Bio-Rad CFX96 real-time detection system using iTaq SYBR Green qPCR master mix (Bio-Rad) and primer pairs as

listed in Table 2.7. PCR conditions consisted of 1 cycle at 95°C for 3 minutes and 40 cycles at 95°C for 5 seconds and 60°C for 30 seconds. Glucuronidase beta (GUSB) was used as an invariant housekeeping gene. Fold change in expression was calculated using the $2^{-\Delta\Delta CT}$ (Livak) method (Livak and Schmittgen, 2001).

Table 2.7: Primers used for qPCR.

Gene	Primer Sequence (5′→3′)
Cdh1	F: TGGAGACGAGACCCTGAG R: TTGAGCACAGACACAGACT
GUSB	F: CTCATTTGGAATTTTGCCGATT R: CCGAGTGAAGATCCCCTTTTTA

2.7. ODE model of temporal control of mitosis

Various models have been constructed to gain insights into the behaviour of the cell cycle. These range from more complex stochastic and deterministic models involving many explicit molecular reactions (and corresponding ordinary differential equations - ODEs) (Csikasz-Nagy et al., 2006; Novak and Tyson, 1993a; 1993b; 2004; Pomerening et al., 2003) to more simple models using only a handful of ODEs (Gelens et al., 2015; Gérard et al., 2013; Santos et al., 2012; Tsai et al., 2014; Yang and Ferrell, 2013). In collaboration with Dr Lendert Gelens, it was built on previous simple models motivated by the fact that simple models can often still capture similar dynamical behaviour as the more complicated models. Moreover, they have the benefit of containing fewer parameters thereby facilitating parameter selection and allowing for a quantitative view into how each individual parameter influences the behaviour of the system.

Dr. Lendert Gelens constructed a simple model that takes into account the synthesis and destruction of Cyclin B1 and the activation and inactivation of Cdk1-cyclin B1 complexes. Cyclin B1 was assumed to be synthesized and degraded at constant rates k_s and a_{deg}, respectively. Moreover, it was assumed that Cyclin B1 bound quickly to Cdk1 and that the Cdk1-cyclin B1 complexes were quickly phosphorylated by the Cdk-activating kinase

(CAK). Under these assumptions, synthesized Cyclin B1 immediately produces active Cdk1-cyclin B1 complexes. However, it is known that the activity of Cdk1-Cyclin B1 is regulated by various other (de)phosphorylations. It is only fully active when Threonine (Thr) 161 is phosphorylated (by CAK) and Thr 14 and Tyrosine (Tyr) 15 are dephosphorylated. The kinase Wee1 (and Myt1) phosphorylates Thr 14 and Tyr 15 and thereby inactivates Cdk1 with a rate constant k_{wee}. Cdk1 itself also inactivates Wee1, leading to a double negative feedback loop (McGowan and Russell, 1993; Mueller et al., 1995a; 1995b; Parker and Piwnica-Worms, 1992; Tang et al., 1993). Similarly, the phosphatase Cdc25 dephosphorylates Tyr15 and activates Cdk1 with a rate constant k_{cdc}, and Cdc25 is in turn activated by Cdk1 forming a positive feedback loop (Hoffmann et al., 1993; Solomon et al., 1990). These interactions led to two simple ODEs describing the time evolution of active Cdk1-cyclin B1 complexes ([Cyc B-Cdk1]) and of total Cyclin B1 ([CycB]):

$$\begin{aligned}\frac{d[CycB-Cdk1](t)}{dt} &= k_s - a_{deg}[CycB-Cdk1](t)\\ &+ k_{cdc}\big([CycB-Cdk1](t)\big)\big([CycB](t)-[CycB-Cdk1](t)\big)\\ &- k_{wee}([CycB-Cdk1](t))[CycB-Cdk1](t)\end{aligned} \tag{2.1}$$

$$\frac{d[CycB](t)}{dt} = k_s - a_{deg}[CycB](t) \tag{2.2}$$

The rate constants k_{cdc} and k_{wee} depend on the concentration of active Cdk1-cyclin B1 complexes ([Cyc B-Cdk1]). This dependency was implemented by the following two Hill functions with high enough Hill exponents, which is a good approximation as long as these (de)phosphorylation events occur on a faster time scale than the modelled time evolution of [CycB-Cdk1] and [CycB]:

$$k_{cdc}([CycB-Cdk1]) = a_{cdc} + b_{cdc}\frac{[CycB-Cdk1]^{n_{cdc}}}{EC50_{cdc}^{n_{cdc}} + [CycB-Cdk1]^{n_{cdc}}} \tag{2.3}$$

$$k_{wee}([CycB-Cdk1]) = a_{wee} + b_{wee}\frac{[CycB-Cdk1]^{n_{wee}}}{EC50_{wee}^{n_{wee}} + [CycB-Cdk1]^{n_{wee}}} \tag{2.4}$$

This ODE system, including the feedback loops involving Wee1 and Cdc25, could turn the system into a bistable switch as long as Wee1 activity is strong enough compared to Cdc25. This is illustrated in Figure 2.5.A. where the Cdk1 activity ([Cyc B-Cdk1]) is shown in function of Cyclin B1 levels ([Cyc B]), assuming that there is no synthesis or degradation of Cyclin B1. The parameters corresponding to the Cdc25 and Wee1 feedback were chosen as follows:

$$
\begin{aligned}
a_{cdc} &= 0.5 min^{-1} \\
b_{cdc} &= 1.5 min^{-1} \\
EC50_{cdc} &= 30nM \\
n_{cdc} &= 10 \\
a_{wee} &= 0.5 min^{-1} \\
b_{wee} &= 1 min^{-1} \\
EC50_{wee} &= 30nM \\
n_{wee} &= 10
\end{aligned}
\tag{2.5}
$$

and the strength of the Wee1 loop (a_{wee} and b_{wee}) was scaled by a factor 1.5, 1, 0.5, 0.25 from top to bottom as shown in Figure 2.5.A. It is worth noting that while the strength of the Wee1 loop was increasing (with respect to the strength of the Cdc25 loop), the region of bistability (gray region) was also increasing, and decreasing its strength decreased this region of bistability. In addition, when the Wee1 feedback loops were strong, Cdk1 activity could be maintained in a more inactive state for a wider range of Cyclin levels. In contrast, when the Wee1 loops were not able to inhibit Cdk1 activity much, the response curve became more linear, such that any increase in Cyclin B1 led to a proportional increase in Cdk1 activity.

Figure 2.5.B. shows the system behaviour in the presence of constant Cyclin synthesis ($k_s = 0.1 nM min^{-1}$) and degradation ($a_{deg} = 7.5\times10^{-4} min^{-1}$). The system was initialized at low concentrations of Cyclin B1 ([Cyc B] = 10) and active Cdk1 ([Cyc B-Cdk1] = 5), shown by point (i). Then Cyclin levels ramped up to a final stationary value of [CycB] = $k_s / a_{deg} \approx$ 133nM, point (f) outside of the plotted range. Cdk1 activity was dramatically different in the presence of the Wee1 feedback loops of varying strength. The stronger the activity of Wee1, the longer Cdk1 activity was kept low, and the higher and the more abrupt the jump in Cdk1 activity was when Cyclin B1 levels reach the threshold T. This bistability involving Wee1 explains the abrupt and all-or-none activation of Cdk1, and therefore mitotic entry, in

various systems (Csikasz-Nagy et al., 2006; Gelens et al., 2015; Novak and Tyson, 1993a; 1993b; 2004; Pomerening et al., 2003; Tsai et al., 2014; Tuck et al., 2013; Yang and Ferrell, 2013).

Next, we included the activation of the Anaphase Promoting Complex/Cyclosome (APC-cdc20) in response to Cdk1 activation. Here, it was envisioned that a similar double-negative feedback loop might be present between APC-cdc20 and Mad2. Mad2 is a critical component of the mitotic checkpoint complex (MCC) or spindle assembly checkpoint (SAC), which inhibits APC-cdc20 activity. Active Mad2 sequesters Cdc20, an essential APC activator and thereby competes with and antagonizes APC (Foster and Morgan, 2012; Izawa and Pines, 2012). Furthermore, it has been shown that APC-cdc20 itself also inhibits SAC (which Mad2 is part of), closing the double negative loop (Foster and Morgan, 2012; Izawa and Pines, 2012; Nilsson et al., 2008; Reddy et al., 2007). This interaction was implemented by assuming that Cdk1 activates the APC-cdc20 in an ultrasensitive manner, as has been shown before (Tsai et al., 2014; Yang and Ferrell, 2013).

Furthermore, it was also assumed that Mad2 could inhibit the APC-cdc20 until it reaches a critical level after which Mad2 can no longer effectively inhibit APC-cdc20. The ODE describing the interaction between the APC-cdc20 and Mad2 is the following:

$$\frac{d[APC](t)}{dt} = a_K + b_K \frac{[CycB - Cdk1](t)^{n_K}}{[CycB - Cdk1](t)^{n_K} + EC50_K^{n_K}}\big(1 - [APC](t)\big) - (a_P + b_P \frac{EC50_P^{n_P}}{[APC](t)^{n_P} + EC50_P^{n_P}})[APC](t) \quad (2.6)$$

where the parameters have been chosen as follows:

$$a_K = 0min^{-1}$$

$$b_K = 0.25min^{-1}$$

$$EC50_K = 0.18$$

$$n_K = 5$$

$$a_P = 0.025min^{-1}$$

$$b_P = 0.5min^{-1}$$

$$EC50_P = 0.18$$

$$n_P = 5 \quad (2.7)$$

Figure 2.5.C. shows the resulting steady-state solutions (APC-cdc20 activities in function of Cdk1 activity) of Eq. (2.6), for varying values of b_P=0.5, 1, 1.5, 2 min^{-1}, which effectively increased the strength of APC inhibition by Mad2. This single ODE also allows for bistability. The width of the bistable region increases with increasing strength of Mad2. The idea behind implementing an additional ODE to describe APC activity is that the resulting bistability allows for two regulatory relationships that are believed to be important in cell cycle regulation: (i) when increasing Cdk1 activity across a threshold, APC activity greatly increases in a sharp and irreversible manner, and (ii) changing the strength of Mad2 allows us to tune this threshold in such a way that when Mad2 activity is strong enough, the APC can never be activated. In this way, the system remains in the low APC activity state (red) and no metaphase to anaphase transition takes place. In other words, implementing a tunable bistable switch in the activity of APC allows the system to dynamically regulate (activate and deactivate) the Spindle Assembly Checkpoint (SAC).

Next, Eqs. (2.1)-(2.4) were combined with Eq. (2.6) to turn this into a model for cell cycle oscillations. Once the APC is active, it ubiquitinates Cyclin B1 and targets it for degradation by the proteasome, which in turn leads to the inactivation of Cdk1 (Holloway et al., 1993; King et al., 1995). It was assumed that both of these events occurred with the same degradation rate b_{deg}, and it was implemented by allowing for additional ultrasensitivity in APC activation in order to avoid the system being arrested in interphase, instead of producing regular time-periodic oscillations in Cyclin B1 and Cdk1 activity. The complete set of equations reads:

$$\begin{aligned}\frac{d[CycB-Cdk1](t)}{dt} &= k_s - a_{deg}[CycB-Cdk1](t) \\ &- b_{deg}[APC]^*(t)[CycB-Cdk1](t) \\ &+ k_{cdc}\big([CycB-Cdk1](t)\big)\big([CycB](t)-[CycB-Cdk1](t)\big) \\ &- k_{wee}\big([CycB-Cdk1](t)\big)[CycB-Cdk1](t)\end{aligned} \tag{2.8}$$

$$\frac{d[CycB](t)}{dt} = k_s - a_{deg}[CycB](t) - b_{deg}[APC]^*(t)[CycB](t) \tag{2.9}$$

$$\begin{aligned}\frac{d[APC](t)}{dt} = \left(a_K + b_K \frac{[CycB-Cdk1](t)^{n_K}}{[CycB-Cdk1](t)^{n_K} + EC50_K^{n_K}}\right)\big(1-[APC](t)\big) - (a_P \\ + b_P \frac{EC50_P^{n_P}}{[APC](t)^{n_P} + EC50_P^{n_P}})[APC](t)\end{aligned} \tag{2.10}$$

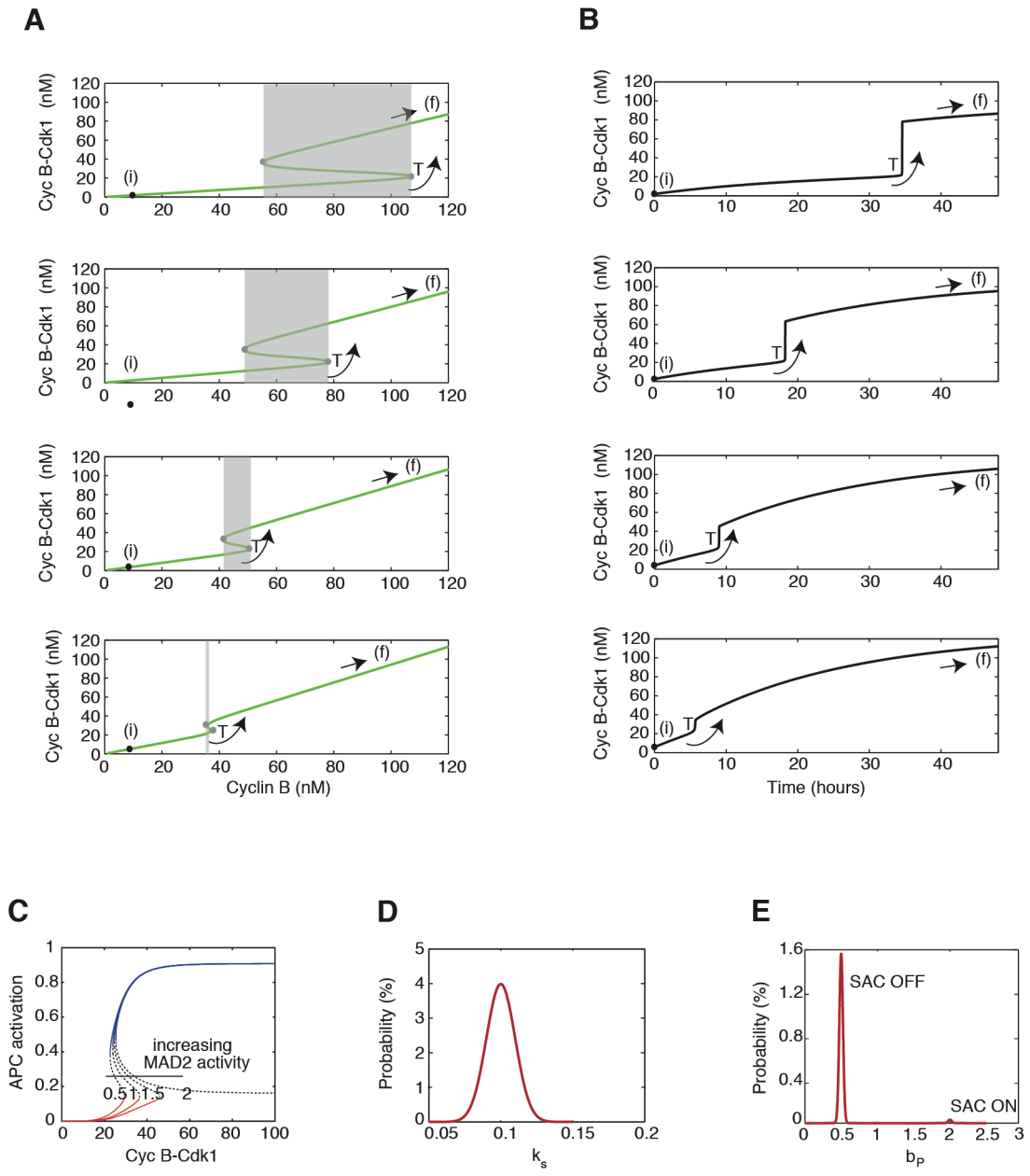


Figure 2.5. Building an ODE model to predict modularity in mitosis. A. Steady state and **B.** time activation dynamics of Cdk1-cyclin B1 with changing Wee1 strength. Steady-state solutions of (CycB-Cdk1 activation as a function of Cyclin B1 accumulation) of Eqs. (2.1)-(2.4), for varying scaling of a_{wee} and b_{wee}, i.e. scaled by a factor 1.5; 1; 0.5; 0.25 (top to bottom). **B.** Shows the corresponding time evolution when initialized at [Cyc B]=10 and [Cyc B-Cdk1]=5. **C.** Steady-state activation dynamics of APC with changing MAD2 strength. Steady-state solutions (APC activity as a function of Cdk1 activity) of Eq. (2.6), for varying values of b_P=0.5; 1; 1.5; $2min^{-1}$. Red line indicates inactive APC and blue line indicates active APC. **D.** Noise distribution functions of Cyclin accumulation rate k_s. **E.** Noise distribution functions of Mad2 strength b_P.

With $[APC]^*(t) = \frac{[APC](t)^{n_{apc}}}{EC50_{apc}^{n_{apc}} + [APC](t)^{n_{apc}}}$, and the basic parameter set given by:

$$k_s = 0.1nMmin^{-1}$$

$$a_{deg} = 0.001min^{-1}$$

$$b_{deg} = 0.02min^{-1}$$

$$a_{cdc} = 0.5min^{-1}$$

$$b_{cdc} = 1.5min^{-1}$$

$$EC50_{cdc} = 30nM$$

$$n_{cdc} = 10$$

$$a_{wee} = 0.5min^{-1}$$

$$b_{wee} = 1min^{-1}$$

$$EC50_{wee} = 30nM$$

$$n_{wee} = 10$$

$$a_K = 0min^{-1}$$

$$b_K = 0.25min^{-1}$$

$$EC50_K = 0.18$$

$$n_K = 5$$

$$a_P = 0.025min^{-1}$$

$$b_P = 0.5min^{-1}$$

$$EC50_P = 0.18$$

$$n_P = 5$$

$$EC50_{apc} = 0.5$$

$$n_{apc} = 10 \qquad (2.11)$$

The parameters k_s and b_{deg} were chosen such that durations of interphase and mitosis (M-Phase) were realistic. a_{deg} was then chosen to be small enough such that Cyclin B1 accumulates to high enough values to flip the Cdk1-cyclin B1 switch and activate Cdk1. Most

of the other parameters are flexible and were chosen to set the threshold values of both the Cdk1-cyclin B1 (Wee1) switch and the Cdk1/APC (Mad2) switch.

Finally, noise was introduced in the model to verify whether this simple model showed qualitatively all the properties observed in our experiments, namely that the mitosis phase is short, constant, and uncorrelated with the total cell cycle length (which is largely determined by interphase duration). Noise was implemented in the form of random variation (normally distributed) around a mean value corresponding to the standard parameters mentioned before. Therefore, noise was added with a standard deviation of $0.01 nM min^{-1}$ to the Cyclin B1 accumulation rate k_s and with a standard deviation of $0.025 min^{-1}$ to the Mad2 strength b_P. This noise introduced changes in cell cycle length. Additionally, in 2% of the simulated cells, the mean value of b_P was increased to 2, mimicking events where the SAC is activated and the cell cycle arrests in M-phase. The resulting distributions of parameter values are shown in Figure 2.5.D and E.

Using an improved Euler method, Eqs. (2.8)-(2.10) were then simulated for 150 hours after an initial transient time of 10 hours. Regular cell cycle oscillations were determined by calculating the oscillation period and verifying whether the system had oscillated with the same period and amplitude for at least three times. If so, the time in interphase was calculated as the time within one oscillation where the system had a Cdk1 activity parameter smaller than 27, while the time in M phase was scored as the time during which the Cdk1 activity parameter was larger than 27. The value 27 was chosen to fall within the range of Cdk1 activities of the middle branch solution in Figure 2.5.A and B for all Wee1 strengths. This simulation was repeated 1000 times and then this data was used to plot probability density functions of interphase and mitotic durations.

Finally, we investigated the effects of perturbing one or both of the two bistable switches: the Cdk1-cyclin B1:Wee1 switch and the APC-cdc20:Mad2 switch. This was done by inhibiting Wee1 and Mad2 activity. In the first case (Cdk1- cyclin B1:Wee1 switch), a_{wee} and b_{wee} rates were decreased by a factor of 7. In the second case (APC-cdc20:Mad2 switch), b_P rate was decreased by a factor of 7.

3. Temporal Insulation of Mitosis

3.1. Summary

The cell cycle is characterized by a sequence of events – G1-, S-, G2- and M-phase – by which a cell gives rise to two daughter cells. Even though the molecular machinery that drives cell division cycles is the same in all tissues, it is known that different cell lines exhibit very different cell division times. To better understand this variability, the cell cycle dynamics of different cell lines was compared. Quantification of the length of cell cycle phases in single cells by live-cell imaging showed high variability in the dynamics of cell cycle phases. An exception to this was mitosis, whose duration remained short and surprisingly constant in different cell types. In addition, contrary to other cell cycle phases, there was no correlation between total cell cycle length and duration of mitosis. In other words, it does not matter if a cell completed the cell cycle at a fast or slow pace - once it reaches mitosis, it completes mitosis in a short and synchronous (constant) manner. It has been shown that positive feedback regulation is crucial to keep mitotic events synchronised (Holt et al., 2008; Santos et al., 2012) and therefore it was hypothesised that positive feedback might be the molecular mechanism that keeps the time of mitosis relatively constant across different cell types with variable cell cycle lengths. By combining live-cell imaging and computational modelling it was possible to show that positive feedback is the molecular mechanism underlying temporal insulation of mitosis. When positive feedback was perturbed the switch-like activation of cyclin dependent kinase 1 (Cdk1) was compromised, leading to a slower mitotic entry and more variable progression through mitosis. Importantly, breaking positive feedback resulted in coupling of duration of mitosis with cell cycle length. The work presented in this chapter showed that positive feedback, a recurrent motif in cell cycle control, may also be important to keep mitosis short, synchronous, and temporally insulated from earlier cell cycle events. This leads us to anticipate that the simple regulatory strategy of positive feedback may also be crucial in creating modularity in other biological systems.

3.2. Aims

The first aim of the work presented in this chapter was to measure cell cycle dynamics in live cells and compare the variability of cell cycle dynamics between different human cell lines. The second aim was to define and characterise the molecular mechanism responsible for keeping mitosis short, constant, and temporally insulated from previous cell cycle events. It was tested whether positive feedback, a recurrent motif in cell cycle regulation, is the molecular mechanism that keeps mitosis as a temporally independent event during cell division.

3.3. Mitosis is short, constant and independent of cell cycle length

3.3.1. Timing of mitosis is short and kept constant in different cell lines

In order to measure cell cycle dynamics in single cells, MCF10A, RPE, and Hela cells stably expressing Cdt1-venus, H2B-Turquoise, and PCNA-mCherry were imaged for two consecutive divisions and the time of different cell cycle phases was measured as described in section 2.5.2.1 (Figure 2.2): G1-phase length was monitored by the appearance and disappearance of Cdt1-venus; S-phase length was defined as the time between appearance and disappearance of nuclear speckles of PCNA-mCherry; G2-phase was measured by monitoring the time between the disappearance of PCNA speckles and nuclear envelope breakdown (NEB), which was characterised by observing the localisation of H2B-Turquoise; mitosis was defined by the time between NEB and nuclear envelope reformation (NER). Total cell cycle length was measured as the time between two consecutive NER events.

The cell cycle of MCF10A cells was determined to be 20.3±4.1 hours. Measuring the dynamics of cell cycle phases in single cells showed that on average, MCF10A cells spent 4.0±1.8 hours in G1-phase, 9.0±1.6 hours in S-phase, and 6.5±2.0 hours in G2-phase (Figure 3.1.A. left panel). Surprisingly, duration of mitosis was quite short (48.0±6.4 minutes) in comparison to the other cell cycle phases. Similar results were seen in RPE and Hela cell lines. The cell cycle of RPE cells was on average 29.0±7.4 hours and cells spent 7.6±4.0 hours in G1-phase, 11.8±3.3 hours in S-phase, 8.7±4.2 hours in G2-phase and only 48.0±7.8 minutes in mitosis (Figure 3.1.A. middle panel). Hela cells spent on average 25.0±4.0 hours in cell cycle. In Hela cells, G1-phase was usually 10.4±3.1 hours long, S-phase was 10.6±2.5 hours long, G2-phase was 3.1±1.1 hours long and mitosis was still short, being 55.7±16.0 minutes long (Figure 3.1.A right panel).

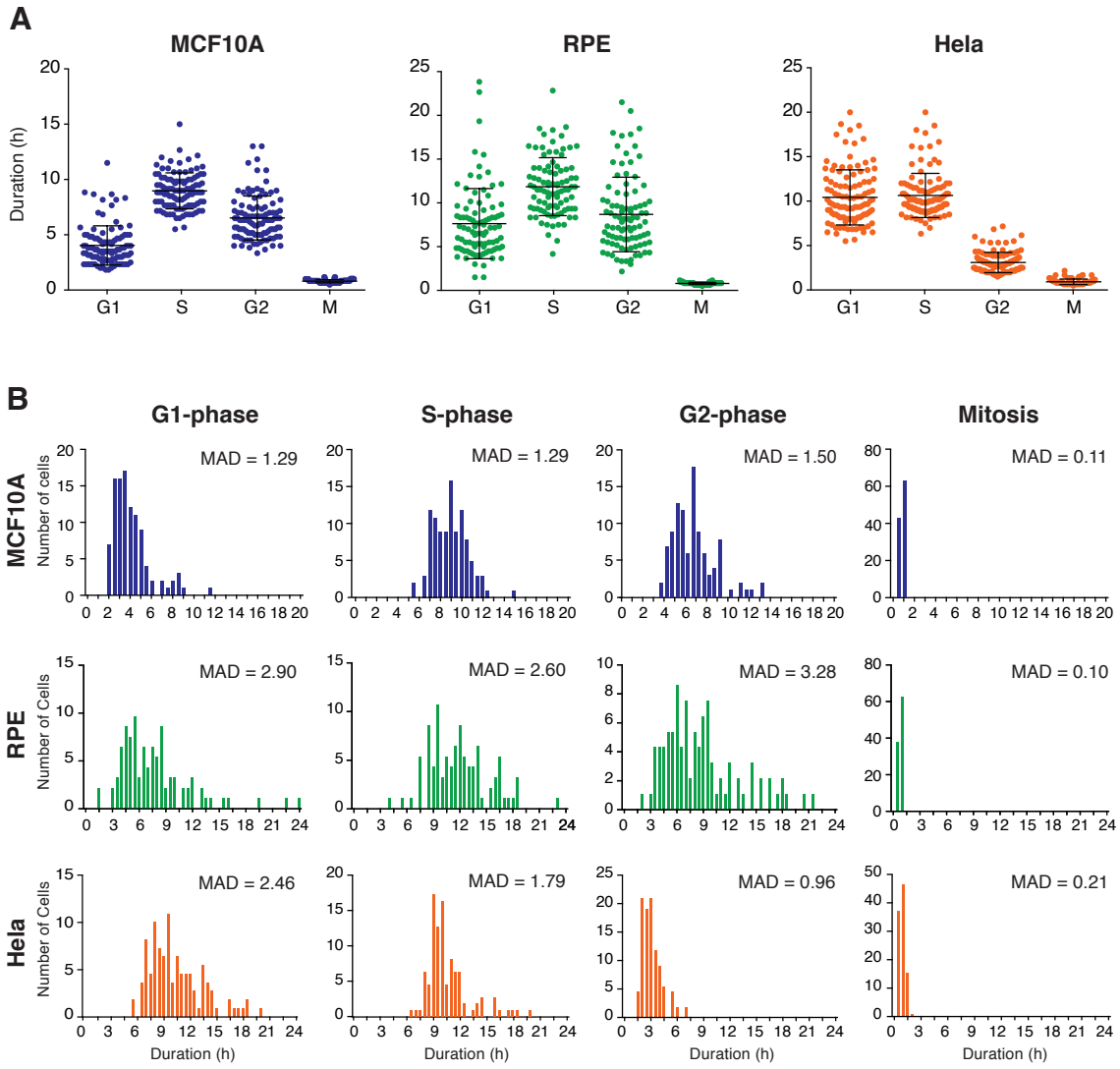


Figure 3.1. Cell cycle dynamics in MCF10A, RPE and Hela cells. Stable lines expressing Cdt1-venus, H2B-Turquoise and PCNA-mCherry. **A.** Time of G1-phase, S-phase, G2-phase and mitosis measured by single live-cell imaging in MCF10A (left panel), RPE (middle panel) and Hela (right panel) cells. Mean ± standard deviations are shown as bars. **B.** Histograms of duration of G1-phase, S-phase, G2-phase and mitosis in MCF10A (top panel), RPE (middle panel) and Hela (bottom panel) cells. Mean absolute deviations (MAD) are shown in hours (n>90).

These results showed that mitosis was always relatively short across the different cell types tested and that cells spend less than 5% of total cell cycle time in mitosis. In addition, plotting the measurements of G1-phase, S-phase, G2-phase, and mitosis durations for multiple individual cells showed that cell-to-cell variability exists in the duration of cell cycle phases, and that the extent of this variability differs for different cell lines, as seen by the calculated mean absolute deviation for G1-phase (MAD=1.29, 2.90 and 2.46 in MCF10A, RPE and Hela cells, respectively), S-phase (MAD=1.29, 2.60 and 1.79 in MCF10A, RPE and HeLa cells, respectively), and G2-phase (MAD=1.50, 3.28 and 0.96 in MCF10A, RPE and Hela cells, respectively) (Figure 3.1.B). The notable exception to this observation was mitosis, which was remarkably constant between cells of the three cell lines tested (MAD=0.11, 0.10 and 0.21 in MCF10A, RPE and Hela cells, respectively). Mean absolute deviation is a measure of dispersion and measures of by how much the values in the data set are likely to differ from the mean.

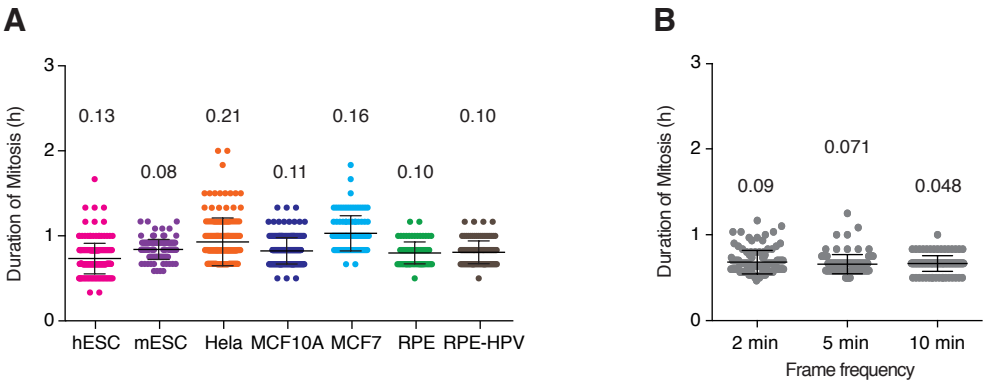


Figure 3.2. Duration of mitosis is short and constant across different cell lines. A. Time of mitosis in single cells as measured by live-cell imaging in seven different human and mouse cell lines (mESC) (n>100). **B.** Time of mitosis in single cells as measured by live-cell imaging in MCF10A cells at different frame frequencies (every 2, 5 and 10 minutes per imaging frame). Mean ± standard deviations are shown as bars and mean absolute deviations (MAD) are shown above in hours (n>100).

As shown in Figure 3.2.A, these observations seem to be true in a variety of different cell lines (normal, cancerous and embryonic cell lines (human and mouse)), where the measured mitotic duration was on average 45 minutes with MAD values between 0.08 and 0.21 hours. To discard the hypothesis that this could be due to under sampling the time of mitosis while imaging cells, increasing the temporal resolution of the acquired images by imaging every 2, 5 and 10 minutes showed no effect on the observed duration of mitosis (in MCF10A cells – 41.0±8.2 minutes, 40.0±6.7 minutes and 40.0±5.5 minutes at a frequency of 2, 5 and 10 minutes, respectively for at least 100 cells) (Figure 3.2.B). Taken together, these results suggest that despite variability in cell-cycle dynamics, duration of mitosis is always short and relatively constant in mammalian cells.

3.3.2. Duration of mitosis does not correlate with cell cycle length

Quantitative measurements of cell-cycle dynamics in individual cells also showed that relative cell cycle length could be predicted by measuring the duration of individual phases during interphase, and vice versa. There was a correlation between the duration of G1-, S-, and G2-phases and the overall cell cycle length in MCF10A, RPE and Hela cells (Pearson correlation coefficient, *r* – MCF10A: G1-phase=0.68, S-phase=0.79, G2-phase=0.77; RPE: G1-phase=0.64, S-phase=0.60, G2-phase=0.66; Hela: G1-phase=0.60, S-phase=0.63, G2-phase=0.48) (Figure 3.3). In other words, cells that spent more time in G1-, S-, or G2-phases have a longer total cell cycle than cells with short G1-, S-, or G2-phases. This appears to be true for all cell cycle phases except for mitosis. Duration of mitosis did not significantly correlate with cell cycle length in any of the cell lines tested, regardless of the overall cell cycle length (Pearson correlation coefficient, *r* – MCF10A=0.3, RPE=0.09 and Hela=0.25) (right panel of Figure 3.3). These observations suggest that even though different cell types have different cell cycle dynamics, timing of mitosis is always short and constant, and mitotic duration is temporally insulated from the variability of earlier cell cycle events.

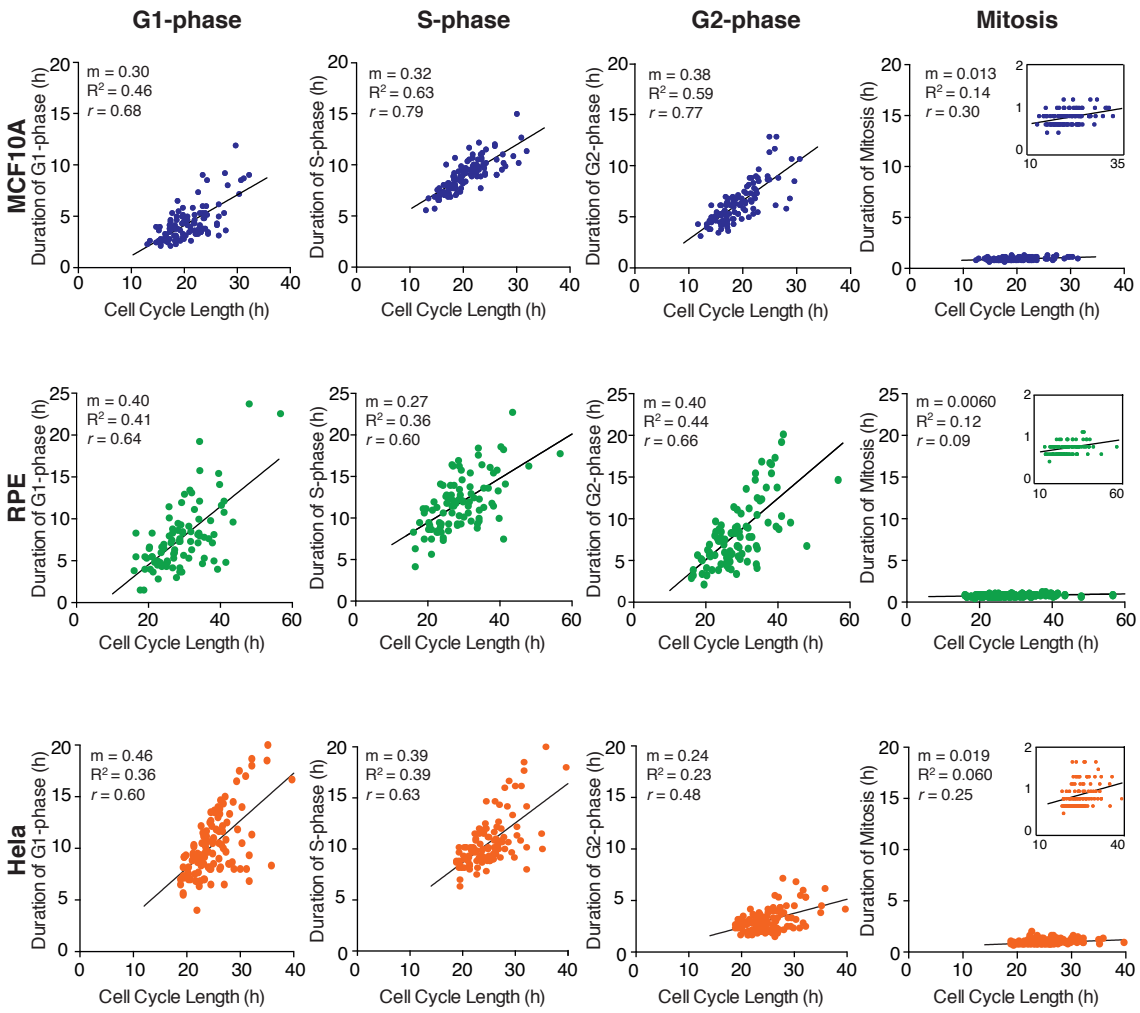


Figure 3.3. Duration of mitosis does not correlate with cell cycle length in single cells. Duration of G1-phase, S-phase, G2-phase and mitosis in single cells as a function of cell-cycle length measured by live-cell imaging in MCF10A (top panel), RPE (middle panel) and Hela (bottom panel) cells. All lines stably expressed Cdt1-venus, H2B-turquoise and PCNA-mCherry. Insect shows same data on a 0-2 hours y axis scale. Slope of the trend line (m), coefficient of determination (R^2) and Pearson correlation coefficient (r) are shown (n>90).

3.3.3. Temperature does not influence the lack of correlation between time of mitosis and cell cycle length

To test the idea that mitosis is temporally uncoupled from variability in the duration of interphase, cell cycle was artificially slowed down and sped up by imaging MCF10A, RPE, and Hela cells at 34ºC (low temperature) and 40ºC (high temperature), respectively, for two division cycles, with images being taken every 10 minutes.

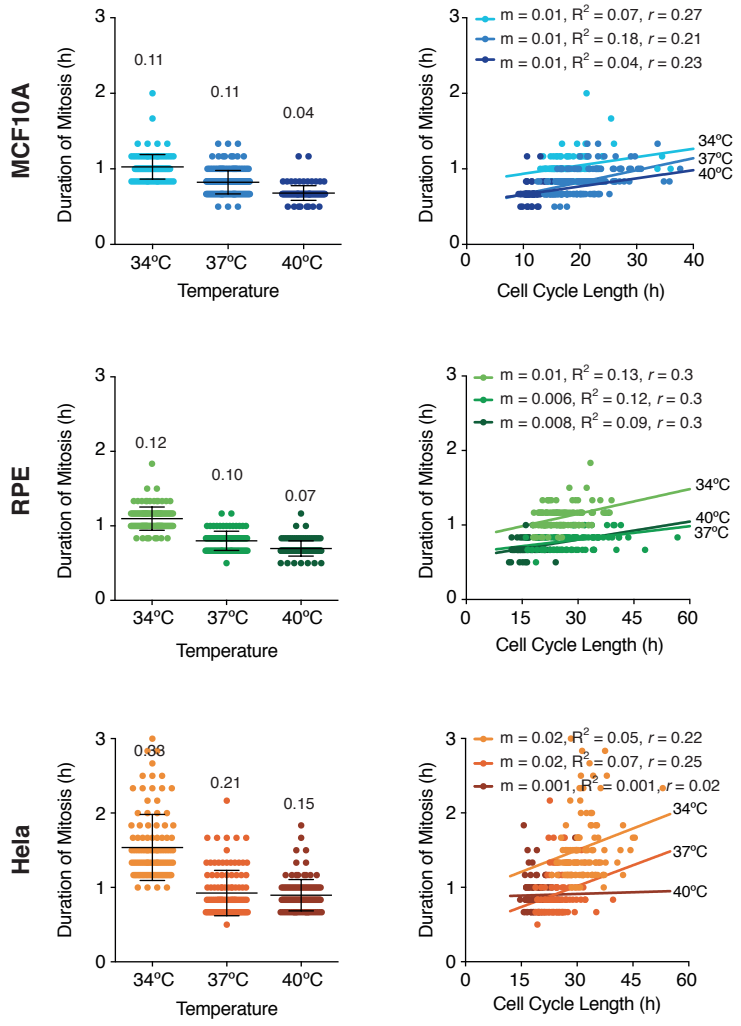


Figure 3.4. Duration of mitosis is constant in temperature-driven changes of cell cycle length. All lines stably expressed Cdt1-venus, H2B-turquoise and PCNA-mCherry. **Left panel –** Duration of mitosis in MCF10A, RPE and Hela cells as measured by live-cell imaging performed at 34ºC, 37ºC and 40ºC. Mean ± standard deviations are shown as bars and mean absolute deviations (MAD) are shown above in hours (n>100). **Right panel –** Duration of mitosis in MCF10A, RPE and Hela cells as a function of cell cycle length measured by live-cell imaging performed at 34ºC, 37ºC and 40ºC. Slope of the trend line (m), coefficient of determination (R^2) and Pearson correlation coefficient (r) are shown (n>100).

Compared to control cells imaged at 37ºC (where mitosis took on average 49.4±9 minutes, 47.9±8 minutes and 55.5±18 minutes in MCF10A, RPE and Hela cells, respectively), duration of mitosis was longer at 34ºC (MCF10A=61.6±9 minutes, RPE=65.8±9 minutes, Hela=92.2±26 minutes) and shorter when cells were imaged at 40ºC (MCF10A=40.8±6 minutes, RPE=41.8±6 minutes, Hela=53.8±12 minutes) (left panel Figure 3.4). However, slowing down or speeding up the cell cycle did not affect variability in mitotic duration as measured by mean absolute deviation values (at 34ºC MAD=0.11, MAD=0.12 and MAD=0.33 in MCF10A, RPE, and Hela cells, respectively and at 40ºC MAD=0.04, MAD=0.07 and MAD=0.15 in MCF10A, RPE, and Hela cells, respectively). Moreover, in these artificial conditions there was still very little correlation between total cell cycle length and duration of mitosis both at low temperature (Pearson correlation coefficient, r – MCF10A=0.27, RPE=0.3 and Hela=0.22) and high temperature (Pearson correlation coefficient, r – MCF10A=0.23, RPE=0.3 and Hela=0.02) (right panel Figure 3.4).

These results support the hypothesis that mitosis is a modular phase during the cell cycle, temporally insulated from earlier cell cycle events.

3.4. Perturbing Spindle Assembly Checkpoint (SAC) does not make mitosis dependent on cell cycle length

In light of the surprising finding that duration of the mitotic phase is consistently and uniquely uncorrelated with total cell cycle length, the next step in this work was to identify the molecular mechanism responsible for keeping the duration of mitosis short, constant, and temporally insulated from variability in previous cell cycle phases. Transitions across different cell cycle phases are heavily controlled by checkpoint regulation. Checkpoints ensure that one cell cycle phase begins only when the previous phase is completed with success, and hence regulate the duration of individual cell cycle phases (Hartwell and Weinert, 1989). There is a checkpoint in the middle of mitosis – the Spindle Assembly Checkpoint (SAC) – that regulates the transition from metaphase to anaphase (Gardner and Burke, 2000; Hoyt et al., 1991; Li and Murray, 1991; Wells, 1996). The SAC guarantees that chromosome segregation, progression to anaphase, and mitotic exit only happen once all the chromosomes are properly aligned in metaphase plate and attached to the mitotic spindle via their kinetochores.

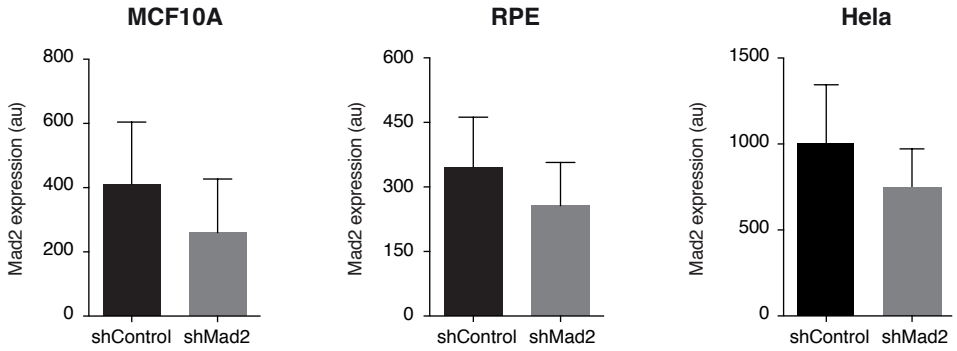


Figure 3.5. Mean expression of Mad2 in MCF10A, RPE and Hela cells stably expressing shMad2 and PCNA-mCherry. Cells lines stably express shControl (shScramble) or shMad2 and PCNA-mCherry. Mean expression of Mad2 protein was measured using immunofluorescence with the antibody MAD2 (BD-Biosciences, cat. no. 610678). Mean ± standard deviation is shown for each cell line (n>5000).

Due to this potential key role in controlling how much time cells stay in mitosis, SAC was a suitable candidate to explain the temporal modularity that was seen in mitosis. To test this hypothesis, the expression of protein Mad2 (a crucial SAC component (Li and Murray, 1991)) was downregulated with short hairpin RNAs (shRNA). MCF10A, RPE, and Hela cells expressing shRNA against Mad2 (shMad2) showed a downregulation of about 20-40% of Mad2 protein, which allowed the cells to be viable and kept in culture (Figure 3.5). Cells stably expressing shMad2 or shControl (shScramble) also expressed PCNA-mCherry in order to measure cell cycle dynamics in these cell lines.

MCF10A, RPE, and Hela cells stably expressing PCNA-mCherry and either shMad2 or shControl (shScramble) were imaged for two consecutive division cycles in order to measure G1-phase and mitosis length. Since Mad2 and SAC play a specific role during mitosis only, Mad2 downregulation showed no significant effect on duration of G1-phase in both MCF10A and RPE (MCF10A: shControl 3.3±1.6 hours and shMad2 3.3±1.8 hours with $p>0.7$ by Mann-Whitney test; RPE: shControl 5.7±2.2 hours and shMad2 6.0±2.8 hours with $p>0.9$ by Mann-Whitney test) (left panel Figure 3.6). In Hela cells, downregulation of Mad2 showed a slight significant effect on G1-phase length, which increased from 8.0±2.2 hours in shControl to 9.0±2.1 hours in shMad2 cells (left panel Figure 3.6).

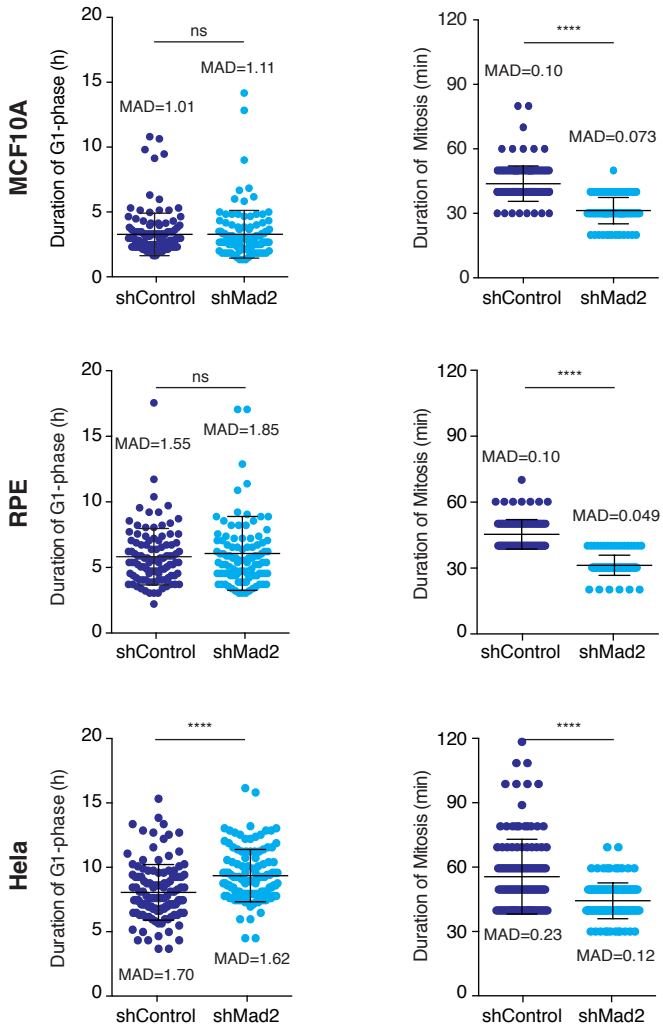


Figure 3.6. Duration of G1-phase and mitosis measured in the presence and partial absence of SAC. All lines stably expressed PCNA-mCherry and shControl or shMad2. **Left panel –** Duration of G1-phase measured in MCF10A, RPE and Hela control lines (shControl) or lines with knockdown (shMad2) of SAC (n>100). **Right panel –** Duration of mitosis measured in MCF10A, RPE and Hela cells in the presence (shControl) or partial absence (shMad2) of SAC. Mean ± standard deviations are shown as bars, mean absolute deviations (MAD) are shown above in hours and p values calculated by Mann-Whitney test are shown (ns=not significant, **** p<0.0001) (n>100).

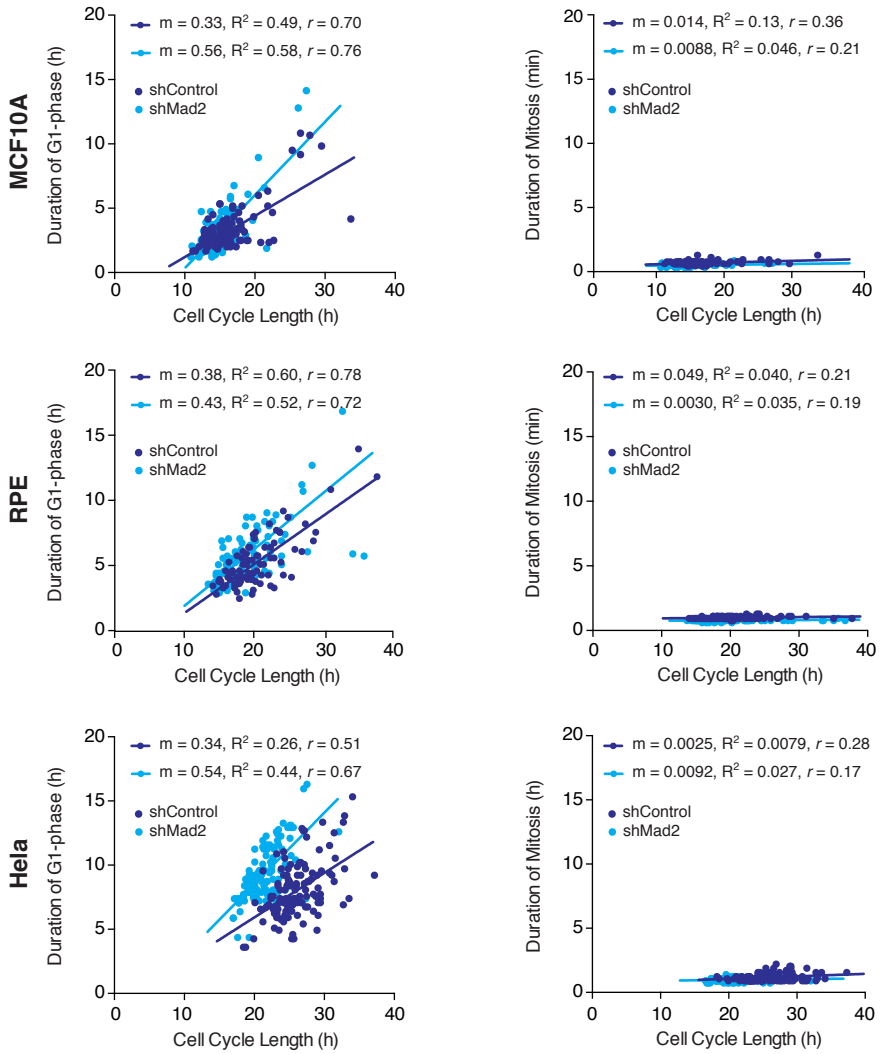


Figure 3.7. Perturbing SAC does not affect temporal insulation of mitosis. All lines stably expressed PCNA-mCherry and shControl or shMad2. **Left panel –** Duration of G1-phase plotted as a function of cell cycle length in MCF10A (top panel), RPE (middle panel) and Hela (bottom panel) cells in without (shControl) or with (shMad2) perturbation of SAC. **Right panel -** Duration of mitosis plotted as a function of cell cycle length in MCF10A (top panel), RPE (middle panel) and Hela (bottom panel) cells in without (shControl) or with (shMad2) perturbation of SAC. Slope of the trend line (m), coefficient of determination (R^2) and Pearson correlation coefficient (r) are shown (n>100).

However, downregulation of Mad2 resulted in a shorter duration of mitosis in all the three cell lines (MCF10A: shControl 43.8±8.0 minutes and shMad2 31.2±6.0 minutes with $p<0.0001$ by Mann-Whitney test; RPE: shControl 43.6±6.0 minutes and shMad2 31.1±4.6 minutes with $p<0.0001$ by Mann-Whitney test; Hela: shControl 55.8±18 minutes and shMad2 44.4±8.4 minutes with $p<0.0001$ by Mann-Whitney test) (right panel Figure 3.6). Nevertheless, in SAC-perturbed cells duration of mitosis was kept constant (with low variability) when compared to control cells in the three cell lines tested as shown by mean absolute deviation values (MCF10A: shControl=0.10 and shMad2=0.073; RPE: shControl=0.10 and shMad2=0.049; Hela: shControl=0.23 and shMad2=0.12) (right panel Figure 3.6).

Importantly, even in the partial absence of SAC, there was a high correlation between duration of G1-phase and cell cycle length in all the three cell lines used (Pearson correlation coefficient, r – MCF10A: shControl=0.70 and shMad2=0.76; RPE: shControl=0.78 and shMad2=0.72; Hela: shControl=0.51 and shMad2=0.67) (left panel Figure 3.7). However, perturbing expression of Mad2 and SAC had no effect on the modularity of mitotic time in relation to total cell cycle length, as seen by the lack of correlation between duration of mitosis and cell cycle time in all cell lines tested (Pearson correlation coefficient, r – MCF10A: shControl=0.36 and shMad2=0.21; RPE: shControl=0.21 and shMad2=0.19; Hela: shControl=0.28 and shMad2=0.17) (right panel Figure 3.7).

Collectively, these results suggest that although SAC is important for the duration of mitosis, it is not the molecular mechanism that keeps duration of mitosis short, constant, and temporally insulated from duration of upstream cell cycle events.

3.5. Positive feedback keeps mitosis temporally insulated from variability of early cell cycle events

Mitotic entry is initiated by a bistable trigger, which is thought to be the basis for a unidirectional and irreversible entry and progression through mitosis (Novak and Tyson, 1993b; Pomerening et al., 2003; Santos et al., 2012; Sha et al., 2003). This bistability is possible because of the switch-like activation of Cdk1 and the spatial redistribution of Cdk1-cyclin B1 complexes due to positive feedback control at the onset of mitosis (Pomerening et al., 2003; Santos et al., 2012; Sha et al., 2003; Tyson and Novak, 2001). Compromising the explosive activation and nuclear import of Cdk1-cyclin B1 has been shown to affect progression through mitosis (Holt et al., 2008; Santos et al., 2012), making positive feedback at mitotic onset a good candidate for the molecular mechanism that keeps duration of mitosis short and relatively constant.

3.5.1. Experimental design to test the role of positive feedback in the temporal modularity of mitosis

Cdk1 activity is required for mitotic entry and progression through mitosis. As illustrated in Figure 3.8, according to the quantitative model for cell cycle progression it is likely that early mitotic events (t_1) require low levels of Cdk1 activity and late mitotic events (t_2) require high levels of Cdk1 activity. In addition, the presence of positive feedback regulation in the activation of Cdk1 gives rise to an explosive, sharp, sigmoidal activation of Cdk1. In such scenario, it is expected that regardless of when a cell enters mitosis, timing between an early and late mitotic event ($\Delta t=t_2-t_1$) should remain short and fairly constant. Consequently, no correlation is expected between when individual cells initiate mitosis (t_1) and duration of mitosis (Δt) (top panel Figure 3.8.A). Breaking positive feedback will compromise the switch-like activation of Cdk1. This will result in a slower and more variable entry and progression through mitosis (Santos et al., 2012). In this scenario, depending on to what extent positive feedback is compromised, cells that entered mitosis early might finish mitosis early as compared to cells that entered mitosis later. Therefore, this may result in a correlation (or coupling) between time when individual cells entered mitosis (t_1) and the duration of mitosis (Δt) (bottom panel Figure 3.8.A).

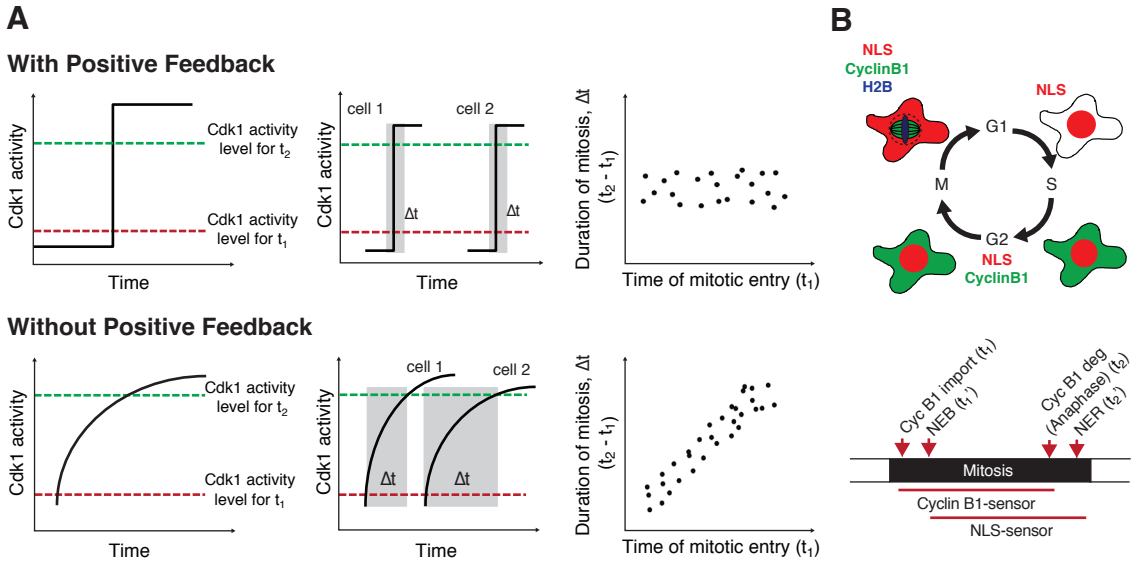


Figure 3.8. Schematic of the experimental design to test wheter positive feedback keeps duration of mitosis constant and uncoupled from previous cell cycle events. A. Expected Cdk1 activation profile and time between an early and a late mitotic event in the presence (top) and absence (bottom) of positive feedback. **B.** Schematic of stable cell lines and biosensors used to measure Cdk1 activity and early (Cyclin B1 import and NEB) and late (Cyclin B1 degradation – anaphase – and NER) mitotic events (more information about the biosensors in section 2.5.2.3).

To test the hypothesis that positive feedback underlies the temporal insulation of mitosis, Cdk1 activation and early and late mitotic events were measured in the presence and absence of positive feedback in single cells. MCF10A, RPE, and Hela cells stably expressing Cyclin B1-YFP, NLS-mCherry and H2B-Turquoise biosensors were used (section 2.5.2.3 and Figure 3.8.B). Cyclin B1 nuclear translocation was used as a proxy of Cdk1 activation, since its nuclear translocation depends on direct phosphorylation by Cdk1 that is crucial for Cyclin B1 redistribution at onset of mitosis (Gavet and Pines, 2010; Pines and Hunter, 1991; Santos et al., 2012).

Early mitotic events (t_1) were measured as Cyclin B1 nuclear import, as well as time of nuclear envelope breakdown (NEB) as determined by H2B-Turquoise localisation. Time of Cyclin B1 degradation, as well as nuclear envelope reformation (NER), were measured as late mitotic events (t_2). Duration of mitosis (Δt) was estimated as the time between Cyclin B1 import and its degradation and/or the time between NEB and NER (Figure 3.8.B). To perturb positive feedback, cells were treated with the small molecule PD166285 (Wee1 inhibitor), a specific Myt1/Wee1 inhibitor (Hashimoto et al., 2006).

3.5.2. Switch-like activation of Cdk1 is compromised when positive feedback is perturbed

At mitosis onset, Cdk1 is activated in a switch-like manner due to positive feedback control. To quantitatively measure Cdk1 activity, time courses of Cdk1 activity in individual cells were fitted to the logistic equation and rise times were calculated from the curve fits for all cells. As expected, in control cells Cdk1 activity had a sharp sigmoidal curve, typical of explosive activation (left panel of Figure 3.9). The fitted rise time is 4.0±1.2 minutes in MCF10A control cells and 6.6±1.3 minutes in Hela control cells. However, in cells treated with Wee1 inhibitor, the sharpness of the curve was lost (right panel of Figure 3.9). Cdk1 activity was a lot more graded as seen by the increased rise time of Cdk1 activation curves – 10.8±3.4 minutes in MCF10A cells and 17.4±7.8 minutes in Hela cells.

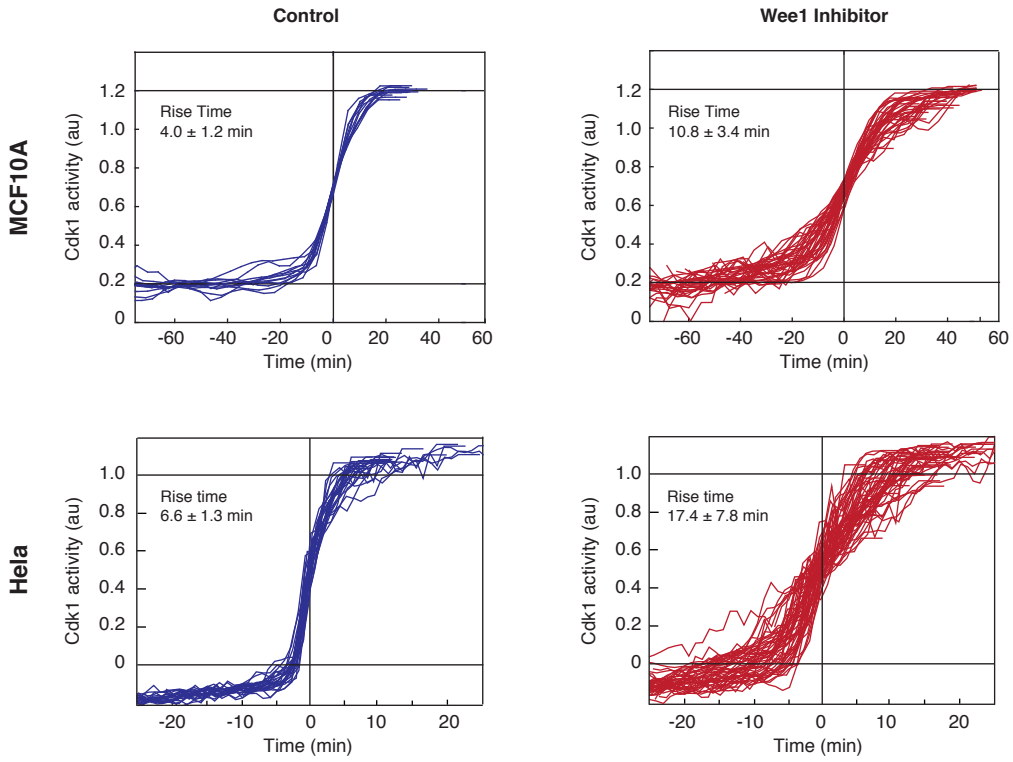


Figure 3.9. Breaking positive feedback results in a graded Cdk1 activation. Quantification of Cdk1 activity over time in MCF10A (top panel) and Hela (bottom panel) cells in the absence (blue) or presence (red) of 1μM of Wee1 inhibitor (PD166285). Individual time courses were fitted to the logistic equation $y=a+b/1+e^{-(t-t0/\tau)}$ and were scaled to their fitted maximum and minimum values (b and a, respectively) and half-maximal times (t0). Rise times (τ) were calculated from the curve fits for all cells and are expressed as Mean ± standard deviation (n>20). Cyclin B1 import was used as a proxy to quantify Cdk1 activity, straight after adding DMSO or Wee1 inhibitor.

3.5.3. Perturbing positive feedback makes mitosis variable

Next it was questioned what was the effect of perturbing positive feedback in duration of mitosis. Positive feedback was perturbed using a range of Wee1 inhibitor concentrations in order to tune the strength of the feedback and duration of mitosis was measured as the time between NEB and NER. Independently of the concentration of the inhibitor used, MCF10A, RPE and Hela cells with compromised positive feedback took longer to complete mitosis and in fact some cells were never able to finish (Figure 3.10). This could be due to cells not being able to satisfy the spindle assembly checkpoint requirements and/or activation of APC-cdc20. These results clearly show that when the positive feedback is broken, mitosis is not short and constant anymore.

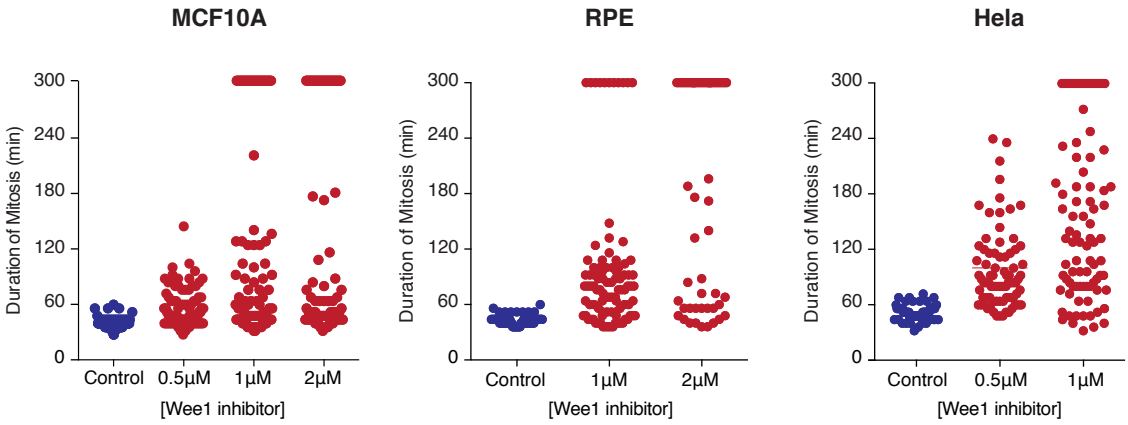


Figure 3.10. Perturbing positive feedback results in a longer and more variable duration of mitosis. Duration of mitosis in MCF10A, RPE and Hela cells stably expressing Cyclin B1-YFP, NLS-mCherry and H2B-Turquoise in the absence (blue) or presence (red) of Wee1 inhibitor (PD166285) at the shown concentrations. DMSO was used as control (n>100). Percentage of cells that entered mitosis but never exited it (300min dots) when treated with Wee1 inhibitor: MCF10A 1μM 24.7% and MCF10A 2μM 45.3%; RPE 1μM 11.6% and RPE 2μM 50.0%; Hela 1μM 23.1%.

3.5.4. Positive feedback keeps mitotic events synchronised

Positive feedback regulation is a recurrent motif in cell cycle control and various functions have been attributed to this type of regulation - for example, keeping synchronicity between cell cycle events (Holt et al., 2008; Skotheim et al., 2008). So, then it was checked whether early and late mitotic events were synchronised in control and Wee1 inhibitor treated cells.

Cyclin B1 nuclear import and time of nuclear envelope breakdown (NEB) were used as early mitotic event and anaphase (time of Cyclin B1 degradation) and nuclear envelope reformation (NER) were used as late mitotic events. In addition to making mitosis time longer and variable, perturbing positive feedback also resulted in loss of synchronicity between early (Cyclin B1 import and NEB) and late mitotic events (Cyclin B1 degradation and NER) in MCF10A, RPE, and Hela cells, as shown in Figure 3.11. This suggests that positive feedback is not only important to keep mitosis short and constant, but also to keep synchronicity between mitotic events which might be essential for cell survival.

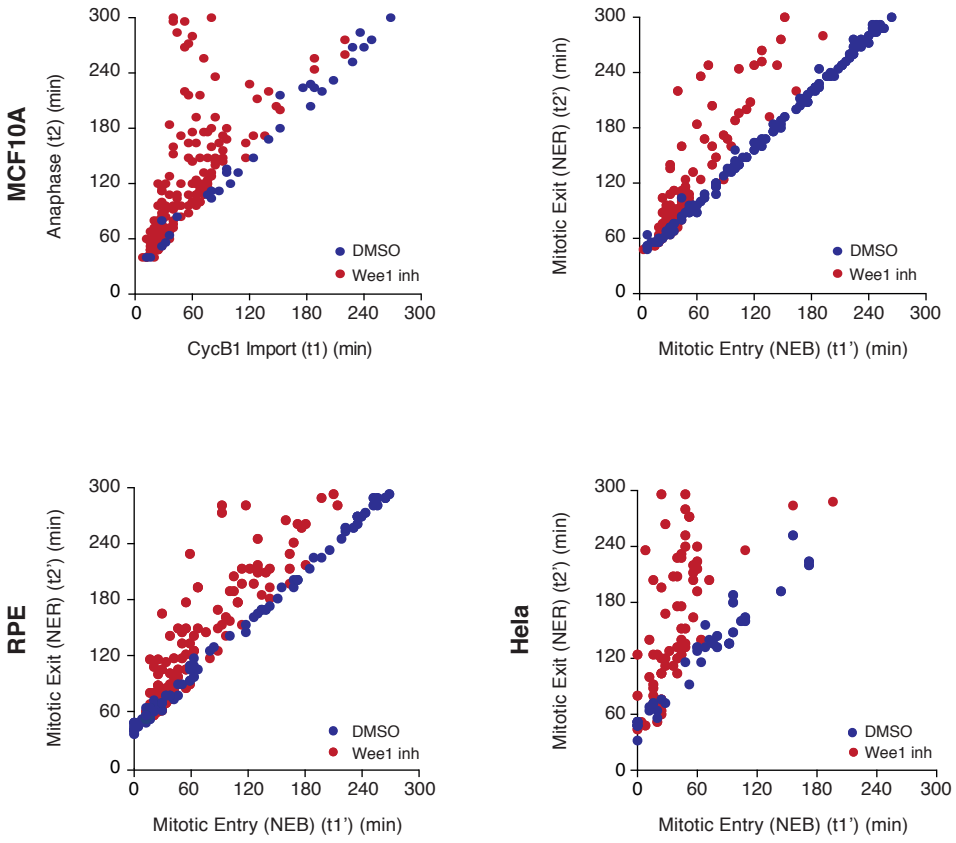


Figure 3.11. Positive feedback keeps early and late mitotic events in sync. All lines stably expressed Cyclin B1-YFP, NLS-mCherry and H2B-Turquoise. **Top panel –** Time of anaphase as a function of Cyclin B1 nuclear import (left) and time of NER as a function of NEB (right) in MCF10A cells either treated with DMSO (blue) or with Wee1 inhibitor (red). **Bottom panel –** Time of NER as a function of NEB in RPE (left panel) and Hela (right panel) cells either treated with DMSO (blue) or with Wee1 inhibitor. NEB – nuclear envelope breakdown, NER – nuclear envelope reformation (n>100).

3.5.5. Positive feedback ensures that duration of mitosis is coupled with mitotic entry

So far, it was possible to point out two consequences of perturbing positive feedback of mitotic entry: mitosis duration became variable and the synchronicity between mitotic events was lost (Figure 3.10 and Figure 3.11). But what happens in terms of coupling duration of mitosis with mitotic entry?

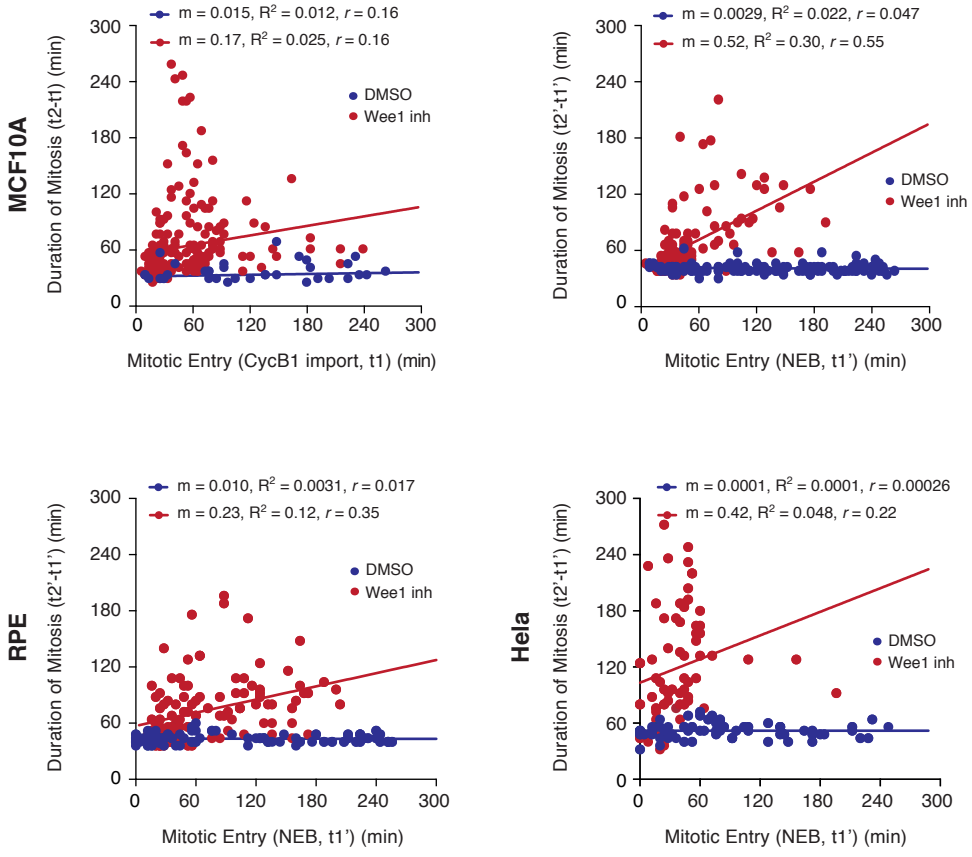


Figure 3.12. Perturbing positive feedback makes duration of mitosis correlate with when cells enter mitosis. All lines stably expressed Cyclin B1-YFP, NLS-mCherry and H2B-Turquoise. **Top panel –** Duration of mitosis as a function of Cyclin B1 nuclear import (left) and time of duration of mitosis as a function of NEB (right) in MCF10A cells either treated with DMSO (blue) or with Wee1 inhibitor (red). **Bottom panel –** Duration of mitosis as a function of NEB in RPE (left panel) and Hela (right panel) cells either treated with DMSO (blue) or with Wee1 inhibitor. Slope of the trend line (m), coefficient of determination (R^2) and Pearson correlation coefficient (*r)* are shown (n>100).

In order to answer this question, cells were either treated with DMSO or Wee1 inhibitor and the time of Cyclin B1 import (t1) or the NEB (t1′) used as mitotic entry time and the duration of mitosis measured as the time between either Cyclin B1 import (t1) and anaphase (t2) or NEB (t1′) and NER (t2′). In control cells with intact feedback regulation, the length of mitosis was kept constant and there was no correlation between the time at which cells entered mitosis (t1 and t1′) and duration of mitosis (t2-t1 or t2′-t1′), suggesting that these events are independent (Pearson correlation coefficient, *r* – MCF10A=0.047, RPE=0.017, Hela=0.00026 for duration of mitosis as a function of NEB; MCF10A=0.16 for duration of mitosis as a function of Cyclin B1 degradation) (Figure 3.12).

Perturbing positive feedback coupled duration of mitosis with the time at which individual cells entered mitosis (Figure 3.12). When positive feedback was compromised, there was a correlation between the time at which cells entered mitosis and duration of mitosis (Pearson correlation coefficient, *r* – MCF10A=0.55, RPE=0.35, Hela=0.22 for duration of mitosis as a function of NEB; MCF10A=0.16 for duration of mitosis as a function of Cyclin B1 degradation). Measuring early and late events with both Cyclin B1-YFP and NLS-mCherry biosensors provided similar results (top panel Figure 3.12). Taken together, these results suggest that positive feedback is important to keep mitotic events synchronised and the time of mitosis insulated from variability in previous cell cycle events.

3.5.6. When positive feedback is compromised, duration of mitosis becomes coupled with upstream cell cycle events

In the beginning of this chapter it was shown that duration of G1-, S- and G2-phases are well correlated with the overall cell cycle length but mitotic time was temporally insulated from variability in previous cell cycle phases. So, next it was addressed whether breaking positive feedback would make duration of mitosis coupled with cell cycle length. The time between two consecutive NER events was measured as cell cycle length and the time between NEB and NER was measured as duration of mitosis in cells treated with either DMSO or Wee1 inhibitor.

Measuring the cell cycle length between two consecutive divisions showed that perturbing positive feedback was sufficient to couple variability in cell cycle length to duration of mitosis in all the cell lines tested (Pearson correlation coefficient, *r* – MCF10A=0.53, Hela=0.83) (Figure 3.13). This experiment strongly indicates that positive feedback is the molecular mechanism responsible for keeping duration of mitosis temporally insulated from variability of upstream cell cycle events.

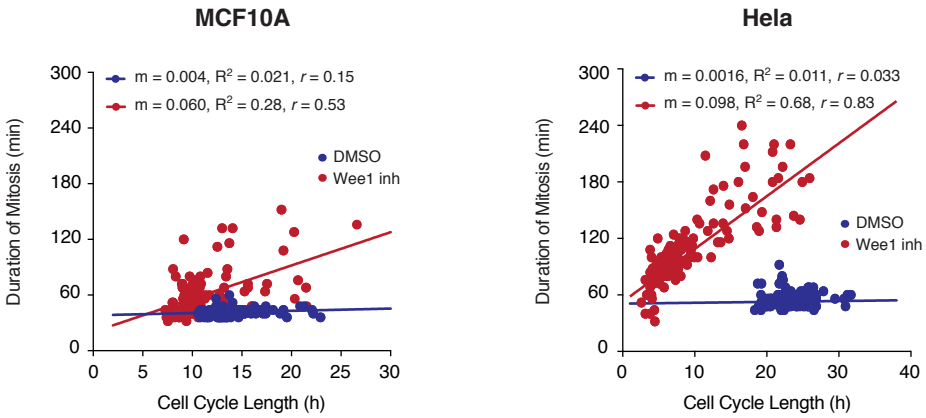


Figure 3.13. Positive feedback keeps mitosis temporally insulated from upstream cell cycle events. All lines stably expressed Cyclin B1-YFP, NLS-mCherry and H2B-Turquoise. Duration of mitosis measured by the time between NEB and NER as a function of cell cycle length in the presence (red) or absence (blue) of Wee1 inhibitor in MCF10A and Hela cells. Slope of the trend line (m), coefficient of determination (R^2) and Pearson correlation coefficient (r) are shown (n>100).

3.5.7. Positive feedback and not SAC affects temporal insulation of mitosis

In order to abolish the contribution of SAC in the temporal insulation of mitosis, positive feedback was compromised using Wee1 inhibitor in the absence of the checkpoint activation. SAC was perturbed in two different ways: either by using cell lines stably expressing shMad2, or by using a specific SAC inhibitor – Reversine – that targets the kinase Msp1 (Santaguida et al., 2010). The MCF10A, RPE, and Hela cell lines used in this study were also expressing NLS-mCherry in order to measure mitotic events and showed downregulation of about 20-40% of Mad2, which allowed the cells to be viable and kept in culture (Figure 3.14). Cells were incubated with Reversine 30 minutes prior to adding Wee1 inhibitor and imaged for 5 hours post-treatment in order to measure the duration of mitosis and mitotic events.

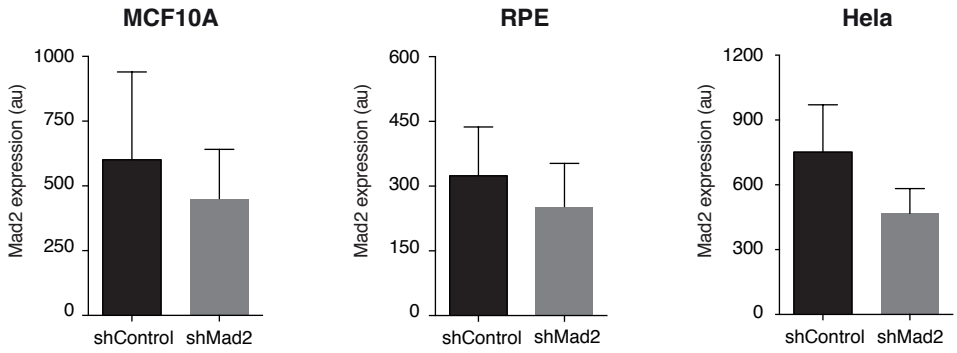


Figure 3.14. Mean expression of Mad2 in MCF10A, RPE and Hela cells stably expressing shMad2 and NLS-mCherry. The cells lines stably express shControl (shScramble) or shMad2 and NLS-mCherry. Mean expression of Mad2 was measured using immunofluorescence with the antibody MAD2 (BD-Biosciences, cat. no. 610678). Mean ± standard deviation is shown for each cell line (n>5000).

3.5.7.1. SAC has no effect on the variability of mitosis duration and synchronicity of mitotic events in the presence of Wee1 inhibitor

The duration of mitosis was measured as the time between NEB and NER in MFC10A, RPE and Hela cells treated with DMSO or Wee1 inhibitor without (shEmpty Vector or shScramble) or with (shMad2) perturbation of the spindle assembly checkpoint. As seen previously, in control cells duration of mitosis decreased when SAC was downregulated (MCF10A: shEmpty Vector 37.5±4.2 minutes, shScramble 37.9±5.1 minutes and shMad2 28.9±4.6 minutes with $p<0.0001$ between shEmpty Vector and shMad2 and between shScramble and shMad2, $p>0.7$ between shEmpty Vector and shScramble, by Mann-Whitney test; RPE: shScramble 43.9±4.5 minutes and shMad2 34.7±3.4 minutes with $p<0.0001$ by Mann-Whitney test; Hela: shScramble 40.1±9.6 minutes and shMad2 30.0±8.0 minutes with $p<0.0001$ by Mann-Whitney test), but mitotic duration remained constant (left panel Figure 3.15).

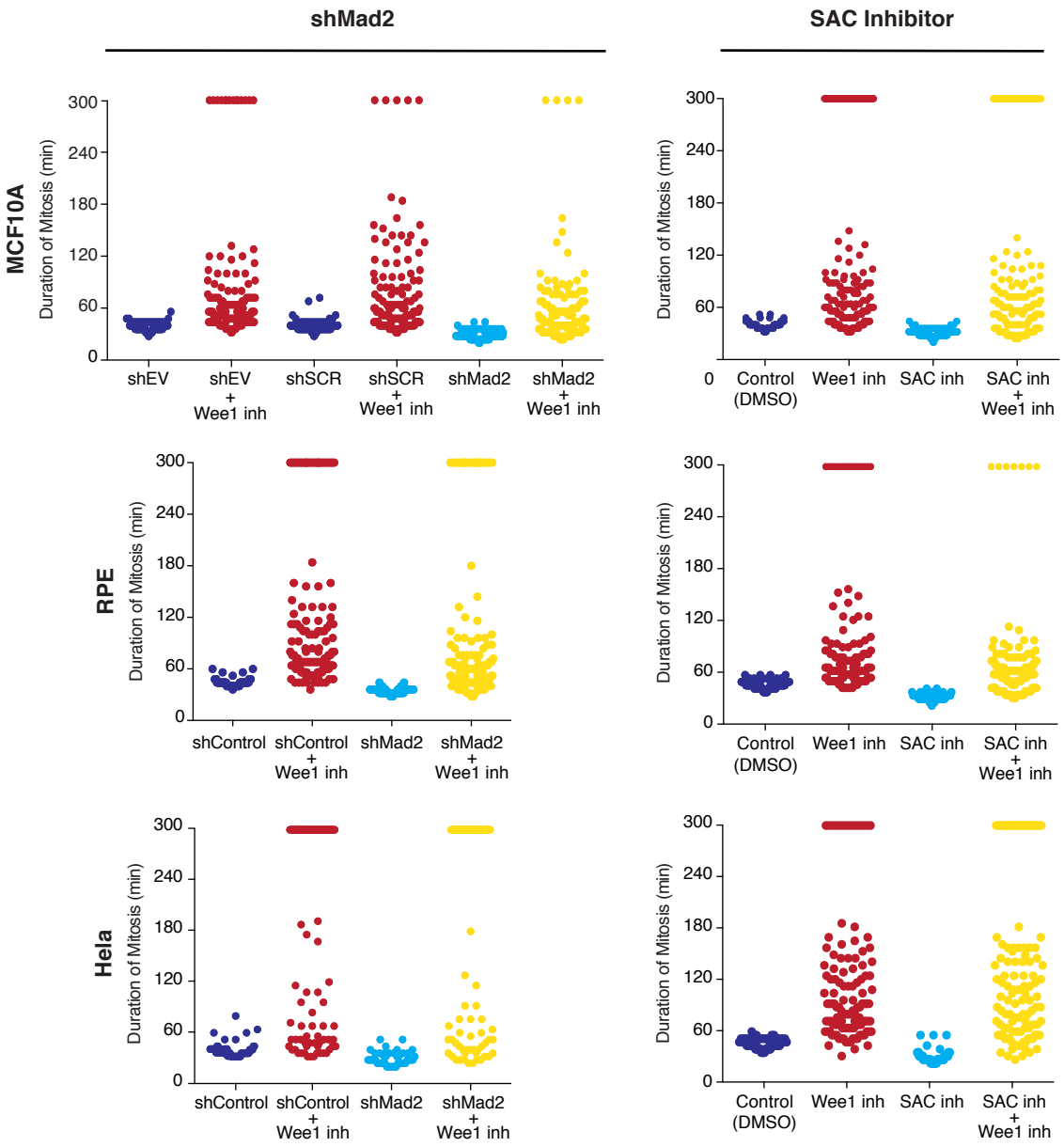


Figure 3.15. Absence of SAC does not make duration of mitosis variable. Left panel – Duration of mitosis measured by the time between NEB and NER in the presence or absence of Wee1 inhibitor in MCF10A, RPE and Hela cells stably expressing NLS-mCherry and shEmpy Vector and/or shScramble as controls or shMad2 for SAC inhibition (n>100). Percentage of cells that entered mitosis but never exited it (300min dots) when treated with Wee1 inhibitor: MCF10A shEV 9.5%, MCF10A shSCR 5.3% and MCF10A shMad2 2.3%; RPE shSCR 17.7% and RPE shMad2 16.7%; Hela shSCR 51.6% and Hela shMad2 53.0%. **Right panel –** Duration of mitosis measured by the time between NEB and NER in MCF10A, RPE, and Hela cells stably expressing NLS-mCherry treated with SAC inhibitor (SAC inh) in the presence or absence of Wee1 inhibitor (Wee1 inh). DMSO was used as control (n>100). Percentage of cells that entered mitosis but never exited it (300min dots) when treated with Wee1 inhibitor: MCF10A+Wee1 inh 28.3%, MCF10A+Sac inh+Wee1 inh 21.0%; RPE+Wee1 inh 14.0%, RPE+Sac inh+Wee1 inh 5.1%; Hela+Wee1 inh 12.4%, Hela+Sac inh+Wee1 inh 22.5%.

Similar results were seen when SAC was perturbed with Reversine; mitosis became shorter and less variable (MCF10A: control 39.6±4.5 minutes and Sac inh 30.7±4.2 minutes with $p<0.0001$ by Mann-Whitney test; RPE: control 43.96±4.9 minutes and Sac inh 29.5±3.8 minutes with $p<0.0001$ by Mann-Whitney test; Hela: control 49.8±5.2 minutes and Sac inh 33.9±5.7 minutes with $p<0.0001$ by Mann-Whitney test) (right panel Figure 3.15). When positive feedback was perturbed using Wee1 inhibitor, mitosis became longer and more variable in both control cells and either SAC downregulated cells or SAC inhibited cells, as shown in Figure 3.15. It was only when positive feedback was compromised that mitotic duration was variable and longer.

Next it was investigated whether synchronicity between early and late mitotic events was affected by a compromised SAC. NEB was measured as an early mitotic event and NER as a late mitotic event in MCF10A, RPE and Hela cells in the presence and absence of positive feedback. SAC downregulation alone was not able to interfere with the synchronicity between early and late mitotic events (Pearson correlation coefficient, r – MCF10A shControl=1.0 and shMad2=1.0, RPE shControl=1.0 and shMad2=1.0, Hela shControl=0.97 and shMad2=1.0 for time of NER as a function of NEB). It was only when positive feedback was perturbed that timing between early and late mitotic events became unsynchronized (Pearson correlation coefficient, r – MCF10A shControl+Wee1 inh=0.90 and shMad2+Wee1 inh=0.96, RPE shControl+Wee1 inh=0.93 and shMad2+Wee1 inh=0.94, Hela shControl+Wee1 inh=0.87 and shMad2+Wee1 inh=0.90 for time of NER as a function of NEB) (left panel Figure 3.16). Similar results were observed when SAC was inhibited with Reversine in the presence or absence of positive feedback inhibitor. Cells where only SAC was inhibited showed similar results to control cells, where there was synchronicity between early and late mitotic events (Pearson correlation coefficient, r – MCF10A Control=1.0 and SAC inh=1.0, RPE Control=1.0 and SAC inh=1.0, Hela Control=1.0 and SAC inh=1.0 for time of NER as a function of NEB). When positive feedback was compromised in the absence or presence of SAC inhibitor, cells lost the synchronicity between early and late mitotic events (Pearson correlation coefficient, r – MCF10A Wee1 inh=0.90 and SAC Inh+Wee1 inh=0.96, RPE Wee1 inh=0.95 and SAC Inh+Wee1 inh=0.97, Hela Wee1 inh=0.87 and SAC Inh+Wee1 inh=0.74 for time of NER as a function of NEB) (right panel Figure 3.16). Positive feedback seems to be the only mechanism involved in keeping mitotic events synchronized.

Taken together, these results suggest that SAC has no role in making mitosis short and constant and keeping mitotic events synchronized, whereas positive feedback seems to be involved in regulation of all these features of mitosis.

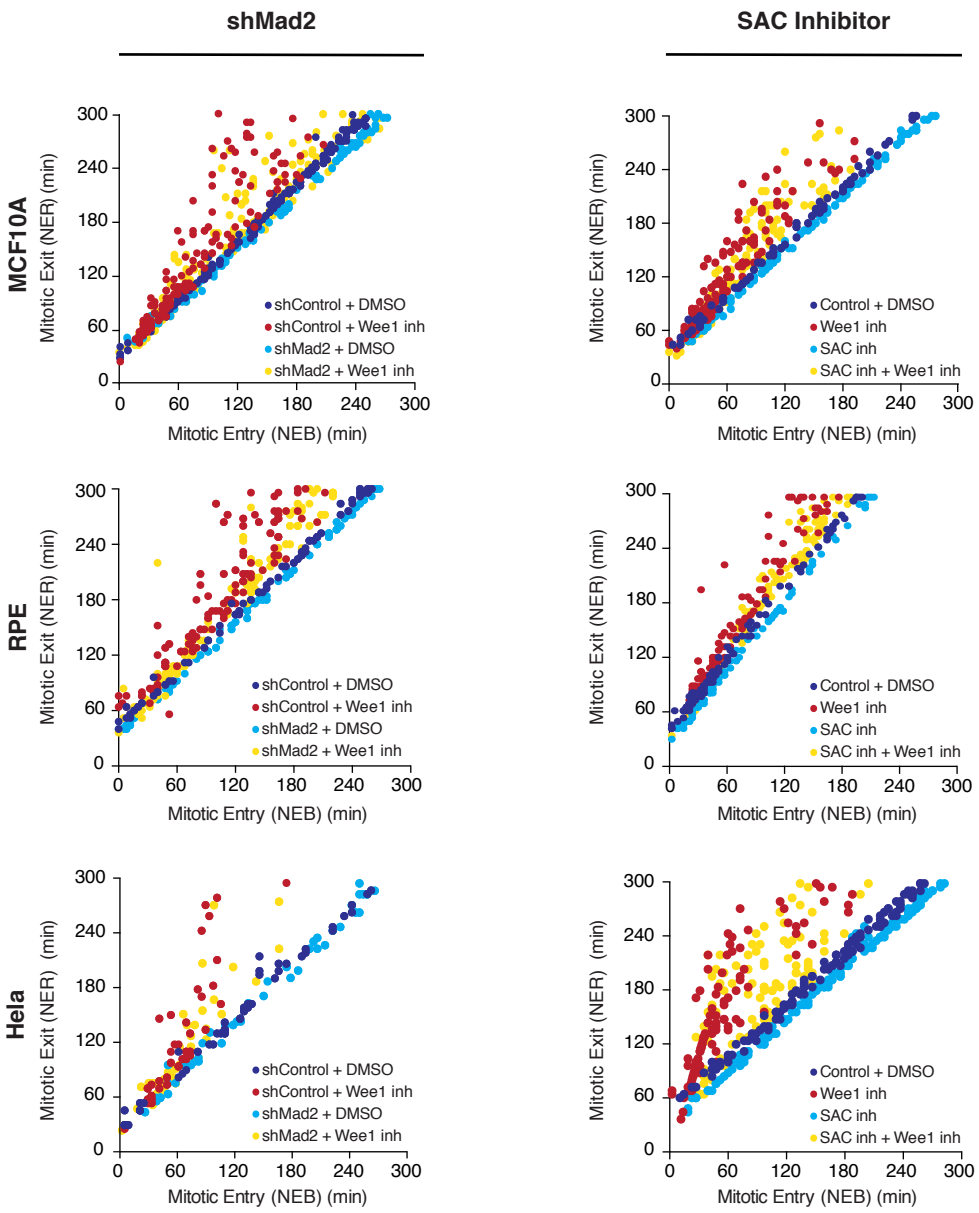


Figure 3.16. SAC has no role in keeping mitotic events synchronized. All cell lines stably expressed NLS-mCherry. **Left panel –** Time of mitotic exit (NER) as a function of mitotic entry (NEB) in control (shScramble) and SAC perturbed (shMad2) MCF10A, RPE, and Hela cells. Cells were either treated with DMSO or Wee1 inhibitor (n>100). **Right panel –** Time of mitotic exit (NER) as a function of time of entry into mitosis (NEB) in control (DMSO) and SAC inhibitor (SAC inh) treated MCF10A, RPE, and Hela cells in the presence or absence of Wee1 inhibitor (Wee1 inh). NEB – nuclear envelope breakdown, NER – nuclear envelope reformation (n>100).

3.5.7.2. SAC does not contribute to temporal insulation of mitosis

Next it was addressed whether SAC is important to couple duration of mitosis (NEB-NER) with time of mitotic entry (NEB). Similarly to the results shown in section 3.4, cells with downregulated SAC behaved very similarly to control cells, where time of mitotic entry was not correlated with duration of mitosis (Pearson correlation coefficient, *r* – MCF10A shControl=0.078 and shMad2=0.020, RPE shControl=0.038 and shMad2=0.096, Hela shControl=0.0053 and shMad2=0.10 for duration of mitosis as a function of NEB). It was only when positive feedback was perturbed that time of mitotic entry was correlated with duration of mitosis, in both the presence and absence of SAC downregulation (Pearson correlation coefficient, *r* – MCF10A shControl+Wee1 inh=0.52 and shMad2+Wee1 inh=0.45, RPE shControl+Wee1 inh=0.50 and shMad2+Wee1 inh=0.52, Hela shControl+Wee1 inh=0.53 and shMad2+Wee1 inh=0.56 for duration of mitosis as a function of NEB) (left panel Figure 3.17).

As before, when SAC was perturbed by treatment with Reversine, similar results were observed. In the absence or presence of SAC inhibition alone, no correlation was found between mitotic entry and duration of mitosis (Pearson correlation coefficient, *r* – MCF10A Control=0.25 and SAC inh=0.17, RPE Control=0.20 and SAC inh=0.061, Hela Control=0.0069 and SAC inh=0.0026 for duration of mitosis as a function of NEB). It was only when positive feedback was perturbed (in cells either treated or not treated with SAC inhibitor) that it was observed a correlation between the time at which each cell entered mitosis and duration of mitosis (Pearson correlation coefficient, *r* – MCF10A Wee1 inh=0.61 and SAC inh+Wee1 inh=0.65, RPE Wee1 inh=0.58 and SAC inh+Wee1 inh=0.68, Hela Wee1 inh=0.44 and SAC inh+Wee1 inh=0.001 for duration of mitosis as a function of NEB) (right panel Figure 3.17).

Then it was tested if duration of mitosis was coupled with the overall cell cycle length when positive feedback was perturbed in the presence or absence of SAC inhibition. As had been demonstrated previously in section 3.4, cells in the presence or absence of SAC inhibition (either expressing shMad2 or treated with SAC inhibitor), showed a lack of correlation between duration of mitosis and cell cycle time (Pearson correlation coefficient, *r* – MCF10A shControl=0.14 and shMad2=0.087, Control=0.11 and SAC inh=0.077; Hela Control=0.021 and SAC inh=0.13 for duration of mitosis as a function of cell cycle length) (Figure 3.18). However, when positive feedback was perturbed in the presence or absence of SAC, duration of mitosis became coupled with cell cycle length (Pearson correlation coefficient, *r* – MCF10A shControl+Wee1 inh=0.60 and shMad2+Wee1 inh=0.54, Wee1 inh=0.61 and SAC inh+Wee1 inh=0.45; Hela Wee1 inh=0.86 and SAC inh+Wee1 inh=0.75 for duration of mitosis as a function of cell cycle length) (Figure 3.18).

These results suggest that positive feedback alone and not SAC activation ensures that mitosis is short, constant and temporally uncoupled from upstream cell cycle events.

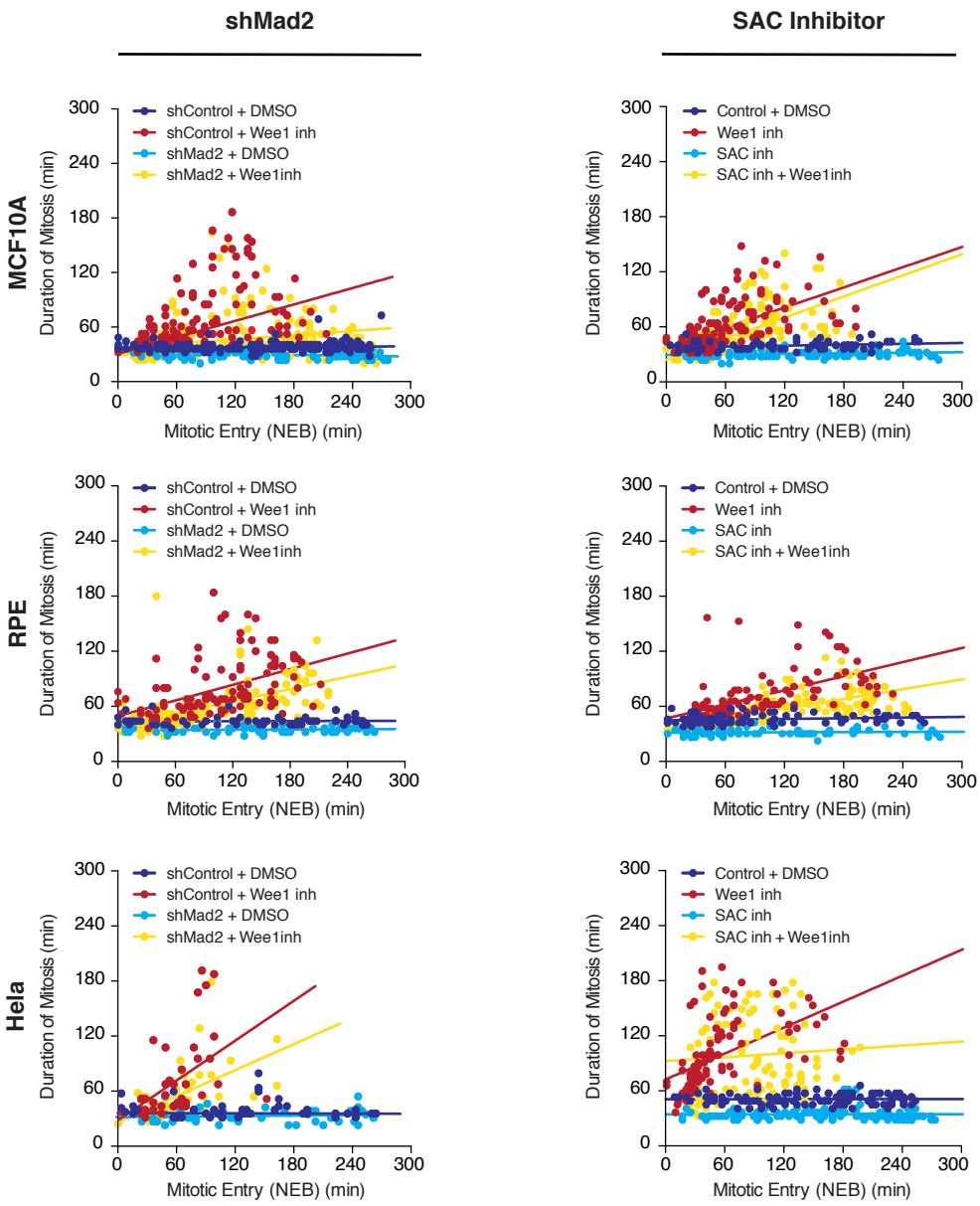


Figure 3.17. SAC inhibition alone cannot uncouple timing of mitotic entry and duration of mitosis. All cell lines stably expressed NLS-mCherry**. Left panel –** Duration of mitosis as a function of mitotic entry (NEB) in control (shSramble) and SAC perturbed (shMad2) MCF10A, RPE and Hela cells. The cells were either treated with DMSO or Wee1 inhibitor (n>100). **Right panel –** Duration of mitosis as a function of mitotic entry (NEB) in control (DMSO) and SAC inhibitied (SAC inh) cells. The cells were wither treated with DMSO or Wee1 inhibitor (Wee1 inh). Trend lines are shown. NEB – nuclear envelope breakdown (n>100).

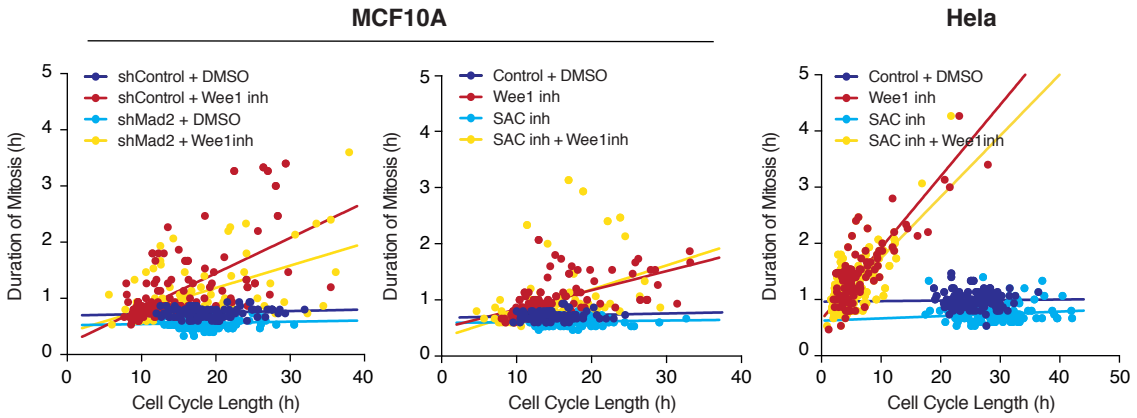


Figure 3.18. SAC does not contribute to duration of mitosis being temporally insulated from duration of upstream cell-cycle events. All cell lines stably expressed NLS-mCherry. **Left panel –** Duration of mitosis as a function of cell cycle length in control (shScramble) and SAC perturbed (shMad2) MCF10A cells. The cells were wither treated with DMSO or Wee1 inhibitor (Wee1 inh) (n>100). **Middle and Right panel –** Duration of mitosis as a function of cell cycle length in control (DMSO) and SAC inhibited (SAC inh) MCF10A and Hela cells. The cells were either treated with DMSO or Wee1 inhibitor (Wee1 inh). Trend lines are shown (n>100).

3.5.8. Breaking Cdk1 activation and spatial positive feedbacks couple duration of mitosis to earlier cell cycle events

In order to rule out the possibility that the results obtained so far were a consequence of inhibiting Wee1 protein, positive feedback regulation was perturbed in three other different ways: firstly, cells were transfected with Cdk1AF (Y14A Y15F), a Cdk1 mutant which cannot be phosphorylated by Wee1; secondly, cells were transfected with Cdc25-CD, a catalytically dead Cdc25C phosphatase that is not able to dephosphorylate tyrosine 15 and activate Cdk1; and finally, cells were treated with Leptomycin B, which blocks the nuclear export of Cyclin B1 and thereby affects the spatial positive feedback needed for mitotic entry (Santos et al., 2012).

MCF10A and Hela cells were transiently transfected with a doxycycline-inducible Cdk1AF construct or with a Cdk1-WT construct, which was used as a control in all the experiments performed. When Cdk1 activity was measured in the presence and absence of positive

feedback, control cells showed a sharp sigmoidal curve as seen before with a fitted rise time of 4.1±1.6 minutes in MCF10A Cdk1-WT cells and 3.5±1.3 minutes in Hela Cdk1-WT cells (left panel Figure 3.19.A and D). In cells expressing Cdk1AF the sharpness of Cdk1 activation curve was lost, becoming steadier as seen by the increased rise time of the curve: 11.9±4.1 minutes in MCF10A cells and 18.6±5.7 minutes in Hela cells (right panel Figure 3.19.A and D). Duration of mitosis also became longer and more variable in both MCF10A and Hela Cdk1AF cells (Figure 3.19.B and E). The only observed difference between this Cdk1AF-based perturbation and the use of Wee1 inhibitor was the fact that using Cdk1AF did not cause cells to fail to finish mitosis. Albeit with a delay, all cells were able to finish mitosis. Moreover, in control cells expressing Cdk1-WT, the length of mitosis (NER-NEB) did not correlate with the time at which individual cells entered mitosis (NEB). However, in the presence of Cdk1AF, duration of mitosis became dependent on the time of mitotic entry - cells that took longer to enter mitosis also took longer to finish it - in both MCF10A and Hela cells (Figure 3.19.C and F).

Cdk1 activation is sharp and explosive due to positive feedback regulation carried out by Wee1 and Cdc25. Cdk1 is kept inactive by a phosphorylation carried out by Wee1. In order to be active, Cdk1 needs to be dephosphorylated by Cdc25C. So, next it was addressed whether perturbing positive feedback in the Cdc25C branch would have the same effects as the ones observed using Wee1 inhibitor or the Cdk1 mutant – Cdk1AF – that affect the Wee1 branch of the positive feedback. Interestingly, the same results were observed. In the presence of Cdc25-CD, Cdk1 activation was more graded with a rise time of 16.5±6.3 minutes in MCF10A cells and 15.2±6.4 minutes in Hela cells (Figure 3.20.A and D). Mitotic duration also became longer (Figure 3.20.B and E), more variable, and correlated with the time at which an individual cell entered mitosis (Figure 3.20.C and F).

The last approach used to test whether positive feedback makes duration of mitosis temporally insulated was to perturb the spatial positive feedback that regulates Cdk1-cyclin B1 sharp redistribution from the cytoplasm to the nucleus at mitotic onset. The basis of this spatial positive feedback is that Cyclin B1 phosphorylation by Cdk1 promotes nuclear localization which in turn promotes more Cyclin B1 phosphorylation (Santos et al., 2012). The sharp Cdk1-cyblin B1 nuclear translocation was perturbed by treating cells with Leptomycin B, which is a potent and specific nuclear export inhibitor. Leptomycin B caused a gradual activation of Cdk1 instead of a switch-like activation as seen in control cells (Figure 3.21.A and D), likely due to a passive accumulation of nuclear Cyclin B1. As for all the other perturbations tested, cells treated with Leptomycin B had longer and more variable duration of mitosis when compared to cells treated with DMSO for both MCF10A and Hela cell lines (Figure 3.21.B and E). Cells treated with Leptomycin B also showed correlation between time of mitotic entry and duration of mitosis, as opposed to DMSO-treated cells where no correlation was found (Figure 3.21.C and F).

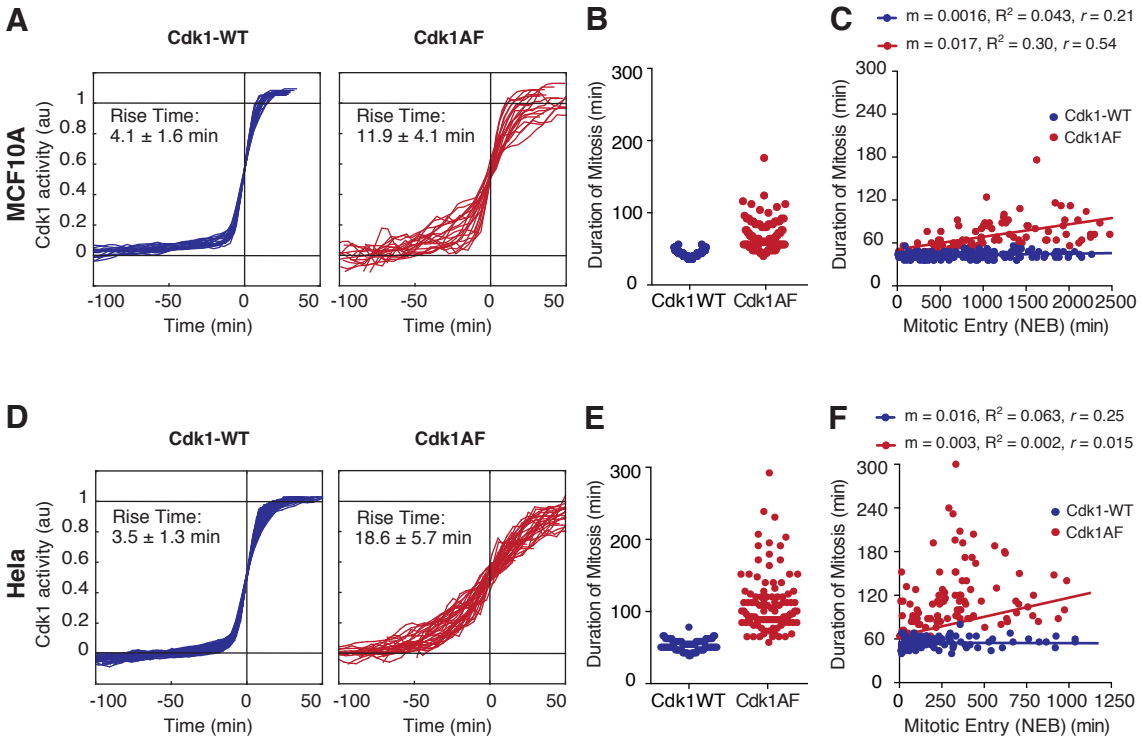


Figure 3.19. Cdk1AF expression makes duration of mitosis longer, more variable, and dependent on time of mitotic entry. A. Quantification of Cdk1 activation over time in MCF10A cells expressing Cdk1-wt (blue) or Cdk1AF (red). The time courses of individual cells were fitted as described in Figure 3.9. Rise times (t) were calculated from the curve fits for all cells and are expressed as Mean ± standard deviation (n>20). **B.** Duration of mitosis (NER-NEB) in MCF10A cells ectopically expressing Cdk1-wt (blue) or Cdk1AF (red) (n>100). **C.** Duration of mitosis as measured by the time between NEB and NER and the onset of mitosis (NEB) in MCF10A cells expressing Cdk1-wt (blue) or Cdk1AF (red). Slope of the trend line (m), coefficient of determination (R^2) and Pearson correlation coefficient (r) are shown (n>100). **D.** Quantification of Cdk1 activation over time in Hela cells expressing Cdk1-wt (blue) or Cdk1AF (red) (n>20). The time courses of individual cells were fitted as described in Figure 3.9. Rise times (t) were calculated from the curve fits for all cells and are expressed as Mean ± standard deviation. **E.** Duration of mitosis (NER-NEB) in Hela cells ectopically expressing Cdk1-wt (blue) or Cdk1AF (red) (n>100). **F.** Duration of mitosis as measured by the time between NEB and NER and the onset of mitosis (NEB) in Hela cells expressing Cdk1-wt (blue) or Cdk1AF (red). Slope of the trend line (m), coefficient of determination (R^2) and Pearson correlation coefficient (r) are shown (n>100).

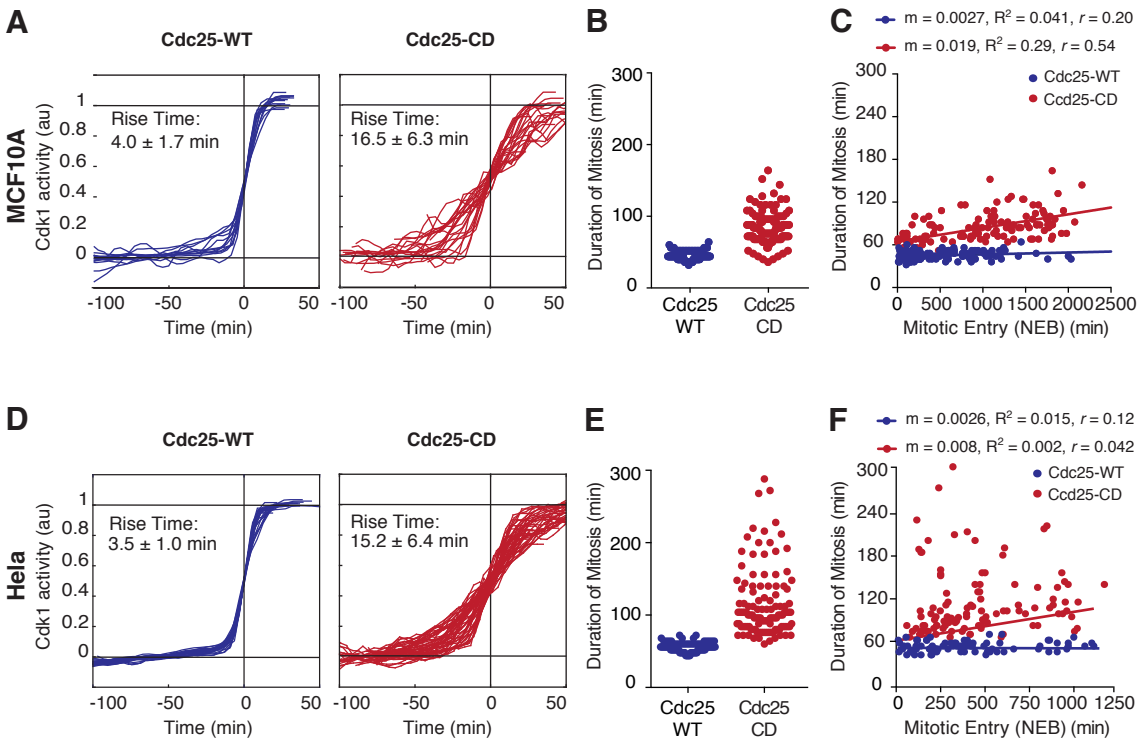


Figure 3.20. Cdc25-CD expression makes mitotic duration coupled with mitotic entry. A. Quantification of Cdk1 activation over time in MCF10A cells expressing Cdc25-WT (blue) or Cdc25-CD (red). The time courses of individual cells were fitted as described in Figure 3.9. Rise times (t) were calculated from the curve fits for all cells and are expressed as Mean ± standard deviation (n>20). **B.** Duration of mitosis (NER-NEB) in MCF10A cells ectopically expressing Cdc25-WT (blue) or Cdc25-CD (red) (n>100). **C.** Duration of mitosis as measured by the time between NEB and NER and the onset of mitosis (NEB) in MCF10A cells expressing Cdc25-WT (blue) or Cdc25-CD (red). Slope of the trend line (m), coefficient of determination (R^2) and Pearson correlation coefficient (*r*) are shown (n>100). **D.** Quantification of Cdk1 activation over time in Hela cells expressing Cdc25-WT (blue) or Cdc25-CD (red). The time courses of individual cells were fitted as described in Figure 3.9. Rise times (t) were calculated from the curve fits for all cells and are expressed as Mean ± standard deviation (n>20). **E.** Duration of mitosis (NER-NEB) in Hela cells expressing Cdc25-WT (blue) or Cdc25-CD (red) (n>100). **F.** Duration of mitosis as measured by the time between NEB and NER and the onset of mitosis (NEB) in Hela cells expressing Cdc25-WT (blue) or Cdc25-CD (red). Slope of the trend line (m), coefficient of determination (R^2) and Pearson correlation coefficient (*r*) are shown (n>100).

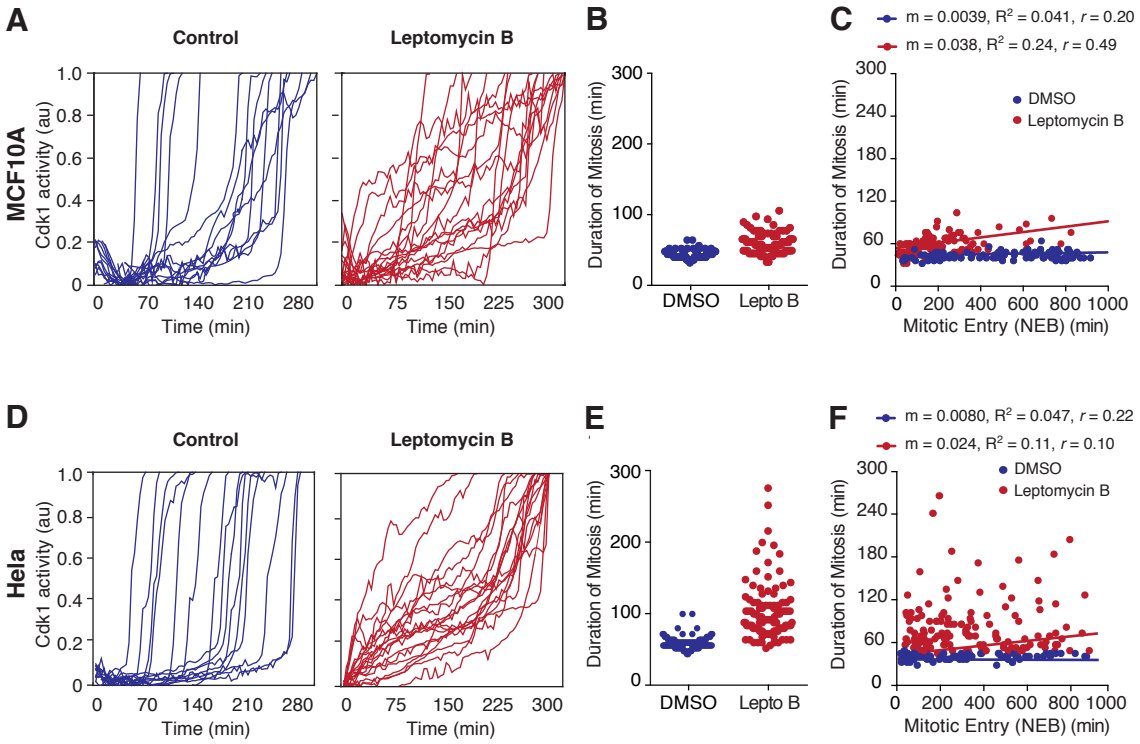


Figure 3.21. Leptomycin B treatment makes duration of mitosis longer and more variable. A. Quantification of Cdk1 activation over time in MCF10A cells in the absence (blue) or presence (red) of Leptomycin B (n>20). **B.** Duration of mitosis (NER-NEB) in MCF10A cells in the absence (blue) or presence (red) of Leptomycin B (n>100). **C.** Duration of mitosis as measured by the time between NEB and NER and the onset of mitosis (NEB) in MCF10A cells in the absence (blue) or presence (red) of Leptomycin B. Slope of the trend line (m), coefficient of determination (R^2) and Pearson correlation coefficient (*r*) are shown (n>100). **D.** Quantification of Cdk1 activation over time in Hela cells in the absence (blue) or presence (red) of Leptomycin B (n>20). **E.** Duration of mitosis (NER-NEB) in Hela cells in the absence (blue) or presence (red) of Leptomycin B (n>100). **F**. Duration of mitosis as measured by the time between NEB and NER and the onset of mitosis (NEB) in Hela cells in the absence (blue) or presence (red) of Leptomycin B. Slope of the trend line (m), coefficient of determination (R^2) and Pearson correlation coefficient (*r*) are shown (n>100).

The fact that similar effects on mitosis were observed for all positive feedback perturbation methods reinforces the conclusion that positive feedback is the molecular mechanism underlying the temporal insulation of mitosis, rather than any unrelated effects as a result of these treatments. All these approaches to perturb positive feedback regulation rendered Cdk1 activation more graded, duration of mitosis longer and more variable, and couple duration of mitosis to time of mitotic entry.

3.5.9. Compromising positive feedback compromises cell viability

All the results observed so far indicate that positive feedback has a crucial role in keeping mitosis short and constant, mitotic events synchronized, and duration of mitosis temporally insulated from variability of earlier cell cycle events. Then it was addressed whether positive feedback is also important for the viability of the new born cells. MCF10A cells were treated with DMSO (as control) or with Wee1 Inhibitor and were imaged for 24 hours in order to follow the cell cycle of their daughter cells. As predicted, perturbing positive feedback not only compromises duration of mitosis and mitotic events in the mother cells but also affects successive cell cycles, i.e. that of the daughter cells (Figure 3.22.A). Breaking positive feedback induced cell death during mitosis or shortly after, so daughter cells never reached a second round of mitotic division (Figure 3.22.B). This suggests that a short and constant mitosis uncoupled from variability in upstream events is a crucial property for fidelity of cell division and cell survival.

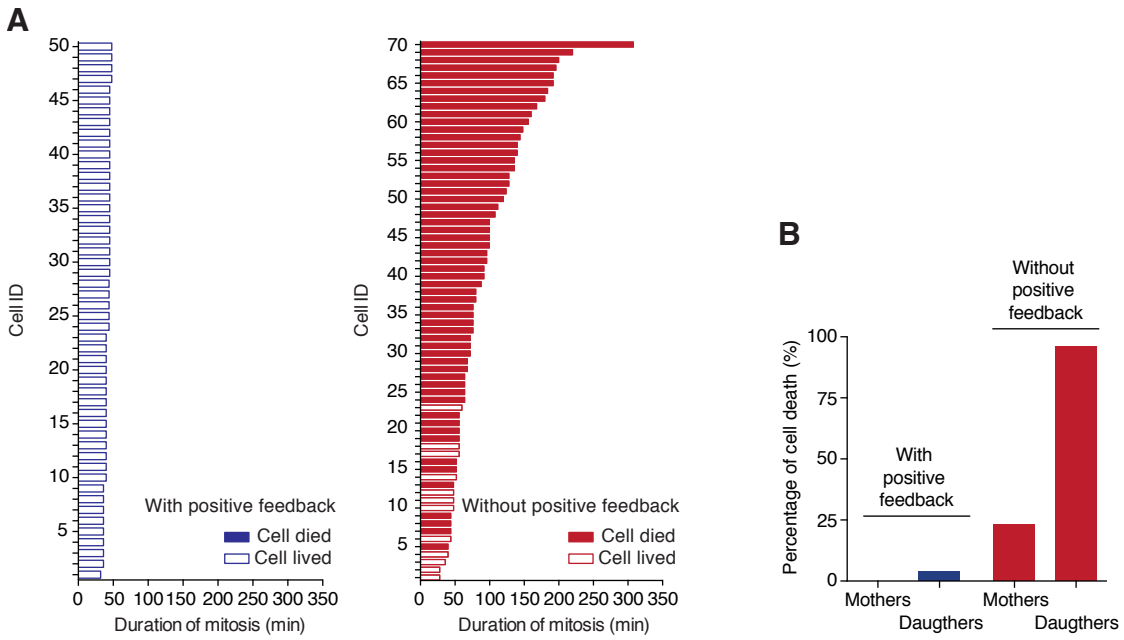


Figure 3.22. Perturbing positive feedback compromises the cell viability. A. Quantification of mitotic duration for individual MCF10A cells stably expressing NLS-mCherry and cell survival in the presence (left) or absence (right) of positive feedback. **B.** Percentage of cells that died during first mitosis (mothers) or right after first mitosis (daughters) when treated with DMSO (with positive feedback) or with Wee1 inhibitor (without positive feedback).

3.6. Mitotic phosphatases role on temporal modularity of mitosis

In addition to the activity of Cdk1 and it regulatory circuit, mitotic duration is also controlled by phosphatases. In fact, inactivation of Cdk1 is not sufficient to finish mitosis - mitotic exit is also dependent on the action of phosphatases, which counteract Cdk1 activity. Immediately prior to mitotic exit, phosphatases promote the controlled removal of mitotic phosphorylations. Different phosphatases from the PP1 and the PP2A families contribute to the reversal of mitotic phosphorylations (Bollen et al., 2009). PP2A is a strong candidate because its subunits B55α and B55*δ* were found to be important for dephosphorylation of Cdk1 substrates during mitotic exit in *Xenopus laevis* extracts (Castilho et al., 2009; Mochida et al., 2009). However, PP1 has also been proposed to contribute to Cdk1 substrate desphosphorylation (Wurzenberger and Gerlich, 2011), and it has been shown that the *Xenopus laevis* and human catalytic subunits PP1α and PP1*γ* are negatively regulated by Cdk (Dohadwala et al., 1994; Kwon et al., 1997; Wu et al., 2009). Thus, it was asked whether phosphatases could also have a role in keeping the time of mitosis short, constant, and uncoupled from previous cell cycle events.

The first approach used to test this hypothesis was carried out by perturbing cells with the specific PP1 family inhibitor Tautomycin (Fujiki and Suganuma, 1993; Takai et al., 1995). MCF10A, RPE, and Hela cells were treated with Tautomycin and imaged for 5 hours. In the three cell lines used, about 80% of the cells entered prematurely into mitosis, but subsequently stalled and failed to exit it (Figure 3.23.A). This shows that PP1 phosphatases are essential for mitotic exit (Figure 3.23.B). However, it was not possible to draw any conclusions regarding the role of PP1 phosphatases in establishing the temporal modularity of mitosis. Tautomycin is a specific inhibitor of PP1 family phosphatases, but it does not discriminate between different PP1 isoforms. Since Tautomycin hits all different PP1 isoforms, this experiment only shows that PP1 phosphatases are essential for mitotic exit but does not discriminate what is the role of different isoforms in this process.

A second approach was used to further investigate the role of phosphatases in keeping the duration of mitosis short and constant. To overcome the drawback of the previous experiments and try to understand what is the role of different PP1 phosphatases isoforms as well as PP2A in mitotic exit, the expression of 3 different isoforms of PP1 phosphatases – PP1A (PP1α), PP1B (PP1β) and PP1C (PP1γ) – and PP2A phosphatase (PP2A-B55α) were downregulated with short hairpin RNAs (shRNA). MCF10A cells showed a protein level downregulation of about 35-55% of PP1 phosphatases and about 40% of PP2A, which allowed the cells to be viable and kept in culture (Figure 3.24). Cells stably expressing shPP1A, shPP1B, shPP1C, shPP2A or shControl (shScramble) also expressed NLS-mCherry in order to measure mitotic events in these cells.

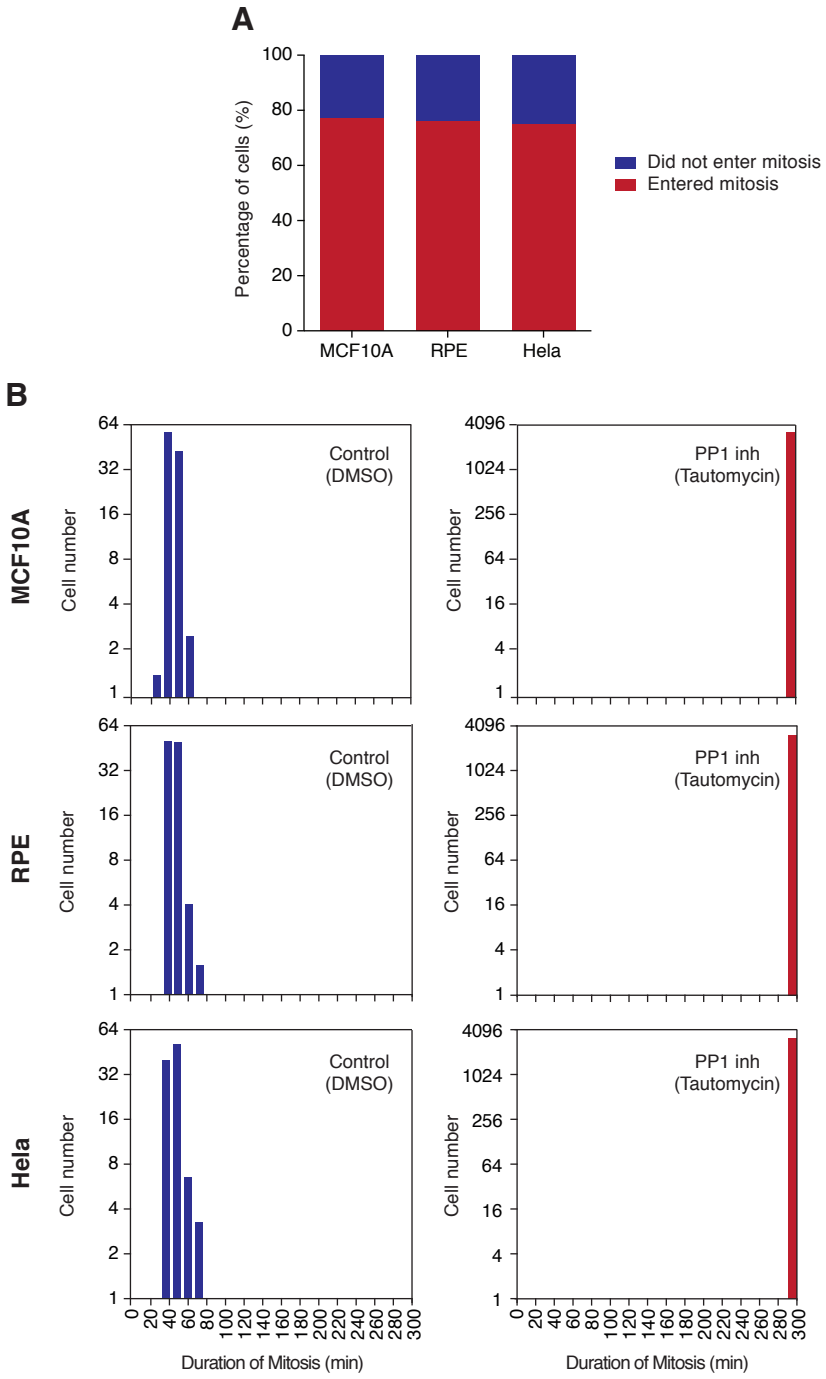


Figure 3.23. PP1 specific inhibitor makes cells arrest at mitosis. A. Percentage of MCF10A, RPE and Hela cells stably expressing NLS-mCherry that successfully entered mitosis after incubation with Tautomycin. **B.** Histograms of duration of mitosis in MCF10A (top panel), RPE (middle panel) and Hela (bottom panel) cells treated either with DMSO (control) or Tautomycin (PP1 inh) (n>100).

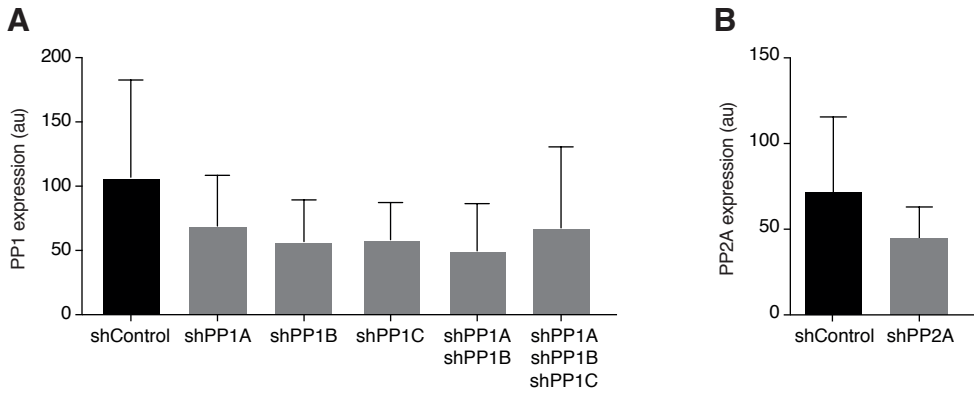


Figure 3.24. Mean expression of PP1 isoforms and PP2A in MCF10A cells stably expressing shPP1 isoforms or shPP2A and NLS-mCherry. A. MCF10A cells stably expressing shControl (shScramble), shPP1A, shPP1B or shPP1C alone or combining shPP1A with shPP1B or shPP1A, shPP1B and shPP1C. Cells also expressed NLS-mCherry. Mean expression of PP1 phosphatase was measured using immunofluorescence with the antibody PP1 (Santa Cruz, cat. no. sc-7482). **B.** MCF10A cells stably expressing shControl (shScramble) or shPP2A and NLS-mCherry. Mean expression of PP2A was measured using immunofluorescence with the antibody PP2A (CST, cat. No. 2290). Mean ± standard deviation is shown for each cell line (n>1000).

MCF10A cells stably expressing shPP1A, shPP1B, shPP1C or shPP2A alone or combining shPP1A with shPP1B or shPP1A, shPP1B and shPP1C, or shControl (shScramble) and NLS-mCherry were imaged for two consecutive division cycles in order to measure duration of mitosis and cell cycle length. Downregulation of mitotic phosphatases resulted in a longer duration of mitosis (shControl 46.6±6.5 minutes; shPP1A 62.0±10.2 minutes; shPP1B 55.5±8.9 minutes; shPP1C 60.0±7.0 minutes; shPP1A and shPP1B 56.5±14.4 minutes; shPP1A, shPP1B and shPP1C 59.4±14.0 minutes; and shPP2A 57.4±8.2 minutes). However, even in perturbed cells, duration of mitosis was kept constant when compared with control cells in all the conditions tested as shown by mean absolute deviation values (shControl=0.091; shPP1A=0.13; shPP1B=0.12; shPP1C=0.071, shPP1A and shPP1B=0.17; shPP1A, shPP1B and shPP1C=0.16; shPP2A=0.11) (Figure 3.25.A).

Perturbing expression of mitotic phosphatases also had no effect in the modularity of mitotic

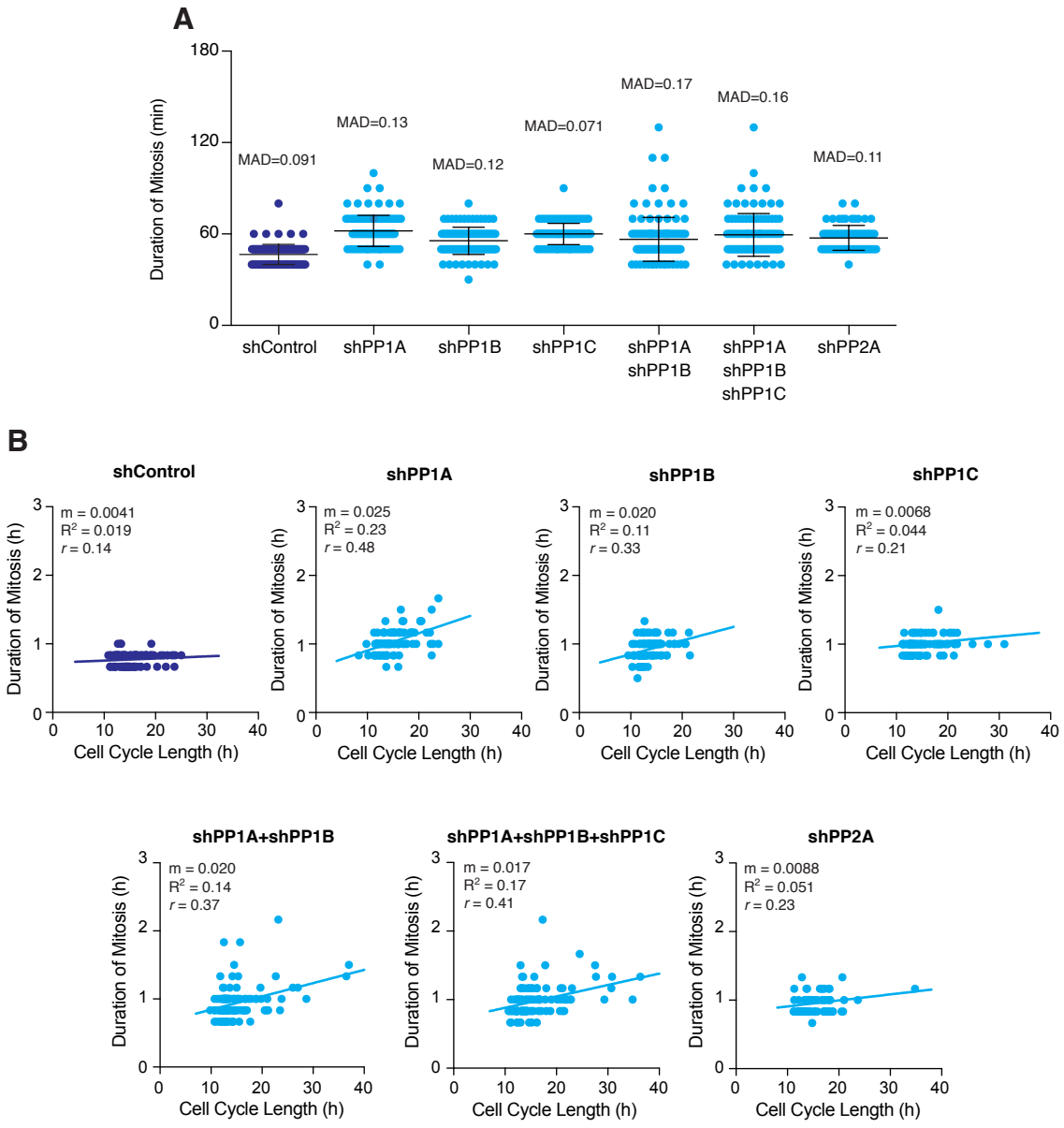


Figure 3.25. Perturbing mitotic phosphatases does not make duration of mitosis more variable and coupled with cell cycle length. All lines stably expressed NLS-mCherry. **A.** Duration of mitosis measured in MCF10A cells in the presence (shControl) or partial knockdown (shPP1A; shPP1B; shPP1C; shPP1A and shPP1B; shPP1A, shPP1B and shPP1C; and shPP2A) of mitotic phosphatases. Mean ± standard deviations are shown as bars and mean absolute deviations (MAD) are shown above in hours (n>100). **B.** Duration of mitosis plotted as a function of cell cycle length in MCF10A cells in the presence (shControl) or partial knockdown (shPP1A; shPP1B; shPP1C; shPP1A and shPP1B; shPP1A, shPP1B and shPP1C; and shPP2A) of mitotic phosphatases. Slope of the trend line (m), coefficient of determination (R^2) and Pearson correlation coefficient (r) are shown (n>70).

time regarding the cell cycle length, as seen by the lack of correlation between duration of mitosis and cell cycle length in the different perturbations used (Pearson correlation coefficient, *r* – shControl=0.14; shPP1B=0.33; shPP1C=0.21; shPP2A=0.23). However, when PP1A was perturbed, either alone or in combination with PP1B or PP1B and PP1C, some degree of correlation between mitotic duration and cell cycle length was found (Pearson correlation coefficient, *r* – shPP1A=0.48; shPP1A and shPP1B=0.37; shPP1A, shPP1B and shPP1C=0.41) (Figure 3.25.B). This is in line with what was shown in *Xenopus laevis*, that PP1α is important for Cdk1 substrate dephosphorylation, in order to drive cells out of mitosis (Dohadwala et al., 1994; Kwon et al., 1997; Wu et al., 2009). Even though PP2A was described as being important for both mitotic entry and mitotic exit, it was not observed a correlation between duration of mitosis and cell cycle length (Pearson correlation coefficient, *r*=0.23), which might be due to a weak downregulation of PP2A (Castilho et al., 2009; Mochida et al., 2009).

To further investigate if mitotic phosphatases have a role in keeping time of mitosis short, constant and independent of cell cycle length, shPhosphatase cells were treated with DMSO or Wee1 inhibitor. As seen previously, in cells treated with DMSO the duration of mitosis was extended when phosphatases were downregulated, but mitotic duration remained constant. When positive feedback was perturbed using Wee1 inhibitor, mitosis became longer and more variable in both control cells and phosphatases downregulated cells as seen in Figure 3.26.A. When looking at synchronicity of events, perturbing mitotic phosphatases alone was not able to interfere with synchronicity between early and late mitotic events (Pearson correlation coefficient, *r* – shControl=1.0; shPP1A=1.0; shPP1B=1.0; shPP1C=1.0; shPP1A and shPP1B=1.0; shPP1A, shPP1B and shPP1C=1.0; shPP2A=1.0). It was only when positive feedback was compromised that mitotic duration became longer, variable and mitotic events unsynchronized (Pearson correlation coefficient, *r* –shControl+Wee1 inh=0.95; shPP1A+ Wee1 inh=0.91; shPP1B+Wee1 inh=0.93 shPP1C+Wee1 inh=0.94; shPP1A and shPP1B+ Wee1 inh=0.92; shPP1A, shPP1B and shPP1C + Wee1 inh=0.93; shPP2A+Wee1 inh=0.94).

Next it was addressed whether mitotic phosphatases were important for the coupling of duration of mitosis with time of mitotic entry. Cells where mitotic phosphatases were downregulated behaved similarly to control cells, where time of mitotic entry was not correlated with time duration of mitosis (Pearson correlation coefficient, *r* – shControl=0.098; shPP1A=0.15; shPP1B=0.0070; shPP1C=0.074; shPP1A and shPP1B=0.030; shPP1A, shPP1B and shPP1C=0.085; shPP2A=0.027). However, when positive feedback was perturbed, time of mitotic entry became correlated with duration of mitosis, with or without mitotic phosphatases downregulation (Pearson correlation coefficient, *r* – shControl+Wee1 inh=0.70; shPP1A+Wee1 inh=0.56; shPP1B+Wee1 inh=0.68; shPP1C+Wee1 inh=0.69; shPP1A and shPP1B+Wee1 inh=0.620; shPP1A, shPP1B and shPP1C+Wee1 inh=0.69; shPP2A+Wee1 inh=0.62) (Figure 3.26.B).

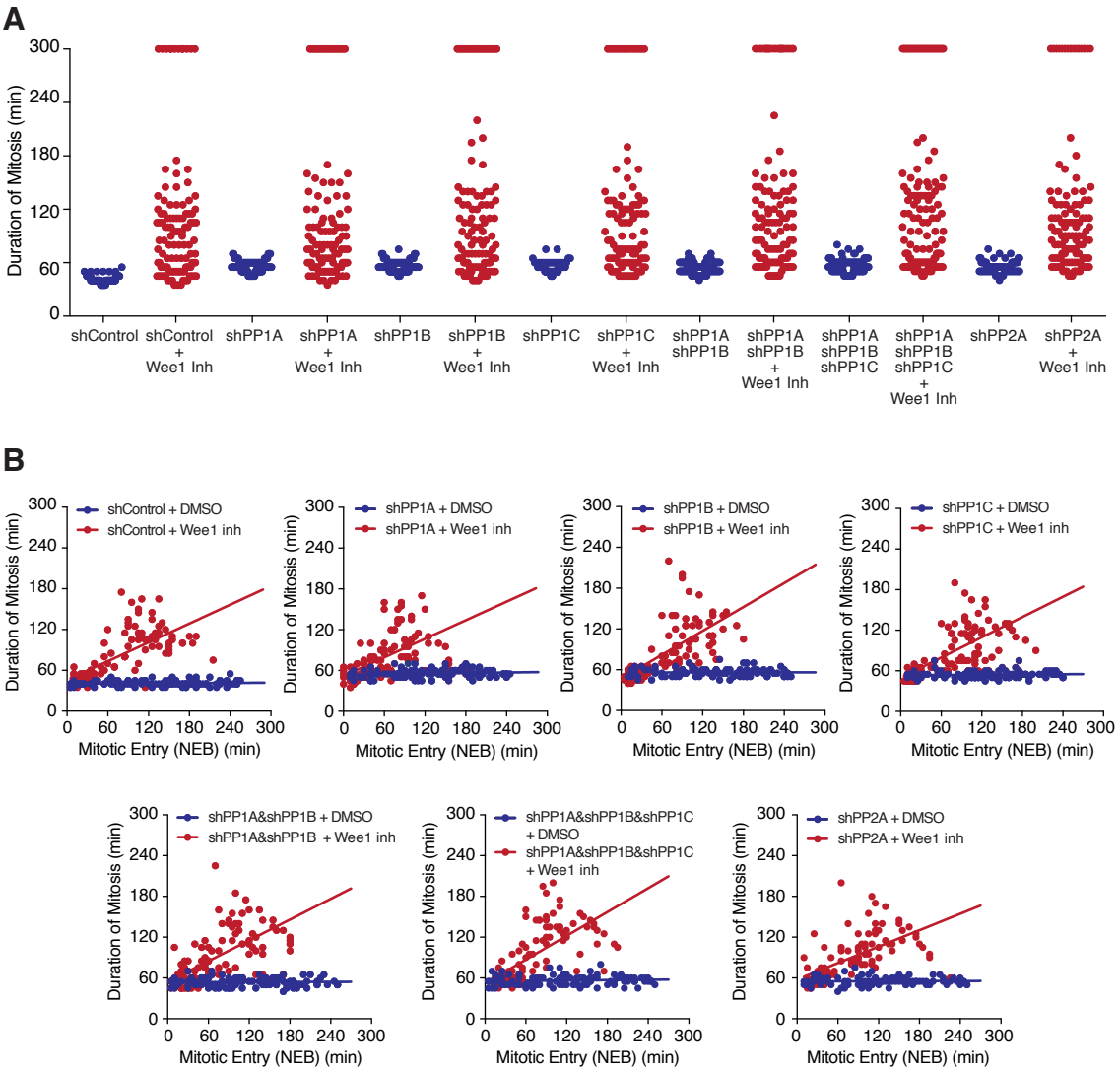


Figure 3.26. Absence of mitotic phosphatases alone does not make duration of mitosis coupled with mitotic entry. All lines stably expressed NLS-mCherry. **A.** Duration of mitosis measured by the time between NEB and NER in the presence or absence of Wee1 inhibitor in MCF10A cells stably expressing shControl (shScramble), shPP1A, shPP1B, shPP1C, shPP1A and shPP1B, shPP1A and shPP1B and shPP1C and shPP2A (n>100). Percentage of cells that entered mitosis but never exited it (300min dots) when treated with Wee1 inhibitor: shControl 10.3%, shPP1A 14.2%, shPP1B 16.8%, shPP1C 13.2%, shPP1A+shPP1B 16.7%, shPP1A+shPP1B+shPP1C 19.7% and shPP2A 12.9%. **B.** Duration of mitosis as a function of mitotic entry (NEB) in control (shScramble) and shPP1A, shPP1B, shPP1C, shPP1A and shPP1B, shPP1A and shPP1B and shPP1C and shPP2A MCF10A cells. The cells were either treated with DMSO or Wee1 inhibitor. Trend lines are shown (n>100).

Taken together, these results suggest that mitotic phosphatases from PP1 and PP2A families might have a role in keeping duration of mitosis short, constant and independent of upstream cell cycle events. However, the efficiency of phosphatases downregulation was not strong enough to allow to derive more supported conclusion in the role of these families of phosphatases in the temporal insulation of mitosis. Even though, these results support what was described before, that both families of phosphatases are important for mitotic entry and mitotic exit and play an important part in the temporal control of mitosis.

3.7. ODE model predicts positive feedback brings about temporal modularity in mitosis

Finally, it was determined whether positive feedback could plausibly be expected to insulate mitosis from previous cell cycle events and thereby generate modularity. In collaboration with Dr. Lendert Gelens, a simple ordinary differential equations (ODE) model was formulated to describe the basic regulatory network that drives cells in and out of mitosis (Figure 3.27.A). A set of deterministic ODEs were implemented with a noisy parameter variation from cell to cell rather than a stochastic Gillespie model, because the number of Cdk1-cyclin B1 complexes in a somatic cell is large ($\approx 1.6\times10^6$) (Sun et al., 2010). The model used consists of 3 ordinary differential equations (ODEs) that simulate the time evolution of the total amount of active Cdk1 ([Cdk1*](t)), and the synthesis and destruction of the mitotic cyclins, Cyclin B1 ([cycB](t)), and active APC-cdc20 ([APC](t)):

$$\frac{d[Cdk1^*](t)}{dt} = k_s - a_{deg} d[Cdk1^*](t) - b_{deg} \frac{[APC](t)^{n_{apc}}}{EC50_{apc}^{n_{apc}} + [APC](t)^{n_{apc}}} [Cdk1^*](t) + \left(a_{cdc} + b_{cdc} \frac{[Cdk1^*](t)^{n_{cdc}}}{EC50_{cdc}^{n_{cdc}} + [Cdk1^*](t)^{n_{cdc}}}\right)([cycB](t) - [Cdk1^*](t)) - \left(a_{wee} + b_{wee} \frac{EC50_{wee}^{n_{wee}}}{EC50_{wee}^{n_{wee}} + [Cdk1^*](t)^{n_{wee}}}\right)[Cdk1^*](t) \quad (3.1)$$

$$\frac{d[cycB](t)}{dt} = k_s - a_{deg} d[cycB](t) - b_{deg} \frac{[APC](t)^{n_{apc}}}{EC50_{apc}^{n_{apc}} + [APC](t)^{n_{apc}}} [cycB](t) \quad (3.2)$$

$$\frac{d[APC](t)}{dt} = \left(a_K + b_K \frac{[CycB - Cdk1](t)^{n_K}}{[CycB - Cdk1](t)^{n_K} + EC50_K^{n_K}}\right)(1 - [APC](t)) - \left(a_P + b_P \frac{EC50_P^{n_P}}{[APC](t)^{n_P} + EC50_P^{n_P}}\right)[APC](t) \quad (3.3)$$

Where the following parameters were chosen:

$$k_s = 0.1 nM min^{-1}$$

$$a_{deg} = 0.001 min^{-1}$$

$$b_{deg} = 0.02 min^{-1}$$

$$a_{cdc} = 0.5 min^{-1}$$

$$b_{cdc} = 1.5 min^{-1}$$

$$EC50_{cdc} = 30 nM$$

$$n_{cdc} = 10$$

$$a_{wee} = 0.5 min^{-1}$$

$$b_{wee} = 1 min^{-1}$$

$$EC50_{wee} = 30 nM$$

$$n_{wee} = 10$$

$$a_K = 0 min^{-1}$$

$$b_K = 0.25 min^{-1}$$

$$EC50_K = 0.18$$

$$n_K = 5$$

$$a_P = 0.025min^{-1}$$

$$b_P = 0.5min^{-1}$$

$$EC50_P = 0.18$$

$$n_P = 5$$

$$EC50_{apc} = 0.5$$

$$n_{apc} = 10 \quad (3.4)$$

The model was firstly used to simulate the time evolution of the concentrations of active Cdk1-cyclin B1 complexes, of total Cyclin B1, and of active APC-cdc20. (Figure 3.27.B). The corresponding steady-state response of active Cdk1-cyclin B1 as a function is also shown in Figure 3.27.C. For intermediate values of Cyclin B1 concentration, two stable solutions existed: high levels of Cdk1 activity (mitosis) and low levels of Cdk1 activity (interphase). One unstable solution (represented as a dashed line) serves as a critical threshold value of Cdk1 activity, below which the system will switch to mitosis (Figure 3.27.C). The solid black line corresponds to the trajectory in the (cyclin B1, active Cdk1-cyclin B1) plane of the cell cycle oscillations toggling between mitosis and interphase, as shown in Figure 3.27.B. The steady-state response of APC-cdc20 activation as a function of Cdk1-cyclin B1 concentration can be observed in Figure 3.27.D. The double-negative feedback loop involving APC-cdc20 and Mad2-cdc20 gave rise to bistability. For intermediate values of active Cdk1-cyclin B1 concentration, two stable solutions existed: high APC activity (solid blue line) and low APC activity (solid red line). The dashed line again shows the threshold value between both solutions.

The region of bistability was greatly extended when Mad2 activity was increased (Figure 3.27.D). Such high Mad2 activity prevents APC-cdc20 activation when Cdk1-cyclin B1 increases, similar to when SAC is active. The solid black line corresponds to the trajectory in the (active Cdk1-cyclinB1, APC-cdc20 activation) plane of the cell cycle oscillations shown in Figure 3.27.B. This shows that after Cdk1-cyclin B1 (in)activation, APC-cdc20 activity quickly changes accordingly, except when Mad2 activity is high.

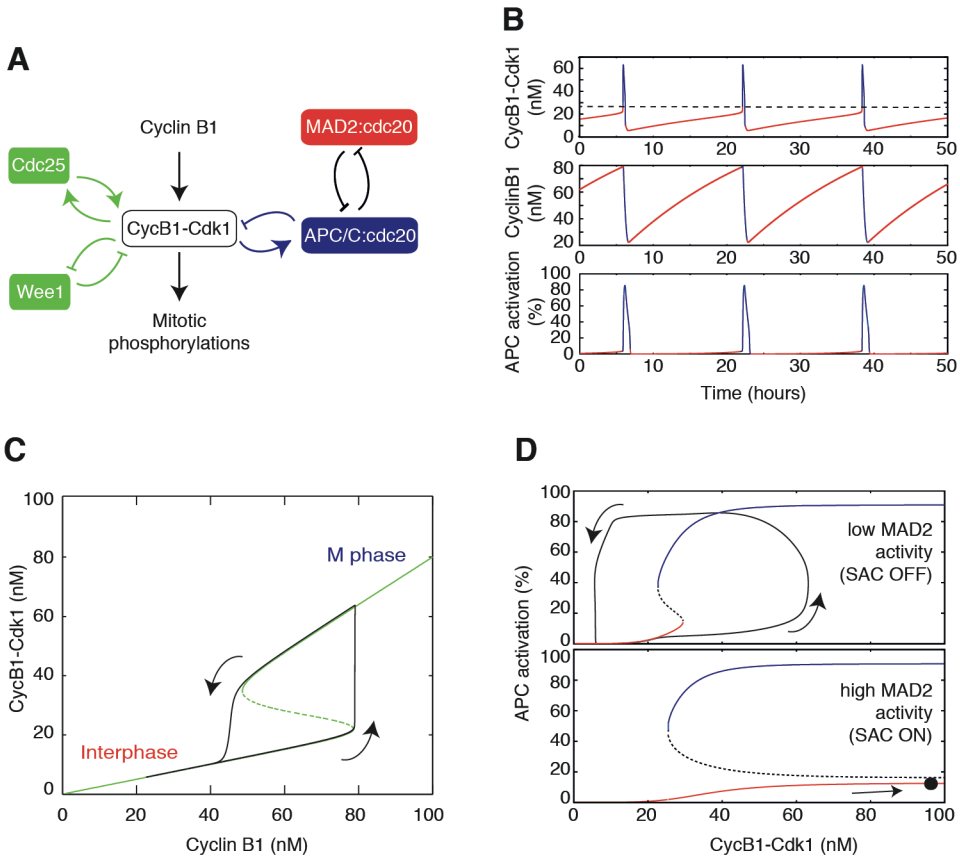


Figure 3.27. ODE model predicts that the double-negative feedback loop involving APC-cdc20 and Mad2-cdc20 gives rise to bistability. A. Wiring diagram showing a simplified Cdk1 regulatory network, including positive and negative feedback loops. **B.** Simulation of the time evolution of the concentration of Cdk1-Cyclin B1 complexes (top), the concentration of Cyclin B1 (middle) and APC-cdc20 activation (bottom). **C.** Steady-state responses of Cdk1-cyclin B1 activation as a function of Cyclin B1 concentration. The positive and double –negative feedback loops including Cdc25, Wee1 and Cdk1-cyclin B1 (A, green) can give rise to bistability. **D.** Steady-state responses of APC-cdc20 activation as a function of active Cdk1-cyclin B1 concentration. The double-negative feedback loop involving APC-cdc20 and Mad2-cdc20 (A, blue/red) can give rise to bistability.

Next, some noise was implemented in the model and the probability of distribution function for the duration of interphase and mitosis was simulated in control cells, in cells were SAC was inhibited, and in the presence or absence of positive feedback regulation (Figure 3.28.A). The duration of interphase was the same, both in control cells and when SAC was inhibited. On the other hand, cells where positive feedback was compromised showed shorter interphase duration, as expected by the premature entry into mitosis after inhibition of Myt1/Wee1. Notably, duration of mitosis, while short and constant both in control and SAC inhibited cells, became longer and more variable when positive feedback was compromised (Figure 3.28.B). Notably, these simulations are well in line with the measured experimental data for MCF10A, RPE, and Hela cells, using either shRNA against Mad2 or Reversine in order to inhibit SAC (Figure 3.29 and Figure 3.30).

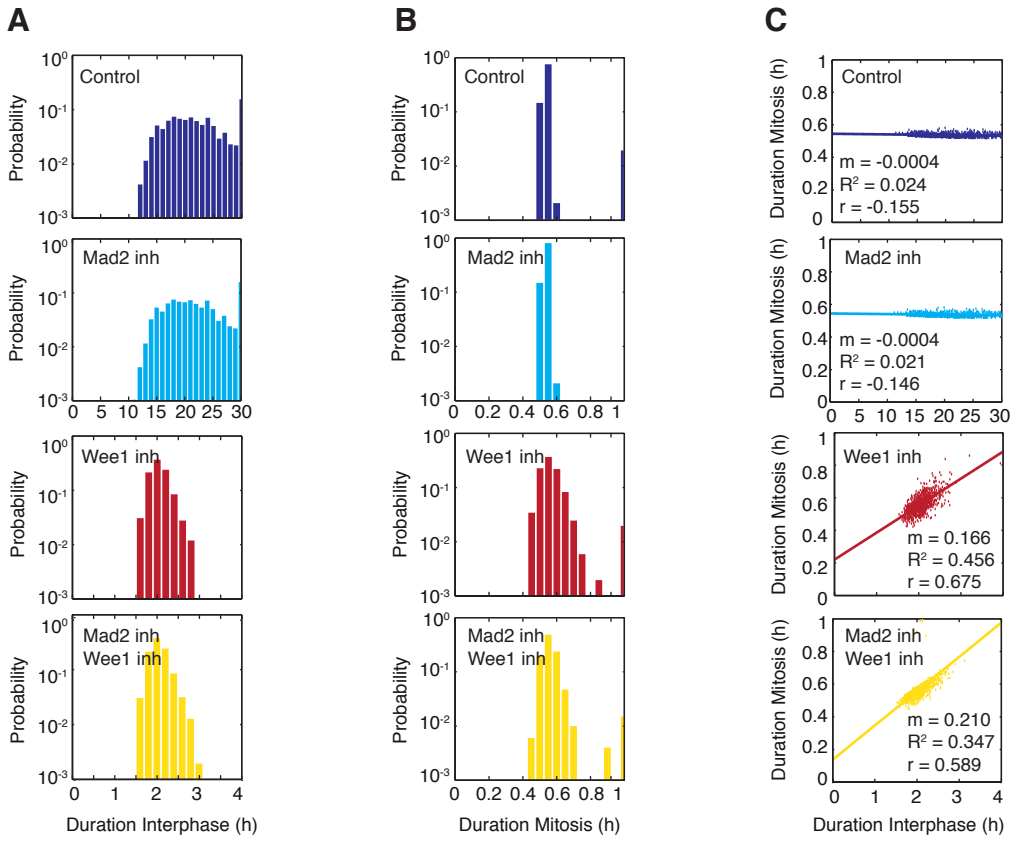


Figure 3.28. ODE modelling predicts that positive feedback promotes temporal modularity in mitosis. A. Simulated probability distribution function (in log scale) of the duration of interphase, **B.** Simulated probability distribution function (in log scale) of the duration of mitosis and **C.** Simulated duration of mitosis as a function of duration of interphase in control cells (control), with inhibition of SAC (Mad2 Inh), with inhibition of the positive feedback loops involving Wee1 (Wee1 Inh), or with inhibition of both SAC and Wee1 positive feedback loops (Mad2 Inh + Wee1 Inh). Slope of the trend line (m), coefficient of determination (R^2) and Pearson correlation coefficient (r) are shown.

Simulating the duration of mitosis as a function of duration of interphase (an approximation of cell cycle length) showed no correlation in control and SAC inhibited cells (Pearson correlation coefficient, *r* – Control=0.155 and Mad2 inh=0.146), suggesting that duration of mitosis is uncoupled with duration of interphase (Figure 3.28.C). When positive feedback was perturbed, both in the presence and absence of SAC inhibition, duration of mitosis became coupled with interphase duration, as seen by the strong correlations (Pearson correlation coefficient, *r* – Wee1 inh=0.675 and Mad2 inh +Wee1 inh=0.589) (Figure 3.28.C).

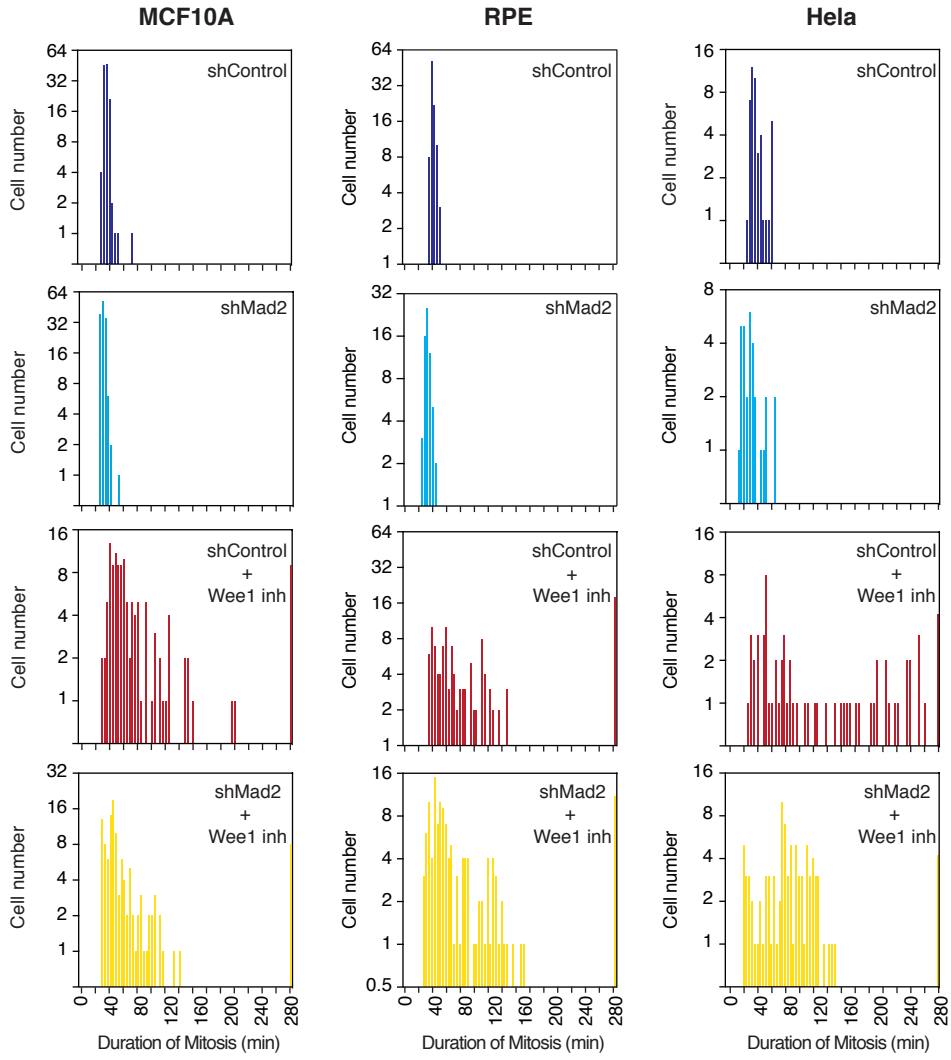


Figure 3.29. Histograms showing duration of mitosis in the absence and presence of Mad2 and with or without positive feedback. All lines stably expressed NLS-mCherry. Histograms are in log scale and show experimentally measured duration of mitosis in MCF10A, RPE and Hela control cells (shScramble), with inhibition of SAC (shMad2), with inhibition of the positive feedback loops involving Wee1 (shControl+Wee1 inh), or with inhibition of both SAC and Wee1 positive feedback loops (shMad2+Wee1 inh) (n>100).

This ODE model predicts that positive feedback accounts for the experimentally observed short, constant duration of mitosis in somatic cells and for the temporal insulation of mitotic duration from variability in duration of upstream cell cycle events. The model therefore predicts that positive feedback provides mitotic regulatory networks the potential to bring about modularity.

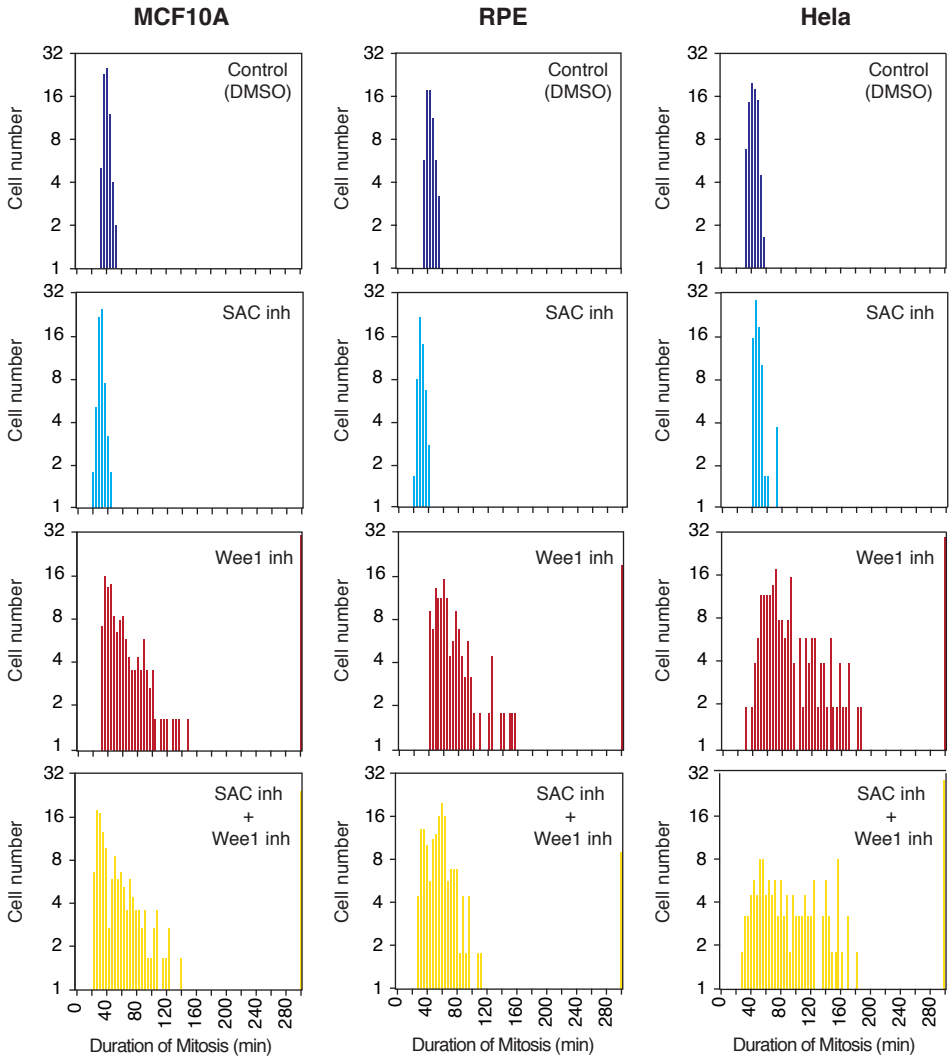


Figure 3.30. Histograms showing duration of mitosis in the absence and presence of Reversine and with or without positive feedback. All lines stably expressed NLS-mCherry. Histograms are in log scale and show experimentally measured duration of mitosis in MCF10A, RPE and Hela control cells (DMSO), with inhibition of SAC (SAC inh), with inhibition of the positive feedback loops involving Wee1 (Wee1 inh), or with inhibition of both SAC and Wee1 positive feedback loops (SAC inh+Wee1 inh) (n>100).

3.8. Highlights from investigating temporal control of mitosis

From all the results presented in this chapter it is possible to derive a few notable conclusions. Studying cell cycle dynamics in different cell lines showed that the cell cycle duration is highly variable in cells with different characteristics and even within cells of the same population. It was also noticed that the duration of mitosis is always short, constant, and uncoupled from variability in total cell cycle length in all cell types tested. Investigating this temporal insulation of mitosis showed that positive feedback is the underlying molecular mechanism which allows this temporal control of mitosis. Enabling modularity in signalling could be considered a new function for positive feedback control, which adds to all the other functions already described for this type of network - including control of synchronicity between events, ordering of events, and irreversible commitment to a decision (Araujo et al., 2016; Holt et al., 2008; López-Avilés et al., 2009; Pomerening et al., 2003; Santos et al., 2012; Sha et al., 2003; Skotheim et al., 2008). This work also shows that it is important to create modularity in cell cycle regulation by temporally insulating mitosis from previous cell cycle events

This work was recently published in Molecular Cell and can be consulted in Appendix A.

4. Temporal Control of Interphase

4.1. Summary

Mitosis is a very short fraction of a typically long cell division cycle. Cells spend on average one hour in mitosis and 23 hours in interphase. The aim of this study was to investigate the mechanisms that act to keep cells out of mitosis, as well as to determine whether cells could go into mitosis before having spent a full 23 hours in interphase. Artificially triggering cell division in freely cycling cells successfully promoted mitotic entry in the majority of cells. In fact, even G1-phase cells where DNA had not been replicated were able to undergo cell division. However, not all cells could divide after this mitotic trigger. Quantification of mitotic entry in single cells showed that there is a refractory period after mitosis where cells are unable to divide in response to a mitotic trigger. Theoretical simulations predicted that modulating the strength of the feedback between Cdk1-cyclin B1 and the Cdk1 regulator APC-Cdh1 allows for modulation of the length of the refractory period. These predictions were tested using human embryonic stem cells (hESC), that have relatively short cell cycles and low levels of APC-Cdh1. The prediction is that these cells lack a refractory period after mitosis and hence can undergo a new mitotic cycle due to a weak Cdk1:APC-Cdh1 feedback loop. Reconstituting the refractory period in hESC by increasing Cdh1 expression levels showed that the period of division cycles can be modulated by changing Cdk1:APC-Cdh1 feedback strength. This raises the interesting possibility that different cell types may fine-tune the period of their cell division cycles by modulating regulatory feedback. This work also suggests that this mechanism of modulating feedback strength might be a simple strategy for temporal regulation in other biological systems.

4.2. Aims

The fact that cells spend a very short fraction of their cell cycle time undergoing mitosis led to the related question on what keeps cells from entering mitosis during so many hours? When are cells able to undergo a new mitotic division? This is a popular question being currently addressed by a few laboratories but here it is addressed from a different angle: by understanding what keeps cells in interphase in the first place. In other words, this study aimed to characterise what regulates when a cell is able to undergo a new mitotic (or division) cycle.

4.3. Cells can respond to a mitotic trigger anytime during the cell cycle

In the previous chapter, mitosis was described as a very short fraction of a typically long cell division cycle. MCF10A cells spent on average 19.3 hours in interphase and 48 minutes in mitosis, which makes mitotic time 3.94% of the overall cell cycle length. Although RPE cells have longer cell division cycles – on average 29.0 hours - they spent only 2.76% of the cell cycle length in mitosis, which was around 48 minutes. Hela cells spent 3.7% of the length of their cell cycle of 25.0 hours in mitosis. These intriguing observations raised the question what keeps cell away from mitosis and when they can undergo a new mitotic cycle.

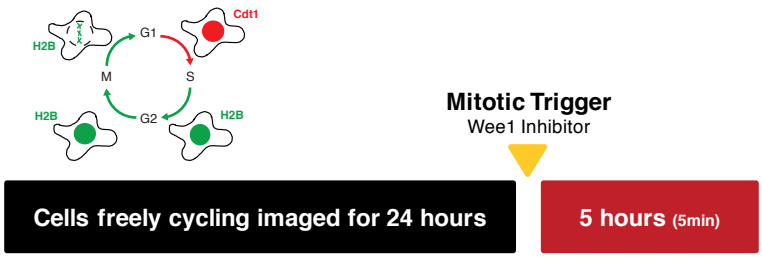


Figure 4.1. Schematic of the experimental design to understand if cells can be pushed into mitosis at any time during the cell cycle. Hela, MCF10A, and RPE cells stably expressing Cdt1-mCherry and H2B-YFP were imaged during 24 hours before adding a mitotic trigger; Wee1 inhibitor. After stimulation, cells were imaged every 5 minutes for 5 more hours.

Why are cells spending such a long time in interphase? Can a cell only respond to a mitotic trigger when they reach 96% completion of their cell cycle? To answer these questions, an experiment was designed to try to determine whether cells can be pushed into mitosis at any time during the cell cycle (Figure 4.1). Freely cycling Hela, MCF10A and RPE cells stably expressing Cdt1-mCherry and H2B-YFP biosensors were imaged for 24 hours in order to capture one division cycle for each cell and know in which phase of the cell cycle individual cells were before treatment with a mitotic trigger. Wee1 inhibitor (PD166285) was used as a "mitotic trigger", releasing Wee1 inhibition of Cdk1 and facilitating entry into mitosis. After stimulation with the mitotic trigger, cells were imaged for five more hours in order to observe what happens to the cells when they receive a signal to enter into mitosis but are not yet on the boundary of G2/M phase.

4.3.1. Wee1 inhibition promotes cell division and acts as a mitotic trigger

In order to measure the percentage of cells that entered into mitosis, Hela, MCF10A and RPE cells were treated with either DMSO or Wee1 inhibitor and imaged for 5 hours after the treatment. Within 5 hours less than 10% of control cells (treated with DMSO) entered in mitosis in all three cell lines used. When Hela, MCF10A, and RPE cells were stimulated with Wee1 inhibitor, cells entered into mitosis prematurely (Figure 4.2). It was observed that even cells which were in G1-phase at the time of treatment were able to respond to Wee1 inhibitor and enter into mitosis. In Hela cells, 55% of cells responded to the mitotic trigger, 21% of which were in G1-phase. The percentage of MCF10A cells that entered into mitosis within 5 hours after stimulation with Wee1 inhibitor was 51.5%, of which 29% were in G1-phase at the time of treatment. RPE cells were less responsive to the mitotic trigger with 32.8% of the cells responding and entering into mitosis. Of these cells, 15% were in G1-phase (Figure 4.2). These results show that cells can in fact be pushed into mitosis when stimulated with a mitotic trigger in any phase of the cell cycle.

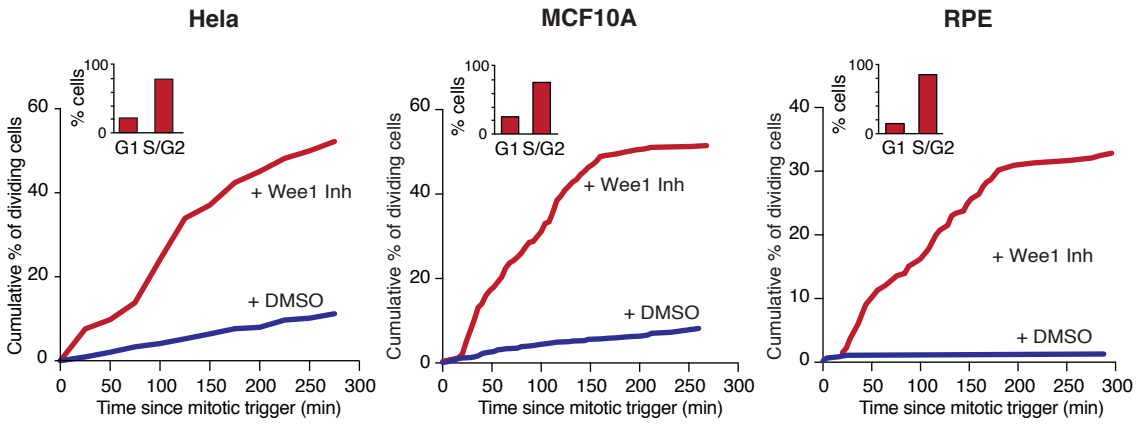


Figure 4.2. Mitotic trigger promotes premature divisions in the majority of cells. Cumulative percentage of dividing cells as a function of time since treatment with mitotic trigger in Hela, MCF10A, and RPE cells stably expressing Cdt1-mCherry and H2B-YFP. Cells were either treated with DMSO (blue) or with Wee1 inhibitor (Wee1 inh) (red). The insect represents the percentage of cells that responded to Wee1 inhibitor and were in either G1-phase or S/G2-phases of the cell cycle at the time of treatment (n>80).

4.3.2. Cells in G1-phase try to replicate DNA before entering in mitosis prematurely

Since even G1-phase cells were able to enter into mitosis when exposed to a mitotic trigger, it was addressed whether these cells try to replicate DNA before entering into mitosis. The hypothesis that these cells might try to replicate DNA before entering into mitosis was based on the quantitative model of temporal regulation of the cell cycle that considers that changing levels of Cdk activity trigger the next cell cycle phase, and specifically that low levels of Cdk activity lead the cells to enter S-phase (Stern and Nurse, 1996).

In order to test this, EdU was added to cells at the same time as the mitotic trigger, since EdU incorporation is a direct measure of active DNA synthesis. In control cells (left panel Figure 4.3.A) EdU staining and expression of Cdt1-mCherry - a marker for G1-phase – are not observed in the same cell. Cdt1 is a marker for G1-phase cells, since Cdt1 needs to be degraded at the G1/S boundary so that the cell can start to replicate DNA. This means that

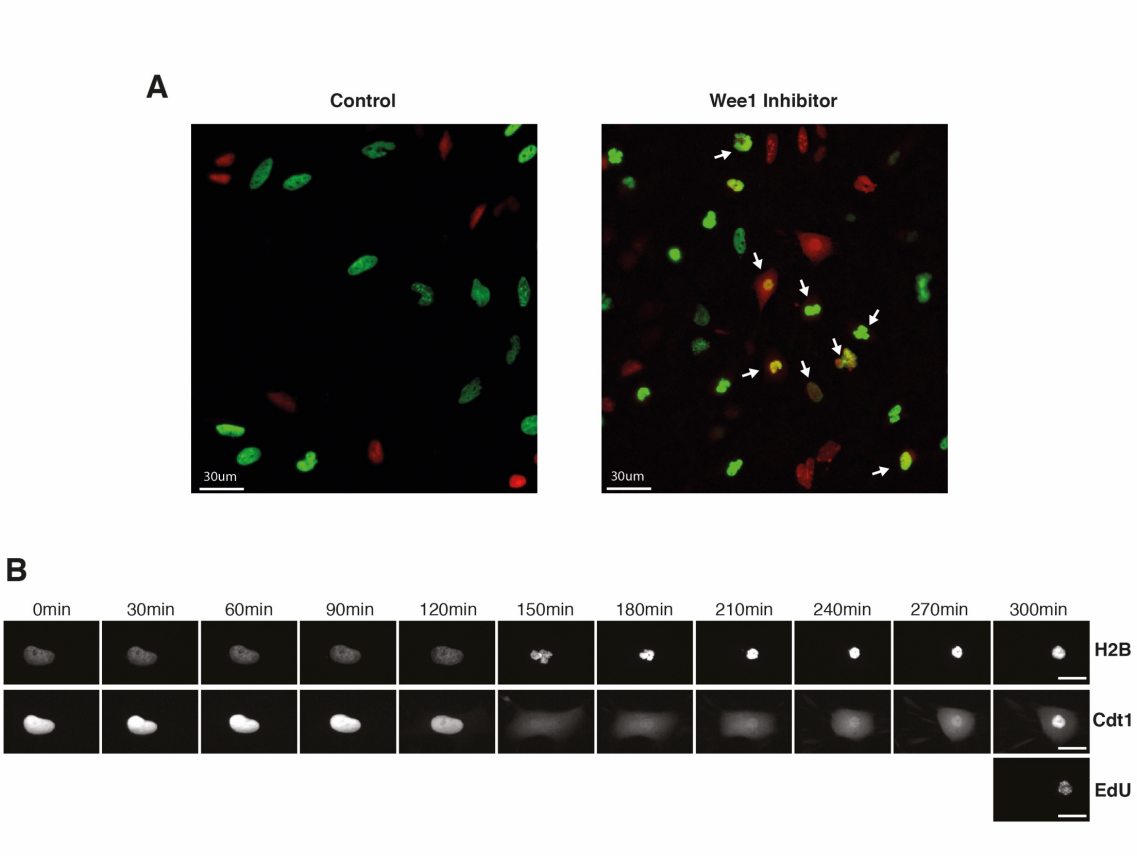


Figure 4.3. When stimulated with a mitotic trigger, cells try to replicate DNA while entering mitosis. A. Hela cells stably expressing Cdt1-mCherry (red) after 5 hours treatment with EdU (green) and either DMSO (control) or Wee1 inhibitor. White arrows mark cells that are positive for both Cdt1 and EdU staining. Scale bar 30μm. **B.** 5 hours montage of a Hela cell stably expressing Cdt1-mcherry and H2B-YFP after stimulation with Wee1 inhibitor. After imaging for 5 hours, this cell was also stained for EdU. Scale bar 15μm.

cells do not experience G1-phase and S-phase simultaneously, as expected. However, in cells stimulated with Wee1 inhibitor (right panel Figure 4.3.A), EdU staining and Cdt1-mCherry expression co-exist in the majority of cells, which means that when G1-phase cells were stimulated with Wee1 inhibitor they tried to replicate DNA before entering into mitosis.

After adding Wee1 inhibitor, cells were imaged for 5 hours in order to follow what happened to the cells. As shown in Figure 4.3.B, when Wee1 inhibitor was added, the cell of interest was in G1-phase because it was expressing Cdt1. Around 150 minutes after treatment with the mitotic trigger, the nuclear envelope broke down as indicated by the re-localisation of H2B, but the cell was still in G1-phase because it had not yet degraded the Cdt1 protein. At the same time, the cell was also replicating DNA (EdU staining is positive). In summary, this experiment showed that when cells are driven into premature mitosis, they 'rush through' the cell cycle even though they are not able to complete any of the cell cycle phases correctly. This is in line with the quantitative model for temporal control of cell cycle that states that cells initiate different cell cycle phases at different Cdk1 thresholds. In addition, Wee1 inhibitor breaks the positive feedback control between Cdk1 and Wee1. As discussed before, positive feedback promotes modularity and exclusion of cellular states. Without positive feedback, cells are now able to be in different, normally excluding states (S-phase and M-phase) at the same time.

4.4. A refractory period after mitosis renders cells unable to undergo a second mitotic division

In order to understand more about the history of cells prior to their exposure to the mitotic trigger, the time since last division was measured. Interestingly, not all the cells in three different cell lines (Hela, MCF10A and RPE) were able to respond to stimulation with Wee1 inhibitor and enter into mitosis. 45% of Hela cells, 48.5% of MCF10A cells, and 67.2% of RPE cells did not respond to the mitotic trigger by entering into mitosis (Figure 4.2). In Figure 4.4.A, it is possible to observe that control cells only divided if their last division was a least around 15 hours before treatment with DMSO. On the other hand, when treated with Wee1 inhibitor, most of the cells entered into mitosis even if they have divided a several hours before the treatment (Figure 4.4.A). However, all the cells that did not respond to the mitotic trigger had a feature in common: they had divided "just" a few hours before being stimulated with Wee1 inhibitor. So, this suggests that there is a lag time after mitosis during which cells are not able to respond to a mitotic trigger.

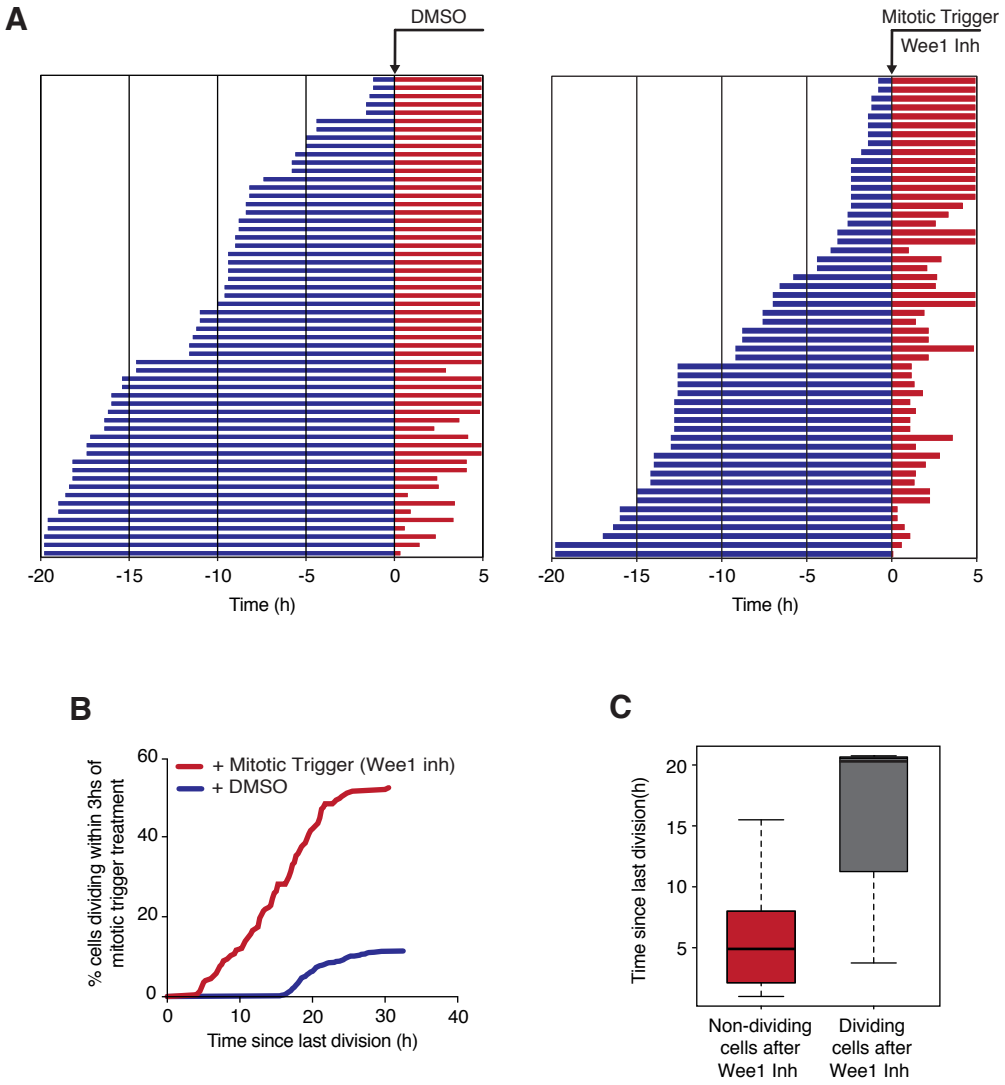


Figure 4.4. Somatic cells have a refractory period after mitosis where they are immune to mitotic triggers. **A.** Bar plot of Hela cells stably expressing Cdt1-mCherry and H2B-YFP representing the time since last division (blue bars) until treated with DMSO (left) or with Wee1 inhibitor (right). The end of red bars represents the time that cells entered mitosis after treatment with DMSO (left) or with Wee1 inhibitor (right) (n>50). **B.** Cumulative percentage of dividing cells as a function of time since mitotic trigger in Hela cells stably expressing Cdt1-mCherry and H2B-YFP either treated with DMSO (blue) or with Wee1 inhibitor (red) (n>100). **C.** Box plot representing the time since last division of Hela cells stable expressing Cdt1-mCherry and H2B-YFP treated with Wee1 inhibitor of non-dividing cells (red) that did not respond to Wee1 inhibitor and cells that responded to Wee1 inhibitor (grey) (n>100).

In fact, cells seem to require a period post-division before being able to respond to mitotic trigger (Figure 4.4.B and C). This means that if a cell has just divided, it would not be able to respond to a mitotic trigger and go into a new round of mitosis. This period was termed a refractory period, whereby the cells must wait until they can enter a new cell division. During this period on average of five hours, the cells are immune to any stimulation that prompts them to enter into mitosis again. After this 5-hour threshold, the number of cells that successfully respond to the mitotic trigger increases exponentially, indicating that the more time has passed since a cell last divided the more it is prone to respond to a mitotic trigger (Figure 4.4.B and C).

4.5. ODE model predicts that the strength of Cdk1-APC feedback controls the refractory period

Next, an ordinary differential equations (ODE) model was formulated in order to understand what might be the molecular mechanism underlying the establishment of a refractory period. This model described the basic regulatory network that control Cdk1 activation – Cyclin B1, Cdc25 and Wee1 – and inactivation – both forms of activated APC: APC-cdc20 and APC-Cdh1 (Figure 4.5.A). It was assumed that as the mass of the cell increases during G1-phase, various other Cyclins (i.e. Cyclin E) accumulate, until a critical mass (of Cyclins) is reached triggering the inhibition of Cdh1, ending the degradation of Cyclin B1 through the APC-Cdh1 activity. Positive feedback loops involving Wee1 and Cdc25 were included in the evolution equation for Cdk1, while APC activity in the form of APC-Cdc20 and APC-Cdh1 were included in the model equations of both Cdk1 and Cyclin through ultrasensitive degradation terms. Finally, the mass of the cell is assumed to grow linearly until cell division upon APC-Cdc20 activation in mitosis (discrete event: $M \rightarrow M / 2$).

$$\frac{dCyc}{dt} = k_s - (a_{deg} + b_{deg}\frac{Cdk1^{ndeg}}{K_{deg}^{ndeg} + Cdk1^{ndeg}} + c_{deg}\frac{Kdeg^{ndeg}}{K_{deg}^{ndeg} + Cdk1^{ndeg}}\frac{Kdeg2^{ndeg2}}{K_{deg2}^{ndeg2} + M^{ndeg2}})\,Cyc \tag{4.1}$$

$$\frac{dCdk1}{dt} = k_s + \left(a_{cdc} + b_{cdc}\frac{Cdk1^{ncdc}}{K_{cdc}^{ncdc} + Cdk1^{ncdc}}\right)(Cyc - Cdk1) - \left(a_{wee} + b_{wee}\frac{K_{wee}^{nwee}}{K_{wee1}^{nwee} + Cdk1^{nwee}}\right)Cdk1 - (a_{deg} + b_{deg}\frac{Cdk1^{ndeg}}{K_{deg}^{ndeg} + Cdk1^{ndeg}} + c_{deg}\frac{Kdeg^{ndeg}}{K_{deg}^{ndeg} + Cdk1^{ndeg}}\frac{Kdeg2^{ndeg2}}{K_{deg2}^{ndeg2} + M^{ndeg2}})\,Cdk1 \tag{4.2}$$

$$\frac{dM}{dt} = k_M \tag{4.3}$$

Where the following parameters were chosen:

$$k_s = 2nMmin^{-1}$$

$$a_{deg} = 0.001min^{-1}$$

$$b_{deg} = 0.4min^{-1}$$

$$c_{deg} = 1min^{-1}$$

$$K_{deg} = 30min^{-1}$$

$$n_{deg} = 20$$

$$a_{cdc} = 0.8min^{-1}$$

$$b_{cdc} = 5min^{-1}$$

$$K_{cdc} = 35min^{-1}$$

$$n_{cdc} = 11$$

$$a_{wee} = 0min^{-1}$$

$$b_{wee} = 3min^{-1}$$

$$K_{wee} = 30min^{-1}$$

$$n_{wee} = 3.5$$

$$K_{deg2} = 30min^{-1}$$

$$n_{deg2} = 20$$

$$K_M = 0.03min^{-1} \quad (4.4)$$

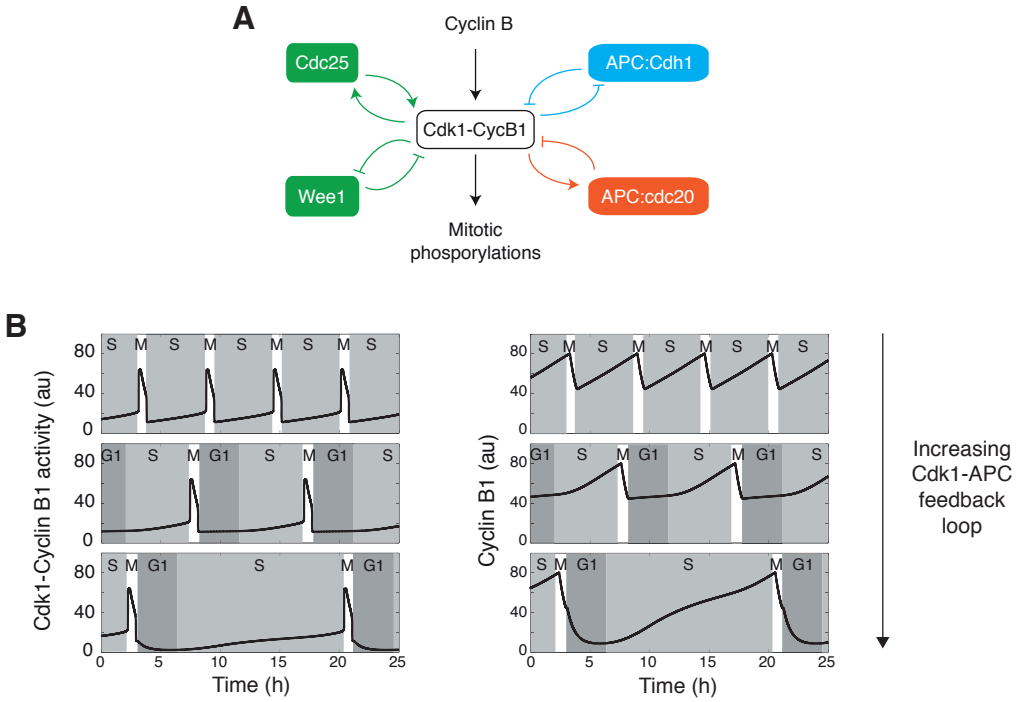


Figure 4.5. ODE model predicts that the strength of Cdk1-APC feedback controls the refractory period. **A.** Wiring diagram showing a simplified Cdk1 regulatory network, including positive and negative feedback loops. **B.** Simulation of the time evolution of the activity of Cdk1-Cyclin B1 complexes (left) and the concentration of Cyclin B1 (right) as the strength of Cdk1:APC is increased (from top to bottom panels).

Figure 4.5 shows typical time traces when varying the strength of feedback by changing K_{deg2} (Cdh1 expression/activity). Doubling the K_{deg2} value, led to differences in Cdk1 activity (left panel Figure 4.5.B) and Cyclin B1 levels (right panel Figure 4.5.B). Changing these parameters allows for a large control over the cell cycle period while maintaining the same amplitude of Cdk1 pulse during mitosis.

The ODE model predicts that a strong Cdk1:APC-Cdh1 feedback loop results in a slowly accumulation of Cyclin B1 and therefore the levels of Cdk1 activity peaks will be more sparse in time and the cell cycles will be longer. In contrast, a weak Cdk1:APC-Cdh1 feedback loop suggests always high levels of Cyclin, Cdk1 activity levels up and down very fast and consequently short cell cycles (Figure 4.5).

4.6. Human embryonic stem cells do not have a refractory period

The ODE model predicted that the strength of the Cdk1:APC-Cdh1 feedback loop is able to control the refractory period, and that this feedback is very strong in somatic cells. The ODE model also predicted that a weak Cdk1:APC-Cdh1 feedback loop will give rise to more frequent peaks in Cdk1 activity and high levels of Cyclin B1. As embryonic stem cells have characteristically shorter cell cycles, with Cdk1 activity peaking more often, next it was addressed whether human embryonic stem cells have a refractory period.

4.6.1. hESC have shorter cell division cycles

Cell cycle length was measured both in pluripotent control cells and cells that were stimulated with BMP4 for 3 days in order to induce differentiation towards mesoderm progenitors. In Figure 4.6 it is possible to observe that post-differentiation, hESC almost double the length of their cell cycle: in control cells cell cycle length was on average 12 hours while in cells stimulated for 3 days with BMP4 was 21 hours.

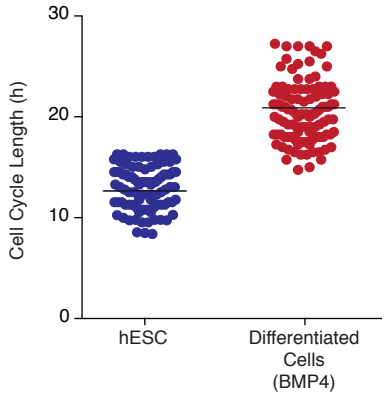


Figure 4.6. After 3 days of differentiation with BMP4, hESC almost double their cell cycle length. Duration of cell cycle length measured by live-cell imaging in H9 pluripotent cells and H9 cells differentiated with BMP4 for 3 days stably expressing NLS-mCherry (n>50). Means are shown as bars.

4.6.2. hESC express very low levels of Cdh1

hES cells have a truncated G1-phase and the ODE model predicted that Cdk1:APC-Cdh1 feedback loop is likely to be weaker in these cells. To test if this feedback loop is effectively weaker in these cells, the endogenous protein levels of Cdh1 were measured by immunofluorescence in pluripotent control cells and cells that were stimulated with BMP4 for 3 days in order to induce differentiation. And in fact, hESC control cells have very low levels of Cdh1 protein (Figure 4.7). In contrast, differentiated hESC have much higher Cdh1 protein levels. This suggests that the Cdk1:APC-Cdh1 feedback loop in embryonic stem cells becomes stronger as cells exit pluripotency and undergo differentiation.

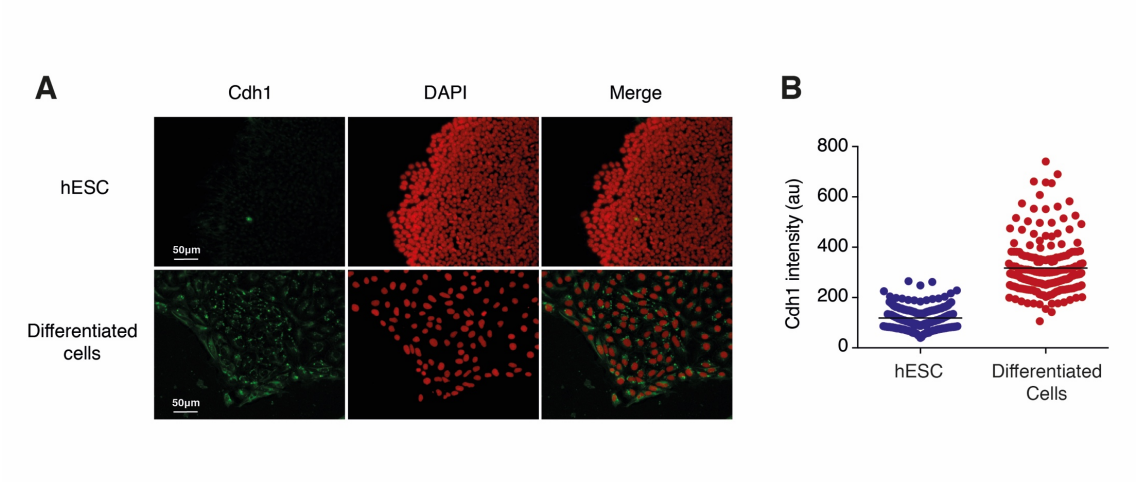


Figure 4.7. Contrary to differentiated cells, hESC express very low levels of APC-Cdh1. A. H9 pluripotent cells and H9 cells differentiated with BMP4 for 3 days were stained for total Cdh1 (green) and DNA (red). Scale bar 50µm **B.** Quantification of Cdh1 intensity (protein levels) in both H9 WT cells and H9 cells differentiated with BMP4 for 3 days (n>200).

4.6.3. Mitotic cyclins are highly expressed in hESC

Another prediction of the ODE model was that cells with a faster cell cycle and low levels of APC-Cdh1 would have high levels of mitotic Cyclins. Cyclin B1 and Cyclin A2 are the most active Cyclins during mitosis, so it was investigated the levels of these two Cyclins in both hESC and differentiated cells. hESC were stimulated with BMP4 for 3 days and endogenous levels of Cyclin B1 and Cyclin A2 were detected by immunofluorescence. Indeed, both Cyclin B1 and Cyclin A2 were highly expressed in hESC in comparison to BMP4 treated cells (Figure 4.8). The percentage of Cyclin B1-positive hESC cells was 61%, around 3 times more than in differentiated cells, where only 18% of cells expressed Cyclin B1 (Figure 4.8.A). A similar trend was observed for Cyclin A2: 75% of hESC were positive for Cyclin A2 in contrast with only 23% of cells differentiated with BMP4 (Figure 4.8.B). These results show that mitotic cyclins are highly expressed in hESC in contrast with very low levels in differentiated cells.

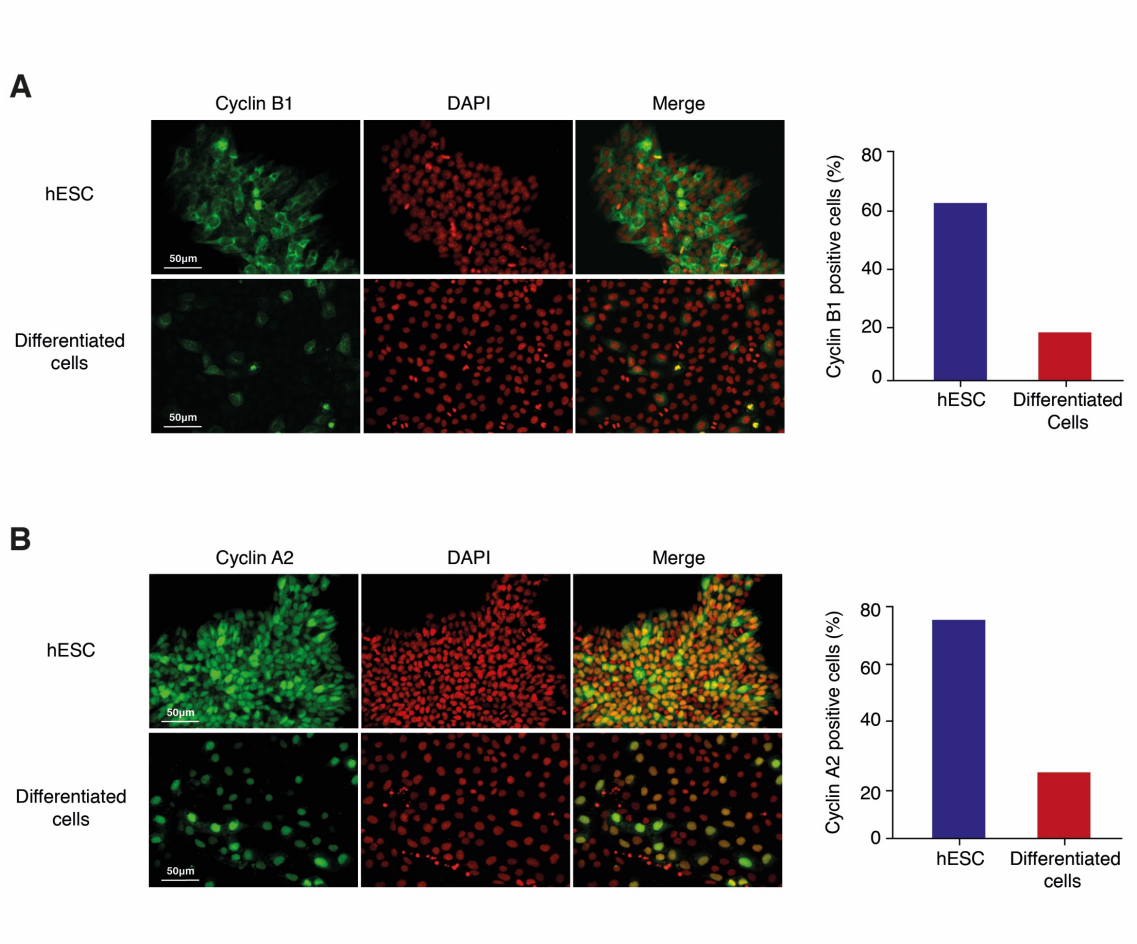


Figure 4.8. hESC express very high levels of Cyclin B1 and Cyclin A2 comparatively to differentiated cells. A. Left panel - H9 pluripotent cells and H9 cells differentiated with BMP4 for 3 days were stained for total Cyclin B1 (green) and DNA (red). Scale bar 50µm**. Right panel -** Quantification of Cyclin B1-positive cells in both H9 WT cells and H9 cells differentiated with BMP4 for 3 days (n>500). **B. Left panel -** H9 pluripotent cells and H9 cells differentiated with BMP4 for 3 days were stained for total Cyclin A2 (green) and DNA (red). Scale bar 50µm**. Right panel -** Quantification of Cyclin A2-positive cells in both H9 pluripotent cells and H9 cells differentiated with BMP4 for 3 days (n>500). A threshold was defined to discriminate between positive and negative cells.

4.6.4. hESC respond immediately to a mitotic trigger

So far, the data indicates that hESC correspond to the system that the ODE model predicted to have weak Cdk1:APC-Cdh1 positive feedback: hESC have smaller cell divisions cycles, low levels of Cdh1 and high expression of mitotic Cyclins. The question is then if hESC have a refractory period or not. To tackle this question, hESC were either stimulated with DMSO or with Wee1 inhibitor to mimic a mitotic trigger. In free cycling hES control cells, 48% of cells divided within a period of 5 hours. When hESC were treated with the mitotic trigger, there was a linear entry intro mitosis and within 120 minutes of adding Wee1 inhibitor to the media near 100% of cells entered into mitosis (Figure 4.9). This is in sharp contrast to somatic cells (Figure 4.2) where not all the cells were able to respond to mitotic trigger and response occurred over a much longer time period. These observations suggest that hESC lack a refractory period and are always ready to undergo another round of cell division. hESC do not have a period after mitosis during which they cannot undergo another round of cell division.

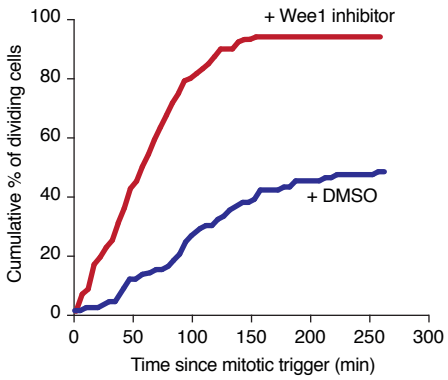


Figure 4.9. hESC enter into mitosis immediately after treatment with Wee1 inhibitor. Cumulative percentage of dividing cells as a function of time since exposure to mitotic trigger in H9 pluripotent cells, treated with either DMSO or with Wee1 inhibitor (n>100).

4.7. Refractory period can be re-established in hESC

It was established experimentally that hESC do not have a refractory period where cells are immune to a mitotic trigger and re-enter cell division when stimulated with Wee1 inhibitor. Next, it was tested if it was possible to re-establish a refractory period in hESC. In order to achieve this, hESC were transduced with a doxycycline-inducible Cdh1 construct, since constitutive over-expression of Cdh1 in hESC induces cell death (data not shown). Cdh1 is an important co-activator of APC/C, so over-expression of Cdh1 should maintain APC/C active for longer and make the Cdk1:APC-Cdh1 feedback stronger.

4.7.1. Ectopic expression of Cdh1 in hESC by a doxycycline-based inducible system

Firstly, it was tested whether inducing the system with different concentrations of doxycycline would induce different levels of Cdh1 expression. H9 iCdh1 (inducible Cdh1) cells were treated with 5µg/mL and 10µg/mL of doxycycline for 3 days and H9 WT (wild type) cells and H9 iCdh1 cells without doxycycline were used as controls. The levels of Cdh1 protein were measured by immunofluorescence.

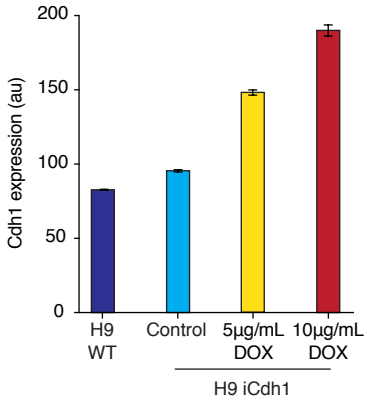


Figure 4.10. Ectopic expression of Cdh1 in hESC can be induced with doxycycline. Quantification of Cdh1 expression levels by immunofluorescence in H9 WT cells and H9 iCdh1 cells 3 days stimulation with 5µg/mL (yellow) or 10µg/mL (red) of doxycycline (DOX). H9 WT cells are represented by dark blue bar and H9 iCdh1 control cells are represented in light blue bar. Standard error of the mean is shown (n=3).

When both controls are compared, H9 iCdh1 cells express a little bit more Cdh1 than H9 WT cells ($p<0.05$), which means that the iCdh1 construct is a little leaky (Figure 4.10). At day 3, both H9 iCdh1 cells either stimulated with 5µg/mL or 10µg/mL of doxycycline showed expression of high levels of Cdh1 when compared with control cells (Figure 4.10).

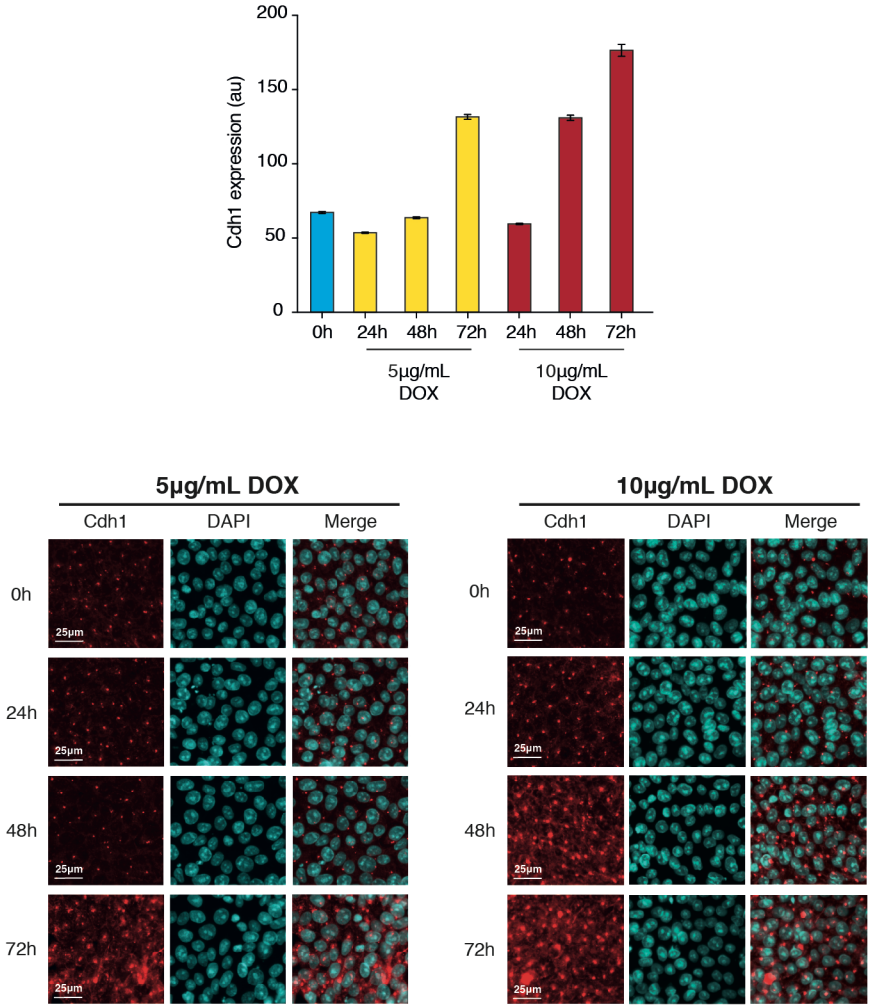


Figure 4.11. Ectopic expression of Cdh1 in hESC is time and dose dependent. Top panel – Quantification of Cdh1 expression levels by immunofluorescence in H9 iCdh1 cells treated for 0, 24, 48 and 72 hours with 5µg/mL (yellow) or 10µg/mL (red) Doxycycline (DOX). Control cells are represented in blue bar (n=3). **Bottom panel –** Immunofluorescence representative images of Cdh1 expression levels in H9 iCdh1 cells treated for 0, 24, 48 and 72 hours with 5µg/mL or 10µg/mL doxycycline. Cdh1 is represented in red and DNA in cyan. Scale bar 25µm.

It was then addressed the time of doxycycline induction of Cdh1. H9 iCdh1 cells were induced with 5 or 10μg/mL of doxycycline during 24, 48 and 72 hours. As shown in Figure 4.11, the over-expression of Cdh1 was gradual over the course of 3 days and dependent on the concentration of doxycycline used. Maximum levels of Cdh1 expression were observed when H9 iCdh1 cells were induced with 10μg/mL doxycycline for 3 days. However, all the experiments shown in the following sections of this chapter using H9 iCdh1 cells were performed by inducing cells with both 5μg/mL and 10μg/mL doxycycline. These results have shown that it is possible to induce overexpression of Cdh1 in hESC and maintain their viability.

4.7.2. Over-expression of Cdh1 reduces the levels of mitotic cyclins in hESC

It was expected that with over-expression of Cdh1 the Cdk1:APC-Cdh1 feedback loop strength would increase. So then, H9 iCdh1 cells over-expressing Cdh1 were tested for mitotic Cyclins levels, using immunofluorescence to detect the endogenous levels of proteins. After 3 days stimulation with either 5μg/mL or 10μg/mL of doxycycline, Cyclin B1 and Cyclin A2 levels decreased to levels similar to those previously seen in differentiated cells (Figure 4.7 and Figure 4.12).

The more Cdh1 was over-expressed, the more drastic was the decrease of percentage of cells expressing Cyclin B1 and Cyclin A2. 57% of untreated cells were expressing Cyclin B1, but this decreased to 29% after treatment with 5μg/mL doxycycline, and only 18% after treatment with 10μg/mL doxycycline for 3 days (Figure 4.12.A). This showed that the decrease of Cyclin B1-positive cells is associated with the increase in levels of Cdh1 expression. This correlation was not as striking for Cyclin A2 levels. Whereas 86% of untreated control cells were positive for Cyclin A2 expression, only 61% and 53% of cells treated with 5μg/mL or 10μg/mL doxycycline, respectively, showed Cyclin A2 expression (Figure 4.12.B).

In summary, these results show that the expression of mitotic Cyclins is inversely correlated with Cdh1 levels. This corroborates the predictions of the ODE model – the stronger the Cdk1:APC-Cdh1 feedback loop is, the lower mitotic Cyclins levels will be.

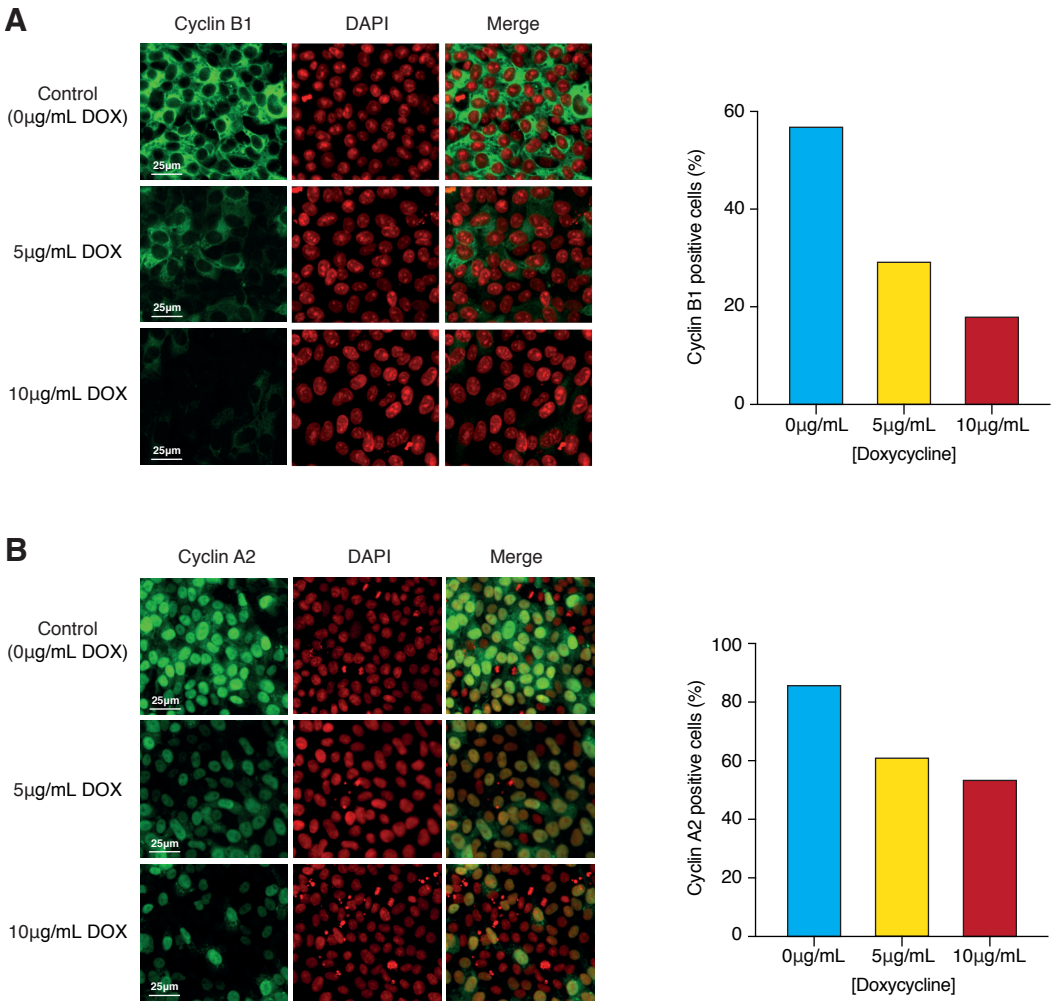


Figure 4.12. Over-expression of Cdh1 in hESC decreases levels of Cyclin B1 and Cyclin A2. A. Left panel - Immunofluorescence representative images of Cyclin B1 expression levels in H9 iCdh1 cells stimulated for 3 days with 0, 5 or 10µg/mL doxycycline (DOX). Scale bar 25µm**. Right panel -** Quantification of Cyclin B1–positive cells in H9 iCdh1 cells stimulated for 3 days with 0 (blue), 5 (yellow), or 10 (red) µg/mL doxycycline (DOX) (n>1000). **B. Left panel -** Immunofluorescence representative images of Cyclin A2 expression levels in H9 iCdh1 cells stimulated for 3 days with 0, 5 or 10µg/mL doxycycline (DOX). Scale bar 25µm**. Right panel -** Quantification of Cyclin A2-positive cells in H9 iCdh1 cells stimulated for 3 days with 0 (blue), 5 (yellow), or 10 (red) µg/mL doxycycline (DOX) (n>1000). A threshold was defined to discriminate between positive and negative cells.

4.7.3. Over-expression of Cdh1 makes G1-phase and cell cycle length longer in hESC

Then it was questioned what would be the effect of over-expressing Cdh1 in hESC on the cell cycle dynamics. To investigate this, H9 iCdh1 cells stably expressing a truncated version of Cdt1-venus and NLS-mCherry were stimulated with 5µg/mL and 10µg/mL doxycycline for 24 hours and then imaged for two consecutive division cycles in order to measure G1-phase and cell cycle length (Figure 4.13.A and B). Control H9 iCdh1 cells that were not stimulated with doxycycline spent 4.9±0.9 hours in G1-phase and took 15.0±1.9 hours to complete a whole cell division cycle. When H9 iCdh1 cells were treated with 5µg/mL doxycycline, G1-phase length increased to 6.9±1.8 hours with a corresponding cell cycle length of 18.4±2.4 hours. Finally, H9 iCdh1 cells treated with 10µg/mL doxycycline spent 7.3±2.0 hours in G1-phase and took 22.5±2.9 hours to conclude one cell division cycle (Figure 4.13.A and B). These results indicate that the more Cdh1 is over-expressed in hESC, the stronger the Cdk1:APC-Cdh1 feedback loop is and hence the longer G1-phase and consequently the overall cell cycle length gets.

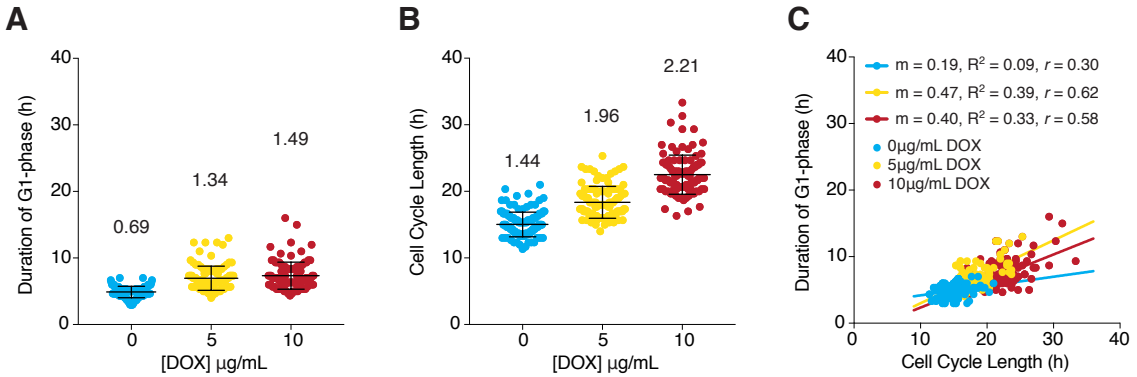


Figure 4.13. G1-phase and cell cycle length increase in hESC over-expressing Cdh1. H9 iCdh1 cells stably expressing Cdt1-venus and NLS-mCherry. **A.** Time of G1-phase measured by live-cell imaging of H9 iCdh1 cells stimulated with 0 (blue), 5 (yellow), and 10 (red) µg/mL doxycycline (DOX). Mean ± standard deviations are shown as bars. and mean absolute deviations (MAD) are shown above in hours (n>100). **B.** Time of cell cycle length measured by live-cell imaging of H9 iCdh1 cells stimulated with 0 (blue), 5 (yellow), and 10 (red) µg/mL doxycycline. Mean ± standard deviation and mean absolute deviations (MAD) are shown above in hours (n>100). **C.** Duration of G1-phase in single cells as a function of total cell-cycle length measured by live-cell imaging of H9 iCdh1 cells stimulated with 0 (blue), 5 (yellow), and 10 (red) µg/mL doxycycline. Slope of the trend line (m), coefficient of determination (R^2) and Pearson correlation coefficient (r) are shown (n>100).

Interestingly, besides increasing the length of G1-phase and the overall cell cycle in hESC, over-expression of Cdh1 also increased the variability of G1-phase and cell cycle length. In untreated control cells duration of G1-phase was not very variable (MAD=0.69), but this variability increased with increasing Cdh1 over-expression (MAD=1.34 and 1.49 in H9 iCdh1 cells treated with 5μg/mL or 10μg/mL doxycycline, respectively) to MAD values similar to those previously seen in somatic cells (Section 3.3.1) (Figure 4.13.A). Cell cycle length variability also increased with over-expression of Cdh1 in H9 iCdh1 cells (MAD=1.44, 1.96 and 2.21 in untreated cells and cells treated with 5μg/mL or 10μg/mL doxycycline, respectively) (Figure 4.13.B). Another interesting observation was that with over-expression of Cdh1 in hESC, duration of G1-phase became correlated with total cell cycle length (Pearson correlation coefficient, r – 0.62 for 5μg/mL of DOX and 0.58 for 10μg/mL of DOX), which was not seen in untreated control cells (Pearson correlation coefficient, r=0.30) (Figure 4.13.C). In hESC G1-phase length is not correlated with total cell cycle length (data not shown), but in somatic cells G1-phase length was shown to be correlated with cell cycle length (Figure 3.3). Taken together, these results suggest that over-expression of Cdh1 in hESC remodels their cell cycle to more closely resemble that of somatic cells.

4.7.4. Over-expression of Cdh1 delays the response of hESC to a mitotic trigger

Finally, it was investigated what happens to hESC over-expressing Cdh1 when they are stimulated with a mitotic trigger (Wee1 inhibitor). H9 iCdh1 cells were stimulated with 5μg/mL and 10μg/mL doxycycline for 24 hours before adding either DMSO or Wee1 inhibitor and then imaged for 5 hours.

As shown in Figure 4.14, untreated control cells responded immediately to stimulation with mitotic trigger, reaching 100% of dividing cells in 20 minutes. However, cells stimulated with 5μg/mL or 10μg/mL doxycycline (and hence expressing high levels of Cdh1) took 30 and 90 minutes, respectively, to reach 100% of cells responding to Wee1 inhibitor (right panel of Figure 4.14.B). Control cells treated with DMSO divided at a normal rate reaching 20% of dividing cells after 5 hours, but this decreased to 12% and 17% in H9 iCdh1 cells stimulated with 5μg/mL and 10μg/mL doxycycline, respectively (left panel of Figure 4.14.B).

These results show that over-expressing Cdh1 in hESC was able to introduce a lag time between when cells are exposed to mitotic trigger and entry into mitosis, which suggests that a refractory period was at least partially re-established in hESC.

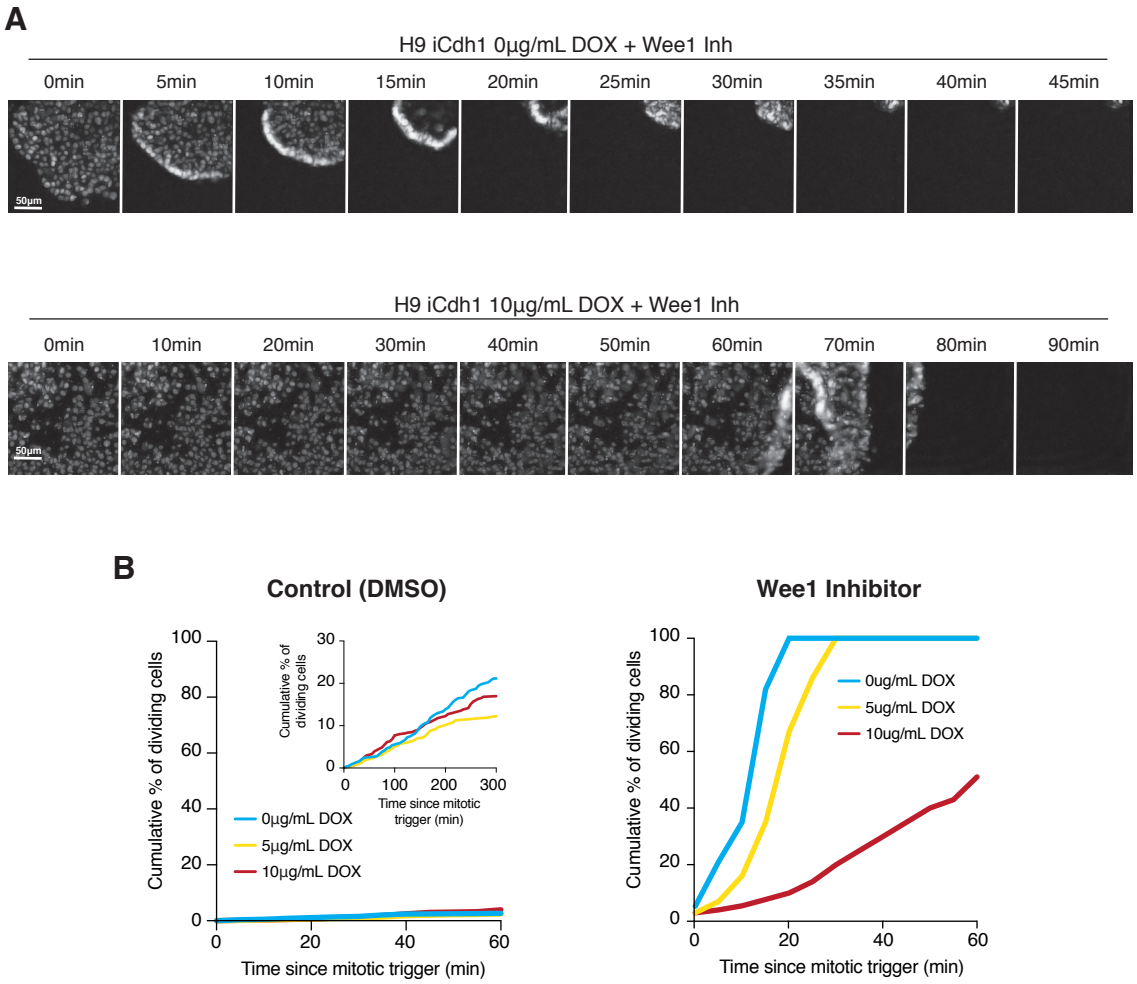


Figure 4.14. Refractory period can be re-established in hESC by over-expressing Cdh1. Montage of H9 iCdh1 cells stably expressing Cdt1-venus and NLS-mCherry stimulated with 0 (top panel) or 10 (bottom panel) µg/mL doxycycline for 24 hours prior to treatment with Wee1 inhibitor. Scale bar 50µm. **B.** Cumulative percentage of dividing cells as a function of time since exposure to mitotic trigger in H9 iCdh1 cells stably expressing Cdt1-venus and NLS-mCherry, treated with either DMSO (left) or with Wee1 inhibitor (right). H9 iCdh1 were stimulated with 0 (blue), 5 (yellow), or 10 (red) µg/mL doxycycline for 24 hours prior to the experiment (n>100).

4.8. Refractory period can be shortened in somatic cells

Since it was possible to re-establish the refractory period in hESC, then it was tested whether the refractory period could also be shortened in somatic cells. To test this hypothesis, the expression of Cdh1 was downregulated with short hairpin RNAs (shRNAs). Hela cells showed a downregulation of about 70% while MCF10A and RPE cells showed a less efficient downregulation of about 20-40% of Cdh1 in comparison to shControl lines (Figure 4.15). Cells stably expressing shCdh1 or shControl (shScramble) also expressed Cdt1-mCherry and H2B-YFP in order to measure G1-phase length and the overall cell cycle length in these cell lines.

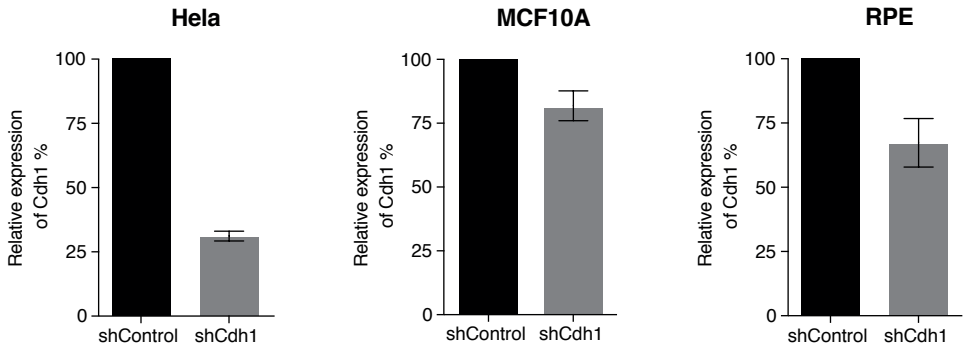


Figure 4.15. Relative expression of Cdh1 mRNA in Hela, MCF10A, and RPE stably expressing shCdh1 and Cdt1-mcherry and H2B-YFP. Relative expression of Cdh1 was measured by qPCR in Hela, MCF10A and RPE cell lines stably expressing shControl (shScramble) or shCdh1 and Cdt1-mCherry and H2B-YFP. Mean ± standard deviation is shown for each cell line (n=3).

4.8.1. Knocking down of Cdh1 shortens the length of G1-phase and cell cycle length in somatic cells

Hela, MCF10A and RPE cells stably expressing either shControl (shScramble) or shCdh1 and Cdt1-venus and H2B-YFP were imaged for two consecutive division cycles in order to measure G1-phase and total cell cycle length. Since Cdh1 plays a major role in activating APC/C from late anaphase until the G1/S transition, Cdh1 downregulation resulted in a major reduction in G1-phase length (Figure 4.16). In all three cell lines, G1-phase length was significantly shorter in Cdh1-depleted cells compared with shControl cells (Hela: shControl 11.5±3.2 hours and shCdh1 8.8±2.0 hours; MCF10A: shControl 6.6±2.8 hours and shCdh1 4.5±1.1 hours; RPE: shControl 11.6±4.9 hours and shCdh1 8.8±2.7 hours). Since G1-phase length became shorter in all three cell lines, total cell cycle length also became shorter (Hela: shControl 26.6±4.3 hours and shCdh1 22.5±2.6 hours; MCF10A: shControl 17.9±4.4 hours and shCdh1 14.4±2.2 hours; RPE: shControl 24.2±5.6 hours and shCdh1 21.0±3.6 hours). In section 4.7.3 it was observed that increasing Cdh1 levels in hESC also increased the variability in G1-phase and cell cycle length, and the inverse was observed when Cdh1 was downregulated in somatic cells. In Hela, MCF10A and RPE, downregulating Cdh1 led to less variability in G1-phase duration and the overall cell cycle length as shown by mean absolute deviation values in Figure 4.16 (G1-phase length: Hela shControl=2.63 and shCdh1=1.58, MCF10A shControl=1.92 and shCdh1=0.82, RPE shControl=3.80 and shCdh1=2.12; Cell Cycle Length: Hela shControl=3.27 and shCdh1=2.08, MCF10A shControl=3.35 and shCdh1=1.74, RPE shControl=4.65 and shCdh1=2.93).

In all three cell lines downregulation of Cdh1 decreased the correlation between duration of G1-phase and cell cycle length (Pearson correlation coefficient, r – Hela shControl=0.66 and shCdh1=0.56; MCF10A shControl=0.81 and shCdh1=0.66; RPE shControl=0.85 and shCdh1=0.61) (right panel Figure 4.16). This corresponds to the reverse effect seen when Cdh1 was over-expressed in hESC and duration of G1-phase became more correlated with cell cycle length as more Cdh1 was over-expressed (Figure 4.13).

Taken together these results suggest that besides being important to establish the refractory period, Cdh1 levels have also an impact on the cell-to-cell variability of cell cycle phase duration and the length of the whole cell division cycle, as well as on the correlation between duration of G1-phase and cell cycle length.

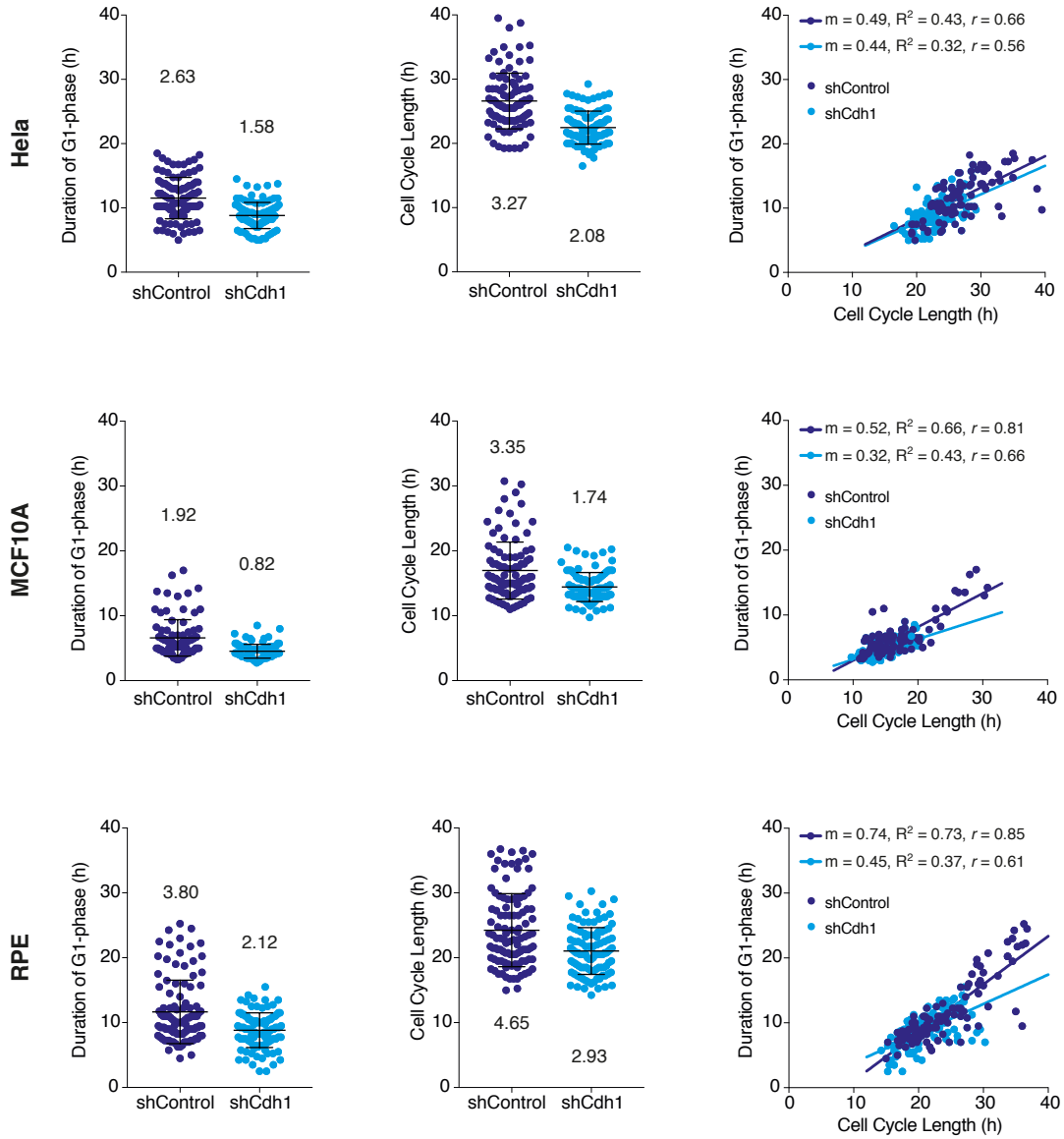


Figure 4.16. Downregulation of Cdh1 in somatic cells decreases duration of G1-phase and cell cycle length. Left panel – Duration of G1-phase measured by live-cell imaging in Hela, MCF10A, and RPE cells stably expressing Cdt1-venus and H2B-YFP in the presence (shControl) or knockdown of Cdh1 (shCdh1). Mean ± standard deviations are shown as bars and mean absolute deviation (MAD) are shown above in hours (n>100). **Middle panel –** Duration of cell division cycle measured by live-cell imaging in Hela, MCF10A and RPE cells stably expressing Cdt1-venus and H2B-YFP in the presence (shControl) or knockdown of Cdh1 (shCdh1). Mean ± standard deviations are shown as bars and mean absolute deviation (MAD) are shown above in hours (n>100). **Right panel –** Duration of G1-phase plotted as a function of cell cycle length in Hela, MCF10A and RPE cells stably expressing Cdt1-venus and H2B-YFP in the presence (shControl) or knockdown of Cdh1 (shCdh1). Slope of the trend line (m), coefficient of determination (R^2) and Pearson correlation coefficient (r) are shown (n>100).

4.8.2. Downregulation of Cdh1 makes somatic cells respond faster to mitotic trigger

Next it was asked whether downregulation of Cdh1 in somatic cells was enough to perturb the refractory period time. To explore this hypothesis, the cumulative percentage of dividing cells was measured in Hela, MCF10A, and RPE cells treated with DMSO or Wee1 inhibitor in the presence (shControl) or downregulation (shCdh1) of Cdh1. As seen previously, less than 10% of cells in both shControl and shCdh1 Hela cell lines divided within 5 hours of treatment with DMSO and the same was observed for RPE cells. In MCF10A cells, less than 25% of the cells divided within 5 hours of DMSO treatment both in the presence (shControl) or knockdown (shCdh1) of Cdh1 (Figure 4.17). However, when Hela cells were stimulated with mitotic trigger, shCdh1 cells responded faster than shControl cells. It was not as striking, but the same trend was also seen in MCF10A and RPE cells. Whenever Cdh1 was down regulated, the cells responded faster to Wee1 inhibition, as the lag time was shorter which indicates that the refractory period had been reduced.

In Hela and MCF10A cells, the cumulative percentage of dividing cells after 5 hours of treatment with the mitotic trigger was essentially the same in shControl lines (51.3% in Hela cells and 56.6% in MCF10A) and shCdh1 lines (51.6% in Hela cells and 55.5% in MCF10A) (Figure 4.17). However, in RPE cells the initial response to the mitotic trigger was similar in shControl and shCdh1 cells, but shCdh1 cells divided much more than shControl cells during the 5 hours that proceeded the mitotic trigger (32.8% in RPE shControl and 48.7% in RPE shCdh1) (Figure 4.17). Together, these results suggest that downregulation of Cdh1 in somatic cells perturbs the refractory period and makes somatic cells more responsive to Wee1 inhibitor stimulation.

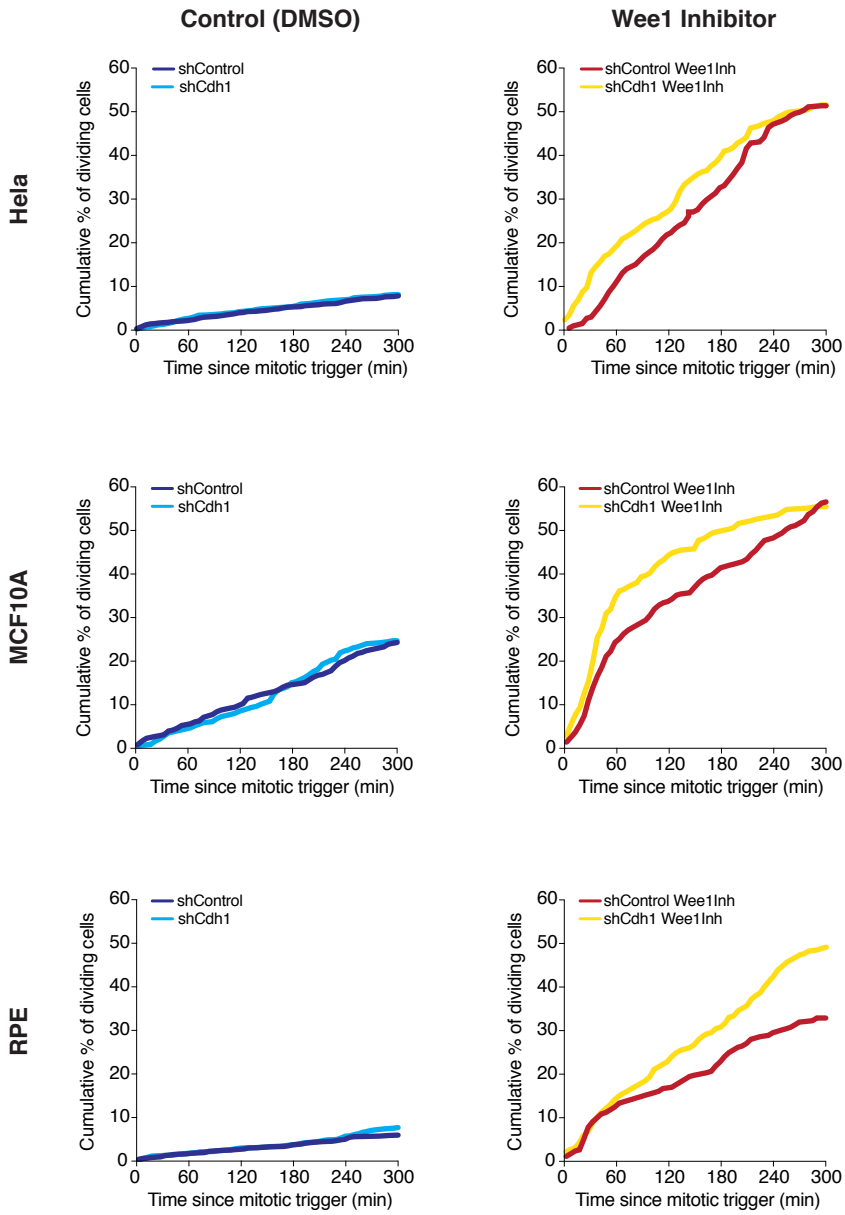


Figure 4.17. Downregulation of Cdh1 decreases response time to a mitotic trigger in somatic cells. Left panel - Cumulative percentage of dividing cells as a function of time since exposure to the mitotic trigger (Wee1 inhibitor) in Hela, MCF10A, and RPE cells stably expressing Cdt1-mCherry and H2B-YFP treated with DMSO in the presence (shControl-dark blue) or knockdown of Cdh1 (shCdh1-light blue) (n>100). **Right panel –** Cumulative percentage of dividing cells as a function of time since exposure to the mitotic trigger in Hela, MCF10A, and RPE cells stably expressing Cdt1-mCherry and H2B-YFP treated with Wee1 inhibitor in the presence (shControl-red) or knockdown of Cdh1 (shCdh1-yellow). (n>100).

4.9. Molecular characterisation of refractory period

Finally, it was addressed if it was possible to characterise molecularly the refractory period. Hela cells spend on average 11 hours in G1-phase and the refractory period has on average a duration of 5 hours, which coincides with G1-phase. For this reason, it was investigated whether G1-phase regulators could be involved in the molecularly establishment of refractory period. Hela, MCF10, RPE, and hES (H9) cells were cultured for 24 hours and then fixed and stained for different G1-phase markers. DAPI staining was used to bin cells into 2N vs. 4N according to DNA content, which allowed for reconstruction of cell cycle trajectory as described by Gut and colleagues (Gut et al., 2015) (in more detail in section 2.5.5). Using this type of analysis, it was possible to derive dynamics of different cell cycle markers throughout different phases of the cell cycle.

Cdt1 protein is a marker for G1-phase and was used as a positive control. It was highly expressed during G1-phase and its levels rapidly decreased at the G1/S transition in Hela, MCF10A, RPE, and hESC. Since hESC have a truncated G1-phase, a major difference in expression dynamics was seen between the three somatic cell lines and hESC. As expected, in somatic cells (Hela, MCF10A, and RPE) (Figure 4.18, Figure 4.19 and Figure 4.20), Cdt1 expression stayed high for a considerably large amount of time, while in hESC high levels of Cdt1 were observed for a very short fraction of time (short G1-phase) (Figure 4.21). In all four cell lines – both somatic and hES cells - Cdt1 levels reach their minimum at the beginning of S-phase and very slowly start to increase again, but never reached levels closer to maximum expression during G1-phase. This shows that Cdt1 staining was a good positive control and supports the use of this type of analysis for the rest of the regulators.

A similar behaviour was observed regarding the activity of Cdh1. Cdh1 activity was calculated by inversion of Cyclin A2 levels, since APC-Cdh1 actively silences Cyclin A2 expression during G1-phase (Geley et al., 2001; Hsu et al., 2002; Lukas et al., 1999; Sørensen et al., 2001). In Hela, MCF10A, and RPE cells, Cdh1 activity was maximal during G1-phase and stayed on until the boundary between G1-phase and S-phase (Figure 4.18, Figure 4.19 and Figure 4.20). However, in hESC Cdh1 activity is maximal at the beginning of G1-phase and rapidly starts to decrease throughout the overall length of G1-phase (Figure 4.21). The fact that in somatic cells Cdh1 activity decreases at the G1/S transition, while in hESC Cdh1 activity decreases during G1-phase, constitutes a major difference in cell cycle dynamics between somatic cells and hESC.

Cdk inhibitors p21 and p27 total levels were very similar in all somatic cell lines – Hela, MCF10A, and RPE cells (Figure 4.18, Figure 4.19 and Figure 4.20). Their maximum levels were observed during G1-phase and decreased in the transition from G1-phase to S-phase. In comparison to Hela and RPE cells, p21 levels in MCF10A cells did not decrease as steeply. All three somatic cell lines showed a small increase in p21 and p27 levels during mitosis.

However, p21 and p27 total levels in hESC behaved in a markedly different way from somatic cells (Figure 4.21). p21 levels had a small increase in a graded manner during G1-phase and underwent a small decrease in the beginning of S-phase. The levels of p21 remained the same during S-phase, starting to rise from the end of S-phase and reaching its maximum levels at G2-phase and mitosis. In hESC, p27 levels were maximum during G1-phase, decreasing from the end of G1-phase and during S-phase. At the end of S-phase, p27 levels started to rise again in a graded manner, reaching again maximum levels at mitosis.

Cyclin A2 and Cyclin B1 levels reached their maximum at mitosis in Hela, MCF10A, RPE, and hESC cells. However, somatic cells and hESC increased Cyclin A2 and Cyclin B1 levels in different dynamics. Hela, MCF10A, and RPE cells have minimum levels of mitotic Cyclins - Cyclin A2 and Cyclin B1 – during G1-phase (Figure 4.18, Figure 4.19 and Figure 4.20). The levels of these two Cyclins increased in a step-like manner during S-phase, attaining maximum levels during G2-phase and mitosis. This confirms that in somatic cells G1-phase is an off-phase for mitotic Cyclins whereas G2-phase and mitosis are on-phases. Conversely, this does not seem to be the case in hESC (Figure 4.21). Like somatic cells, in G1-phase hESC have very low levels of Cyclin A2 and Cyclin B1, but the accumulation of both mitotic Cyclins is much more graded than in somatic cells and reaches maximum levels at G2-phase and mitosis.

In order to progress from G1-phase to S-phase, pRB needs to be hyper-phosphorylated. Cdk4-Cyclin D1 complexes phosphorylate Rb Ser780 during G1-phase in a cell cycle-dependent manner in order to promote dissociation of Rb from E2F1 (Kitagawa et al., 1996). Cdk4-Cyclin D1 is also responsible for phosphorylation of Rb Ser807/881, which disrupts the C-pocket of Rb that is one of primary locations of phosphatases binding on inactive pRB (Connell-Crowley et al., 1997; Lees et al., 1991; Zarkowska and Mittnacht, 1997). In Hela, MCF10A, and RPE cells phosphorylation levels of Rb on Ser780 and on Ser807/811 were very low during G1-phase (Figure 4.18, Figure 4.19 and Figure 4.20). However, at the G1/S transition phosphorylation levels of these three serine residues started to increase, reaching maximum levels at G2-phase and mitosis. The phosphorylation levels of Ser780 and Ser807/811 increased during S-phase in a step-like manner in both Hela and RPE cells, while MCF10A cells showed a more graded increase. In hESC the phosphorylation levels of pRB acted in a different manner. Phosphorylation of Ser780 increased during G1-phase and decreased during S-phase. At the S/G2-phase transition, phosphorylation of Ser780 started to increase, attaining maximum levels during mitosis (Figure 4.21). Phosphorylation of pRB Ser807/811 slowly increased in a cell cycle-dependent manner in hESC, from G1-phase to mitosis.

The phosphorylation of Cdc6 Ser54 by Cdk2-cyclin A2 complexes leads to re-localization of Cdc6 from the nucleus to the cytoplasm in order to prevent re-replication of DNA during S-phase (Petersen et al., 1999). This phosphorylation is a read out for Cdk2-cyclin A2 activity. So as expected, the phosphorylation levels of Cdc6 Ser54 increased in a cell cycle-dependent manner in all three somatic cells lines tested – Hela, MCF10A, and RPE cells (Figure 4.18, Figure 4.19 and Figure 4.20). A different trend was observed in hESC: at the beginning of G1-phase, phosphorylation levels of Ser54 peaked and then decreased gradually until the middle of S-phase before starting to increase again and peaking at mitosis (Figure 4.21).

The activity levels of p21 and p27 were estimated by inverting the inhibitory phosphorylation levels of p21 Thr145 and p27 Thr187. Pim-1 phosphorylates p21 at Thr145 in order to stabilize and inactivate p21, increasing the rate of cell proliferation (Zhang et al., 2007). Cdk2-Cyclin E complexes phosphorylate p27 Thr187, targeting it for degradation (Sheaff et al., 1997). p21 and p27 activity levels were maximal in G1-phase in Hela, MCF10A, and RPE cells and decreased in a cell cycle-dependent manner, reaching minimum levels at mitosis (Figure 4.18, Figure 4.19 and Figure 4.20). In hESC, p21 activity levels had exactly the same trend as in somatic cells (Figure 4.21). Although p27 activity levels were high at the beginning of G1-phase as observed in somatic cells, they decreased during G1-phase and increased again during S-phase, peaking at S/G2-phase transition (Figure 4.21). After that, p27 activity levels started to decrease again, reaching minimum levels at the end of mitosis.

Although fluctuation of Emi1 levels in all four lines tested looked very different, they were minimal at the beginning of G1-phase and maximal during mitosis. In Hela and MCF10A cells, Emi1 levels increased from the beginning of G1-phase until mitosis in a cell cycle-dependent manner (Figure 4.18 and Figure 4.19). In RPE cells, Emi1 levels increased at the beginning of G1-phase and then decreased until the G1/S transition (Figure 4.20). During S-phase Emi1 levels increased in step-like manner reaching high levels in mitosis. In hESC, Emi1 levels increased in a gradual manner during G1-phase and were maintained during S-phase and G2-phase, starting to rise again at the end of G2-phase and reaching maximum levels during mitosis (Figure 4.21).

By comparing the expression and activity levels of important cell cycle players in Hela, MCF10A, and RPE cells that have a refractory period and hESC that do not have a refractory period, it was possible to suggest some important molecular features of the refractory period. Taking into account the results presented above, the refractory period resembles a time that is characterised by extreme low levels of the mitotic cyclins Cyclin A2 and Cyclin B1, high levels of p21 and p27 expression, low levels of Rb phosphorylation, high levels of Cdh1 activity and modestly increasing levels of Cdk2 activity.

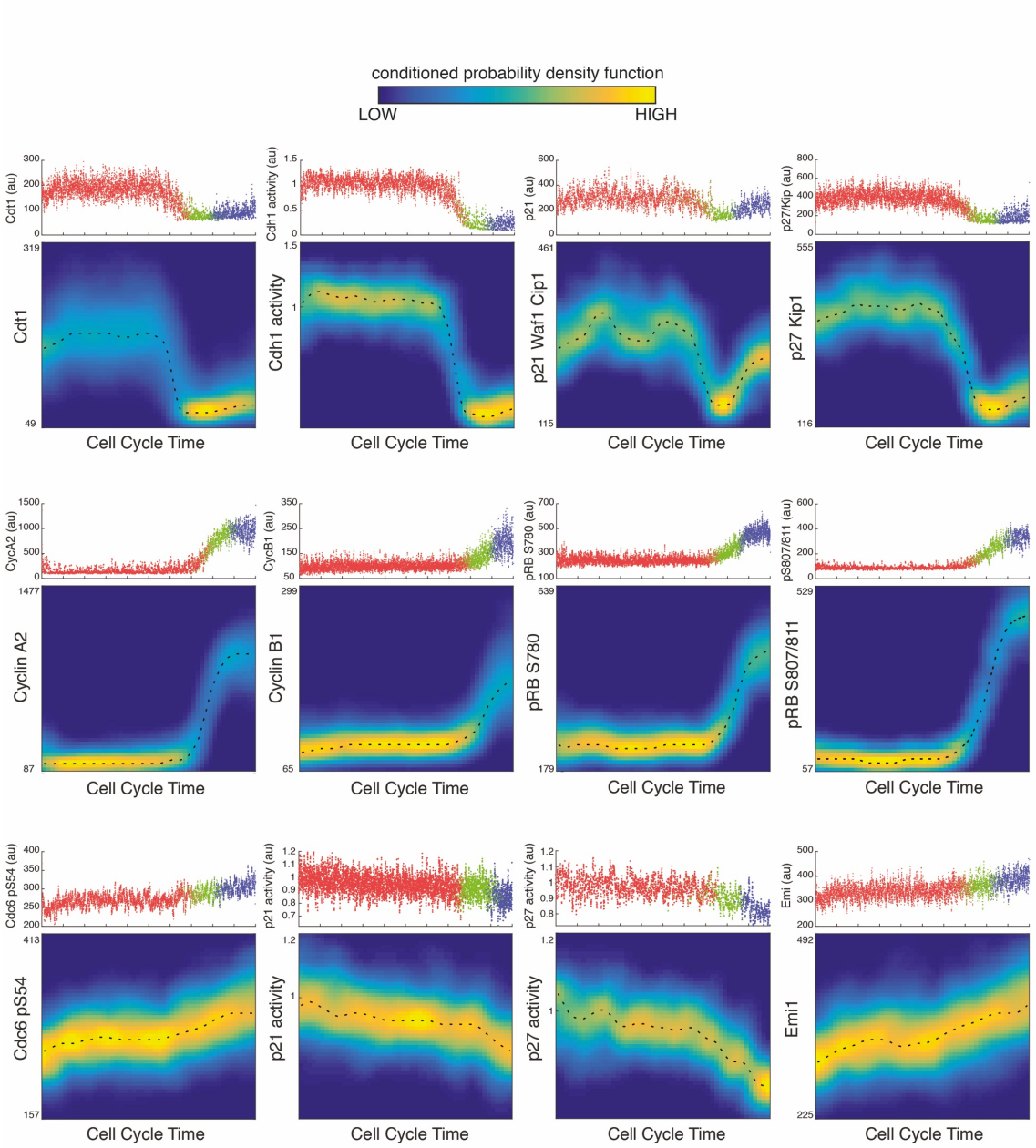


Figure 4.18. Cell cycle trajectory of G1-phase regulators in Hela cells. The figures in the top panel represent the scatter plot of cell cycle time vs mean nuclear intensity of the cell cycle regulator from single cell quantification. This recapitulates the dynamics of the respective cell cycle regulator. The figures in the lower panel are the heat map representation of the 2D-kernel density estimation from the figures in the top panel conditioned to X-axis (i.e. cell cycle time). The density weighted average of mean intensity of the cell cycle regulators shown as dotted line represents the estimated trajectory of the cell cycle regulator during cell cycle progression.

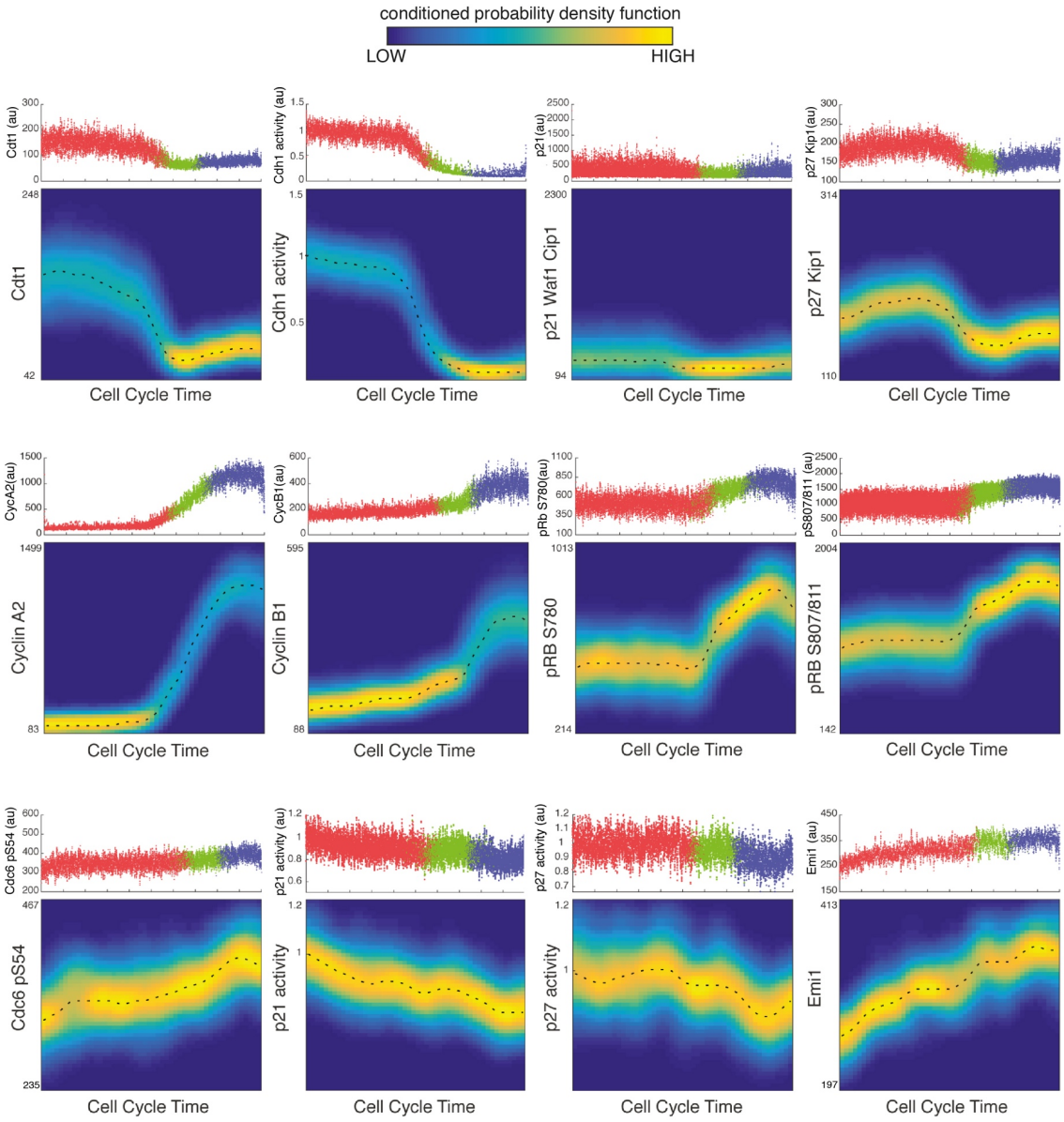


Figure 4.19. Cell cycle trajectory of G1-phase regulators in MCF10A cells. The figures in the top panel represent the scatter plot of cell cycle time vs mean nuclear intensity of the cell cycle regulator from single cell quantification. This recapitulates the dynamics of the respective cell cycle regulator. The figures in the lower panel are the heat map representation of the 2D-kernel density estimation from the figures in the top panel conditioned to X-axis (i.e. cell cycle time). The density weighted average of mean intensity of the cell cycle regulators shown as dotted line represents the estimated trajectory of the cell cycle regulator during cell cycle progression.

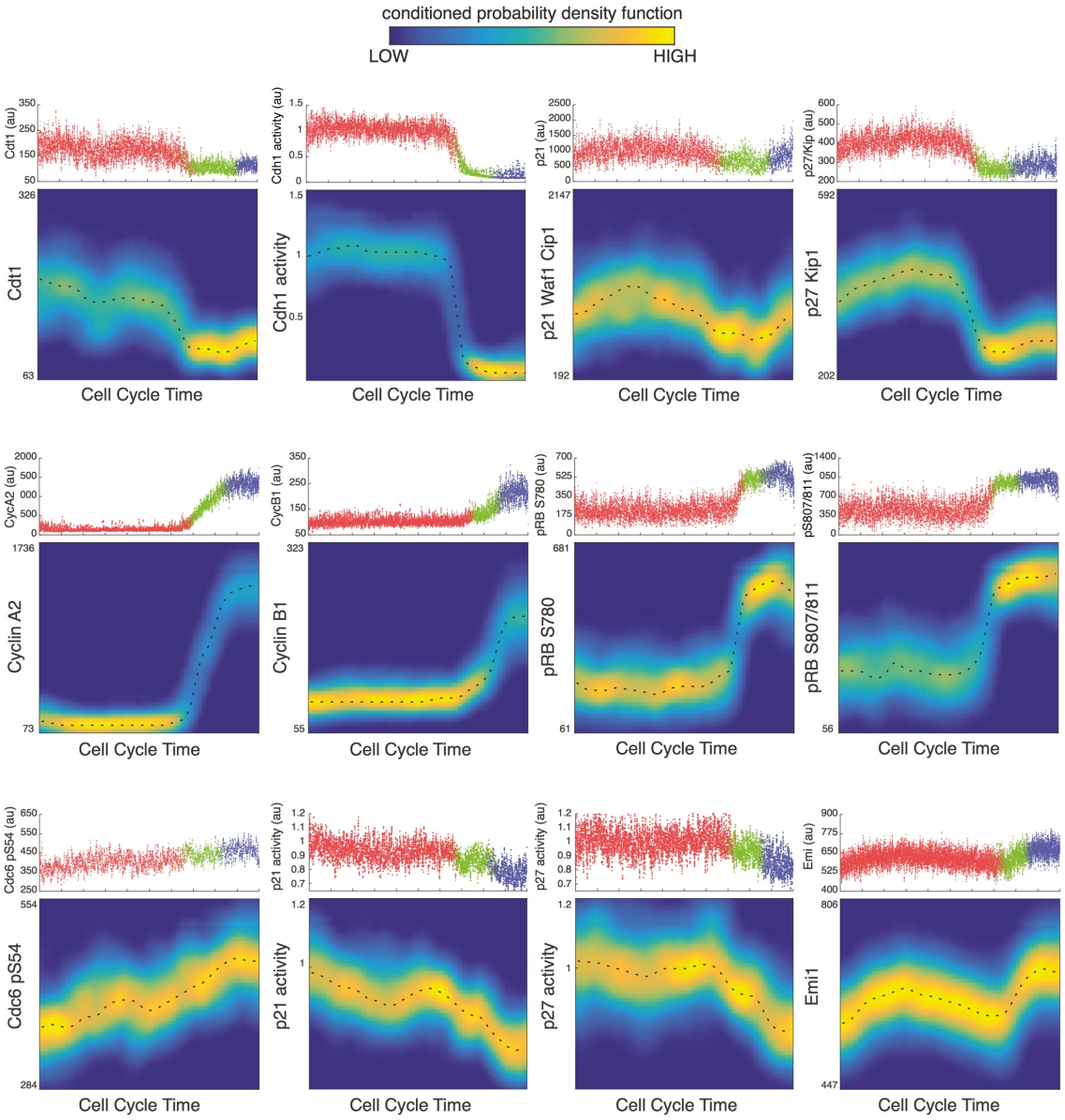


Figure 4.20. Cell cycle trajectory of G1-phase regulators in RPE cells. The figures in the top panel represent the scatter plot of cell cycle time vs mean nuclear intensity of the cell cycle regulator from single cell quantification. This recapitulates the dynamics of the respective cell cycle regulator. The figures in the lower panel are the heat map representation of the 2D-kernel density estimation from the figures in the top panel conditioned to X-axis (i.e. cell cycle time). The density weighted average of mean intensity of the cell cycle regulators shown as dotted line represents the estimated trajectory of the cell cycle regulator during cell cycle progression.

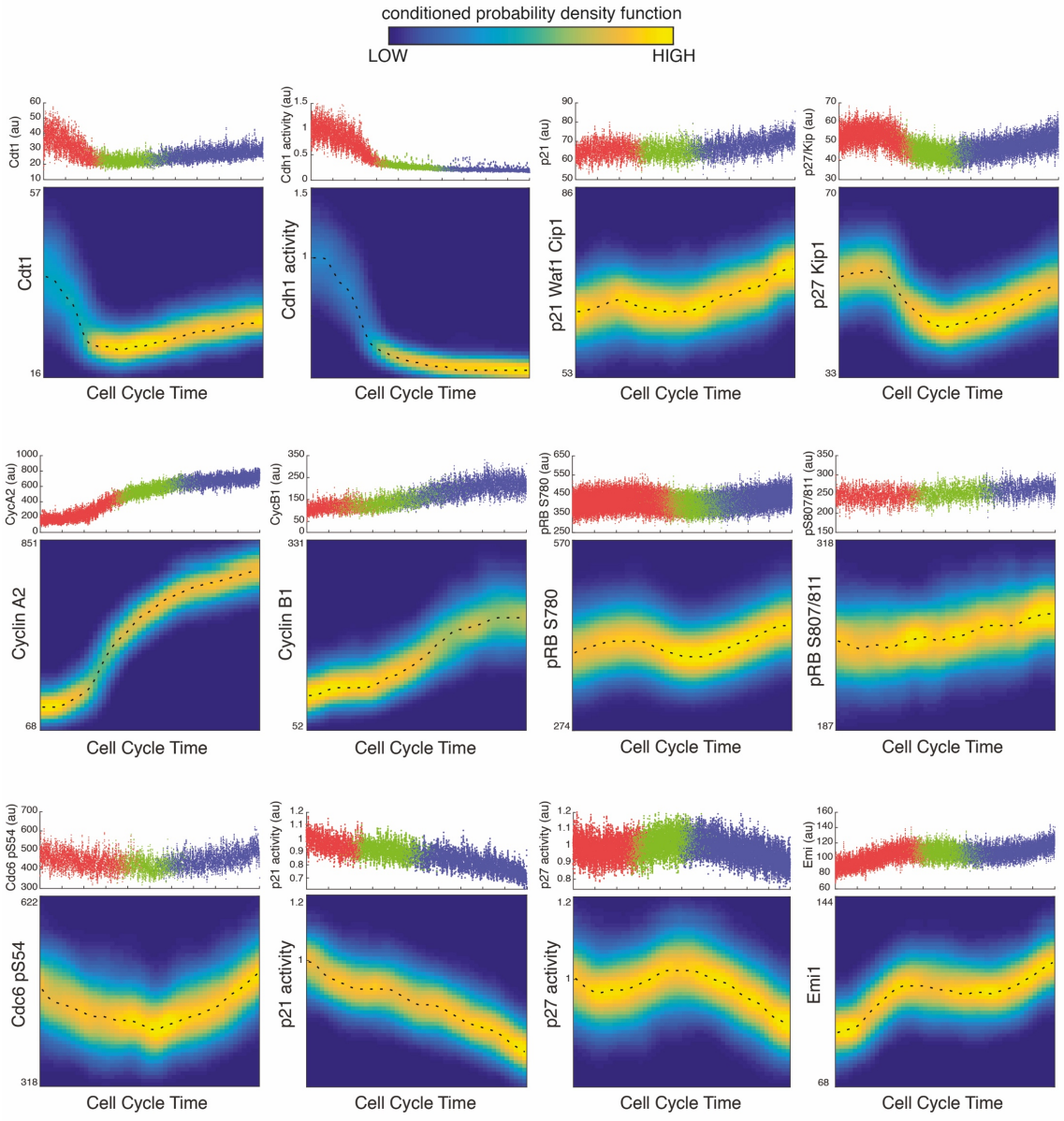


Figure 4.21. Cell cycle trajectory of G1-phase regulators in hESC cells. The figures in the top panel represent the scatter plot of cell cycle time vs mean nuclear intensity of the cell cycle regulator from single cell quantification. This recapitulates the dynamics of the respective cell cycle regulator. The figures in the lower panel are the heat map representation of the 2D-kernel density estimation from the figures in the top panel conditioned to X-axis (i.e. cell cycle time). The density weighted average of mean intensity of the cell cycle regulators shown as dotted line represents the estimated trajectory of the cell cycle regulator during cell cycle progression.

4.10. Major highlights of temporal control of interphase

The main aim of the work presented in this chapter was to understand the stage at which cells become competent to undergo a new round of mitosis. To tackle this question, different cell lines expressing cell cycle sensors were treated with Wee1 inhibitor as a proxy for a mitotic trigger. When freely cycling cells were challenged with Wee1 inhibitor, some cells responded to the mitotic trigger but other cells did not. It was found that after mitosis there is a refractory period, during which cells are immune to mitotic triggers and cannot undergo another round of mitosis. It was also shown that this mitotic refractory period was dependent on the strength of the Cdk1:APC-Cdh1 feedback loop. hESCs lack a mitotic refractory period, but when Cdh1 was ectopically expressed in these cells it was possible to re-establish the refractory period. This confirms the ODE prediction that by modulating the strength of the Cdk1:APC-Cdh1 feedback loop it is possible to change the length of the refractory period. In line with this reasoning, post-mitotic, non-dividing cells such as neurons express high levels of APC-Cdh1, which is likely to result in stronger Cdk1:CyclinB1-APC:Cdh1 feedback regulation and thereby a longer interphase. This work also provides evidence for the theory that modulating feedback strength is a simple regulatory strategy which allows cells to tune the period of division cycles.

5. Cell Cycle Dynamics in Single Cells: a preliminary comparative study

5.1. Summary

The molecular machinery that regulates cell division appeared more than a billion years ago and is well conserved over the course of evolution and between different species. However, within the same organism, the length of the cell cycle varies between different cell types. Early divisions in an embryo happen every 4.4 hours whereas some post-mitotic cells, like neurons, stay all their lives in a post-mitotic state and never re-enter the cell cycle. In this chapter, it was asked whether measuring cell cycle dynamics at single cell level with multiple cell cycle biosensors in different cell lines would allow to infer similarities and/or differences between cell cycle dynamics in normal and cancer cells. Preliminary quantification of the length of time of the different cell cycle phases in single cells by live-cell imaging showed high variability between cells within a population. A combination of experimental approaches based on single cell imaging with computational analyses was used in order to understand globally the temporal dynamics of cell division in different cell lines. For that purpose, proliferative differences between normal and cancer cells were measured and comparative cell cycle dynamics were analysed. With these experiments, preliminary results showed that it might be possible to infer regulatory principles that underlie proper functioning of the cell cycle in human cells and understand potential cell cycle hallmarks for malignancy.

5.2. Aims

The aim of the work presented in this chapter was to use different set of biosensors to measure cell cycle dynamics by live cell imaging in pairwise normal and cancer cell lines in order to identify similarity and or differences in cell cycle regulation that distinguish healthy and malignant cells

5.3. Different cell lines have different cell cycle dynamics

In chapter 3 it was shown that it is possible to measure cell cycle dynamics in single cells stably expressing Cdt1-venus, H2B-turquoise and PCNA-mCherry as cell cycle biosensors. However, a different set of biosensors was also built. Measuring cell cycle dynamics with two different set of sensors allows for a more robust outcome and ensure that artefacts are not being introduced. This second set of sensors was composed by Dnmt1-CFP, DNA Ligase-YFP and H2B-mCherry and the time of different cell cycle phases was measured as described in section 2.5.2.2: G1-phase length was monitored by nuclear localization of Dnmt1 and DNA Ligase; S-phase starting point was considered to be the time that Dnmt1 and DNA Ligase start to speckle and S-phase length was defined as the time between appearance and disappearance of DNA Ligase speckles; G2-phase was measured by monitoring the time between the disappearance of DNA Ligase speckles and the disappearance of Dnmt1 speckles or nuclear envelope breakdown (NEB); mitosis was defined as the time between nuclear envelope breakdown (NEB) and nuclear envelope reformation (NER), and cell cycle length was measured as the time between two consecutive NER events.

MCF10A, RPE, and Hela cells stably expressing Dnmt1-CFP, DNA Ligase-YFP and H2B-mCherry biosensors were imaged for two consecutive days and in order to measure cell cycle dynamics and compare with the results obtained with the previous set of sensors used (Cdt1-venus, H2B-turquoise and PCNA-mCherry). The cell cycle length of the two normal somatic cell lines, MCF10A (21.7±4.5 hours) and RPE (23.9±4.3 hours), was found to be very similar to the cell cycle length of Hela cells (24.6±3.4 hours) – a regularly used cancer cell line (Figure 5.1.A). However, the length of different cell cycle phases was strikingly different between normal and cancer cell lines. Both MCF10A and RPE cells spend less time in G1-phase – 4.6±1.1 hours and 5.9±2.3 hours, respectively – in comparison to 8.4±2.6 hours in Hela cells. MCF10A, RPE, and Hela cells spent the largest fraction of their cell cycle in S-phase (MCF10A=7.9±1.5 hours, RPE=10.0±1.4 hours and Hela=9.4±2.0 hours), since S-phase involves the careful replication of DNA and hence is one of the most critical phases of the cell cycle. Unexpectedly, and contrary to what was seen for G1-phase length, Hela cells had

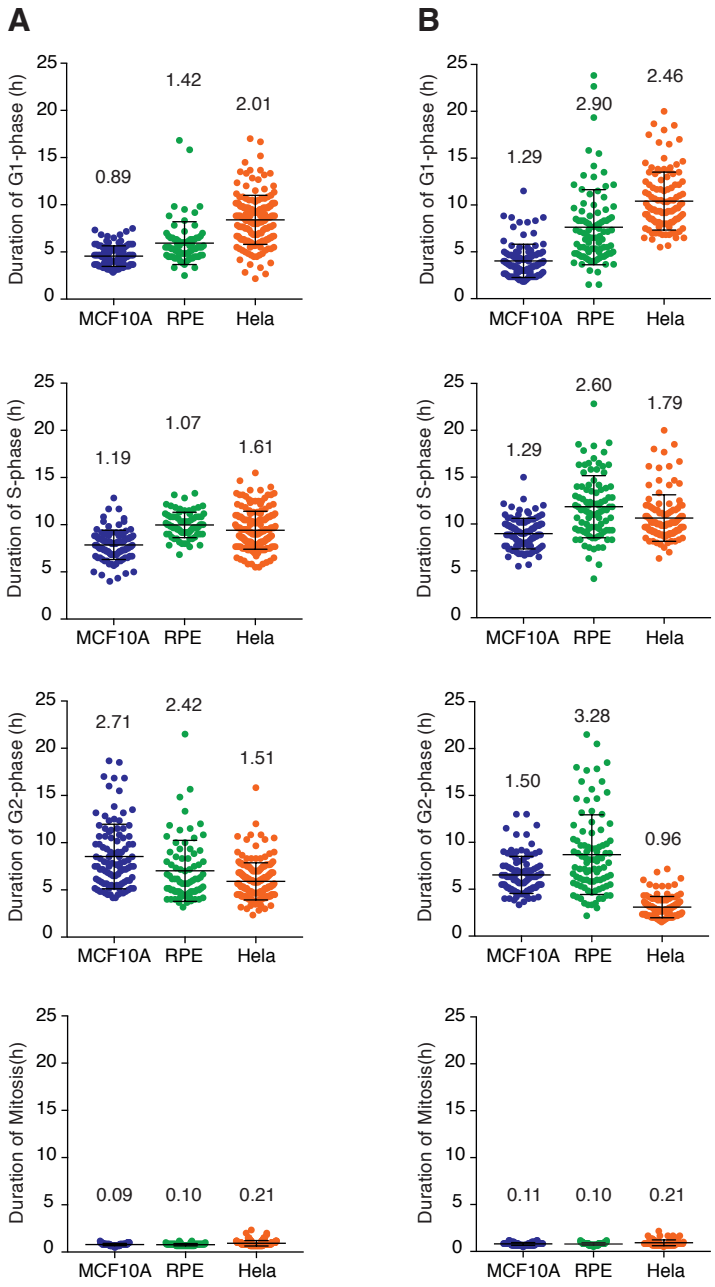


Figure 5.1. Cell cycle dynamics of three somatic cell lines measured with two different sets of cell cycle biosensors. A. Time of G1-phase, S-phase, G2-phase, and mitosis (from top to bottom, respectively) measured by live-cell imaging in MCF10A (blue), RPE (green) and Hela (orange) cells stably expressing Dnmt1-CFP, DNA Ligase-YFP and H2B-mCherry. **B.** Time of G1-phase, S-phase, G2-phase and mitosis (from top to bottom, respectively) measured by live-cell imaging in MCF10A (blue), RPE (green) and Hela (orange) cells stably expressing Cdt1-venus, PCNA-mCherry and H2B-Turquoise. Mean ± standard deviations are shown as bars and mean absolute deviations (MAD) are shown above in hours (n>80).

a much short G2-phase (5.9±2.0 hours) in comparison to MCF10A (8.5±3.4 hours) and RPE cells (7.2±3.4 hours). This may be explained by the fact that G2-phase is the time to repair any DNA damage that occurs during S-phase and cancer cells might have means to overcome this surveillance mechanism. However, and as seen previously, duration of mitosis was always short across the three different cell lines (MCF10A=47.8±7.2 minutes, RPE=47.8±8.9 minutes, and Hela=55.8±16.9 minutes) (Figure 5.1.A).

All three cell lines – MCF10A, RPE and Hela – showed large variability in the time of G1-phase (MAD=0.89, 1.42 and 2.01 in MCF10A, RPE, and Hela cells, respectively), S-phase (MAD=1.19, 1.07 and 1.61 in MCF10A, RPE, and Hela cells, respectively), and G2-phase (MAD=2.71, 2.42 and 1.51 in MCF10A, RPE, and Hela cells, respectively) as indicated by their MAD values. As expected, mitosis was kept remarkably constant across normal and cancer cell lines (MAD=0.09, 0.10 and 0.21 in MCF10A, RPE, and Hela cells, respectively).

Using two different sets of cell cycle biosensors allowed to confirm that the cell cycle dynamics measured are not dependent on a single set of biosensors. Using Cdt1, DNA Ligase, PCNA and Dnmt1 allowed for the comparison between them and avoided introducing artefacts, since more than one protein at each time was used to read the length of the different cell cycle phases. In general, the cell cycle dynamics measured using the two different sets of biosensors as shown in Figure 5.2 is very similar. Besides some slight differences – time of G2-phase in RPE for example - between the different sets of biosensors, the trends are exactly the same. MCF10A cells were the ones with the shortest G1-phase and Hela cells had the longest G1-phase. RPE cells spent the longest fraction of their cell cycle in S-phase, while MCF10A cells spent less time duplicating DNA. Hela cells were the fastest in G2-phase, spending less time repairing DNA than normal cells. MCF10A and RPE cells had longer G2-phases than Hela cells. The most difference between the two sets of cell cycle biosensors was seen in measurements of RPE G2-phase length, probably because this is one of the most variable phases of the cell cycle where the cell stops to make sure that all DNA damage is repaired before proceeding to mitosis. Mitotic time was very similar in all three cell lines when measured with the two different sets of cell cycle biosensors.

As previously shown, measuring cell cycle dynamics of MCF10A, RPE, and Hela cells with Cdt1-venus, PCNA-mCherry, and H2B-Turquoise disclosed that the relative length of interphase could be used to anticipate the duration of the overall cell cycle length (Figure 3.3). When Dnmt1-CFP, DNA Ligase-YFP and H2B-mCherry biosensors were used to measure cell cycle dynamics of MCF10A, RPE, and Hela cells the same tendency was observed. There was a correlation between duration of G1-, S-, and G2-phases and the corresponding total cell cycle length. Meaning, it is possible to foresee how long the cell cycle is going to be by knowing how long the duration of G1-, S- or G2-phase was for a certain cell (Figure 3.3 and Figure 5.2).

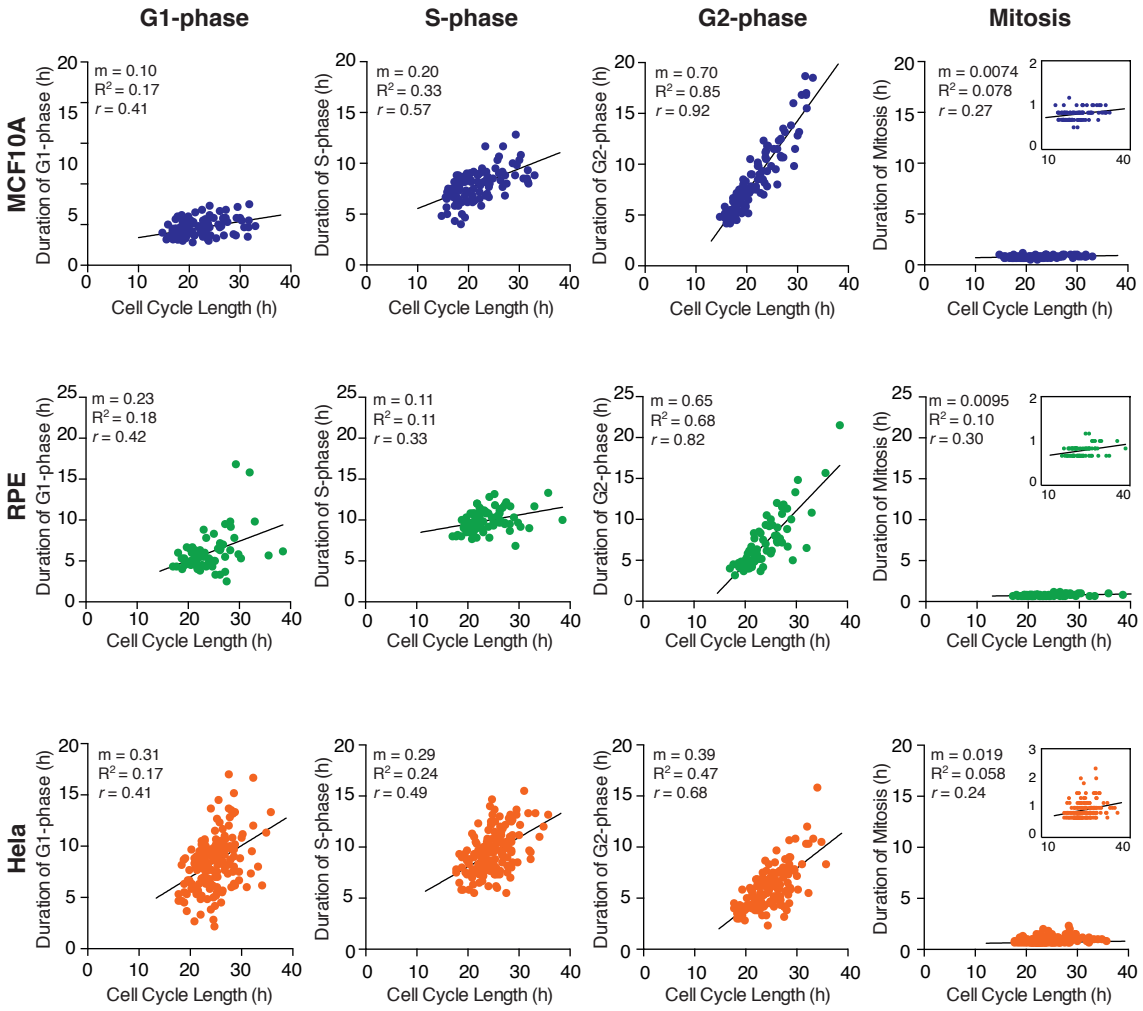


Figure 5.2. A different set of cell cycle biosensors also show that duration of interphase correlates with cell cycle length. Duration of G1-phase, S-phase, G2-phase, and mitosis in single cells as a function of cell cycle length measured by live-cell imaging in MCF10A (top panel), RPE (middle panel) and Hela (bottom panel) cells. All lines stable expressed Dnmt1-CFP, DNA Ligase-YFP, and H2B-mCherry. Insect shows same data on a 0-2 or 0-3 hours y axis scale. Slope of the trend line (m), coefficient of determination (R^2) and Pearson correlation coefficient (r) are shown (n>80).

As extensively studied in chapter 3, regardless of the overall cell cycle length for individual cells, there was no correlation between duration of mitosis and cell cycle length in all cell lines tested using this second set of cell cycle biosensors (Pearson correlation coefficient, *r* – MCF10A=0.27, RPE=0.30 and Hela=0.24 using Dnmt1-CFP, DNA Ligase-YFP and H2B-mCherry) (right panel Figure 3.3 and right panel Figure 5.2).

Taken together, these results show that using two different sets of cell cycle biosensors still allows for a very similar measurement of cell cycle dynamics as proposed before (Easwaran et al., 2005; Sakaue-Sawano et al., 2008a; Sporbert et al., 2005) (Figure 5.2 and Figure 3.3). Although exact timing of different cell cycle phases was not exactly the same, the overall trends are conserved. Any differences might be due to intrinsic noise and the inherent variability that exists between cells in the same population.

5.4. Comparing cell cycle dynamics in normal cells vs. paired cancer cells

In the previous section, it was observed that cancer and normal cells have different cell cycle dynamics. So, next it was investigated whether the cell cycle dynamics would also be different when comparing paired normal and cancer cells. To this end, a pair of normal and cancer cell lines was used. The pair was comprised of the epithelial non-tumorigenic breast cell line MCF10A and the adenocarcinoma-derived epithelial breast cell line MCF7. In order to measure cell cycle dynamics in paired normal vs. cancer cells, MCF10A and MCF7 cells stably expressing Cdt1-venus, PCNA-mCherry, and H2B-Turquoise were imaged for two consecutive division cycles and the length of different cell cycle phases measured as described in section 2.5.2.1.

5.4.1. A pair of normal vs. cancerous cells behave differently throughout the different cell cycle phases

There were obvious differences between the overall cell cycle length of normal cells and their cancerous counterparts. MCF10A cells had an average cell cycle length of 20.3±4.1 hours and their paired cancer cells, MCF7, took 35.0±6.2 hours to conclude their cell cycle. In Figure 5.3 the length of G1-, S-, G2-phases and mitosis in normal and cancerous cells is compared.

Duration of G1-phase in MCF10A cells was much shorter (4.0±1.8 hours) when compared with MCF7 cells (9.4±3.7 hours) and also less variable (MAD: MCF10A=1.29 and MCF7=2.82). Although S-phase was the longest phase in both MCF10A and MCF7 cells it was extremely different between these two lines. MCF7 cells spent on average 20.3±4.1 hours in S-phase (the same amount of time that MCF10A cells needed to go through one division cycle) and MCF10A cells finished S-phase in 9.0±1.6 hours. In terms of variability, S-phase time of MCF7 cells was much more variable (MAD=3.24) than the duration of S-phase in MCF10A cells (MAD=1.29).

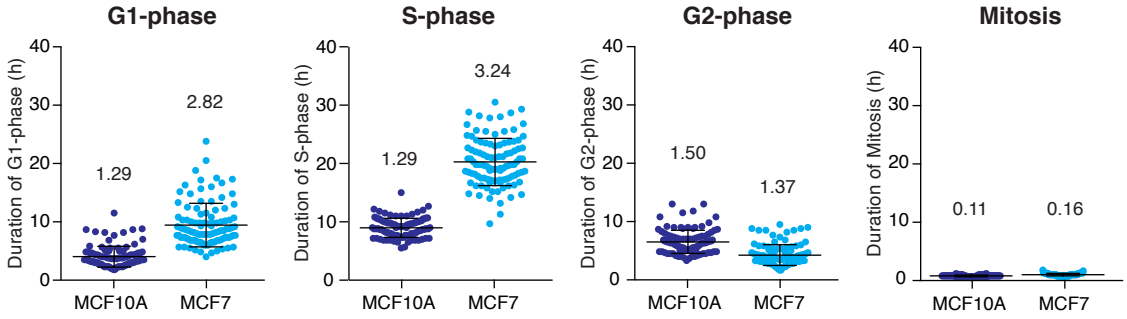


Figure 5.3. Time of different cell cycle phases in paired normal vs. cancer cell lines. Duration of G1-phase, S-phase, G2-phase, and mitosis measured by live-cell imaging in MCF10A (dark blue) and MCF7 (light blue) cells stably expressing Cdt1-venus, PCNA-mCherry, and H2B-Turquoise. Mean ± standard deviations are shown as bars and mean absolute deviations (MAD) are shown above in hours (n>100).

As seen previously, G2-phase was shorter and more constant in cancer cells – MCF7 – when compared to the duration of G2-phase in their normal counterpart. Besides having a very long S- phase, MCF7 cells spent on average 4.2±1.8 hours in G2-phase, while MCF10A spent 6.5±2.0 hours (p<0.0001 by Mann-Whitney test). When comparing mitotic time, as expected from all the results presented in previous chapters, it was always short and constant across different cell types, including normal and cancer cell lines (right panel Figure 5.3). Both cell lines spent less than 5% of their cell cycle length in mitosis. Although MCF7 cells spent slightly more time in mitosis than MF10A cells (48.0±6.4 minutes and 61.8±12.6 minutes, respectively), both cell types showed very low variability on duration of mitosis time as shown by the mean absolute deviation values (MCF10A=0.10 and MCF7=0.16).

Correlations between different cell cycle phases and the relative cell cycle length showed that cancer cells have the same behaviour as normal cells. There was a strong correlation between G1-, S- and G2-phases and the total cell cycle length in MCF7 cells as well as MCF10A cells (Figure 3.3). In both cell lines, duration of mitosis did not correlate with cell cycle length (Pearson correlation coefficient, r – MCF10A=0.30 and MCF7=0.16).

Taken together these results suggest that the length and variability of cell cycle phases between normal and cancer cells is very different which impacts in their specific cell cycle dynamics. However, the temporal insulation of mitosis seems to be a feature common to all cell types independently of their function or disease state.

5.4.2. Interdependency of different cell cycle phases time is different in normal and cancer cells

Next, it was addressed how time of individual cell cycle phases correlate with each other and if it was possible to observe different trends when comparing a pair of normal and cancer cells. In order to investigate this, the percentage of time that an individual cell spent in each of the four different cell cycle phases was calculated. In this way, it was possible to compare data from two different cell lines without introducing artefacts. The dependence of each different cell cycle phase on the other three cell cycle phases is shown in Figure 5.4. The first striking observation is that independently of the cell type (normal or cancerous), G1-, S- and G2-phases durations are highly correlative, while mitosis is independent from the three interphase cell cycle phases (Pearson correlation coefficient, r – G1-phase vs M in MCF10A=-0.29 and MCF7=-0.26; S-phase vs M in MCF10A=0.21 and MCF7=0.09; G2-phase vs M in

MCF10A=-0.039 and MCF7=0.15). This corroborates previous observations that mitosis is temporally independent from upstream cell cycle events. G1-phase was strongly inversely correlated with S-phase in MCF7 cells (Pearson correlation coefficient, r = -0.79). In MCF10A cells G1-phase was also inversely correlated with S-phase (Pearson correlation coefficient, r – MCF10A=-0.47). G2-phase was also highly inversely correlated with G1-phase in MCF10A cells, which was not observed in MCF7 cells (Pearson correlation coefficient, r – MCF10A=-0.59; MCF7=-0.36).

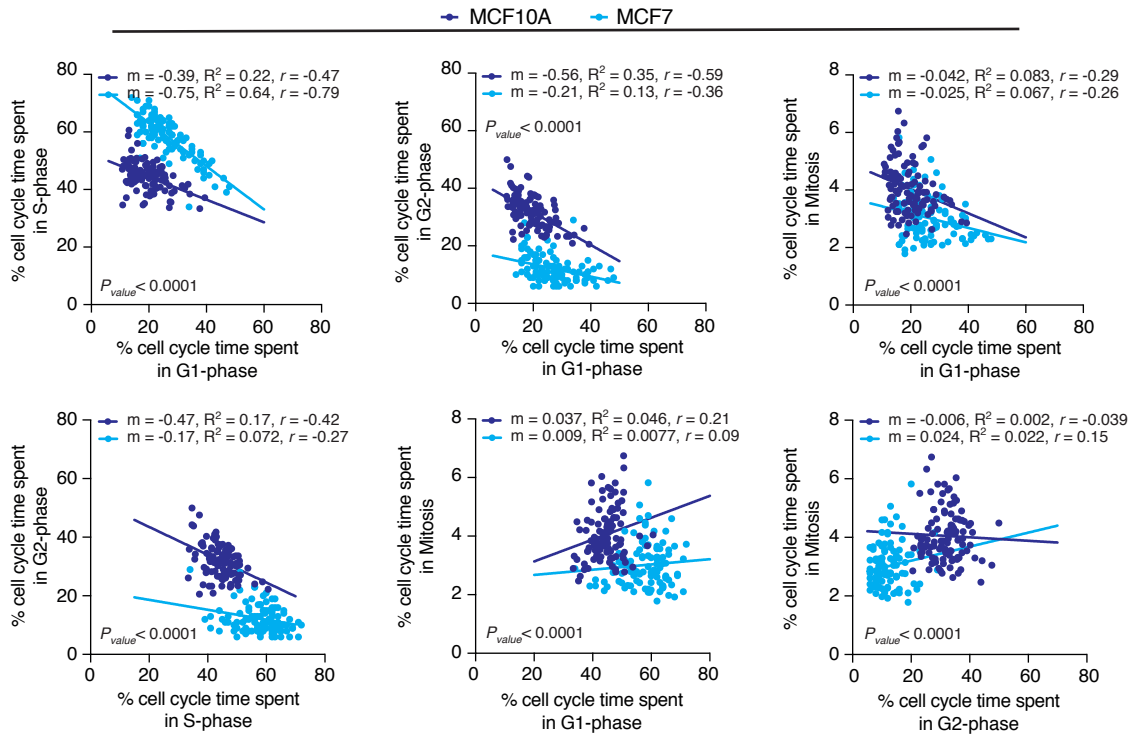


Figure 5.4. G1-phase is inversely correlated with S-phase and G2-phase in normal cells but not in cancer cells. Stable lines expressing Cdt1-venus, PCNA-mCherry, and H2B-Turquoise. Percentage of timing of G1-phase, S-phase, G-phase, and mitosis as a function of the other three cell cycle phases in MCF10A (dark blue dots) and MCF7 (light blue dots) cells as measured by live-cell imaging. Slope of the trend line (m), coefficient of determination (R^2), Pearson correlation coefficient (r) and p values calculated by Mann-Whitney test are shown (n>100).

Another interesting observation came when S-phase and G2-phase were compared. In normal cells, MCF10A, S-phase was strongly inversely correlated with G2-phase (Pearson correlation coefficient, *r* – MCF10A=-0.42), which might be due to fact that cells that spend less time in S-phase are more likely to carry some faults in the replicated DNA, and hence need to spend more time in G2-phase in order to repair it in preparation for entry into mitosis. On the other hand, in MCF7 cells there was no correlation between S-phase and G2-phase (Pearson correlation coefficient, *r* – MCF7=-0.27). This is in line with previous suggestions that cancer cell lines – Hela and MCF7 cells – have very short G2-phases and hence spend a short amount of time repairing DNA.

This type of analysis points to the importance of looking at the dynamics of the different cell cycle phases to understand potential functional differences between cell lines. The results presented here suggest that normal cell lines have different cell cycle dynamics from cancer cell lines. G1-phase was inversely correlated with S-phase and G2-phase in MCF10A (normal) cells but not in cancerous MCF7 cells. Looking at cell cycle dynamics in different cell lines might allow to infer regulatory principles underlying proper functioning of different human cell types.

5.5. Major highlights of cell cycle dynamics in single cells

In this chapter, it was presented preliminary evidence that measuring cell cycle dynamics with two different sets of cell cycle biosensors gives very similar measurements of the dynamics of different cell cycle phases. Intrinsic noise and variability within the same population of cells might account for small differences observed between the measurements taken using the two sets of biosensors. Moreover, normal and paired cancerous cells have very different cell cycle dynamics which might impact directly on their cell function. However, temporal insulation of mitosis seems to be a common feature of all cell lines, independently of their function or disease state. This type of approach suggests that it might be possible to infer regulatory principles fundamental for proper functioning of the cell cycle in human cells and understand potential cell cycle hallmarks of malignancy.

6. Discussion

6.1. Feedback regulation is important for temporal control of cell division

In all the cell lines where duration of mitosis was measured, the length of mitosis as well as the overall cell cycle length scales well with the number of chromosomes (Figure 6.1). Mouse embryonic stem cells have 40 chromosomes and undergo a shorter mitotic time and cell cycle length. In contrast, the cancer cell lines MCF7 and Hela both have 82 chromosomes and also have the longest duration of mitosis, with MCF7 also displaying the longest overall cell cycle length. Hence, there appears to be some degree of correlation between chromosome number and mitosis and cell cycle duration – cells with higher number of chromosomes have a longer duration of mitosis and cell cycle length. This could be a consequence of the time needed to replicate and segregate chromosomes, which are the two main functions of a cell division cycle (Morgan, 2007).

When studied at the single-cell level, cells within the same population have highly variable cell cycle lengths. This seems to be a consequence of high variability in the dynamics of interphase duration – G1-phase, S-phase and G2-phase – that was not seen in mitotic duration. Surprisingly, duration of mitosis was found to be always short, constant and independent of variability of earlier cell cycle phases, showing no correlation with cell cycle length. In addition, it was possible to predict how long the cell cycle of a certain cell was going to be based on how long G1-, S- and G2-phases were and vice versa.

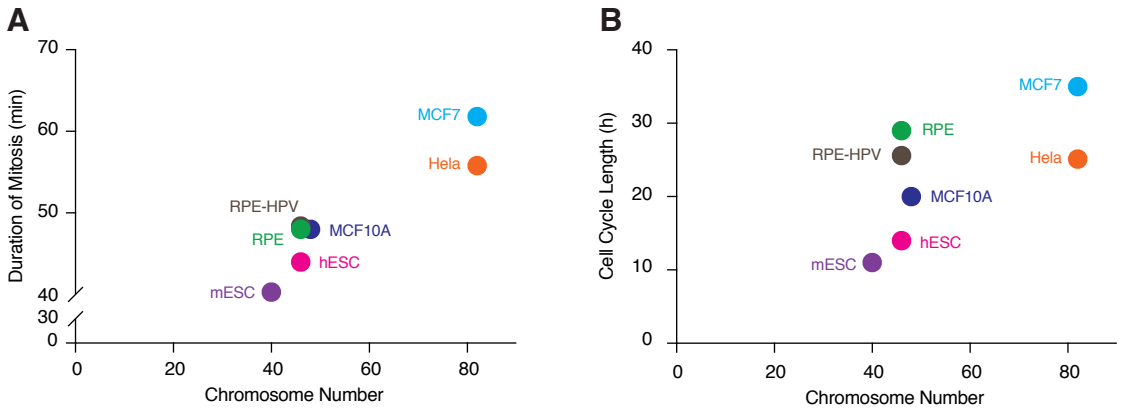


Figure 6.1. Duration of mitosis as well as the overall cell cycle length scales well with chromosome number. A. Duration of mitosis as a function of chromosome number measured by live imaging in seven different human and mouse cell lines (mESC). **B.** Cell cycle length as a function of chromosome number measured by live imaging in seven different human and mouse cell lines (mESC).

However, this is not the case for mitosis. There is no correlation between the time that it takes to complete mitosis and the overall cell cycle length. This suggests that it does not seem to matter how long a cell stayed in interphase and how long it took for previous events to happen, once it enters mitosis it completes mitosis decisively within a short and reasonably constant time. This indicates that duration of mitosis is temporally insulated from variability of earlier cell cycle events, i.e. events during interphase.

One of the models proposed to control time in the cell cycle is checkpoint controls, which assure that one cell cycle stage begins only when the previous one finishes with success. Spindle assembly checkpoint takes stage at metaphase in order to make sure that all chromosomes are perfectly aligned at metaphase plate and all kinetochores are bound to mitotic spindle microtubules. However, when the role of spindle assembly checkpoint in mitotic duration was further investigated, it was shown that compromising spindle assembly checkpoint failed to couple duration of mitosis and cell cycle length. When plotting the measurements of mitotic duration in normal cells, the histograms of mitotic time have a narrow distribution and are slightly positively skewed - this corresponds to the cells that

spent slightly more time to finish mitosis, probably because the checkpoint was on for longer time. Downregulating the spindle assembly checkpoint resulted in removing the skew in the distribution, which means that in normal cycling cells the delay that the checkpoint causes in mitosis is minimal and that without the checkpoint, mitosis can proceed as fast as possible (Figure 3.28, Figure 3.29 and Figure 3.30). Without full function of the spindle assembly checkpoint, the duration of mitosis gets shorter and less variable. So, the spindle assembly checkpoint is not the underlying mechanism keeping mitosis short and constant, but rather induces small amount of variability in mitotic duration that is minimal in normal cells.

The work described in this thesis proposes that positive feedback within the network that regulates mitosis, is the molecular mechanism that insulates duration of mitosis from variability in earlier cell cycle events. This is supported by the fact that compromising the switch-like activation of the Cdk1-cyclin B1 complex compromised the ability of cells to complete mitosis in a timely, constant manner. When positive feedback was perturbed in various manners, duration of mitosis became coupled with interphase duration and the overall cell cycle length. Similar to the case with G1-, S- and G2-phases, where it is possible to predict cell cycle length by knowing how long a cell spent in one of these interphase phases, when positive feedback is broken it is also possible to predict the cell cycle length of a certain cell by knowing how long that cell spent in mitosis. This is also true regardless of whether the spindle assembly checkpoint is also inhibited, confirming that this checkpoint has no role in the time insulation of mitosis.

These results are consistent with earlier studies in *Xenopus laevis* extracts, a system where checkpoint control is inactive. The lag time between phosphorylation of Cdc25 – an early mitotic event - and phosphorylation of Cdc27 – a late mitotic event – was shown to be constant regardless of how long extracts stayed in interphase (Georgi et al., 2002).Thus, it did not matter how long *Xenopus laevis* extracts spent in interphase, the duration of mitosis was kept constant. The same authors also observed that once Cdk1 became active, the nuclear envelope broke down and chromatin condensed within the same constant lag time. This suggests that a short and constant duration of mitosis that is uncoupled from early cell cycle events is not specific to mammalian somatic cells, but rather is a general conserved design principle of cell cycle regulation.

In the absence of positive feedback, mitotic time became considerably longer and much more variable in individual cells, leading cells to die during mitosis or shortly after. It is not surprising that cells that have longer durations of mitosis die because they will have the checkpoints on and the cells are wired to not stay that long in mitosis. However, this phenomenon was also observed in cells treated with Wee1 inhibitor that took only 50 minutes to complete mitosis. Positive feedback is thought to help achieve the Cdk1 activation thresholds that underlay proper progression and exit from mitosis, in addition to other roles such as keeping synchronicity between events (Holt et al., 2008; Skotheim et al., 2008).

Another consequence of breaking positive feedback was the loss of synchronicity between early and late mitotic events (Figure 3.11). So, in the absence of positive feedback a cell might be able to reform the nuclear envelope, but possibly progresses out of mitosis with many features that the cellular machinery interprets as defects – therefore, soon after finishing mitosis checkpoint control mechanisms take place and might trigger cell death. This further suggests that a constant mitotic duration uncoupled with previous cell cycle events is crucial for fidelity of cell division and cell survival. The elegant work of Reijo-Pera and colleagues also supports this hypothesis. In early embryonic divisions of *in vitro* fertilized human embryos, a constant duration of cytokinesis (15 minutes) was shown to be essential to ensure embryo viability and progression through embryo development (Wong et al., 2010). Georgi and colleagues also identified that early and late mitotic events happen in a synchronous way, independently of how long *Xenopus laevis* extracts stayed in mitosis (Georgi et al., 2002). Holt and colleagues also showed that APC activation by Cdk1 and the resulting degradation of securin and segregation of sister chromatids happens in a synchronized way (Holt et al., 2008). Together, this evidence supports the hypothesis that a constant duration of mitosis is advantageous for cells and that this feature was actively conserved throughout evolution as a mechanism to temporally insulate mitosis and ensure cell survival and fidelity.

In addition to the Cdk1-based regulatory networks and the spindle assembly checkpoint, temporal control of mitosis is also dependent on and regulated by mitotic phosphatases, namely members of PP1 and PP2A families. Both PP1 and PP2A phosphatases have been implicated in mitotic entry and mitotic exit by counteracting phosphorylation on Cdk1 substrates (Bollen et al., 2009; Castilho et al., 2009; Dohadwala et al., 1994; Kwon et al., 1997; Mochida, 2015; Wu et al., 2009; Wurzenberger and Gerlich, 2011). PP1 phosphatases were described to have a major role in mitotic exit and compromising their activity with a specific inhibitor (tautomycin) stalled cells in mitosis by preventing mitotic exit (Figure 3.23). This is in line with work presented by Winkler and colleagues, where the over-expression of a potent nuclear inhibitor of PP1 caused spindle assembly and chromosome congression defects, leading to cell death (Winkler et al., 2015). In general, it has been difficult to understand the contribution of phosphatases PP1 and PP2A to the control of cell cycle progression in vertebrates, due to lack of availability of specific inhibitors and the functional redundancy between isoforms, making multi-target knockdown experiments rather informative (Cheng et al., 2000; Kirchner et al., 2007; Trinkle-Mulcahy et al., 2001; Varmuza et al., 1999). PP1 isoforms – α, β and γ – are encoded by separate genes, but are more than 89% identical in amino acid sequence (Barker et al., 1994; 1993; Sasaki et al., 1990; Trinkle-Mulcahy et al., 2001). To further investigate if mitotic phosphatases had a role in keeping time of mitosis short and constant, different PP1 isoforms and PP2A-B55 were knocked down in MCF10A cells. The knockdown of single isoforms and combined knockdown of different isoforms produced a consistent phenotype – mitotic time increased by around 5 minutes (Figure 3.25). However, mitosis was still very constant. A slight correlation between duration

of mitosis and cell cycle length was observed in cells lacking PP1A, showing that this particular isoform might have some influence in keeping duration of mitosis temporally insulated from upstream events (Figure 3.25). However, contrary to what was expected, PP1- and PP2A-depleted cells showed no correlation between duration of mitosis and time of mitotic entry. It was only when positive feedback was perturbed that duration of mitosis became longer, more variable, and correlated with specific time of mitotic entry (Figure 3.26). This suggests that, unlike the spindle assembly checkpoint which induces some slight variability in mitosis duration, mitotic phosphatases seem to be important to keep the time of mitosis short, constant and independent of previous cell cycle events. Yet, this does not seem to be the best approach to study the role of PP1 and PP2A phosphatase families in cell cycle regulation, since the percentages of knockdown achieved were very variable and the phenotypes obtained were not very severe. In future, it would be important to try to dissect more the role of different phosphatases in mitosis maybe by using CRISPR technology to make an inducible knockout or by designing more specific inhibitors that would target only one isoform at the time.

In order to support the idea that positive feedback is the molecular mechanism underlying temporal insulation of mitosis, a simple ODE model was developed in collaboration with Dr Lendert Gelens from KU Leuven. And indeed, the model predicted that positive feedback in Cdk1-cyclin B1 regulatory network alone could give rise to a short mitotic duration and uncouple duration of mitosis from interphase duration. Despite being a qualitative understanding of the system, the ODE model confirms that the assumptions that were made about how the system works are true, since simulated and experimental data demonstrated qualitatively the same behaviour. In addition, the model predicted that the double-negative feedback loop involving APC-cdc20 and Mad2-cdc20 can give rise to bistability, since there are two different states of APC activity (high and low). The bistable region increases when Mad2 activity increases, preventing the activation of APC-cdc20 and mitotic exit in a similar manner as active spindle assembly checkpoint.

Recently, Atay and colleagues used the pheromone response network in budding yeast to study the design principles necessary to build a network that brings about modularity. Using both computational and experimental analysis, the authors discovered that the positive feedback switch that drives re-entry into the cell cycle controls the insulation of the feedforward motif controlling the cell cycle inhibitor Far1. If Cdk-cyclin complexes target Far1 for degradation before cell cycle entry, the switch-like interface between cell cycle and pheromone signalling is broken and the feedforward motif is not able to predict the network behaviour (Atay et al., 2016). In concordance with the work presented in this thesis, positive feedback is the key mechanism responsible for keeping length of mitosis constant in time, not only in mammalian cells but probably in all eukaryotes.

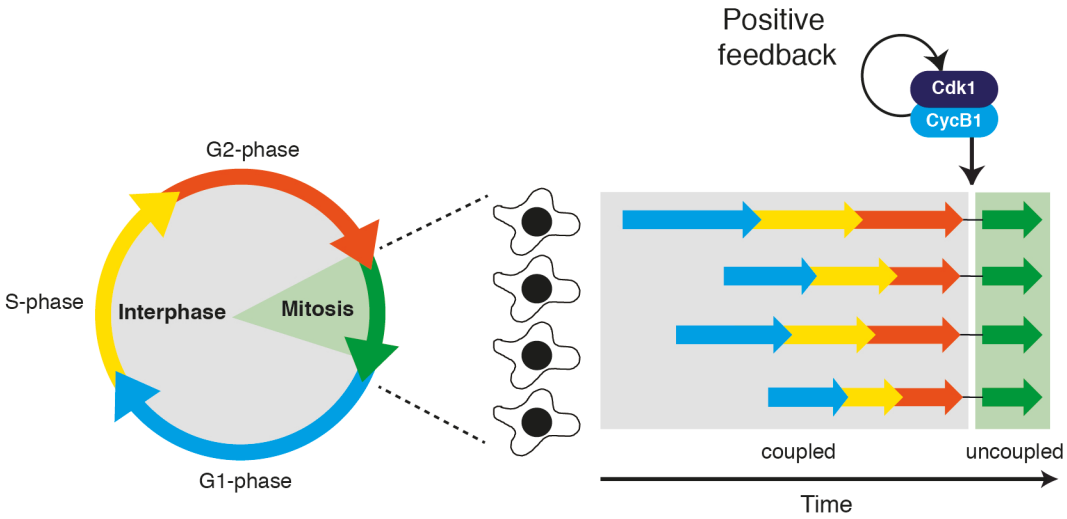


Figure 6.2. Positive feedback keeps duration of mitosis temporally insulated from upstream cell cycle events. Quantitative cell measurements of different cell cycle phases in single cells showed that mitosis is short, constant and surprisingly uncoupled from the high variability of earlier cell cycle phases. Positive feedback control is responsible for this modularity and this suggests that it might enable modularity in other biological systems.

One of the most important steps forward in our understanding of the systems-level biology of cellular decision-making has been the appreciation of the fact that there are simple and ubiquitous motifs that define how genes and proteins regulate each other's activities (Alon, 2007). Positive feedback loops are an example of such recurrent cellular strategies and have been shown to bring about amplification, maintenance, and rapid switching of activities in time and space (Chang and Ferrell, 2013; Ferrell, 2002; Santos et al., 2012). In this way, these regulatory networks can be the basis for unidirectional, coherent, and all-or-none cellular events (Ferrell and Machleder, 1998; He et al., 2009; Holt et al., 2008; López-Avilés et al., 2009; Novak et al., 2007; Skotheim et al., 2008; Xiong and Ferrell, 2003). The work presented here shows that positive feedback regulation can generate temporal insulation and bring about modularity. In mammalian cells, coupling timing of G1-, S- and G2-phases may provide cells with the potential to couple growth, DNA replication, and repair and all the cell cycle events that are likely to influence and depend on one another (Figure 6.2). A delay in cell growth might delay G1-phase and consequently, commitment to DNA replication. An error or delay in DNA replication might postpone the completion of DNA repair. However, when entering mitosis, cells will undergo dramatic biochemical and morphological changes, stopping most metabolic and transcriptional activity in preparation for an even segregation of chromosomes and distributions of other cellular components in two new daughter cells. Uncoupling mitosis from earlier events might allow individual cells to avoid noise and variability in upstream cell cycle phases and irreversibly commit to segregate chromosomes into two daughter cells in a short, fast, and all-or-none manner. This work describes a new role for positive feedback; bringing about modularity in signalling. Given the fact that modularity is emerging as an important and widespread feature of biological systems (Atay and Skotheim, 2014; Atay et al., 2016; Hartwell et al., 1999; Jaitin et al., 2014; Treutlein et al., 2014), it suggests that positive feedback may prove to be a recurrent cellular strategy to temporally uncouple events beyond the cell cycle field and without restriction to mammalian cells.

After finding out what is the molecular mechanism determining how cells spend such a short and constant time of their cell cycle length in mitosis, the next logical question to ask was why do cells stay in interphase on average for more than 24 hours? And importantly, do cells need to wait all these hours to be competent to enter into mitosis? The work presented in chapter 4 of this thesis contributes the understanding of the mechanism that keep cells out of mitosis and highlight one more time to that feedback regulation of Cdk1 activity plays a crucial role.

Evidence was found that, in fact, cells do not need to wait the whole time in interphase to respond to a mitotic trigger. When free cycling somatic cells were exposed to Wee1 inhibitor, used as a proxy of a mitotic trigger, most of the cells were able to respond to it (Figure 4.2). Intriguingly, the group of cells that responded also included G1-phase cells. This phenomenon raised the question of whether these G1-phase cells that responded to the

mitotic trigger tried to replicate DNA before entering mitosis, since different thresholds of Cdk1 activity are thought to drive these different cell cycle phases (Stern and Nurse, 1996). Indeed, cells that were in G1-phase that responded to the mitotic trigger and initiated mitosis, also tried to replicate their DNA (Figure 4.3). Positive feedback mechanisms that control mitotic entry also insulate mitotic duration and when the cells were exposed to the mitotic trigger, thereby breaking positive feedback, mitosis was not insulated anymore (Figure 3.13). So, positive feedback is protecting cells from entering into mitosis prematurely, but when positive feedback is broken this protection is lost and different cell cycle events happen in a disordered way. Cells treated with Wee1 inhibitor, will start to release Cdk1 inhibition and a lower activity threshold is enough to trigger S-phase as shown in figure 4.3. The mitotic trigger releases the inhibitory phosphorylation on Cdk1, making it easier to activate it. Low levels of Cdk1 will trigger S-phase and as they increase it will finally trigger mitosis (Stern and Nurse, 1996). This is why cells that were in G1-phase were able to respond to the mitotic trigger and jump to mitosis in less than 23 hours. This shows the importance that feedback control has in separating different cell cycle states – interphase and mitosis.

However, not all the cells responded to mitotic trigger. Why not? After further investigation, it was found that all the cells that did not respond to the mitotic trigger shared a common feature – they had "just" left mitosis. Thus, there is a refractory period of approximately five hours after mitosis where cells are immune to any mitotic trigger (Figure 4.4). This means that a cell that had just divided cannot go into mitosis again. The data indicates that cells need to wait at least five hours in order to be able to enter a second round of mitosis. It is likely that this is the minimum time that cells need to prepare to commit to DNA replication by hyper-phosphorylating Rb and releasing E2F factor from its inhibition in order to start the all-or-none wave of transcription need to prepare for DNA replication (Doncic et al., 2015; Skotheim et al., 2008). Moreover, this might also be the time where the cells require growth before being able to commit to the next division cycle. Although the role of G1/S transition in cell size control in mammalian cells is still not very well understood (Dolznig et al., 2004; Killander and Zetterberg, 1965), it is known to be important in budding yeast, as described by many labs (Di Talia et al., 2007; Hartwell and Unger, 1977; Schmoller et al., 2015). Though, these are all possible explanations to what cells might be able to do because Cdk1 activity is low and the work presented in the chapter 4 of this thesis describes the mechanism which is keeping Cdk1 activity down and does not allow cells to initiate mitosis prematurely – feedback control between Cdk1 and APC-Cdh1.

An ODE model predicted that modulating the strength of the feedback loop between Cdk1 and APC-Cdh1 is enough to control the refractory period (Figure 4.5). Somatic cells have a robust Cdk1:APC-Cdh1 feedback loop with levels of Cyclins accumulating very slowly and therefore Cdk1 activity peaks are more sparse in time, which makes cell division cycles longer. In contrast, a weak Cdk1:APC-Cdh1 feedback loop should give rise to quickly oscillating levels of Cdk1 activity because Cyclins do not get degraded. In fact, there is a very

well-known system with short cell cycles, permanently high levels of Cyclins, and frequent peaks of Cdk1 activity – embryonic cells (Murray and Kirschner, 1989). For a long time, it was thought that APC/C was not functional in embryonic cells, since Cdk activity is high throughout their whole cell cycle (Fujii-Yamamoto et al., 2005; White et al., 2005; Yang et al., 2011). Moreover, the short G1-phase was seen as a result of the inability of major APC/C targets to oscillate (Fujii-Yamamoto et al., 2005; Stead et al., 2002; Yang et al., 2011). It was recently found in embryonic stem cells that Cdk activity is increased because APC/C activity is reduced, leading to a different balance and more limited oscillation of Cdk activity (Ballabeni et al., 2011).

Human embryonic stem cells were indeed found to have shorter cell cycles than differentiated cells or somatic cells (Figure 4.6). Moreover, hESC express very low levels of Cdh1 in contrast with differentiated cells that highly express Cdh1 (Figure 4.7). This might be due to the lengthening of G1-phase that happens upon differentiation (Becker et al., 2010; Calder et al., 2013; White and Dalton, 2005) and the fact that mitotic Cyclins need to be silenced during G1-phase in order prevent a premature commitment to a next cell cycle in somatic cells (Geley et al., 2001; Hsu et al., 2002; Lukas et al., 1999; Murray and Kirschner, 1989; Sørensen et al., 2001). The work of Bar-On and colleagues support this idea, since the authors found that the activity of APC-Cdh1 increases during the differentiation of human embryonic stem cells (Bar-On et al., 2010). In addition, as predicted by the ODE model, hESC express high levels of mitotic Cyclins – Cyclin B1 and Cyclin A2 – when compared to differentiated cells (Figure 4.8). This is in line with the fact that embryonic cells express high levels of mitotic cyclins and that increasing levels of mitotic cyclins is enough to drive cells into mitosis (Kang and Pomerening, 2012; Yang and Ferrell, 2013). Finally, it was revealed that hESC were much more responsive to treatment with the mitotic trigger than somatic cells, which highly suggests that hESC lack a refractory period and are programmed to go into rounds of division without the need to wait, which are the predicted characteristics of a system with a weak Cdk1:APC-Cdh1 feedback loop.

To reverse this phenotypic lack of a refractory period, Cdh1 was over-expressed in hESC in order to strengthen the Cdk1:APC-Cdh1 feedback loop. Over-expression of Cdh1 was found to be inversely correlated with both Cyclin B1 and Cyclin A2 levels in hESC (Figure 4.12). APC/C has a partial role in triggering mitotic exit by targeting Cyclin B1 for degradation, and further activation of Cdh1 that binds to APC/C in late anaphase targets Cyclin A for degradation during G1-phase (Geley et al., 2001; Hsu et al., 2002; Lukas et al., 1999; Murray and Kirschner, 1989; Sørensen et al., 2001). This is in line with what was observed: the more active APC/C becomes due to over-expression of its activator Cdh1, the more it will degrade mitotic Cyclins. Moreover, over-expression of Cdh1 in hESCs also led to lengthening of G1-phase, similar to what is observed as hESCs differentiate (Becker et al., 2010; Calder et al., 2013; White and Dalton, 2005). Increasing the level of Cdh1 also made G1-phase length correlate with cell cycle length, which is more similar to what is observed in somatic cells

(Figure 3.3 and 4.13). In addition, over-expression of Cdh1 increased variability in duration of G1-phase and length of the whole cell division cycle. This supports the idea that the cell cycle is remodelled as the cells transit from a pluripotent state to a differentiated state, with rising levels of APC-Cdh1 being probably one of the first changes observed (Ballabeni et al., 2011; Eguren et al., 2013; Wäsch et al., 2010). Lastly, when treated with a mitotic trigger, hESC over-expressing Cdh1 showed a lag time between receiving the trigger and responding to it. In fact, over-expression of Cdh1 made the cells three times slower to respond to the mitotic trigger in comparison with control hESC (Figure 4.14).

Since it appears to be possible to re-establish a refractory period in hESC, it was also attempted to the shorten this period in somatic cells. Cdh1 was knocked down in three somatic cell lines – Hela, MCF10A, and RPE cells – in order to shorten the refractory period. Indeed, knocking down Cdh1 expression in somatic cells was able to shorten G1-phase and consequently the overall cell cycle length in all three cell lines (Figure 4.16). Knockdown of Cdh1 had already been shown to cause shortened G1 phase and accumulation of DNA damage (Sigl et al., 2009; Yuan et al., 2014). So, just by changing one component of one feedback loop it was possible to make somatic cells look more like embryonic cells and embryonic cells look more like somatic cells. When stimulated with mitotic triggers, cells lacking Cdh1 responded more often and in a quicker way than normal somatic cells (Figure 4.17). This evidence is highly consistent with the fact that depletion of Cdh1 in cultured post-mitotic cells led to a re-entry into the cell cycle (Almeida et al., 2005; Liu and Greene, 2001). The changes in cell cycle behaviour observed when over-expressing Cdh1 in hESC and knocking down Cdh1 in somatic cells suggest that simply by changing levels of Cdh1, an important co-activator of APC/C, it is possible to modulate the strength of the Cdk1:APC-Cdh1 feedback loop in order to drive different cell cycle structures.

Comparing the expression and activity levels of important cell cycle players in somatic cells and hESC suggests that the refractory period is a time where both Cyclin B1 and Cyclin A2 levels are low, Rb is hypophosphorylated, Cdh1 activity levels are high and where Cdk2-Cyclin A activity levels start to increase. Recent work from Cappell and colleagues proposed that the inactivation of APC-Cdh1 is the ultimate and irreversible commitment point to S-phase in mammalian cells. These authors, as well as Barr and collegues, further posit that APC-Cdh1 is inactivated in a switch-like manner by Cdk2-cyclin E within less than one hour prior to DNA replication. Moreover, proliferating cells that directly enter G1-phase have a minimum time window of 4 hours before inactivating APC-Cdh1 (Barr et al., 2016; Cappell et al., 2016).These observations further support the idea that the refractory period might coincide with the time that cells need to overcome the restriction point and commit to a new division cycle, which is reminiscent of the minimum time during which cells are immune to a mitotic trigger – 5 hours.

The proposed mechanism that controls the mitotic refractory period is represented in Figure 6.3. In somatic cells the Cdk1:APC-Cdh1 feedback loop is very strong which results in longer G1-phases and a refractory period during which cells are immune to treatment with a mitotic trigger. In embryonic stem cells, the Cdk1:APC-Cdh1 feedback loop is weak, and this results in very short G1-phases and the inexistence of a refractory period. So, in principle, embryonic stem cells will always be able to respond to a mitotic trigger. This simple mechanism suggests that by changing the strength of a feedback network it is possible to increase or decrease G1-phase duration, an idea that was born out experimentally.

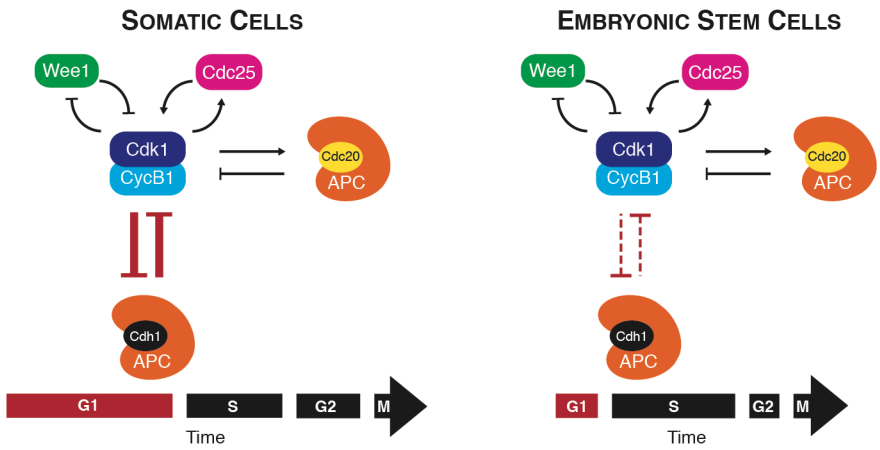


Figure 6.3. Cdk1:APC-Cdh1 feedback strength modulates the length of refractory period. Modulating feedback strength of Cdk1:APC-Cdh1 can drive different cell division cycles: a strong feedback is present in somatic cells and a weak feedback is present in embryonic stem cells.

Modulating feedback strength may be a simple regulatory strategy that allows cells to tune the period of division cycles. In embryonic cells and somatic cells the machinery that controls cell division is exactly the same and only by changing the feedback strength between Cdk1 and APC-Cdh1 does it give rise to fundamentally different cell division cycles. This appears to be related to the function of these different cell types. One of the characteristics of embryonic cells is self-renewal, so cells are programmed to divide repeatedly. In contrast, an important goal of cells in a somatic tissue is to keep division very controlled by ensuring correct replication and repair of DNA before segregation of the sister chromatids in order to maintain tissue integrity and stability. In addition, Cdh1 is highly expressed in neurons (Gieffers et al., 1999), which makes the Cdk1:APC-Cdh1 feedback very strong and is possibly a major mechanism for keeping neurons from undergoing cell division. This is also true for other mammalian tissues, suggesting that Cdh1 might be found ubiquitously in post-mitotic cells (Gieffers et al., 1999).

In addition to Cdh1, other cell cycle regulators seem to acquire different functions in post-mitotic cells in order to avoid re-entry into the cell cycle. The work of Jord and colleagues recently showed that non-dividing cells can use the mitotic clock-like regulatory network to coordinate subcellular reorganization associated with differentiation in multiciliated progenitor cells (Jord et al., 2017). Multiciliogenesis relies on the massive production of centrioles and that, like in cycling cells, polo-like kinase 1, Cdk1, and APC-cdc20 activity coordinates the timing of centriole biogenesis in multiciliated progenitor cells. Moreover, in neurons, APC-cdc20 promotes presynaptic differentiation and dendrite growth and morphogenesis (Kim et al., 2009; Yang et al., 2009b), while APC-Cdh1 is responsible for axonal growth and patterning (Konishi et al., 2004). Although the different players of the cell cycle machinery remain the same in all tissues, it is likely that they have different functions and interact with each other in different ways - for example by changing the strength or signal of a feedback loop. This is a very resource-inexpensive strategy to maintain cell integrity and function, and could possibly explain the evolutionary conservation of the players of cell cycle control machinery across all cell types in the eukaryote kingdom (Cao et al., 2014; Cross et al., 2011; Harashima et al., 2013).

6.2. Monitoring cell cycle dynamics in single cells as a way to derive regulatory principles in cell division

This work was initiated in 2014 and one of its main goals was to develop tools to measure the length of the four different cell cycle phases by live cell imaging, using different sensors for each cell cycle phase. At the time, the original FUCCI system was already available but did not allow the ability to distinguish between S-phase and G2-phase. In order to fulfil this goal, two different sets of cell cycle biosensors were designed. The first set of biosensors was comprised of Cdt1-venus, H2B-Turquoise, and PCNA-mCherry (described in chapters 2 and 3) and the second set of biosensors was composed by Dnmt1-CFP, DNA Ligase-YFP and H2B-mCherry, to confirm all the results obtained.

Since all the biosensors used are being over-expressed in the cells, a few assessments were used in order to prevent misreading of cell cycle phase dynamics. To ensure that the measuring of duration of different cell cycle phases did not include artefacts, the cell lines were selected by FACS for the lowest levels of expression that were enough to distinguish them from the non-labelled cells. Moreover, in each set of sensors the length of each cell cycle phase can be measured by two different sensors. In the set that includes Dnmt1-CFP, DNA Ligase-YFP, and H2B-mCherry, the beginning of G1-phase can be measured by observing nuclear envelope reformation using localisation of H2B or nuclear diffusion of Dnmt1 and DNA Ligase. The end of G1-phase is measured by the appearance of DNA Ligase speckles that mark the beginning of S-phase. S-phase length can be measure as the time between the appearance and disappearance of DNA Ligase speckles, or the time between the appearance of DNA Ligase speckles and the time of appearance of Dnmt1 speckles that mark the beginning of G2-phase. G2-phase length can be measured as the time between appearance of Dnmt1 speckles and the diffusion of Dnmt1 into the cytoplasm at the beginning of mitosis, or as the time between the disappearance of DNA ligase speckles and the diffusion of DNA ligase into the cytoplasm at the beginning of mitosis. Mitotic time can be measured by observing chromatin shape and dynamics using H2B, or by observing the time between diffusion of both Dnmt1 and DNA ligase into the cytoplasm with NEB, and consequent NER. The same is true for the sensor set that is comprised of Cdt1-venus, H2B-Turquoise, and PCNA-mCherry. G1-phase duration can be measured as the time between nuclear envelope reformation (observed using H2B) or nuclear diffusion of PCNA, and the disappearance of Cdt1 at the boundary between G1/S transition. S-phase duration can be measured as the time between the appearance and disappearance of PCNA speckles or the time between Cdt1 degradation and the disappearance of PCNA speckles. G2-phase time can be measured as the time between the disappearance of PCNA speckles and the diffusion of PCNA into the cytoplasm with NEB, or as the time between the disappearance of PCNA speckles and chromosome condensation, which is observed using H2B. Duration of mitosis can be measured by observing the localisation of H2B, or as the time between diffusion of PCNA

into the cytoplasm upon NEB and then re-localisation to the nucleus upon the subsequent NER. In fact, there is always more than one possibility to measure the length of the different cell cycle phases. The ideal scenario would be to use knock-in-based CRISPR technology to fluorescently tag and observe endogenous proteins, but this approach also has some limitations. The potential disadvantage is that CRISPR-based knock-ins may not be very bright which can lead to phototoxicity while imaging at high intensities. In order to image cells for long periods – 2 to 3 days – a compromise needs to be made between the amount of light to which cells are exposed and how frequently the cells are imaged, in order to perturb the cells as little as possible. If cells are exposed for long periods of time to a strong light, it may interfere with cell cycle dynamics and may lead to cell death.

Preliminary data described in chapter 5 showed that measuring cell cycle dynamics in single cells with the two sets of biosensors gives very similar measurements in three different cell lines – Hela, MCF10A, and RPE cells (Figure 5.1). Although the average time that different cell types spent in the different cell cycle phases was not exactly the same when measured by the two different sets of biosensors, the trends remain identical. Hela cells spent the longest amount of time in G1-phase, while MCF10A spent the least. RPE cells spent the largest fraction of their cell cycle duplicating DNA, while MCF10A cells went quickly through S-phase. It might be that in order to compensate for a fast DNA replication, MCF10A cells spent more time in G2-phase, while Hela cells spent less time repairing DNA than normal cells.

Perhaps a more informed way of analysing this data would be to look at the correlations between the duration of different cell cycle phases and the overall cell cycle length. When comparing the results regarding both set of sensors, the same tendency was observed (Figure 3.3 and Figure 5.2). There was a correlation between duration of G1-, S- and G2-phases and the overall cell cycle length, making it possible to predict how long the cell cycle of a certain cell is going to be by knowing how long it stayed in one of the three interphase phases. Another feature that was observed (and has been seen before): the duration of mitosis was always short, constant, and independent of variability in upstream cell cycle events – this was observed independently of which set of biosensors was used and which cell type was studied. Since Hela cells have been used for decades as a model system to study cell cycle regulation, the time that they spend in each phase of the cell cycle has been documented previously using different live cell probes and is very similar to the dynamics measured in this work (Hahn et al., 2009; Tsuchida et al., 2015). Hela cells spent on average 80% of their cell cycle in G1-phase and S-phase, 15% in G2-phase and 5% in mitosis, which confirms the reliability of both sets of biosensors.

Preliminary data of cell cycle dynamics in MCF10A and MCF7 also allowed to infer some similarities and differences between these two cell types. MCF10A cells had an average cell cycle length of 20.3±4.1 hours and MCF7 took 35.0±6.2 hours to conclude their cell cycle. Both

cell lines spent the largest fraction of their cell cycle time in replicating DNA. Another intriguing observation was that MCF7 cells have much shorter and less variable G2-phases than MCF10A cells (Figure 5.3). This was also observed in Hela cells (Figure 3.1.A and Figure 5.2), suggesting that cancer cells might be able to overcome DNA repair during G2-phase and progress into mitosis while carrying some errors that propagate into the next generation of cells. These preliminary results showed that normal and cancer cell lines have different interphase dynamics, even though the temporal insulation of mitosis seems to be a feature common to all cell types independent of their function or disease state.

Differences between MCF10A cells and MCF7 cells were highlighted when individual cell cycle phases were compared in relation to the overall cell cycle length. When the percentage of time that an individual cell spent in each of the four different cell cycle phases was calculated, it was possible to see that the duration of interphase phases is dependent on each other, while duration of mitosis is independent from all the three interphase phases (Figure 5.4). A strong inverse correlation between length of G1-phase and length of S-phase was found in MCF7 cells. G1-phase and G2-phase were also inversely correlated in MCF10A cells but not in MCF7 cells. In normal cells (MCF10A cells), S-phase length was strongly inversely correlated with G2-phase length, while in cancer cells (MCF7) there was no correlation between these two cell cycle phases. As suggested before, it is possible that cancer cells might circumvent DNA-repair mechanisms which leads to shorter G2-phases. It is known that genes which encode components of the DNA damage response pathway, and specifically of DNA repair pathways, are among the most frequently mutated genes in cancer (Ciriello et al., 2013; Reinhardt et al., 2009). It will be interesting to determine whether these types of analyses involving pairs of different untransformed and transformed cell lines could reveal common cell cycle regulatory principles shared by cancer cells.

The work presented in this thesis shows that measuring cell cycle dynamics with two different sets of cell cycle biosensors gives very similar measurements of the dynamics of different cell cycle phases in different cell lines. Intrinsic noise and variability within the same population of cells might account for small differences observed between the measurements taken using the two sets of biosensors. However, temporal insulation of mitosis seems to be a common feature of all cell lines, independently of their function or disease state, normal and paired cancerous cells have very different cell cycle dynamics which might impact directly on their cell function.

Looking at the cell cycle dynamics of different cell lines, especially when comparing normal and disease state cells with this type of quantitative approaches, it might be possible to understand how different cell types regulate their cell cycle machinery in order to drive different cell cycle phases, and in turn how cell cycle dynamics relates to cell function. Interestingly, when comparing the interphase dynamics of a pair of normal and cancer cells, MCF10A cells and MCF7 cells stably expressing Cdt1-venus, PCNA-mCherry and H2B-Turquoise sensors, it is possible to observe that they separate very well (Figure 6.4). To further investigate this, a large-scale analysis should be performed, including a wide pallet of paired cancer and normal cells lines.

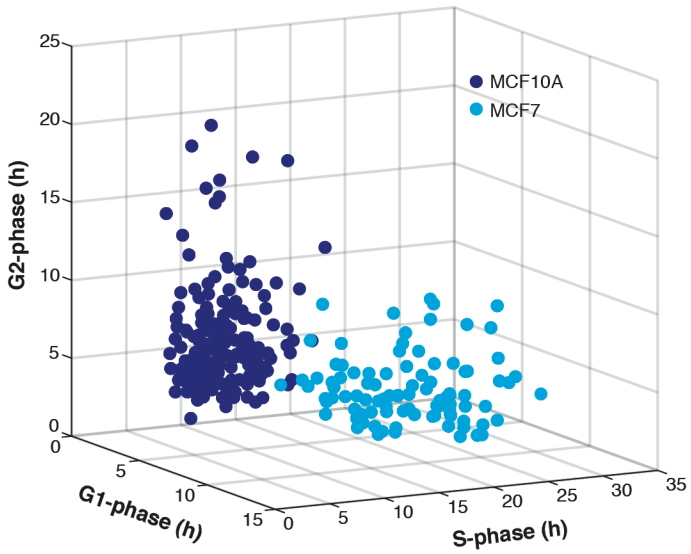


Figure 6.4. 3D representation of duration of G1-, S- and G2-phases of MCF10A and MCF7 cells. MCF10A and MCF7 cells stably expressing Cdt1-venus, H2B-Turquoise and PCNA-mCherry were imaged for two consecutive divisions in order to measure cell cycle dynamics. The relationship between the duration of G1-, S- and G2-phases of each cell were plotted in a 3D map.

It is widely known that the cell cycle is remodelled when cells change from a pluripotent state to a differentiated state. This not only occurs in embryonic cells but also in adult tissues (Becker et al., 2010; Calder et al., 2013; White and Dalton, 2005). B cells and Naïve T cells have short cell cycles to maintain their immature population and differentiate and lengthen their cell cycle when stimulated by an antigen (Hawkins et al., 2009; Kinjyo et al., 2015; Marchingo et al., 2014; Turner et al., 2008). This further suggests that cell cycle dynamics is closely related to cell function. In sum, the study of cell cycle dynamics in single cells by live cell imaging combined with further mathematical analysis such as principle component analysis, might allow us to infer regulatory principles that are fundamental for proper functioning of the cell cycle in human cells, comprehend how time is regulated in the cell cycle, and understand and define the cell cycle hallmarks of malignancy.

7. Final conclusions

The work presented in this thesis combined experimental work with mathematical modelling to quantitatively measure cell cycle dynamics in different cell types. This resulted in new insights into new roles of feedback regulation in the temporal regulation of cell division.

On one hand, this work furthered the understanding of the quantitative mechanisms controlling the cell cycle by identifying the role that the strength of systems-level feedback plays in cell cycle control, using mammalian cells with different characteristics as a model. Mitotic duration was shown to be short, constant, and independent of variability of upstream cell cycle events in all different cell types tested, from embryonic stem cells to normal cells and cancer cells. The core network that is responsible for this insulation of mitotic duration is the positive feedback mechanism that drives Cdk1-cyclin B1 activation at the beginning of mitosis. If this feedback mechanism is impaired in any cell type, mitosis time becomes longer, more variable, and coupled with upstream cell cycle events.

On the other hand, this work also suggested that modulating the strength of feedback control is enough to drive different cell cycle profiles. Somatic cells have a refractory period of five hours after mitosis where they are immune to any stimuli to divide. Conversely, embryonic stem cells - which have short G1-phases and are required to divide repeatedly - lack this refractory period. In fact, the duration of this refractory period can be established by modulating the strength of the Cdk1:APC-Cdh1 feedback loop. The experiments presented in this thesis have provided evidence that somatic cells have a strong Cdk1:APC-Cdh1 feedback loop whereas hESC have a weaker Cdk1:APC-Cdh1 feedback loop, which gives rise to distinct cell cycle dynamics.

Finally, it was demonstrated the utility of studying cell cycle dynamics in single cells by live cell imaging. Preliminary results showed that the duration of G1-, S-, and G2-phases are very

variable amongst cells within the same population, which was not true for mitosis. This type of analysis could be used in the future to compare normal and cancer cells in order to infer common regulatory principles underlying cell cycle regulation in these two different contexts.

In conclusion, the work presented in this thesis highlighted the power of combining quantitative measurements in single cells with mathematical modelling to understand temporal control in cell division. In this context, it also confirmed the key role of feedback regulation in the temporal control of both interphase and mitosis. Moreover, the combination of multidisciplinary approaches used in these studies will hopefully continue to shed light on some of the temporal control principles regulating cell division in mammalian cells. A quantitative understanding of the spatial-temporal control of mitosis and interphase in different cell models will also potentially lead to transformative insights into cell cycle control in health and disease states.

8. Future directions

Although the work presented here has furthered our understanding of how time is regulated in both interphase and mitosis, a lot is still yet to be unveiled. It would be important to fully understand the role of phosphatases during mitosis and how they help Cdk1 to orchestrate all the events in mitosis in a timely ordered manner. Perhaps this could help us to understand the reason why mitosis duration needs to be insulated from the previous cell cycle events and translate that to other biological systems. It was also found in this work that modulating the Cdk1:APC-Cdh1 feedback results in different cell cycle dynamics – to better understand how this occurs during development, it would be important to characterise the timeline of changes in cell cycle machinery when a stem cell commits to differentiation and remodels its cell cycle in order to accommodate a new function and purpose. Moreover, it would be important to understand what really happens first: the commitment to a new cell fate, or the remodelling of the cell cycle, as well as to what extent modulating a feedback loop is a reversible process.

In order to understand the potential compromise between different cell states, a robust and broad analysis of cell cycle dynamics should be done. Cell cycle dynamics should be measured in more pairs of cancer and normal cell lines as well as in human embryonic stem cells in order to have a stronger idea of what the differences might be between a healthy and a non-healthy cell. This further study might also reveal some similarities between stem cells and cancer cells that can be helpful in the design of new drugs to fight exclusively cancer cells and not the stem cells in adult tissues. After this, the next step would be to study cell cycle dynamics in primary cell cultures of human tissues with different characteristics, or monitor the different cell cycle phases *in vivo* in mice models that express cell cycle biosensors. This would allow us to understand the cell cycle dynamics of cells in the context of a tissue within a live organism. Further advances in the design of cell cycle biosensors would also improve the accuracy of measurements of the length of the different cell cycle phases. Two new FUCCI systems are now available and allow for a more accurate measure

of the length of the different cell cycle dynamics (Bajar et al., 2016; Sakaue-Sawano et al., 2017). Preliminary experiments should be done in previously characterised cell lines in order to understand how accurate these two systems are and refine the automating tracking and analysis techniques in order to improve the quality and quantity of data. Then, this approach could be implemented in *in vivo* systems in order to properly achieve an understanding of how time is controlled during cell cycle in different cell types in different tissues.

In a wider context, it would be important to elucidate the mechanism behind the control of cell division in a *in vivo* context in order to understand how perturbations in human cell cycle machinery are related to distinct states such as development and cancer. This would allow for the design of predictive models of specific cell cycle dynamics that could be helpful to develop new ways of targeting distinct cell populations within a whole organism, as well as, for example, specifically target cancer cells or prevent healthy cells from succumbing to malignancy.

9. References

Abbas, T., and Dutta, A. (2009). p21 in cancer: intricate networks and multiple activities. Nat. Rev. Cancer *9*, 400–414.

Abe, T., Sakaue-Sawano, A., Kiyonari, H., Shioi, G., Inoue, K.-I., Horiuchi, T., Nakao, K., Miyawaki, A., Aizawa, S., and Fujimori, T. (2013). Visualization of cell cycle in mouse embryos with Fucci2 reporter directed by Rosa26 promoter. Development *140*, 237–246.

Abrieu, A., Brassac, T., Galas, S., Fisher, D., Labbe, J.C., and Doree, M. (1998). The Polo-like kinase Plx1 is a component of the MPF amplification loop at the G2/M-phase transition of the cell cycle in Xenopus eggs. J. Cell Sci. *111*, 1751–1757.

Al-Dewachi, H.S., Appleton, D.R., Watson, A.J., and Wright, N.A. (1979). Variation in the cell cycle time in the crypts of Lieberkühn of the mouse. Virchows Arch., B, Cell Pathol. *31*, 37–44.

Alberts, B., Bray, D., Hopkin, K., Johnson, A., Lewis, J., Raff, M., Roberts, K., and Walter, P. (2013). Essential Cell Biology, Fourth Edition (Garland Science).

Aligianni, S., Lackner, D.H., Klier, S., Rustici, G., Wilhelm, B.T., Marguerat, S., Codlin, S., Brazma, A., de Bruin, R.A.M., and Bähler, J. (2009). The fission yeast homeodomain protein Yox1p binds to MBF and confines MBF-dependent cell-cycle transcription to G1-S via negative feedback. PLoS Genet. *5*, e1000626.

Alizadeh, M., Wada, M., Gelfman, C.M., Handa, J.T., and Hjelmeland, L.M. (2001). Downregulation of Differentiation Specific Gene Expression by Oxidative Stress in ARPE-19 Cells. Invest. Ophthalmol. Vis. Sci. *42*, 2706–2713.

Almeida, A., Bolaños, J.P., and Moreno, S. (2005). Cdh1/Hct1-APC is essential for the survival of postmitotic neurons. J. Neurosci. *25*, 8115–8121.

Alon, U. (2007). Network motifs: theory and experimental approaches. Nat. Rev. Genet. *8*, 450–461.

Amon, A., Tyers, M., Futcher, B., and Nasmyth, K. (1993). Mechanisms that help the yeast cell cycle clock tick: G2 cyclins transcriptionally activate G2 cyclins and repress G1 cyclins. Cell *74*, 993–1007.

Andrews, B., and Measday, V. (1998). The cyclin family of budding yeast: abundant use of a good idea. Trends Genet. *14*, 66–72.

Araujo, A.R., Gelens, L., Sheriff, R.S.M., and Santos, S.D.M. (2016). Positive Feedback Keeps Duration of Mitosis Temporally Insulated from Upstream Cell-Cycle Events. Mol. Cell *64*, 362–375.

Arias, E.E., and Walter, J.C. (2007). Strength in numbers: preventing rereplication via multiple mechanisms in eukaryotic cells. Genes Dev. *21*, 497–518.

Atay, O., and Skotheim, J.M. (2014). Modularity and predictability in cell signaling and decision making. Mol. Biol. Cell *25*, 3445–3450.

Atay, O., Doncic, A., and Skotheim, J.M. (2016). Switch-like Transitions Insulate Network Motifs to Modularize Biological Networks. Cell Syst. *3*, 121–132.

Azzam, R., Chen, S.L., Shou, W., Mah, A.S., Alexandru, G., Nasmyth, K., Annan, R.S., Carr, S.A., and Deshaies, R.J. (2004). Phosphorylation by cyclin B-Cdk underlies release of mitotic exit activator Cdc14 from the nucleolus. Science *305*, 516–519.

Baguley, B.C., and Leung, E. (2011). Heterogeneity pf phenotype in breast cancer. In Breast Cancer - Carcinogenesis, Cell Growth and Signalling Pathways, (InTech).

Bajar, B.T., Lam, A.J., Badiee, R.K., Oh, Y.-H., Chu, J., Zhou, X.X., Kim, N., Kim, B.B., Chung, M., Yablonovitch, A.L., et al. (2016). Fluorescent indicators for simultaneous reporting of all four cell cycle phases. Nat. Methods *13*, 993–996.

Ballabeni, A., Park, I.-H., Zhao, R., Wang, W., Lerou, P.H., Daley, G.Q., and Kirschner, M.W. (2011). Cell cycle adaptations of embryonic stem cells. Proc. Natl. Acad. Sci. USA *108*, 19252–19257.

Bar-On, O., Shapira, M., Skorecki, K., Hershko, A., and Hershko, D.D. (2010). Regulation of APC/C (Cdh1) ubiquitin ligase in differentiation of human embryonic stem cells. Cell Cycle *9*, 1986–1989.

Barker, H.M., Brewis, N.D., Street, A.J., Spurr, N.K., and Cohen, P.T. (1994). Three genes for protein phosphatase 1 map to different human chromosomes: sequence, expression and gene localisation of protein serine/threonine phosphatase 1 beta (PPP1CB). Biochim. Biophys. Acta *1220*, 212–218.

Barker, H.M., Craig, S.P., Spurr, N.K., and Cohen, P.T. (1993). Sequence of human protein serine/threonine phosphatase 1 gamma and localization of the gene (PPP1CC) encoding it to chromosome bands 12q24.1-q24.2. Biochim. Biophys. Acta *1178*, 228–233.

Barr, A.R., Heldt, F.S., Zhang, T., Bakal, C., and Novak, B. (2016). A Dynamical Framework for the All-or-None G1/S Transition. Cell Syst. *2*, 27–37.

Bartek, J., and Lukas, J. (2001). Pathways governing G1/S transition and their response to DNA damage. FEBS Letters *490*, 117–122.

Bartek, J., Lukas, C., and Lukas, J. (2004). Checking on DNA damage in S phase. Nat. Rev. Mol. Cell Biol. *5*, 792–804.

Baserga, R. (1985). The Biology of Cell Reproduction (Cambridge: Harvard University Press).

Becker, K.A., Ghule, P.N., Therrien, J.A., Lian, J.B., Stein, J.L., van Wijnen, A.J., and Stein, G.S. (2006). Self-renewal of human embryonic stem cells is supported by a shortened G1 cell cycle phase. J. Cell Physiol. *209*, 883–893.

Becker, K.A., Stein, J.L., Lian, J.B., van Wijnen, A.J., and Stein, G.S. (2010). Human embryonic stem cells are pre-mitotically committed to self-renewal and acquire a lengthened G1 phase upon lineage programming. J. Cell Physiol. *222*, 103–110.

Becskei, A., and Serrano, L. (2000). Engineering stability in gene networks by autoregulation. Nature *405*, 590–593.

Benmaamar, R., and Pagano, M. (2005). Involvement of the SCF complex in the control of Cdh1 degradation in S-phase. Cell Cycle *4*, 1230–1232.

Berdougo, E., Nachury, M.V., Jackson, P.K., and Jallepalli, P.V. (2008). The nucleolar phosphatase Cdc14B is dispensable for chromosome segregation and mitotic exit in human cells. Cell Cycle *7*, 1184–1190.

Bertoli, C., Skotheim, J.M., and de Bruin, R.A.M. (2013). Control of cell cycle transcription during G1 and S phases. Nat. Rev. Mol. Cell Biol. *14*, 518–528.

Bollen, M., Gerlich, D.W., and Lesage, B. (2009). Mitotic phosphatases: from entry guards to exit guides. Trends Cell Biol. *19*, 531–541.

Booher, R.N., Holman, P.S., and Fattaey, A. (1997). Human Myt1 is a cell cycle-regulated kinase that inhibits Cdc2 but not Cdk2 activity. J. Biol. Chem. *272*, 22300–22306.

Bornstein, G., Bloom, J., Sitry-Shevah, D., Nakayama, K., Pagano, M., and Hershko, A. (2003). Role of the SCFSkp2 ubiquitin ligase in the degradation of p21Cip1 in S phase. J. Biol. Chem. *278*, 25752–25757.

Bosco, G., Du, W., and Orr-Weaver, T.L. (2001). DNA replication control through interaction of E2F-RB and the origin recognition complex. Nat. Cell Biol. *3*, 289–295.

Bouchoux, C., and Uhlmann, F. (2011). A quantitative model for ordered Cdk substrate dephosphorylation during mitotic exit. Cell *147*, 803–814.

Boutros, R., Dozier, C., and Ducommun, B. (2006). The when and wheres of CDC25 phosphatases. Curr. Opin. Cell Biol. *18*, 185–191.

Böhmer, R.M., Scharf, E., and Assoian, R.K. (1996). Cytoskeletal integrity is required throughout the mitogen stimulation phase of the cell cycle and mediates the anchorage-dependent expression of cyclin D1. Mol. Biol. Cell *7*, 101–111.

Brandeis, M., Rosewell, I., Carrington, M., Crompton, T., Jacobs, M.A., Kirk, J., Gannon, J., and Hunt, T. (1998). Cyclin B2-null mice develop normally and are fertile whereas cyclin B1-null mice die in utero. Proc. Natl. Acad. Sci. USA *95*, 4344–4349.

Budhavarapu, V.N., White, E.D., Mahanic, C.S., Chen, L., Lin, F.-T., and Lin, W.-C. (2012). Regulation of E2F1 by APC/C Cdh1 via K11 linkage-specific ubiquitin chain formation. Cell Cycle *11*, 2030–2038.

Calder, A., Roth-Albin, I., Bhatia, S., Pilquil, C., Lee, J.H., Bhatia, M., Levadoux-Martin, M., McNicol, J., Russell, J., Collins, T., et al. (2013). Lengthened G1 Phase Indicates Differentiation Status in Human Embryonic Stem Cells. Stem Cells Dev. *22*, 279–295.

Campanero, M.R., and Flemington, E.K. (1997). Regulation of E2F through ubiquitin-proteasome-dependent degradation: stabilization by the pRB tumor suppressor protein. Proc. Natl. Acad. Sci. USA *94*, 2221–2226.

Cao, L., Chen, F., Yang, X., Xu, W., Xie, J., and Yu, L. (2014). Phylogenetic analysis of CDK and cyclin proteins in premetazoan lineages. BMC Evol. Biol. *14*, 10.

Cappell, S.D., Chung, M., Jaimovich, A., Spencer, S.L., and Meyer, T. (2016). Irreversible APC(Cdh1) Inactivation Underlies the Point of No Return for Cell-Cycle Entry. Cell *166*, 167–180.

Capra, F. (1996). The web of life: A new scientific understanding of living systems. New York: Anchor.

Cardoso, M.C., Joseph, C., Rahn, H.P., Reusch, R., Nadal-Ginard, B., and Leonhardt, H. (1997). Mapping and use of a sequence that targets DNA ligase I to sites of DNA replication in vivo. J. Cell Biol. *139*, 579–587.

Carmena, M., Wheelock, M., Funabiki, H., and Earnshaw, W.C. (2012). The chromosomal passenger complex (CPC): from easy rider to the godfather of mitosis. Nat. Rev. Mol. Cell Biol. *13*, 789–803.

Carrano, A.C., Eytan, E., Hershko, A., and Pagano, M. (1999). SKP2 is required for ubiquitin-mediated degradation of the CDK inhibitor p27. Nat. Cell Biol. *1*, 193–199.

Castilho, P.V., Williams, B.C., Mochida, S., Zhao, Y., and Goldberg, M.L. (2009). The M Phase Kinase Greatwall (Gwl) Promotes Inactivation of PP2A/B55δ, a Phosphatase Directed Against CDK Phosphosites. Mol. Biol. Cell *20*, 4777–4789.

Chan, F.K., Zhang, J., Cheng, L., Shapiro, D.N., and Winoto, A. (1995). Identification of human and mouse p19, a novel CDK4 and CDK6 inhibitor with homology to p16ink4. Mol. Cell Biol. *15*, 2682–2688.

Chang, J.B., and Ferrell, J.E. (2013). Mitotic trigger waves and the spatial coordination of the Xenopus cell cycle. Nature *500*, 603–607.

Chang, L., and Barford, D. (2014). Insights into the anaphase-promoting complex: a molecular machine that regulates mitosis. Curr. Opin. Struct. Biol. *29*, 1–9.

Chang, L., Zhang, Z., Yang, J., McLaughlin, S.H., and Barford, D. (2015). Atomic structure of the APC/C and its mechanism of protein ubiquitination. Nature *522*, 450–454.

Chen, F., Archambault, V., Kar, A., Lio, P., D'Avino, P.P., Sinka, R., Lilley, K., Laue, E.D., Deak, P., Capalbo, L., et al. (2007). Multiple protein phosphatases are required for mitosis in Drosophila. Curr. Biol. *17*, 293–303.

Chen, J., Saha, P., Kornbluth, S., Dynlacht, B.D., and Dutta, A. (1996). Cyclin-binding motifs are essential for the function of p21CIP1. Mol. Cell Biol. *16*, 4673–4682.

Chen, M.S., Hurov, J., White, L.S., Woodford-Thomas, T., and Piwnica-Worms, H. (2001). Absence of apparent phenotype in mice lacking Cdc25C protein phosphatase. Mol. Cell Biol. *21*, 3853–3861.

Chen, P.L., Scully, P., Shew, J.Y., Wang, J.Y., and Lee, W.H. (1989). Phosphorylation of the retinoblastoma gene product is modulated during the cell cycle and cellular differentiation. Cell *58*, 1193–1198.

Cheng, A., Dean, N.M., and Honkanen, R.E. (2000). Serine/threonine protein phosphatase type 1gamma1 is required for the completion of cytokinesis in human A549 lung carcinoma cells. J. Biol. Chem. *275*, 1846–1854.

Ciriello, G., Miller, M.L., Aksoy, B.A., Senbabaoglu, Y., Schultz, N., and Sander, C. (2013). Emerging landscape of oncogenic signatures across human cancers. Nat. Genet. *45*, 1127–1133.

Collin, P., Nashchekina, O., Walker, R., and Pines, J. (2013). The spindle assembly checkpoint works like a rheostat rather than a toggle switch. Nat. Cell Biol. *15*, 1378–1385.

Conklin, J.F., and Sage, J. (2009). Keeping an eye on retinoblastoma control of human embryonic stem cells. J. Cell. Biochem. *108*, 1023–1030.

Connell-Crowley, L., Harper, J.W., and Goodrich, D.W. (1997). Cyclin D1/Cdk4 regulates retinoblastoma protein-mediated cell cycle arrest by site-specific phosphorylation. Mol. Biol. Cell *8*, 287–301.

Costanzo, M., Nishikawa, J.L., Tang, X., Millman, J.S., Schub, O., Breitkreuz, K., Dewar, D., Rupes, I., Andrews, B., and Tyers, M. (2004). CDK activity antagonizes Whi5, an inhibitor of G1/S transcription in yeast. Cell *117*, 899–913.

Coudreuse, D., and Nurse, P. (2010). Driving the cell cycle with a minimal CDK control network. Nature *468*, 1074–1079.

Coverley, D., Laman, H., and Laskey, R.A. (2002). Distinct roles for cyclins E and A during DNA replication complex assembly and activation. Nat. Cell Biol. *4*, 523–528.

Crasta, K., Lim, H.H., Giddings, T.H., Winey, M., and Surana, U. (2008). Inactivation of Cdh1 by synergistic action of Cdk1 and polo kinase is necessary for proper assembly of the mitotic spindle. Nat. Cell Biol. *10*, 665–675.

Cross, F.R., Hoek, M., McKinney, J.D., and Tinkelenberg, A.H. (1994). Role of Swi4 in cell cycle regulation of CLN2 expression. Mol. Cell Biol. *14*, 4779–4787.

Cross, F.R., Archambault, V., Miller, M., and Klovstad, M. (2002). Testing a mathematical model of the yeast cell cycle. Mol. Biol. Cell *13*, 52–70.

Cross, F.R., Buchler, N.E., and Skotheim, J.M. (2011). Evolution of networks and sequences in eukaryotic cell cycle control. Philos. Trans. R. Soc. Lond., B, Biol. Sci. *366*, 3532–3544.

Csikasz-Nagy, A., Battogtokh, D., Chen, K.C., Novak, B., and Tyson, J.J. (2006). Analysis of a generic model of eukaryotic cell-cycle regulation. Biophys. J. *90*, 4361–4379.

Culotti, J., and Hartwell, L.H. (1971). Genetic control of the cell division cycle in yeast. 3. Seven genes controlling nuclear division. Exp. Cell Res. *67*, 389–401.

de Bruin, R.A.M., McDonald, W.H., Kalashnikova, T.I., Yates, J., and Wittenberg, C. (2004). Cln3 activates G1-specific transcription via phosphorylation of the SBF bound repressor Whi5. Cell *117*, 887–898.

DeGregori, J., Kowalik, T., and Nevins, J.R. (1995). Cellular targets for activation by the E2F1 transcription factor include DNA synthesis- and G1/S-regulatory genes. Mol. Cell Biol. *15*, 4215–4224.

Deibler, R.W., and Kirschner, M.W. (2010). Quantitative reconstitution of mitotic CDK1 activation in somatic cell extracts. Mol. Cell *37*, 753–767.

Di Talia, S., Skotheim, J.M., Bean, J.M., Siggia, E.D., and Cross, F.R. (2007). The effects of molecular noise and size control on variability in the budding yeast cell cycle. Nature *448*, 947–951.

Di Talia, S., Wang, H., Skotheim, J.M., Rosebrock, A.P., Futcher, B., and Cross, F.R. (2009). Daughter-specific transcription factors regulate cell size control in budding yeast. PLoS Biol. *7*, e1000221.

Diaz-Martinez, L.A., Tian, W., Li, B., Warrington, R., Jia, L., Brautigam, C.A., Luo, X., and Yu, H. (2015). The Cdc20-binding Phe box of the spindle checkpoint protein BubR1 maintains the mitotic checkpoint complex during mitosis. J. Biol. Chem. *290*, 2431–2443.

Dick, A.E., and Gerlich, D.W. (2013). Kinetic framework of spindle assembly checkpoint signalling. Nat. Cell Biol. *15*, 1370–1377.

Dohadwala, M., da Cruz e Silva, E.F., Hall, F.L., Williams, R.T., Carbonaro-Hall, D.A., Nairn, A.C., Greengard, P., and Berndt, N. (1994). Phosphorylation and inactivation of protein phosphatase 1 by cyclin-dependent kinases. Proc. Natl. Acad. Sci. USA *91*, 6408–6412.

Dolznig, H., Grebien, F., Sauer, T., Beug, H., and Müllner, E.W. (2004). Evidence for a size-sensing mechanism in animal cells. Nat. Cell Biol. *6*, 899–905.

Doncic, A., Atay, O., Valk, E., Grande, A., Bush, A., Vasen, G., Colman-Lerner, A., Loog, M., and Skotheim, J.M. (2015). Compartmentalization of a bistable switch enables memory to cross a feedback-driven transition. Cell *160*, 1182–1195.

Doncic, A., Falleur-Fettig, M., and Skotheim, J.M. (2011). Distinct interactions select and maintain a specific cell fate. Mol. Cell *43*, 528–539.

Draetta, G. (1993). Cdc2 activation: the interplay of cyclin binding and Thr161 phosphorylation. Trends Cell Biol. *3*, 287–289.

Draetta, G., Brizuela, L., Potashkin, J., and Beach, D. (1987). Identification of p34 and p13, human homologs of the cell cycle regulators of fission yeast encoded by cdc2+ and suc1+. Cell *50*, 319–325.

Duensing, A., Liu, Y., Tseng, M., Malumbres, M., Barbacid, M., and Duensing, S. (2006). Cyclin-dependent kinase 2 is dispensable for normal centrosome duplication but required for oncogene-induced centrosome overduplication. Oncogene *25*, 2943–2949.

Dulić, V., Kaufmann, W.K., Wilson, S.J., Tlsty, T.D., Lees, E., Harper, J.W., Elledge, S.J., and Reed, S.I. (1994). p53-dependent inhibition of cyclin-dependent kinase activities in human fibroblasts during radiation-induced G1 arrest. Cell *76*, 1013–1023.

Dulić, V., Lees, E., and Reed, S.I. (1992). Association of human cyclin E with a periodic G1-S phase protein kinase. Science *257*, 1958–1961.

Dunn, K.C., Aotaki-Keen, A.E., Putkey, F.R., and Hjelmeland, L.M. (1996). ARPE-19, a human retinal pigment epithelial cell line with differentiated properties. Exp. Eye Res. *62*, 155–169.

Dunphy, W.G., and Kumagai, A. (1991). The cdc25 protein contains an intrinsic phosphatase activity. Cell *67*, 189–196.

Dunphy, W.G., Brizuela, L., Beach, D., and Newport, J. (1988). The Xenopus cdc2 protein is a component of MPF, a cytoplasmic regulator of mitosis. Cell *54*, 423–431.

Dynlacht, B.D., Flores, O., Lees, J.A., and Harlow, E. (1994). Differential regulation of E2F transactivation by cyclin/cdk2 complexes. Genes Dev. *8*, 1772–1786.

Easwaran, H.P., Leonhardt, H., and Cardoso, M.C. (2005). Cell cycle markers for live cell analyses. Cell Cycle *4*, 453–455.

Eguren, M., Manchado, E., and Malumbres, M. (2011). Non-mitotic functions of the Anaphase-Promoting Complex. Semin. Cell Dev. Biol. *22*, 572–578.

Eguren, M., Porlan, E., Manchado, E., García-Higuera, I., Cañamero, M., Fariñas, I., and Malumbres, M. (2013). The APC/C cofactor Cdh1 prevents replicative stress and p53-dependent cell death in neural progenitors. Nat. Commun. *4*, 2880.

el-Deiry, W.S., Tokino, T., Velculescu, V.E., Levy, D.B., Parsons, R., Trent, J.M., Lin, D., Mercer, W.E., Kinzler, K.W., and Vogelstein, B. (1993). WAF1, a potential mediator of p53 tumor suppression. Cell *75*, 817–825.

Elia, A.E.H., Cantley, L.C., and Yaffe, M.B. (2003a). Proteomic screen finds pSer/pThr-binding domain localizing Plk1 to mitotic substrates. Science *299*, 1228–1231.

Elia, A.E.H., Rellos, P., Haire, L.F., Chao, J.W., Ivins, F.J., Hoepker, K., Mohammad, D., Cantley, L.C., Smerdon, S.J., and Yaffe, M.B. (2003b). The molecular basis for phosphodependent substrate targeting and regulation of Plks by the Polo-box domain. Cell *115*, 83–95.

Elowitz, M.B., and Leibler, S. (2000). A synthetic oscillatory network of transcriptional regulators. Nature *403*, 335–338.

Elzen, den, N., and Pines, J. (2001). Cyclin A is destroyed in prometaphase and can delay chromosome alignment and anaphase. J. Cell Biol. *153*, 121–136.

Errico, A., Deshmukh, K., Tanaka, Y., Pozniakovsky, A., and Hunt, T. (2010). Identification of substrates for cyclin dependent kinases. Adv. Enzyme Regul. *50*, 375–399.

Eser, U., Falleur-Fettig, M., Johnson, A., and Skotheim, J.M. (2011). Commitment to a cellular transition precedes genome-wide transcriptional change. Mol. Cell *43*, 515–527.

Essers, J., Theil, A.F., Baldeyron, C., van Cappellen, W.A., Houtsmuller, A.B., Kanaar, R., and Vermeulen, W. (2005). Nuclear dynamics of PCNA in DNA replication and repair. Mol. Cell Biol. *25*, 9350–9359.

Evans, T., Rosenthal, E.T., Youngblom, J., Distel, D., and Hunt, T. (1983). Cyclin: a protein specified by maternal mRNA in sea urchin eggs that is destroyed at each cleavage division. Cell *33*, 389–396.

Ezhevsky, S.A., Ho, A., Becker-Hapak, M., Davis, P.K., and Dowdy, S.F. (2001). Differential regulation of retinoblastoma tumor suppressor protein by G(1) cyclin-dependent kinase complexes in vivo. Mol. Cell Biol. *21*, 4773–4784.

Faast, R., White, J., Cartwright, P., Crocker, L., Sarcevic, B., and Dalton, S. (2004). Cdk6-cyclin D3 activity in murine ES cells is resistant to inhibition by p16(INK4a). Oncogene *23*, 491–502.

Famulski, J.K., and Chan, G.K. (2007). Aurora B kinase-dependent recruitment of hZW10 and hROD to tensionless kinetochores. Curr. Biol. *17*, 2143–2149.

Fang, G., Yu, H., and Kirschner, M.W. (1998). The checkpoint protein MAD2 and the mitotic regulator CDC20 form a ternary complex with the anaphase-promoting complex to control anaphase initiation. Genes Dev. *12*, 1871–1883.

Fattaey, A., and Booher, R.N. (1997). Myt1: a Wee1-type kinase that phosphorylates Cdc2 on residue Thr14. Prog. Cell Cycle Res. *3*, 233–240.

Ferguson, A.M., White, L.S., Donovan, P.J., and Piwnica-Worms, H. (2005). Normal cell cycle and checkpoint responses in mice and cells lacking Cdc25B and Cdc25C protein phosphatases. Mol. Cell Biol. *25*, 2853–2860.

Ferrell, J.E. (1999). Xenopus oocyte maturation: new lessons from a good egg. Bioessays *21*, 833–842.

Ferrell, J.E. (2000). What do scaffold proteins really do? Sci. STKE *2000*, 52pe1–pe1.

Ferrell, J.E., and Machleder, E.M. (1998). The biochemical basis of an all-or-none cell fate switch in Xenopus oocytes. Science *280*, 895–898.

Ferrell, J.E. (2002). Self-perpetuating states in signal transduction: positive feedback, double-negative feedback and bistability. Curr. Opin. Cell Biol. *14*, 140–148.

Ferrell, J.E. (2013). Feedback loops and reciprocal regulation: recurring motifs in the systems biology of the cell cycle. Curr. Opin. Cell Biol. *25*, 676–686.

Ferrell, J.E., and Xiong, W. (2001). Bistability in cell signaling: How to make continuous processes discontinuous, and reversible processes irreversible. Chaos *11*, 227–236.

Ferrell, J.E., Tsai, T.Y.-C., and Yang, Q. (2011). Modeling the cell cycle: why do certain circuits oscillate? Cell *144*, 874–885.

Fisher, R.P., and Morgan, D.O. (1994). A novel cyclin associates with MO15/CDK7 to form the CDK-activating kinase. Cell *78*, 713–724.

Floyd, S., Pines, J., and Lindon, C. (2008). APC/C Cdh1 targets aurora kinase to control reorganization of the mitotic spindle at anaphase. Curr. Biol. *18*, 1649–1658.

Fluckiger, A.-C., Marcy, G., Marchand, M., Négre, D., Cosset, F.-L., Mitalipov, S., Wolf, D., Savatier, P., and Dehay, C. (2006). Cell cycle features of primate embryonic stem cells. Stem Cells *24*, 547–556.

Forester, C.M., Maddox, J., Louis, J.V., Goris, J., and Virshup, D.M. (2007). Control of mitotic exit by PP2A regulation of Cdc25C and Cdk1. Proc. Natl. Acad. Sci. USA *104*, 19867–19872.

Foster, D.A., Yellen, P., Xu, L., and Saqcena, M. (2010). Regulation of G1 Cell Cycle Progression: Distinguishing the Restriction Point from a Nutrient-Sensing Cell Growth Checkpoint(s). Genes Cancer *1*, 1124–1131.

Foster, S.A., and Morgan, D.O. (2012). The APC/C subunit Mnd2/Apc15 promotes Cdc20 autoubiquitination and spindle assembly checkpoint inactivation. Mol. Cell *47*, 921–932.

Frescas, D., and Pagano, M. (2008). Deregulated proteolysis by the F-box proteins SKP2 and beta-TrCP: tipping the scales of cancer. Nat. Rev. Cancer *8*, 438–449.

Fujii-Yamamoto, H., Kim, J.M., Arai, K.-I., and Masai, H. (2005). Cell cycle and developmental regulations of replication factors in mouse embryonic stem cells. J. Biol. Chem. *280*, 12976–12987.

Fujiki, H., and Suganuma, M. (1993). Tumor promotion by inhibitors of protein phosphatases 1 and 2A: the okadaic acid class of compounds. Adv. Cancer Res. *61*, 143–194.

Fujita, M., Yamada, C., Tsurumi, T., Hanaoka, F., Matsuzawa, K., and Inagaki, M. (1998). Cell cycle- and chromatin binding state-dependent phosphorylation of human MCM heterohexameric complexes. A role for cdc2 kinase. J. Biol. Chem. *273*, 17095–17101.

Fujita, M., Ishimi, Y., Nakamura, H., Kiyono, T., and Tsurumi, T. (2002). Nuclear organization of DNA replication initiation proteins in mammalian cells. J. Biol. Chem. *277*, 10354–10361.

Furnari, B., Rhind, N., and Russell, P. (1997). Cdc25 mitotic inducer targeted by chk1 DNA damage checkpoint kinase. Science *277*, 1495–1497.

Gardner, R.D., and Burke, D.J. (2000). The spindle checkpoint: two transitions, two pathways. Trends Cell Biol. *10*, 154–158.

Gautier, J., and Maller, J.L. (1991). Cyclin B in Xenopus oocytes: implications for the mechanism of pre-MPF activation. Embo J. *10*, 177–182.

Gavet, O., and Pines, J. (2010). Progressive activation of CyclinB1-Cdk1 coordinates entry to mitosis. Dev. Cell *18*, 533–543.

Gelens, L., Huang, K.C., and Ferrell, J.E. (2015). How Does the Xenopus laevis Embryonic Cell Cycle Avoid Spatial Chaos? Cell Rep. *12*, 892–900.

Geley, S., Kramer, E., Gieffers, C., Gannon, J., Peters, J.M., and Hunt, T. (2001). Anaphase-promoting complex/cyclosome-dependent proteolysis of human cyclin A starts at the beginning of mitosis and is not subject to the spindle assembly checkpoint. J. Cell Biol. *153*, 137–148.

Geng, Y., Yu, Q., Sicinska, E., Das, M., Schneider, J.E., Bhattacharya, S., Rideout, W.M., Bronson, R.T., Gardner, H., and Sicinski, P. (2003). Cyclin E ablation in the mouse. Cell *114*, 431–443.

Georgi, A.B., Stukenberg, P.T., and Kirschner, M.W. (2002). Timing of events in mitosis. Curr. Biol. *12*, 105–114.

Gérard, C., Tyson, J.J., and Novak, B. (2013). Minimal models for cell-cycle control based on competitive inhibition and multisite phosphorylations of Cdk substrates. Biophys. J. *104*, 1367–1379.

Gibson, D.G., Young, L., Chuang, R.-Y., Venter, J.C., Hutchison, C.A., and Smith, H.O. (2009). Enzymatic assembly of DNA molecules up to several hundred kilobases. Nat. Methods *6*, 343–345.

Gieffers, C., Peters, B.H., Kramer, E.R., Dotti, C.G., and Peters, J.M. (1999). Expression of the CDH1-associated form of the anaphase-promoting complex in postmitotic neurons. Proc. Natl. Acad. Sci. USA *96*, 11317–11322.

Ginsberg, D., Vairo, G., Chittenden, T., Xiao, Z.X., Xu, G., Wydner, K.L., DeCaprio, J.A., Lawrence, J.B., and Livingston, D.M. (1994). E2F-4, a new member of the E2F transcription factor family, interacts with p107. Genes Dev. *8*, 2665–2679.

Glotzer, M., Murray, A.W., and Kirschner, M.W. (1991). Cyclin is degraded by the ubiquitin pathway. Nature *349*, 132–138.

González, T., Seoane, M., Caamaño, P., Viñuela, J., Domínguez, F., and Zalvide, J. (2003). Inhibition of Cdk4 activity enhances translation of p27kip1 in quiescent Rb-negative cells. J. Biol. Chem. *278*, 12688–12695.

Gould, K.L., and Nurse, P. (1989). Tyrosine phosphorylation of the fission yeast cdc2+ protein kinase regulates entry into mitosis. Nature *342*, 39–45.

Graña, X., Garriga, J., and Mayol, X. (1998). Role of the retinoblastoma protein family, pRB, p107 and p130 in the negative control of cell growth. Oncogene *17*, 3365–3383.

Gray, C.H., Good, V.M., Tonks, N.K., and Barford, D. (2003). The structure of the cell cycle protein Cdc14 reveals a proline-directed protein phosphatase. Embo J. *22*, 3524–3535.

Grosskortenhaus, R., and Sprenger, F. (2002). Rca1 inhibits APC-Cdh1(Fzr) and is required to prevent cyclin degradation in G2. Dev. Cell *2*, 29–40.

Gu, Y., Turck, C.W., and Morgan, D.O. (1993). Inhibition of CDK2 activity in vivo by an associated 20K regulatory subunit. Nature *366*, 707–710.

Guan, K.L., Jenkins, C.W., Li, Y., Nichols, M.A., Wu, X., O'Keefe, C.L., Matera, A.G., and Xiong, Y. (1994). Growth suppression by p18, a p16INK4/MTS1- and p14INK4B/MTS2-related CDK6 inhibitor, correlates with wild-type pRb function. Genes Dev. *8*, 2939–2952.

Guhr, A., Kurtz, A., Friedgen, K., and Löser, P. (2006). Current state of human embryonic stem cell research: an overview of cell lines and their use in experimental work. Stem Cells

24, 2187–2191.

Guidi, G.M., and Goldbeter, A. (1997). Bistability without Hysteresis in Chemical Reaction Systems: A Theoretical Analysis of Irreversible Transitions between Multiple Steady States. J. Phys. Chem. A *101*, 9367–9376.

Guidi, G.M., and Goldbeter, A. (1998). Bistability without Hysteresis in Chemical Reaction Systems: The Case of Nonconnected Branches of Coexisting Steady States. J. Phys. Chem. A *102*, 7813–7820.

Gut, G., Tadmor, M.D., Pe'er, D., Pelkmans, L., and Liberali, P. (2015). Trajectories of cell-cycle progression from fixed cell populations. Nat. Methods *12*, 951–954.

Hahn, A.T., Jones, J.T., and Meyer, T. (2009). Quantitative analysis of cell cycle phase durations and PC12 differentiation using fluorescent biosensors. Cell Cycle *8*, 1044–1052.

Hanashiro, K., Kanai, M., Geng, Y., Sicinski, P., and Fukasawa, K. (2008). Roles of cyclins A and E in induction of centrosome amplification in p53-compromised cells. Oncogene *27*, 5288–5302.

Hannon, G.J., and Beach, D. (1994). p15INK4B is a potential effector of TGF-beta-induced cell cycle arrest. Nature *371*, 257–261.

Harashima, H., Dissmeyer, N., and Schnittger, A. (2013). Cell cycle control across the eukaryotic kingdom. Trends Cell Biol. *23*, 345–356.

Harbour, J.W., and Dean, D.C. (2000). The Rb/E2F pathway: expanding roles and emerging paradigms. Genes Dev. *14*, 2393–2409.

Harbour, J.W., Luo, R.X., Dei Santi, A., Postigo, A.A., and Dean, D.C. (1999). Cdk phosphorylation triggers sequential intramolecular interactions that progressively block Rb functions as cells move through G1. Cell *98*, 859–869.

Hardwick, K.G., Johnston, R.C., Smith, D.L., and Murray, A.W. (2000). MAD3 encodes a novel component of the spindle checkpoint which interacts with Bub3p, Cdc20p, and Mad2p. J. Cell Biol. *148*, 871–882.

Harper, J.W., Adami, G.R., Wei, N., Keyomarsi, K., and Elledge, S.J. (1993). The p21 Cdk-interacting protein Cip1 is a potent inhibitor of G1 cyclin-dependent kinases. Cell *75*, 805–816.

Harper, J.W., Elledge, S.J., Keyomarsi, K., Dylancht, B., Tsai, L.H., Zhang, P., Dobrowolski, S., Bai, C., Connell-Crowley, L., and Swindell, E. (1995). Inhibition of cyclin-dependent kinases by p21. Mol. Biol. Cell *6*, 387–400.

Hartwell, L.H. (1978). Cell division from a genetic perspective. J. Cell Biol. *77*, 627–637.

Hartwell, L.H., and Unger, M.W. (1977). Unequal division in Saccharomyces cerevisiae and its implications for the control of cell division. J. Cell Biol. *75*, 422–435.

Hartwell, L.H., and Weinert, T.A. (1989). Checkpoints: controls that ensure the order of cell cycle events. Science *246*, 629–634.

Hartwell, L.H., Culotti, J., and Reid, B. (1970). Genetic control of the cell-division cycle in yeast. I. Detection of mutants. Proc. Natl. Acad. Sci. USA *66*, 352–359.

Hartwell, L.H., Culotti, J., Pringle, J.R., and Reid, B.J. (1974). Genetic control of the cell division cycle in yeast. Science *183*, 46–51.

Hartwell, L.H., Hopfield, J.J., Leibler, S., and Murray, A.W. (1999). From molecular to modular cell biology. Nature *402*, C47–C52.

Hartwell, L.H., Mortimer, R.K., Culotti, J., and Culotti, M. (1973). Genetic Control of the Cell Division Cycle in Yeast: V. Genetic Analysis of cdc Mutants. Genetics *74*, 267–286.

Hashimoto, O., Shinkawa, M., Torimura, T., Nakamura, T., Selvendiran, K., Sakamoto, M., Koga, H., Ueno, T., and Sata, M. (2006). Cell cycle regulation by the Wee1 inhibitor PD0166285, pyrido [2,3-d] pyimidine, in the B16 mouse melanoma cell line. BMC Cancer *6*, 292.

Hasty, J., McMillen, D., Isaacs, F., and Collins, J.J. (2001). Computational studies of gene regulatory networks: in numero molecular biology. Nat. Rev. Genet. *2*, 268–279.

Hatakeyama, M., and Weinberg, R.A. (1995). The role of RB in cell cycle control. Prog. Cell Cycle Res. *1*, 9–19.

Hateboer, G., Kerkhoven, R.M., Shvarts, A., Bernards, R., and Beijersbergen, R.L. (1996). Degradation of E2F by the ubiquitin-proteasome pathway: regulation by retinoblastoma family proteins and adenovirus transforming proteins. Genes Dev. *10*, 2960–2970.

Havens, C.G., Ho, A., Yoshioka, N., and Dowdy, S.F. (2006). Regulation of late G1/S phase transition and APC Cdh1 by reactive oxygen species. Mol. Cell Biol. *26*, 4701–4711.

Hawkins, E.D., Markham, J.F., McGuinness, L.P., and Hodgkin, P.D. (2009). A single-cell pedigree analysis of alternative stochastic lymphocyte fates. Proc. Natl. Acad. Sci. USA *106*, 13457–13462.

He, S., Nakada, D., and Morrison, S.J. (2009). Mechanisms of stem cell self-renewal. Annu. Rev. Cell Dev. Biol. *25*, 377–406.

Heim, A., Konietzny, A., and Mayer, T.U. (2015). Protein phosphatase 1 is essential for Greatwall inactivation at mitotic exit. EMBO Rep. *16*, 1501–1510.

Helin, K., Harlow, E., and Fattaey, A. (1993). Inhibition of E2F-1 transactivation by direct binding of the retinoblastoma protein. Mol. Cell Biol. *13*, 6501–6508.

Hendrickson, M., Madine, M., Dalton, S., and Gautier, J. (1996). Phosphorylation of MCM4 by cdc2 protein kinase inhibits the activity of the minichromosome maintenance complex. Proc. Natl. Acad. Sci. USA *93*, 12223–12228.

Hershko, A., Ganoth, D., Sudakin, V., Dahan, A., Cohen, L.H., Luca, F.C., Ruderman, J.V., and Eytan, E. (1994). Components of a system that ligates cyclin to ubiquitin and their regulation by the protein kinase cdc2. J. Biol. Chem. *269*, 4940–4946.

Hégarat, N., Rata, S., and Hochegger, H. (2016). Bistability of mitotic entry and exit switches during open mitosis in mammalian cells. Bioessays *38*, 627–643.

Hirai, H., Roussel, M.F., Kato, J.Y., Ashmun, R.A., and Sherr, C.J. (1995). Novel INK4 proteins, p19 and p18, are specific inhibitors of the cyclin D-dependent kinases CDK4 and CDK6. Mol. Cell Biol. *15*, 2672–2681.

Hoffmann, I., Clarke, P.R., Marcote, M.J., Karsenti, E., and Draetta, G. (1993). Phosphorylation and activation of human cdc25-C by cdc2--cyclin B and its involvement in the self-amplification of MPF at mitosis. Embo J. *12*, 53–63.

Holloway, S.L., Glotzer, M., King, R.W., and Murray, A.W. (1993). Anaphase is initiated by proteolysis rather than by the inactivation of maturation-promoting factor. Cell *73*, 1393–1402.

Holmes, J.K., and Solomon, M.J. (1996). A predictive scale for evaluating cyclin-dependent kinase substrates. A comparison of p34cdc2 and p33cdk2. J. Biol. Chem. *271*, 25240–25246.

Holt, L.J., Krutchinsky, A.N., and Morgan, D.O. (2008). Positive feedback sharpens the anaphase switch. Nature *454*, 353–357.

Howell, B.J., Moree, B., Farrar, E.M., Stewart, S., Fang, G., and Salmon, E.D. (2004). Spindle checkpoint protein dynamics at kinetochores in living cells. Curr. Biol. *14*, 953–964.

Hoyt, M.A., Totis, L., and Roberts, B.T. (1991). S. cerevisiae genes required for cell cycle arrest in response to loss of microtubule function. Cell *66*, 507–517.

Hsu, J.Y., Reimann, J.D.R., Sørensen, C.S., Lukas, J., and Jackson, P.K. (2002). E2F-dependent accumulation of hEmi1 regulates S phase entry by inhibiting APC(Cdh1). Nat. Cell Biol. *4*, 358–366.

Hu, L., Plafker, K., Vorozhko, V., Zuna, R.E., Hanigan, M.H., Gorbsky, G.J., Plafker, S.M., Angeletti, P.C., and Ceresa, B.P. (2009). Human papillomavirus 16 E5 induces bi-nucleated cell formation by cell-cell fusion. Virology *384*, 125–134.

Humbert, C., Giroud, F., and Brugal, G. (1990). Detection of S cells and evaluation of DNA denaturation protocols by image cytometry of fluorescent BrdUrd labelling. Cytometry *11*, 481–489.

Hwang, H.C., and Clurman, B.E. (2005). Cyclin E in normal and neoplastic cell cycles. Oncogene *24*, 2776–2786.

Irniger, S., Piatti, S., Michaelis, C., and Nasmyth, K. (1995). Genes involved in sister chromatid separation are needed for B-type cyclin proteolysis in budding yeast. Cell *81*, 269–278.

Ito, D., Saito, Y., and Matsumoto, T. (2012). Centromere-tethered Mps1 pombe homolog (Mph1) kinase is a sufficient marker for recruitment of the spindle checkpoint protein Bub1, but not Mad1. Proc. Natl. Acad. Sci. USA *109*, 209–214.

Izawa, D., and Pines, J. (2012). Mad2 and the APC/C compete for the same site on Cdc20 to ensure proper chromosome segregation. J. Cell Biol. *199*, 27–37.

Izumi, T., and Maller, J.L. (1993). Elimination of cdc2 phosphorylation sites in the cdc25 phosphatase blocks initiation of M-phase. Mol. Biol. Cell *4*, 1337–1350.

Izumi, T., Walker, D.H., and Maller, J.L. (1992). Periodic changes in phosphorylation of the Xenopus cdc25 phosphatase regulate its activity. Mol. Biol. Cell *3*, 927–939.

Jablonski, S.A., Chan, G.K., Cooke, C.A., Earnshaw, W.C., and Yen, T.J. (1998). The hBUB1 and hBUBR1 kinases sequentially assemble onto kinetochores during prophase with hBUBR1 concentrating at the kinetochore plates in mitosis. Chromosoma *107*, 386–396.

Jackman, M., Lindon, C., Nigg, E.A., and Pines, J. (2003). Active cyclin B1–Cdk1 first appears on centrosomes in prophase. Nat. Cell Biol. *5*, 143–148.

Jaitin, D.A., Kenigsberg, E., Keren-Shaul, H., Elefant, N., Paul, F., Zaretsky, I., Mildner, A., Cohen, N., Jung, S., Tanay, A., et al. (2014). Massively parallel single-cell RNA-seq for marker-free decomposition of tissues into cell types. Science *343*, 776–779.

Jaquenoud, M., van Drogen, F., and Peter, M. (2002). Cell cycle-dependent nuclear export of Cdh1p may contribute to the inactivation of APC/C(Cdh1). Embo J. *21*, 6515–6526.

Jaspersen, S.L., Charles, J.F., and Morgan, D.O. (1999). Inhibitory phosphorylation of the

APC regulator Hct1 is controlled by the kinase Cdc28 and the phosphatase Cdc14. Curr. Biol. *9*, 227–236.

Jeffrey, P.D., Tong, L., and Pavletich, N.P. (2000). Structural basis of inhibition of CDK-cyclin complexes by INK4 inhibitors. Genes Dev. *14*, 3115–3125.

Jelluma, N., Dansen, T.B., Sliedrecht, T., Kwiatkowski, N.P., and Kops, G.J.P.L. (2010). Release of Mps1 from kinetochores is crucial for timely anaphase onset. J. Cell Biol. *191*, 281–290.

Jiang, W., Wells, N.J., and Hunter, T. (1999). Multistep regulation of DNA replication by Cdk phosphorylation of HsCdc6. Proc. Natl. Acad. Sci. USA *96*, 6193–6198.

Johnson, A., and Skotheim, J.M. (2013). Start and the restriction point. Curr. Opin. Cell Biol. *25*, 717–723.

Johnson, V.L., Scott, M.I.F., Holt, S.V., Hussein, D., and Taylor, S.S. (2004). Bub1 is required for kinetochore localization of BubR1, Cenp-E, Cenp-F and Mad2, and chromosome congression. J. Cell Sci. *117*, 1577–1589.

Jord, Al, A., Shihavuddin, A., Servignat d'Aout, R., Faucourt, M., Genovesio, A., Karaiskou, A., Sobczak-Thépot, J., Spassky, N., and Meunier, A. (2017). Calibrated mitotic oscillator drives motile ciliogenesis. Science *358*, 803–806.

Kamura, T., Hara, T., Kotoshiba, S., Yada, M., Ishida, N., Imaki, H., Hatakeyama, S., Nakayama, K., and Nakayama, K.I. (2003). Degradation of p57Kip2 mediated by SCFSkp2-dependent ubiquitylation. Proc. Natl. Acad. Sci. USA *100*, 10231–10236.

Kang, Q., and Pomerening, J.R. (2012). Punctuated cyclin synthesis drives early embryonic cell cycle oscillations. Mol. Biol. Cell *23*, 284–296.

Kapinas, K., Grandy, R., Ghule, P., Medina, R., Becker, K., Pardee, A., Zaidi, S.K., Lian, J., Stein, J., van Wijnen, A., et al. (2013). The Abbreviated Pluripotent Cell Cycle. J. Cell Physiol. *228*, 9–20.

Kempe, H., Schwabe, A., Crémazy, F., Verschure, P.J., and Bruggeman, F.J. (2015). The volumes and transcript counts of single cells reveal concentration homeostasis and capture biological noise. Mol. Biol. Cell *26*, 797–804.

Killander, D., and Zetterberg, A. (1965). Quantitative cytochemical studies on interphase growth: I. Determination of DNA, RNA and mass content of age determined mouse fibroblasts *in vitro* and of intercellular variation in generation time. Exp. Cell Res. *38*, 272–284.

Kim, A.H., Puram, S.V., Bilimoria, P.M., Ikeuchi, Y., Keough, S., Wong, M., Rowitch, D., and Bonni, A. (2009). A centrosomal Cdc20-APC pathway controls dendrite morphogenesis in postmitotic neurons. Cell *136*, 322–336.

Kim, S.Y., and Ferrell, J.E., Jr. (2007). Substrate Competition as a Source of Ultrasensitivity in the Inactivation of Wee1. Cell *128*, 1133–1145.

King, R.W., Peters, J.M., Tugendreich, S., Rolfe, M., Hieter, P., and Kirschner, M.W. (1995). A 20S complex containing CDC27 and CDC16 catalyzes the mitosis-specific conjugation of ubiquitin to cyclin B. Cell *81*, 279–288.

Kinjyo, I., Qin, J., Tan, S.-Y., Wellard, C.J., Mrass, P., Ritchie, W., Doi, A., Cavanagh, L.L., Tomura, M., Sakaue-Sawano, A., et al. (2015). Real-time tracking of cell cycle progression during CD8+ effector and memory T-cell differentiation. Nat. Commun. *6*, 1–13.

Kirchner, J., Gross, S., Bennett, D., and Alphey, L. (2007). Essential, overlapping and redundant roles of the Drosophila protein phosphatase 1 alpha and 1 beta genes. Genetics *176*, 273–281.

Kisielewska, J., Lu, P., and Whitaker, M. (2005). GFP-PCNA as an S-phase marker in embryos during the first and subsequent cell cycles. Biol. Cell *97*, 221–229.

Kitagawa, M., Higashi, H., Jung, H.K., Suzuki-Takahashi, I., Ikeda, M., Tamai, K., Kato, J., Segawa, K., Yoshida, E., Nishimura, S., et al. (1996). The consensus motif for phosphorylation by cyclin D1-Cdk4 is different from that for phosphorylation by cyclin A/E-Cdk2. Embo J. *15*, 7060–7069.

Kiviet, D.J., Nghe, P., Walker, N., Boulineau, S., Sunderlikova, V., and Tans, S.J. (2014). Stochasticity of metabolism and growth at the single-cell level. Nature *514*, 376–379.

Kobayashi, H., Stewart, E., Poon, R., Adamczewski, J.P., Gannon, J., and Hunt, T. (1992). Identification of the domains in cyclin A required for binding to, and activation of, p34cdc2 and p32cdk2 protein kinase subunits. Mol. Biol. Cell *3*, 1279–1294.

Koff, A., Giordano, A., Desai, D., Yamashita, K., Harper, J.W., Elledge, S., Nishimoto, T., Morgan, D.O., Franza, B.R., and Roberts, J.M. (1992). Formation and activation of a cyclin E-cdk2 complex during the G1 phase of the human cell cycle. Science *257*, 1689–1694.

Koledova, Z., Krämer, A., Kafkova, L.R., and Divoky, V. (2010). Cell-cycle regulation in embryonic stem cells: centrosomal decisions on self-renewal. Stem Cells Dev. *19*, 1663–1678.

Kolupaeva, V., and Janssens, V. (2013). PP1 and PP2A phosphatases-cooperating partners in modulating retinoblastoma protein activation. Febs J. *280*, 627–643.

Konishi, Y., Stegmüller, J., Matsuda, T., Bonni, S., and Bonni, A. (2004). Cdh1-APC controls axonal growth and patterning in the mammalian brain. Science *303*, 1026–1030.

Kornbluth, S., Sebastian, B., Hunter, T., and Newport, J. (1994). Membrane localization of the kinase which phosphorylates p34cdc2 on threonine 14. Mol. Biol. Cell *5*, 273–282.

Kramer, E.R., Scheuringer, N., Podtelejnikov, A.V., Mann, M., and Peters, J.M. (2000). Mitotic regulation of the APC activator proteins CDC20 and CDH1. Mol. Biol. Cell *11*, 1555–1569.

Krämer, A., Lukas, J., and Bartek, J. (2004). Checking out the centrosome. Cell Cycle *3*, 1390–1393.

Krek, W., Ewen, M.E., Shirodkar, S., Arany, Z., Kaelin, W.G., and Livingston, D.M. (1994). Negative regulation of the growth-promoting transcription factor E2F-1 by a stably bound cyclin A-dependent protein kinase. Cell *78*, 161–172.

Kumagai, A., and Dunphy, W.G. (1992). Regulation of the cdc25 protein during the cell cycle in Xenopus extracts. Cell *70*, 139–151.

Kumagai, A., and Dunphy, W.G. (1996). Purification and molecular cloning of Plx1, a Cdc25-regulatory kinase from Xenopus egg extracts. Science *273*, 1377–1380.

Kumagai, A., Yakowec, P.S., and Dunphy, W.G. (1998). 14-3-3 proteins act as negative regulators of the mitotic inducer Cdc25 in Xenopus egg extracts. Mol. Biol. Cell *9*, 345–354.

Kwon, Y.G., Lee, S.Y., Choi, Y., Greengard, P., and Nairn, A.C. (1997). Cell cycle-dependent phosphorylation of mammalian protein phosphatase 1 by cdc2 kinase. Proc. Natl. Acad. Sci. USA *94*, 2168–2173.

Labbe, J.C., Picard, A., Peaucellier, G., Cavadore, J.C., Nurse, P., and Doree, M. (1989).

Purification of MPF from starfish: identification as the H1 histone kinase p34cdc2 and a possible mechanism for its periodic activation. Cell *57*, 253–263.

Lasorella, A., Stegmüller, J., Guardavaccaro, D., Liu, G., Carro, M.S., Rothschild, G., la Torre-Ubieta, de, L., Pagano, M., Bonni, A., and Iavarone, A. (2006). Degradation of Id2 by the anaphase-promoting complex couples cell cycle exit and axonal growth. Nature *442*, 471–474.

Laurent, M., and Kellershohn, N. (1999). Multistability: a major means of differentiation and evolution in biological systems. Trends Biochem. Sci. *24*, 418–422.

Lee, C., Hong, B., Choi, J.M., Kim, Y., Watanabe, S., Ishimi, Y., Enomoto, T., Tada, S., Kim, Y., and Cho, Y. (2004). Structural basis for inhibition of the replication licensing factor Cdt1 by geminin. Nature *430*, 913–917.

Lee, M.G., and Nurse, P. (1987). Complementation used to clone a human homologue of the fission yeast cell cycle control gene cdc2. Nature *327*, 31–35.

Lees, J.A., Buchkovich, K.J., Marshak, D.R., Anderson, C.W., and Harlow, E. (1991). The retinoblastoma protein is phosphorylated on multiple sites by human cdc2. Embo J. *10*, 4279–4290.

Leonhardt, H., Rahn, H.P., Weinzierl, P., Sporbert, A., Cremer, T., Zink, D., and Cardoso, M.C. (2000). Dynamics of DNA replication factories in living cells. J. Cell Biol. *149*, 271–280.

Li, J., Ran, C., Li, E., Gordon, F., Comstock, G., Siddiqui, H., Cleghorn, W., Chen, H.-Z., Kornacker, K., Liu, C.-G., et al. (2008). Synergistic function of E2F7 and E2F8 is essential for cell survival and embryonic development. Dev. Cell *14*, 62–75.

Li, R., and Murray, A.W. (1991). Feedback control of mitosis in budding yeast. Cell *66*, 519–531.

Li, X., Zhao, Q., Liao, R., Sun, P., and Wu, X. (2003). The SCF(Skp2) ubiquitin ligase complex interacts with the human replication licensing factor Cdt1 and regulates Cdt1 degradation. J. Biol. Chem. *278*, 30854–30858.

Lincoln, A.J., Wickramasinghe, D., Stein, P., Schultz, R.M., Palko, M.E., De Miguel, M.P., Tessarollo, L., and Donovan, P.J. (2002). Cdc25b phosphatase is required for resumption of meiosis during oocyte maturation. Nat. Genet. *30*, 446–449.

Lindon, C., and Pines, J. (2004). Ordered proteolysis in anaphase inactivates Plk1 to contribute to proper mitotic exit in human cells. J. Cell Biol. *164*, 233–241.

Lindqvist, A., van Zon, W., Karlsson Rosenthal, C., and Wolthuis, R.M.F. (2007). Cyclin B1–Cdk1 Activation Continues after Centrosome Separation to Control Mitotic Progression. PLoS Biol. *5*, e123–11.

Lischetti, T., Zhang, G., Sedgwick, G.G., Bolanos-Garcia, V.M., and Nilsson, J. (2014). The internal Cdc20 binding site in BubR1 facilitates both spindle assembly checkpoint signalling and silencing. Nat. Commun. *5*, 5563.

Listovsky, T., and Sale, J.E. (2013). Sequestration of CDH1 by MAD2L2 prevents premature APC/C activation prior to anaphase onset. J. Cell Biol. *203*, 87–100.

Liu, D.X., and Greene, L.A. (2001). Neuronal apoptosis at the G1/S cell cycle checkpoint. Cell Tissue Res. *305*, 217–228.

Liu, D., Matzuk, M.M., Sung, W.K., Guo, Q., Wang, P., and Wolgemuth, D.J. (1998). Cyclin A1 is required for meiosis in the male mouse. Nat. Genet. *20*, 377–380.

Liu, E., Li, X., Yan, F., Zhao, Q., and Wu, X. (2004). Cyclin-dependent kinases phosphorylate human Cdt1 and induce its degradation. J. Biol. Chem. *279*, 17283–17288.

Liu, F., Stanton, J.J., Wu, Z., and Piwnica-Worms, H. (1997). The human Myt1 kinase preferentially phosphorylates Cdc2 on threonine 14 and localizes to the endoplasmic reticulum and Golgi complex. Mol. Cell Biol. *17*, 571–583.

Liu, Q., Guntuku, S., Cui, X.S., Matsuoka, S., Cortez, D., Tamai, K., Luo, G., Carattini-Rivera, S., DeMayo, F., Bradley, A., et al. (2000). Chk1 is an essential kinase that is regulated by Atr and required for the G(2)/M DNA damage checkpoint. Genes Dev. *14*, 1448–1459.

Livak, K.J., and Schmittgen, T.D. (2001). Analysis of relative gene expression data using real-time quantitative PCR and the 2(-Delta Delta C(T)) Method. Methods *25*, 402–408.

Lobjois, V., Jullien, D., Bouché, J.-P., and Ducommun, B. (2009). The polo-like kinase 1 regulates CDC25B-dependent mitosis entry. Biochim. Biophys. Acta *1793*, 462–468.

Lohka, M.J., and Maller, J.L. (1988). Induction of metaphase chromosome condensation in human sperm by Xenopus egg extracts. Exp. Cell Res. *179*, 303–309.

Lohka, M.J., and Masui, Y. (1983). Formation in vitro of sperm pronuclei and mitotic chromosomes induced by amphibian ooplasmic components. Science *220*, 719–721.

Lohka, M.J., Hayes, M.K., and Maller, J.L. (1988). Purification of maturation-promoting factor, an intracellular regulator of early mitotic events. Proc. Natl. Acad. Sci. USA *85*, 3009–3013.

London, N., and Biggins, S. (2014). Mad1 kinetochore recruitment by Mps1-mediated phosphorylation of Bub1 signals the spindle checkpoint. Genes Dev. *28*, 140–152.

Lord, P.G., and Wheals, A.E. (1981). Variability in individual cell cycles of Saccharomyces cerevisiae. J. Cell Sci. *50*, 361–376.

López-Avilés, S., Kapuy, O., Novak, B., and Uhlmann, F. (2009). Irreversibility of mitotic exit is the consequence of systems-level feedback. Nature *459*, 592–595.

Lu, L.X., Domingo-Sananes, M.R., Huzarska, M., Novak, B., and Gould, K.L. (2012). Multisite phosphoregulation of Cdc25 activity refines the mitotic entrance and exit switches. Proc. Natl. Acad. Sci. USA *109*, 9899–9904.

Lukas, C., Sørensen, C.S., Kramer, E., Santoni-Rugiu, E., Lindeneg, C., Peters, J.M., Bartek, J., and Lukas, J. (1999). Accumulation of cyclin B1 requires E2F and cyclin-A-dependent rearrangement of the anaphase-promoting complex. Nature *401*, 815–818.

Lukas, J., Herzinger, T., Hansen, K., Moroni, M.C., Resnitzky, D., Helin, K., Reed, S.I., and Bartek, J. (1997). Cyclin E-induced S phase without activation of the pRb/E2F pathway. Genes Dev. *11*, 1479–1492.

Lundgren, K., Walworth, N., Booher, R., Dembski, M., Kirschner, M., and Beach, D. (1991). mik1 and wee1 cooperate in the inhibitory tyrosine phosphorylation of cdc2. Cell *64*, 1111–1122.

Luo, X., Fang, G., Coldiron, M., Lin, Y., Yu, H., Kirschner, M.W., and Wagner, G. (2000). Structure of the Mad2 spindle assembly checkpoint protein and its interaction with Cdc20. Nat. Struct. Biol. *7*, 224–229.

Luo, X., Tang, Z., Rizo, J., and Yu, H. (2002). The Mad2 spindle checkpoint protein undergoes similar major conformational changes upon binding to either Mad1 or Cdc20. Mol. Cell *9*, 59–71.

Ma, S., Vigneron, S., Robert, P., Strub, J.M., Cianferani, S., Castro, A., and Lorca, T. (2016). Greatwall dephosphorylation and inactivation upon mitotic exit is triggered by PP1. J. Cell Sci. *129*, 1329–1339.

Mailand, N., Podtelejnikov, A.V., Groth, A., Mann, M., Bartek, J., and Lukas, J. (2002). Regulation of G(2)/M events by Cdc25A through phosphorylation-dependent modulation of its stability. Embo J. *21*, 5911–5920.

Malumbres, M., and Barbacid, M. (2001). To cycle or not to cycle: a critical decision in cancer. Nat. Rev. Cancer *1*, 222–231.

Malumbres, M., and Barbacid, M. (2005). Mammalian cyclin-dependent kinases. Trends Biochem. Sci. *30*, 630–641.

Malumbres, M., and Barbacid, M. (2009). Cell cycle, CDKs and cancer: a changing paradigm. Nat. Rev. Cancer *9*, 153–166.

Malumbres, M., Harlow, E., Hunt, T., Hunter, T., Lahti, J.M., Manning, G., Morgan, D.O., Tsai, L.-H., and Wolgemuth, D.J. (2009). Cyclin-dependent kinases: a family portrait. Nat. Cell Biol. *11*, 1275–1276.

Mandal, M., Bandyopadhyay, D., Goepfert, T.M., and Kumar, R. (1998). Interferon-induces expression of cyclin-dependent kinase-inhibitors p21WAF1 and p27Kip1 that prevent activation of cyclin-dependent kinase by CDK-activating kinase (CAK). Oncogene *16*, 217–225.

Mantel, C., Guo, Y., Lee, M.R., Kim, M.-K., Han, M.-K., Shibayama, H., Fukuda, S., Yoder, M.C., Pelus, L.M., Kim, K.-S., et al. (2007). Checkpoint-apoptosis uncoupling in human and mouse embryonic stem cells: a source of karyotpic instability. Blood *109*, 4518–4527.

Marchingo, J.M., Kan, A., Sutherland, R.M., Duffy, K.R., Wellard, C.J., Belz, G.T., Lew, A.M., Dowling, M.R., Heinzel, S., and Hodgkin, P.D. (2014). T cell signaling. Antigen affinity, costimulation, and cytokine inputs sum linearly to amplify T cell expansion. Science *346*, 1123–1127.

Margolis, S.S., Walsh, S., Weiser, D.C., Yoshida, M., Shenolikar, S., and Kornbluth, S. (2003). PP1 control of M phase entry exerted through 14-3-3-regulated Cdc25 dephosphorylation. Embo J. *22*, 5734–5745.

Marti, A., Wirbelauer, C., Scheffner, M., and Krek, W. (1999). Interaction between ubiquitin-protein ligase SCFSKP2 and E2F-1 underlies the regulation of E2F-1 degradation. Nat. Cell Biol. *1*, 14–19.

Masui, Y., and Markert, C.L. (1971). Cytoplasmic control of nuclear behavior during meiotic maturation of frog oocytes. J. Exp. Zool. *177*, 129–145.

Matsuoka, S., Huang, M., and Elledge, S.J. (1998). Linkage of ATM to cell cycle regulation by the Chk2 protein kinase. Science *282*, 1893–1897.

Matsusaka, T., and Pines, J. (2004). Chfr acts with the p38 stress kinases to block entry to mitosis in mammalian cells. J. Cell Biol. *166*, 507–516.

Mäkelä, T.P., Tassan, J.P., Nigg, E.A., Frutiger, S., Hughes, G.J., and Weinberg, R.A. (1994). A cyclin associated with the CDK-activating kinase MO15. Nature *371*, 254–257.

McGarry, T.J., and Kirschner, M.W. (1998). Geminin, an inhibitor of DNA replication, is degraded during mitosis. Cell *93*, 1043–1053.

McGowan, C.H., and Russell, P. (1993). Human Wee1 kinase inhibits cell division by

phosphorylating p34cdc2 exclusively on Tyr15. Embo J. *12*, 75–85.

McGowan, C.H., and Russell, P. (1995). Cell cycle regulation of human WEE1. Embo J. *14*, 2166–2175.

Méndez, J., Zou-Yang, X.H., Kim, S.-Y., Hidaka, M., Tansey, W.P., and Stillman, B. (2002). Human origin recognition complex large subunit is degraded by ubiquitin-mediated proteolysis after initiation of DNA replication. Mol. Cell *9*, 481–491.

Michael, W.M., and Newport, J. (1998). Coupling of mitosis to the completion of S phase through Cdc34-mediated degradation of Wee1. Science *282*, 1886–1889.

Michael, W.M., Ott, R., Fanning, E., and Newport, J. (2000). Activation of the DNA replication checkpoint through RNA synthesis by primase. Science *289*, 2133–2137.

Miller, M.E., and Cross, F.R. (2001). Cyclin specificity: how many wheels do you need on a unicycle? J. Cell Sci. *114*, 1811–1820.

Minshull, J., Golsteyn, R., Hill, C.S., and Hunt, T. (1990). The A- and B-type cyclin associated cdc2 kinases in Xenopus turn on and off at different times in the cell cycle. Embo J. *9*, 2865–2875.

Mocciaro, A., and Schiebel, E. (2010). Cdc14: a highly conserved family of phosphatases with non-conserved functions? J. Cell Sci. *123*, 2867–2876.

Mocciaro, A., Berdougo, E., Zeng, K., Black, E., Vagnarelli, P., Earnshaw, W., Gillespie, D., Jallepalli, P., and Schiebel, E. (2010). Vertebrate cells genetically deficient for Cdc14A or Cdc14B retain DNA damage checkpoint proficiency but are impaired in DNA repair. J. Cell Biol. *189*, 631–639.

Mochida, S. (2015). PP1 inactivates Greatwall to release PP2A-B55 from mitotic confinement. EMBO Rep. *16*, 1411–1412.

Mochida, S., Ikeo, S., Gannon, J., and Hunt, T. (2009). Regulated activity of PP2A–B55δ is crucial for controlling entry into and exit from mitosis in Xenopus egg extracts. Embo J. *28*, 2777–2785.

Mochida, S., Rata, S., Hino, H., Nagai, T., and Novak, B. (2016). Two Bistable Switches Govern M Phase Entry. Curr. Biol. *26*, 3361–3367.

Montagnoli, A., Fiore, F., Eytan, E., Carrano, A.C., Draetta, G.F., Hershko, A., and Pagano, M. (1999). Ubiquitination of p27 is regulated by Cdk-dependent phosphorylation and trimeric complex formation. Genes Dev. *13*, 1181–1189.

Moore, J.D., Kirk, J.A., and Hunt, T. (2003). Unmasking the S-phase-promoting potential of cyclin B1. Science *300*, 987–990.

Morgan, D.O. (2007). The Cell Cycle (New Science Press).

Morris, V.B., Cowan, R., and Culpin, D. (1979). Variability of cell cycle times measured in vivo in embryonic chick retina by continuous labelling with BUdR. Nature *280*, 68–71.

Moyle, M.W., Kim, T., Hattersley, N., Espeut, J., Cheerambathur, D.K., Oegema, K., and Desai, A. (2014). A Bub1-Mad1 interaction targets the Mad1-Mad2 complex to unattached kinetochores to initiate the spindle checkpoint. J. Cell Biol. *204*, 647–657.

Mueller, P.R., Coleman, T.R., and Dunphy, W.G. (1995a). Cell cycle regulation of a Xenopus Wee1-like kinase. Mol. Biol. Cell *6*, 119–134.

Mueller, P.R., Coleman, T.R., Kumagai, A., and Dunphy, W.G. (1995b). Myt1: a membrane-associated inhibitory kinase that phosphorylates Cdc2 on both threonine-14 and tyrosine-15. Science *270*, 86–90.

Murphy, M., Stinnakre, M.G., Senamaud-Beaufort, C., Winston, N.J., Sweeney, C., Kubelka, M., Carrington, M., Bréchot, C., and Sobczak-Thépot, J. (1997). Delayed early embryonic lethality following disruption of the murine cyclin A2 gene. Nat. Genet. *15*, 83–86.

Murray, A.W., and Kirschner, M.W. (1989). Cyclin synthesis drives the early embryonic cell cycle. Nature *339*, 275–280.

Murray, A.W., Solomon, M.J., and Kirschner, M.W. (1989). The role of cyclin synthesis and degradation in the control of maturation promoting factor activity. Nature *339*, 280–286.

Musacchio, A., and Salmon, E.D. (2007). The spindle-assembly checkpoint in space and time. Nat. Rev. Mol. Cell Biol. *8*, 379–393.

Nagahama, H., Minamishima, Y.A., Matsumoto, M., Nakamichi, I., Kitagawa, K., Shirane, M., Tsunematsu, R., Tsukiyama, T., Ishida, N., Kitagawa, M., et al. (2000). Targeted disruption of Skp2 results in accumulation of cyclin E and p27(Kip1), polyploidy and centrosome overduplication. Embo J. *19*, 2069–2081.

Nagy, A., Rossant, J., Nagy, R., Abramow-Newerly, W., and Roder, J.C. (1993). Derivation of completely cell culture-derived mice from early-passage embryonic stem cells. Proc. Natl. Acad. Sci. USA *90*, 8424–8428.

Nash, P., Tang, X., Orlicky, S., Chen, Q., Gertler, F.B., Mendenhall, M.D., Sicheri, F., Pawson, T., and Tyers, M. (2001). Multisite phosphorylation of a CDK inhibitor sets a threshold for the onset of DNA replication. Nature *414*, 514–521.

Nasmyth, K. (2001). Disseminating the genome: joining, resolving, and separating sister chromatids during mitosis and meiosis. Annu. Rev. Genet. *35*, 673–745.

Nasmyth, K.A., and Reed, S.I. (1980). Isolation of genes by complementation in yeast: molecular cloning of a cell-cycle gene. Proc. Natl. Acad. Sci. USA *77*, 2119–2123.

Neumann, B., Walter, T., Hériché, J.-K., Bulkescher, J., Erfle, H., Conrad, C., Rogers, P., Poser, I., Held, M., Liebel, U., et al. (2010). Phenotypic profiling of the human genome by time-lapse microscopy reveals cell division genes. Nature *464*, 721–727.

Nilsson, J., Yekezare, M., Minshull, J., and Pines, J. (2008). The APC/C maintains the spindle assembly checkpoint by targeting Cdc20 for destruction. Nat. Cell Biol. *10*, 1411–1420.

Nishitani, H., Lygerou, Z., and Nishimoto, T. (2004). Proteolysis of DNA replication licensing factor Cdt1 in S-phase is performed independently of geminin through its N-terminal region. J. Biol. Chem. *279*, 30807–30816.

Noble, M.E., Endicott, J.A., Brown, N.R., and Johnson, L.N. (1997). The cyclin box fold: protein recognition in cell-cycle and transcription control. Trends Biochem. Sci. *22*, 482–487.

Noda, A., Ning, Y., Venable, S.F., Pereira-Smith, O.M., and Smith, J.R. (1994). Cloning of senescent cell-derived inhibitors of DNA synthesis using an expression screen. Exp. Cell Res. *211*, 90–98.

Novak, B., and Tyson, J.J. (1993a). Numerical analysis of a comprehensive model of M-phase control in Xenopus oocyte extracts and intact embryos. J. Cell Sci. *106 (Pt 4)*, 1153–1168.

Novak, B., and Tyson, J.J. (2003). Modelling the controls of the eukaryotic cell cycle. Biochem. Soc. Trans. *31*, 1526–1529.

Novak, B., and Tyson, J.J. (1993b). Modeling the Cell Division Cycle: M-phase Trigger, Oscillations, and Size Control. J. Theor. Biol. *165*, 101–134.

Novak, B., and Tyson, J.J. (2004). A model for restriction point control of the mammalian cell cycle. J. Theor. Biol. *230*, 563–579.

Novak, B., and Tyson, J.J. (2008). Design principles of biochemical oscillators. Nat. Rev. Mol. Cell Biol. *9*, 981–991.

Novak, B., Tyson, J.J., Gyorffy, B., and Csikasz-Nagy, A. (2007). Irreversible cell-cycle transitions are due to systems-level feedback. Nat. Cell Biol. *9*, 724–728.

Nowakowski, R.S., Lewin, S.B., and Miller, M.W. (1989). Bromodeoxyuridine immunohistochemical determination of the lengths of the cell cycle and the DNA-synthetic phase for an anatomically defined population. J. Neurocytol. *18*, 311–318.

Nurse, P. (1975). Genetic control of cell size at cell division in yeast. Nature *256*, 547–551.

Nurse, P. (1990). Universal control mechanism regulating onset of M-phase. Nature *344*, 503–508.

Nurse, P., and Bissett, Y. (1981). Gene required in G1 for commitment to cell cycle and in G2 for control of mitosis in fission yeast. Nature *292*, 558–560.

Nurse, P., Thuriaux, P., and Nasmyth, K. (1976). Genetic control of the cell division cycle in the fission yeast Schizosaccharomyces pombe. Mol. Gen. Genet. *146*, 167–178.

Ohtani, K., Tsujimoto, A., Ikeda, M., and Nakamura, M. (1998). Regulation of cell growth-dependent expression of mammalian CDC6 gene by the cell cycle transcription factor E2F. Oncogene *17*, 1777–1785.

Oikonomou, C., and Cross, F.R. (2011). Rising cyclin-CDK levels order cell cycle events. Plos One *6*, e20788.

Okamoto, K., and Sagata, N. (2007). Mechanism for inactivation of the mitotic inhibitory kinase Wee1 at M phase. Proc. Natl. Acad. Sci. USA *104*, 3753–3758.

Ortega, S., Malumbres, M., and Barbacid, M. (2002). Cyclin D-dependent kinases, INK4 inhibitors and cancer. Biochim. Biophys. Acta *1602*, 73–87.

Pagliuca, F.W., Collins, M.O., Lichawska, A., Zegerman, P., Choudhary, J.S., and Pines, J. (2011). Quantitative proteomics reveals the basis for the biochemical specificity of the cell-cycle machinery. Mol. Cell *43*, 406–417.

Pardee, A.B. (1974). A restriction point for control of normal animal cell proliferation. Proc. Natl. Acad. Sci. USA *71*, 1286–1290.

Parker, L.L., and Piwnica-Worms, H. (1992). Inactivation of the p34cdc2-cyclin B complex by the human WEE1 tyrosine kinase. Science *257*, 1955–1957.

Parry, D.H., and O'Farrell, P.H. (2001). The schedule of destruction of three mitotic cyclins can dictate the timing of events during exit from mitosis. Curr. Biol. *11*, 671–683.

Pavletich, N.P. (1999). Mechanisms of cyclin-dependent kinase regulation: structures of Cdks, their cyclin activators, and Cip and INK4 inhibitors. J. Mol. Biol. *287*, 821–828.

Peters, J.-M. (2006). The anaphase promoting complex/cyclosome: a machine designed to destroy. Nat. Rev. Mol. Cell Biol. *7*, 644–656.

Petersen, B.O., Lukas, J., Sørensen, C.S., Bartek, J., and Helin, K. (1999). Phosphorylation of mammalian CDC6 by cyclin A/CDK2 regulates its subcellular localization. Embo J. *18*, 396–410.

Piggott, J.R., Rai, R., and Carter, B.L. (1982). A bifunctional gene product involved in two phases of the yeast cell cycle. Nature *298*, 391–393.

Pines, J., and Hunter, T. (1991). Human cyclins A and B1 are differentially located in the cell and undergo cell cycle-dependent nuclear transport. J. Cell Biol. *115*, 1–17.

Pines, J., and Hunter, T. (1992). Cyclins A and B1 in the human cell cycle. Ciba Found. Symp. *170*, 187–96–discussion196–204.

Pines, J. (2011). Cubism and the cell cycle: the many faces of the APC/C. Nat. Rev. Mol. Cell Biol. *12*, 427–438.

Polyak, K., Kato, J.Y., Solomon, M.J., Sherr, C.J., Massague, J., Roberts, J.M., and Koff, A. (1994a). p27Kip1, a cyclin-Cdk inhibitor, links transforming growth factor-beta and contact inhibition to cell cycle arrest. Genes Dev. *8*, 9–22.

Polyak, K., Lee, M.H., Erdjument-Bromage, H., Koff, A., Roberts, J.M., Tempst, P., and Massague, J. (1994b). Cloning of p27Kip1, a cyclin-dependent kinase inhibitor and a potential mediator of extracellular antimitogenic signals. Cell *78*, 59–66.

Pomerening, J.R. (2009). Positive-feedback loops in cell cycle progression. FEBS Letters *583*, 3388–3396.

Pomerening, J.R. (2008). Uncovering mechanisms of bistability in biological systems. Current Opinion in Biotechnology *19*, 381–388.

Pomerening, J.R., Kim, S.Y., and Ferrell, J.E. (2005). Systems-level dissection of the cell-cycle oscillator: bypassing positive feedback produces damped oscillations. Cell *122*, 565–578.

Pomerening, J.R., Sontag, E.D., and Ferrell, J.E. (2003). Building a cell cycle oscillator: hysteresis and bistability in the activation of Cdc2. Nat. Cell Biol. *5*, 346–351.

Potapova, T.A., Sivakumar, S., Flynn, J.N., Li, R., and Gorbsky, G.J. (2011). Mitotic progression becomes irreversible in prometaphase and collapses when Wee1 and Cdc25 are inhibited. Mol. Biol. Cell *22*, 1191–1206.

Prescott, D.M. (1976). Reproduction of eukaryotic cells.

Primorac, I., and Musacchio, A. (2013). Panta rhei: the APC/C at steady state. J. Cell Biol. *201*, 177–189.

Qu, Y., Han, B., Yu, Y., Yao, W., Bose, S., Karlan, B.Y., Giuliano, A.E., and Cui, X. (2015). Evaluation of MCF10A as a Reliable Model for Normal Human Mammary Epithelial Cells. Plos One *10*, e0131285.

Queralt, E., and Uhlmann, F. (2008). Cdk-counteracting phosphatases unlock mitotic exit. Curr. Opin. Cell Biol. *20*, 661–668.

Rape, M., and Kirschner, M.W. (2004). Autonomous regulation of the anaphase-promoting complex couples mitosis to S-phase entry. Nature *432*, 588–595.

Rape, M., Reddy, S.K., and Kirschner, M.W. (2006). The processivity of multiubiquitination by the APC determines the order of substrate degradation. Cell *124*, 89–103.

Ray, D., Terao, Y., Fuhrken, P.G., Ma, Z.-Q., DeMayo, F.J., Christov, K., Heerema, N.A.,

Franks, R., Tsai, S.Y., Papoutsakis, E.T., et al. (2007). Deregulated CDC25A expression promotes mammary tumorigenesis with genomic instability. Cancer Res. *67*, 984–991.

Reddy, S.K., Rape, M., Margansky, W.A., and Kirschner, M.W. (2007). Ubiquitination by the anaphase-promoting complex drives spindle checkpoint inactivation. Nature *446*, 921–925.

Reimann, J.D., Gardner, B.E., Margottin-Goguet, F., and Jackson, P.K. (2001). Emi1 regulates the anaphase-promoting complex by a different mechanism than Mad2 proteins. Genes Dev. *15*, 3278–3285.

Reinhardt, H.C., Jiang, H., Hemann, M.T., and Yaffe, M.B. (2009). Exploiting synthetic lethal interactions for targeted cancer therapy. Cell Cycle *8*, 3112–3119.

Ridenour, D.A., McKinney, M.C., Bailey, C.M., and Kulesa, P.M. (2012). CycleTrak: a novel system for the semi-automated analysis of cell cycle dynamics. Dev. Biol. *365*, 189–195.

Rieder, C.L., and Cole, R.W. (1998). Entry into mitosis in vertebrate somatic cells is guarded by a chromosome damage checkpoint that reverses the cell cycle when triggered during early but not late prophase. J. Cell Biol. *142*, 1013–1022.

Rieder, C.L., Cole, R.W., Khodjakov, A., and Sluder, G. (1995). The checkpoint delaying anaphase in response to chromosome monoorientation is mediated by an inhibitory signal produced by unattached kinetochores. J. Cell Biol. *130*, 941–948.

Rogers, S., Fey, D., McCloy, R.A., Parker, B.L., Mitchell, N.J., Payne, R.J., Daly, R.J., James, D.E., Caldon, C.E., Watkins, D.N., et al. (2016). PP1 initiates the dephosphorylation of MASTL, triggering mitotic exit and bistability in human cells. J. Cell Sci. *129*, 1340–1354.

Russell, P., and Nurse, P. (1986). cdc25+ functions as an inducer in the mitotic control of fission yeast. Cell *45*, 145–153.

Russell, P., and Nurse, P. (1987). Negative regulation of mitosis by wee1+, a gene encoding a protein kinase homolog. Cell *49*, 559–567.

Saha, P., Chen, J., Thome, K.C., Lawlis, S.J., Hou, Z.H., Hendricks, M., Parvin, J.D., and Dutta, A. (1998). Human CDC6/Cdc18 associates with Orc1 and cyclin-cdk and is selectively eliminated from the nucleus at the onset of S phase. Mol. Cell Biol. *18*, 2758–2767.

Sakaue-Sawano, A., and Miyawaki, A. (2014). Visualizing spatiotemporal dynamics of multicellular cell-cycle progressions with fucci technology. Cold Spring Harb. Protoc. *2014*, pii:pdb.prot080408.

Sakaue-Sawano, A., Kurokawa, H., Morimura, T., Hanyu, A., Hama, H., Osawa, H., Kashiwagi, S., Fukami, K., Miyata, T., Miyoshi, H., et al. (2008a). Visualizing spatiotemporal dynamics of multicellular cell-cycle progression. Cell *132*, 487–498.

Sakaue-Sawano, A., Ohtawa, K., Hama, H., Kawano, M., Ogawa, M., and Miyawaki, A. (2008b). Tracing the silhouette of individual cells in S/G2/M phases with fluorescence. Chem. Biol. *15*, 1243–1248.

Sakaue-Sawano, A., Yo, M., Komatsu, N., Hiratsuka, T., Kogure, T., Hoshida, T., Goshima, N., Matsuda, M., Miyoshi, H., and Miyawaki, A. (2017). Genetically Encoded Tools for Optical Dissection of the Mammalian Cell Cycle. Mol. Cell *68*, 626–640.e5.

Sanchez, I., and Dylancht, B. (2005). New insights into cyclins, CDKs, and cell cycle control. Semin. Cell Dev. Biol. *16*, 311–321.

Sandler, O., Mizrahi, S.P., Weiss, N., Agam, O., Simon, I., and Balaban, N.Q. (2015). Lineage correlations of single cell division time as a probe of cell-cycle dynamics. Nature *519*, 468–

471.

Santaguida, S., and Musacchio, A. (2009). The life and miracles of kinetochores. Embo J. *28*, 2511–2531.

Santaguida, S., Tighe, A., D'Alise, A.M., Taylor, S.S., and Musacchio, A. (2010). Dissecting the role of MPS1 in chromosome biorientation and the spindle checkpoint through the small molecule inhibitor reversine. J. Cell Biol. *190*, 73–87.

Santaguida, S., Vernieri, C., Villa, F., Ciliberto, A., and Musacchio, A. (2011). Evidence that Aurora B is implicated in spindle checkpoint signalling independently of error correction. Embo J. *30*, 1508–1519.

Santamaría, D., Barrière, C., Cerqueira, A., Hunt, S., Tardy, C., Newton, K., Cáceres, J.F., Dubus, P., Malumbres, M., and Barbacid, M. (2007). Cdk1 is sufficient to drive the mammalian cell cycle. Nature *448*, 811–815.

Santos, S.D.M., Wollman, R., Meyer, T., and Ferrell, J.E., Jr. (2012). Spatial Positive Feedback at the Onset of Mitosis. Cell *149*, 1500–1513.

Sasaki, K., Shima, H., Kitagawa, Y., Irino, S., Sugimura, T., and Nagao, M. (1990). Identification of members of the protein phosphatase 1 gene family in the rat and enhanced expression of protein phosphatase 1 alpha gene in rat hepatocellular carcinomas. Jpn. J. Cancer Res. *81*, 1272–1280.

Satyanarayana, A., and Kaldis, P. (2009). Mammalian cell-cycle regulation: several Cdks, numerous cyclins and diverse compensatory mechanisms. Oncogene *28*, 2925–2939.

Savatier, P., Huang, S., Szekely, L., Wiman, K.G., and Samarut, J. (1994). Contrasting patterns of retinoblastoma protein expression in mouse embryonic stem cells and embryonic fibroblasts. Oncogene *9*, 809–818.

Schmoller, K.M., Turner, J.J., Kõivomägi, M., and Skotheim, J.M. (2015). Dilution of the cell cycle inhibitor Whi5 controls budding-yeast cell size. Nature *526*, 268–272.

Schwob, E., Böhm, T., Mendenhall, M.D., and Nasmyth, K. (1994). The B-type cyclin kinase inhibitor p40SIC1 controls the G1 to S transition in S. cerevisiae. Cell *79*, 233–244.

Sczaniecka, M., Feoktistova, A., May, K.M., Chen, J.-S., Blyth, J., Gould, K.L., and Hardwick, K.G. (2008). The spindle checkpoint functions of Mad3 and Mad2 depend on a Mad3 KEN box-mediated interaction with Cdc20-anaphase-promoting complex (APC/C). J. Biol. Chem. *283*, 23039–23047.

Serrano, M., Hannon, G.J., and Beach, D. (1993). A new regulatory motif in cell-cycle control causing specific inhibition of cyclin D/CDK4. Nature *366*, 704–707.

Sha, W., Moore, J., Chen, K., Lassaletta, A.D., Yi, C.-S., Tyson, J.J., and Sible, J.C. (2003). Hysteresis drives cell-cycle transitions in Xenopus laevis egg extracts. Proc. Natl. Acad. Sci. USA *100*, 975–980.

Sheaff, R.J., Groudine, M., Gordon, M., Roberts, J.M., and Clurman, B.E. (1997). Cyclin E-CDK2 is a regulator of p27Kip1. Genes Dev. *11*, 1464–1478.

Sherr, C.J., and Roberts, J.M. (1999). CDK inhibitors: positive and negative regulators of G1-phase progression. Genes Dev. *13*, 1501–1512.

Sherr, C.J., and McCormick, F. (2002). The RB and p53 pathways in cancer. Cancer Cell *2*, 103–112.

Shields, R. (1977). Transition probability and the origin of variation in the cell cycle. Nature *267*, 704–707.

Shou, W., Seol, J.H., Baskerville, C., Moazed, D., Chen, Z.W., Jang, J., Shevchenko, A., Charbonneau, H., and Deshaies, R.J. (1999). Exit from mitosis is triggered by Tem1-dependent release of the protein phosphatase Cdc14 from nucleolar RENT complex. Cell *97*, 233–244.

Shou, W., Azzam, R., Chen, S.L., Huddleston, M.J., Baskerville, C., Charbonneau, H., Annan, R.S., Carr, S.A., and Deshaies, R.J. (2002). Cdc5 influences phosphorylation of Net1 and disassembly of the RENT complex. BMC Mol. Biol. *3*, 3.

Sigl, R., Wandke, C., Rauch, V., Kirk, J., Hunt, T., and Geley, S. (2009). Loss of the mammalian APC/C activator FZR1 shortens G1 and lengthens S phase but has little effect on exit from mitosis. J. Cell Sci. *122*, 4208–4217.

Skotheim, J.M., Di Talia, S., Siggia, E.D., and Cross, F.R. (2008). Positive feedback of G1 cyclins ensures coherent cell cycle entry. Nature *454*, 291–296.

Skoufias, D.A., Indorato, R.-L., Lacroix, F., Panopoulos, A., and Margolis, R.L. (2007). Mitosis persists in the absence of Cdk1 activity when proteolysis or protein phosphatase activity is suppressed. J. Cell Biol. *179*, 671–685.

Smith, P.J., Blunt, N., Wiltshire, M., Hoy, T., Teesdale-Spittle, P., Craven, M.R., Watson, J.V., Amos, W.B., Errington, R.J., and Patterson, L.H. (2000). Characteristics of a novel deep red/infrared fluorescent cell-permeant DNA probe, DRAQ5, in intact human cells analyzed by flow cytometry, confocal and multiphoton microscopy. Cytometry *40*, 280–291.

Smolen, P., Baxter, D.A., and Byrne, J.H. (2000). Mathematical modeling of gene networks. Neuron *26*, 567–580.

Solomon, M.J., Glotzer, M., Lee, T.H., Philippe, M., and Kirschner, M.W. (1990). Cyclin activation of p34cdc2. Cell *63*, 1013–1024.

Soule, H.D., Maloney, T.M., Wolman, S.R., Peterson, W.D., Brenz, R., McGrath, C.M., Russo, J., Pauley, R.J., Jones, R.F., and Brooks, S.C. (1990). Isolation and characterization of a spontaneously immortalized human breast epithelial cell line, MCF-10. Cancer Res. *50*, 6075–6086.

Soule, H.D., Vazguez, J., Long, A., Albert, S., and Brennan, M. (1973). A human cell line from a pleural effusion derived from a breast carcinoma. J. Natl. Cancer Inst. *51*, 1409–1416.

Spencer, F., and Hieter, P. (1992). Centromere DNA mutations induce a mitotic delay in Saccharomyces cerevisiae. Proc. Natl. Acad. Sci. USA *89*, 8908–8912.

Spencer, S.L., Cappell, S.D., Tsai, F.-C., Overton, K.W., Wang, C.L., and Meyer, T. (2013). The proliferation-quiescence decision is controlled by a bifurcation in CDK2 activity at mitotic exit. Cell *155*, 369–383.

Sporbert, A., Domaing, P., Leonhardt, H., and Cardoso, M.C. (2005). PCNA acts as a stationary loading platform for transiently interacting Okazaki fragment maturation proteins. Nucleic Acids Res. *33*, 3521–3528.

Stead, E., White, J., Faast, R., Conn, S., Goldstone, S., Rathjen, J., Dhingra, U., Rathjen, P., Walker, D., and Dalton, S. (2002). Pluripotent cell division cycles are driven by ectopic Cdk2, cyclin A/E and E2F activities. Oncogene *21*, 8320–8333.

Stegmüller, J., Konishi, Y., Huynh, M.A., Yuan, Z., Dibacco, S., and Bonni, A. (2006). Cell-intrinsic regulation of axonal morphogenesis by the Cdh1-APC target SnoN. Neuron *50*, 389–400.

Stern, B., and Nurse, P. (1996). A quantitative model for the cdc2 control of S phase and mitosis in fission yeast. Trends Genet. *12*, 345–350.

Stewart, S., and Fang, G. (2005). Destruction box-dependent degradation of aurora B is mediated by the anaphase-promoting complex/cyclosome and Cdh1. Cancer Res. *65*, 8730–8735.

Strausfeld, U., Labbe, J.C., Fesquet, D., Cavadore, J.C., Picard, A., Sadhu, K., Russell, P., and Doree, M. (1991). Dephosphorylation and activation of a p34cdc2/cyclin B complex in vitro by human CDC25 protein. Nature *351*, 242–245.

Strauss, B., Harrison, A., Coelho, P.A., Yata, K., Zernicka-Goetz, M., and Pines, J. (2018). Cyclin B1 is essential for mitosis in mouse embryos, and its nuclear export sets the time for mitosis. J. Cell Biol. *217*, 179–193.

Sugimoto, N., Tatsumi, Y., Tsurumi, T., Matsukage, A., Kiyono, T., Nishitani, H., and Fujita, M. (2004). Cdt1 phosphorylation by cyclin A-dependent kinases negatively regulates its function without affecting geminin binding. J. Biol. Chem. *279*, 19691–19697.

Sugiyama, M., Sakaue-Sawano, A., Iimura, T., Fukami, K., Kitaguchi, T., Kawakami, K., Okamoto, H., Higashijima, S.-I., and Miyawaki, A. (2009). Illuminating cell-cycle progression in the developing zebrafish embryo. Proc. Natl. Acad. Sci. USA *106*, 20812–20817.

Sullivan, M., and Morgan, D.O. (2007). Finishing mitosis, one step at a time. Nat. Rev. Mol. Cell Biol. *8*, 894–903.

Sun, T., Yang, X., Wang, W., Zhang, X., Xu, Q., Zhu, S., Kuchta, R., Chen, G., and Liu, X. (2010). Cellular abundance of Mps1 and the role of its carboxyl terminal tail in substrate recruitment. J. Biol. Chem. *285*, 38730–38739.

Surana, U., Robitsch, H., Price, C., Schuster, T., Fitch, I., Futcher, A.B., and Nasmyth, K. (1991). The role of CDC28 and cyclins during mitosis in the budding yeast S. cerevisiae. Cell *65*, 145–161.

Sutterlüty, H., Chatelain, E., Marti, A., Wirbelauer, C., Senften, M., Müller, U., and Krek, W. (1999). p45SKP2 promotes p27Kip1 degradation and induces S phase in quiescent cells. Nat. Cell Biol. *1*, 207–214.

Swaffer, M.P., Jones, A.W., Flynn, H.R., Snijders, A.P., and Nurse, P. (2016). CDK Substrate Phosphorylation and Ordering the Cell Cycle. Cell *167*, 1750–1761.e16.

Sweeney, E.E., McDaniel, R.E., Maximov, P.Y., Fan, P., and Jordan, V.C. (2012). Models and Mechanisms of Acquired Antihormone Resistance in Breast Cancer: Significant Clinical Progress Despite Limitations. Horm. Mol. Biol. Clin. Investig. *9*, 143–163.

Sørensen, C.S., Lukas, C., Kramer, E.R., Peters, J.M., Bartek, J., and Lukas, J. (2001). A conserved cyclin-binding domain determines functional interplay between anaphase-promoting complex-Cdh1 and cyclin A-Cdk2 during cell cycle progression. Mol. Cell Biol. *21*, 3692–3703.

Tada, S., Li, A., Maiorano, D., Méchali, M., and Blow, J.J. (2001). Repression of origin assembly in metaphase depends on inhibition of RLF-B/Cdt1 by geminin. Nat. Cell Biol. *3*, 107–113.

Takai, A., Sasaki, K., Nagai, H., Mieskes, G., Isobe, M., Isono, K., and Yasumoto, T. (1995). Inhibition of specific binding of okadaic acid to protein phosphatase 2A by microcystin-LR, calyculin-A and tautomycin: method of analysis of interactions of tight-binding ligands with target protein. Biochem. J. *306 (Pt 3)*, 657–665.

Takeda, D.Y., Parvin, J.D., and Dutta, A. (2005). Degradation of Cdt1 during S phase is Skp2-

independent and is required for efficient progression of mammalian cells through S phase. J. Biol. Chem. *280*, 23416–23423.

Tamm, C., Pijuan Galitó, S., and Annerén, C. (2013). A comparative study of protocols for mouse embryonic stem cell culturing. Plos One *8*, e81156.

Tanaka, K. (2001). Mitosis (Chichester, UK: John Wiley & Sons, Ltd).

Tang, Z., Coleman, T.R., and Dunphy, W.G. (1993). Two distinct mechanisms for negative regulation of the Wee1 protein kinase. Embo J. *12*, 3427–3436.

Thomson, J.A., Itskovitz-Eldor, J., Shapiro, S.S., Waknitz, M.A., Swiergiel, J.J., Marshall, V.S., and Jones, J.M. (1998). Embryonic stem cell lines derived from human blastocysts. Science *282*, 1145–1147.

Tominaga, Y., Li, C., Wang, R.-H., and Deng, C.-X. (2006). Murine Wee1 plays a critical role in cell cycle regulation and pre-implantation stages of embryonic development. Int. J. Biol. Sci. *2*, 161–170.

Toyoshima, H., and Hunter, T. (1994). p27, a novel inhibitor of G1 cyclin-Cdk protein kinase activity, is related to p21. Cell *78*, 67–74.

Traverso, E.E., Baskerville, C., Liu, Y., Shou, W., James, P., Deshaies, R.J., and Charbonneau, H. (2001). Characterization of the Net1 cell cycle-dependent regulator of the Cdc14 phosphatase from budding yeast. J. Biol. Chem. *276*, 21924–21931.

Treutlein, B., Brownfield, D.G., Wu, A.R., Neff, N.F., Mantalas, G.L., Espinoza, F.H., Desai, T.J., Krasnow, M.A., and Quake, S.R. (2014). Reconstructing lineage hierarchies of the distal lung epithelium using single-cell RNA-seq. Nature *509*, 371–375.

Trinkle-Mulcahy, L., Sleeman, J.E., and Lamond, A.I. (2001). Dynamic targeting of protein phosphatase 1 within the nuclei of living mammalian cells. J. Cell Sci. *114*, 4219–4228.

Truman, A.W., Kitazono, A.A., Fitz Gerald, J.N., and Kron, S.J. (2001). Cell Cycle: Regulation by Cyclins (Chichester, UK: John Wiley & Sons, Ltd).

Trunnell, N.B., Poon, A.C., Kim, S.Y., and Ferrell, J.E. (2011). Ultrasensitivity in the Regulation of Cdc25C by Cdk1. Mol. Cell *41*, 263–274.

Tsai, T.Y.-C., Theriot, J.A., and Ferrell, J.E. (2014). Changes in oscillatory dynamics in the cell cycle of early Xenopus laevis embryos. PLoS Biol. *12*, e1001788.

Tsai, T.Y.-C., Choi, Y.S., Ma, W., Pomerening, J.R., Tang, C., and Ferrell, J.E. (2008). Robust, tunable biological oscillations from interlinked positive and negative feedback loops. Science *321*, 126–129.

Tsuchida, E., Kaida, A., Pratama, E., Ikeda, M.-A., Suzuki, K., Harada, K., and Miura, M. (2015). Effect of X-Irradiation at Different Stages in the Cell Cycle on Individual Cell-Based Kinetics in an Asynchronous Cell Population. Plos One *10*, e0128090.

Tsvetkov, L.M., Yeh, K.H., Lee, S.J., Sun, H., and Zhang, H. (1999). p27(Kip1) ubiquitination and degradation is regulated by the SCF(Skp2) complex through phosphorylated Thr187 in p27. Curr. Biol. *9*, 661–664.

Tuck, C., Zhang, T., Potapova, T., Malumbres, M., and Novak, B. (2013). Robust mitotic entry is ensured by a latching switch. Biol. Open *2*, 924–931.

Turner, D.A., Hayward, P.C., Baillie-Johnson, P., Rué, P., Broome, R., Faunes, F., and Martinez Arias, A. (2014). Wnt/β-catenin and FGF signalling direct the specification and

maintenance of a neuromesodermal axial progenitor in ensembles of mouse embryonic stem cells. Development *141*, 4243–4253.

Turner, M.L., Hawkins, E.D., and Hodgkin, P.D. (2008). Quantitative regulation of B cell division destiny by signal strength. J. Immunol. *181*, 374–382.

Tyson, J., and Othmer, H. (1978). The Dynamics of Feedback Control Circuits in Biochemical Pathways. Prog. Theor. Biol. *5*, 1–62.

Tyson, J.J., and Novak, B. (2001). Regulation of the eukaryotic cell cycle: molecular antagonism, hysteresis, and irreversible transitions. J. Theor. Biol. *210*, 249–263.

Uhlmann, F., Bouchoux, C., and López-Avilés, S. (2011). A quantitative model for cyclin-dependent kinase control of the cell cycle: revisited. Philos. Trans. R. Soc. Lond., B, Biol. Sci. *366*, 3572–3583.

Uto, K., Inoue, D., Shimuta, K., Nakajo, N., and Sagata, N. (2004). Chk1, but not Chk2, inhibits Cdc25 phosphatases by a novel common mechanism. Embo J. *23*, 3386–3396.

van den Brink, S.C., Baillie-Johnson, P., Balayo, T., Hadjantonakis, A.-K., Nowotschin, S., Turner, D.A., and Martinez Arias, A. (2014). Symmetry breaking, germ layer specification and axial organisation in aggregates of mouse embryonic stem cells. Development *141*, 4231–4242.

Varmuza, S., Jurisicova, A., Okano, K., Hudson, J., Boekelheide, K., and Shipp, E.B. (1999). Spermiogenesis Is Impaired in Mice Bearing a Targeted Mutation in the Protein Phosphatase 1cγ Gene. Dev. Biol. *205*, 98–110.

Vázquez-Novelle, M.D., Esteban, V., Bueno, A., and Sacristán, M.P. (2005). Functional homology among human and fission yeast Cdc14 phosphatases. J. Biol. Chem. *280*, 29144–29150.

Verma, R., Annan, R.S., Huddleston, M.J., Carr, S.A., Reynard, G., and Deshaies, R.J. (1997). Phosphorylation of Sic1p by G1 Cdk required for its degradation and entry into S phase. Science *278*, 455–460.

Vigneron, S., Brioudes, E., Burgess, A., Labbé, J.C., Lorca, T., and Castro, A. (2009). Greatwall maintains mitosis through regulation of PP2A. Embo J. *28*, 2786–2793.

Visintin, R., Craig, K., Hwang, E.S., Prinz, S., Tyers, M., and Amon, A. (1998). The phosphatase Cdc14 triggers mitotic exit by reversal of Cdk-dependent phosphorylation. Mol. Cell *2*, 709–718.

Visintin, R., Hwang, E.S., and Amon, A. (1999). Cfi1 prevents premature exit from mitosis by anchoring Cdc14 phosphatase in the nucleolus. Nature *398*, 818–823.

Vlach, J., Hennecke, S., and Amati, B. (1997). Phosphorylation-dependent degradation of the cyclin-dependent kinase inhibitor p27. Embo J. *16*, 5334–5344.

Vodermaier, H.C. (2004). APC/C and SCF: controlling each other and the cell cycle. Curr. Biol. *14*, R787–R796.

Wang, Y., and Burke, D.J. (1995). Checkpoint genes required to delay cell division in response to nocodazole respond to impaired kinetochore function in the yeast Saccharomyces cerevisiae. Mol. Cell Biol. *15*, 6838–6844.

Wasserman, W.J., and Masui, Y. (1976). A cytoplasmic factor promoting oocyte maturation: its extraction and preliminary characterization. Science *191*, 1266–1268.

Wasserman, W.J., and Smith, L.D. (1978). The cyclic behavior of a cytoplasmic factor controlling nuclear membrane breakdown. J. Cell Biol. *78*, R15–R22.

Watanabe, N., Broome, M., and Hunter, T. (1995). Regulation of the human WEE1Hu CDK tyrosine 15-kinase during the cell cycle. Embo J. *14*, 1878–1891.

Wäsch, R., Robbins, J.A., and Cross, F.R. (2010). The emerging role of APC/CCdh1 in controlling differentiation, genomic stability and tumor suppression. Oncogene *29*, 1–10.

Wäsch, R., and Cross, F.R. (2002). APC-dependent proteolysis of the mitotic cyclin Clb2 is essential for mitotic exit. Nature *418*, 556–562.

Weinert, T.A., and Hartwell, L.H. (1988). The RAD9 gene controls the cell cycle response to DNA damage in Saccharomyces cerevisiae. Science *241*, 317–322.

Welburn, J.P.I., Tucker, J.A., Johnson, T., Lindert, L., Morgan, M., Willis, A., Noble, M.E.M., and Endicott, J.A. (2007). How tyrosine 15 phosphorylation inhibits the activity of cyclin-dependent kinase 2-cyclin A. J. Biol. Chem. *282*, 3173–3181.

Wells, W.A. (1996). The spindle-assembly checkpoint: aiming for a perfect mitosis, every time. Trends Cell Biol. *6*, 228–234.

White, J., and Dalton, S. (2005). Cell cycle control of embryonic stem cells. Stem Cell Rev *1*, 131–138.

White, J., Stead, E., Faast, R., Conn, S., Cartwright, P., and Dalton, S. (2005). Developmental activation of the Rb-E2F pathway and establishment of cell cycle-regulated cyclin-dependent kinase activity during embryonic stem cell differentiation. Mol. Biol. Cell *16*, 2018–2027.

Wijnen, H., Landman, A., and Futcher, B. (2002). The G(1) cyclin Cln3 promotes cell cycle entry via the transcription factor Swi6. Mol. Cell Biol. *22*, 4402–4418.

Winkler, C., De Munter, S., Van Dessel, N., Lesage, B., Heroes, E., Boens, S., Beullens, M., Van Eynde, A., and Bollen, M. (2015). The selective inhibition of protein phosphatase-1 results in mitotic catastrophe and impaired tumor growth. J. Cell Sci. *128*, 4526–4537.

Wirt, S.E., and Sage, J. (2010). p107 in the public eye: an Rb understudy and more. Cell Div. *5*, 9.

Wohlschlegel, J.A., Dwyer, B.T., Dhar, S.K., Cvetic, C., Walter, J.C., and Dutta, A. (2000). Inhibition of eukaryotic DNA replication by geminin binding to Cdt1. Science *290*, 2309–2312.

Wolf, F., Wandke, C., Isenberg, N., and Geley, S. (2006). Dose-dependent effects of stable cyclin B1 on progression through mitosis in human cells. Embo J. *25*, 2802–2813.

Won, K.A., and Reed, S.I. (1996). Activation of cyclin E/CDK2 is coupled to site-specific autophosphorylation and ubiquitin-dependent degradation of cyclin E. Embo J. *15*, 4182–4193.

Wong, C.C., Loewke, K.E., Bossert, N.L., Behr, B., De Jonge, C.J., Baer, T.M., and Reijo Pera, R.A. (2010). Non-invasive imaging of human embryos before embryonic genome activation predicts development to the blastocyst stage. Nat. Biotechnol. *28*, 1115–1121.

Woo, R.A., and Poon, R.Y.C. (2003). Cyclin-dependent kinases and S phase control in mammalian cells. Cell Cycle *2*, 316–324.

Wu, J.Q., Guo, J.Y., Tang, W., Yang, C.-S., Freel, C.D., Chen, C., Nairn, A.C., and Kornbluth, S. (2009). PP1-mediated dephosphorylation of phosphoproteins at mitotic exit is controlled

by inhibitor-1 and PP1 phosphorylation. Nat. Cell Biol. *11*, 644–651.

Wurzenberger, C., and Gerlich, D.W. (2011). Phosphatases: providing safe passage through mitotic exit. Nat. Rev. Mol. Cell Biol. *12*, 469–482.

Xiong, W., and Ferrell, J.E. (2003). A positive-feedback-based bistable "memory module" that governs a cell fate decision. Nature *426*, 460–465.

Xiong, Y., Hannon, G.J., Zhang, H., Casso, D., Kobayashi, R., and Beach, D. (1993). p21 is a universal inhibitor of cyclin kinases. Nature *366*, 701–704.

Xu, M., Sheppard, K.A., Peng, C.Y., Yee, A.S., and Piwnica-Worms, H. (1994). Cyclin A/CDK2 binds directly to E2F-1 and inhibits the DNA-binding activity of E2F-1/DP-1 by phosphorylation. Mol. Cell Biol. *14*, 8420–8431.

Yamano, H., Gannon, J., and Hunt, T. (1996). The role of proteolysis in cell cycle progression in Schizosaccharomyces pombe. Embo J. *15*, 5268–5279.

Yan, Z., DeGregori, J., Shohet, R., Leone, G., Stillman, B., Nevins, J.R., and Williams, R.S. (1998). Cdc6 is regulated by E2F and is essential for DNA replication in mammalian cells. Proc. Natl. Acad. Sci. USA *95*, 3603–3608.

Yang, Q., and Ferrell, J.E. (2013). The Cdk1-APC/C cell cycle oscillator circuit functions as a time-delayed, ultrasensitive switch. Nat. Cell Biol. *15*, 519–525.

Yang, V.S., Carter, S.A., Hyland, S.J., Tachibana-Konwalski, K., Laskey, R.A., and Gonzalez, M.A. (2011). Geminin escapes degradation in G1 of mouse pluripotent cells and mediates the expression of Oct4, Sox2, and Nanog. Curr. Biol. *21*, 692–699.

Yang, X., Feng, M., Jiang, X., Wu, Z., Li, Z., Aau, M., and Yu, Q. (2009a). miR-449a and miR-449b are direct transcriptional targets of E2F1 and negatively regulate pRb-E2F1 activity through a feedback loop by targeting CDK6 and CDC25A. Genes Dev. *23*, 2388–2393.

Yang, Y., Kim, A.H., Yamada, T., Wu, B., Bilimoria, P.M., Ikeuchi, Y., la Iglesia, de, N., Shen, J., and Bonni, A. (2009b). A Cdc20-APC ubiquitin signaling pathway regulates presynaptic differentiation. Science *326*, 575–578.

Yao, G., Lee, T.J., Mori, S., Nevins, J.R., and You, L. (2008). A bistable Rb-E2F switch underlies the restriction point. Nat. Cell Biol. *10*, 476–482.

Yoshida, K., and Inoue, I. (2004). Regulation of Geminin and Cdt1 expression by E2F transcription factors. Oncogene *23*, 3802–3812.

Yoshida, S., and Toh-e, A. (2002). Budding yeast Cdc5 phosphorylates Net1 and assists Cdc14 release from the nucleolus. Biochem. Biophys. Res. Commun. *294*, 687–691.

Yu, J., Zhao, Y., Li, Z., Galas, S., and Goldberg, M.L. (2006). Greatwall kinase participates in the Cdc2 autoregulatory loop in Xenopus egg extracts. Mol. Cell *22*, 83–91.

Yuan, X., Srividhya, J., De Luca, T., Lee, J.-H.E., and Pomerening, J.R. (2014). Uncovering the role of APC-Cdh1 in generating the dynamics of S-phase onset. Mol. Biol. Cell *25*, 441–456.

Zachariae, W., Schwab, M., Nasmyth, K., and Seufert, W. (1998). Control of cyclin ubiquitination by CDK-regulated binding of Hct1 to the anaphase promoting complex. Science *282*, 1721–1724.

Zarkowska, T., and Mittnacht, S. (1997). Differential phosphorylation of the retinoblastoma protein by G1/S cyclin-dependent kinases. J. Biol. Chem. *272*, 12738–12746.

Zetterberg, A., and Larsson, O. (1985). Kinetic analysis of regulatory events in G1 leading to proliferation or quiescence of Swiss 3T3 cells. Proc. Natl. Acad. Sci. USA *82*, 5365–5369.

Zhang, C., Baffi, J., Cousins, S.W., and Csaky, K.G. (2003). Oxidant-induced cell death in retinal pigment epithelium cells mediated through the release of apoptosis-inducing factor. J. Cell Sci. *116*, 1915–1923.

Zhang, Y., Wang, Z., and Magnuson, N.S. (2007). Pim-1 kinase-dependent phosphorylation of p21Cip1/WAF1 regulates its stability and cellular localization in H1299 cells. Mol. Cancer Res. *5*, 909–922.

Zhao, Y., Haccard, O., Wang, R., Yu, J., Kuang, J., Jessus, C., and Goldberg, M.L. (2008). Roles of Greatwall kinase in the regulation of cdc25 phosphatase. Mol. Biol. Cell *19*, 1317–1327.

Zhou, Y., Ching, Y.-P., Ng, R.W.M., and Jin, D.-Y. (2003). Differential expression, localization and activity of two alternatively spliced isoforms of human APC regulator CDH1. Biochem. J. *374*, 349–358.

Zielke, N., Korzelius, J., van Straaten, M., Bender, K., Schuhknecht, G.F.P., Dutta, D., Xiang, J., and Edgar, B.A. (2014). Fly-FUCCI: A versatile tool for studying cell proliferation in complex tissues. Cell Rep. *7*, 588–598.

10. Appendices

Appendix A

Publications:

Positive Feedback Keeps Duration of Mitosis Temporally Insulated from Upstream Cell-Cycle Events

Ana Rita Araujo,[1,2] Lendert Gelens,[3] Rahuman S.M. Sheriff,[1,2,4] and Silvia D.M. Santos[1,2,5,*]

[1] Quantitative Cell Biology Lab, MRC-Clinical Sciences Centre (CSC), London W12 0NN, UK

[2] Institute of Clinical Sciences (ICS), Faculty of Medicine, Imperial College London, London SW7 2AZ, UK

[3] Laboratory of Dynamics in Biological Systems, Department of Cellular and Molecular Medicine, University of Leuven, 3000 Leuven, Belgium

[4] European Bioinformatics Institute, EMBL-EBI, Hinxton, Cambridge CB10 1SD, UK

[5] Lead Contact *Correspondence: silvia.santos@imperial.ac.uk

http://dx.doi.org/10.1016/j.molcel.2016.09.018

Published in:

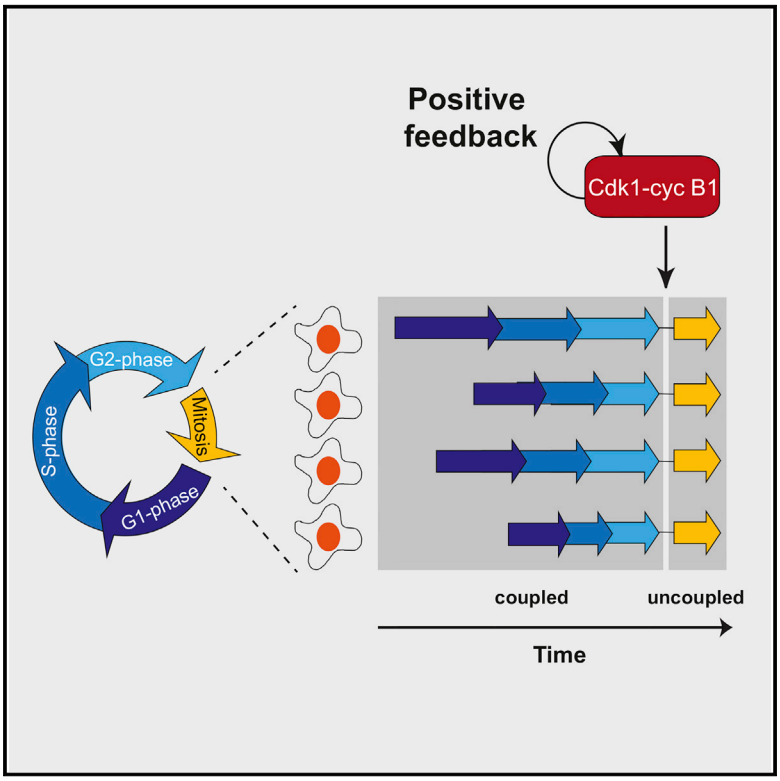
Molecular Cell, 64, 362–375, October 20, 2016

Article

Molecular Cell

Positive Feedback Keeps Duration of Mitosis Temporally Insulated from Upstream Cell-Cycle Events

Graphical Abstract



Authors

Ana Rita Araujo, Lendert Gelens, Rahuman S.M. Sheriff, Silvia D.M. Santos

Correspondence

silvia.santos@imperial.ac.uk

In Brief

Araujo et al. show by quantitative single cell measurements that mitosis is short, fairly constant, and, surprisingly, uncoupled from the highly variable duration of earlier cell-cycle phases. They propose that positive feedback is responsible for this modularity and predict that it might enable modularity in other biological systems.

Highlights

- Duration of mitosis in single cells is short and remarkably constant
- Duration of mitosis is temporally insulated from variability in early cell-cycle phases
- Positive feedback keeps duration of mitosis short, constant, and insulated
- Positive feedback can be a cellular strategy to bring about modularity in signaling

Araujo et al., 2016, Molecular Cell *64*, 362–375
October 20, 2016 © 2016 The Authors. Published by Elsevier Inc.
http://dx.doi.org/10.1016/j.molcel.2016.09.018

CellPress

Molecular Cell
Article

Positive Feedback Keeps Duration of Mitosis Temporally Insulated from Upstream Cell-Cycle Events

Ana Rita Araujo,[1,2] Lendert Gelens,[3] Rahuman S.M. Sheriff,[1,2,4] and Silvia D.M. Santos[1,2,5,*]
[1]Quantitative Cell Biology Lab, MRC-Clinical Sciences Centre (CSC), London W12 0NN, UK
[2]Institute of Clinical Sciences (ICS), Faculty of Medicine, Imperial College London, London SW7 2AZ, UK
[3]Laboratory of Dynamics in Biological Systems, Department of Cellular and Molecular Medicine, University of Leuven, 3000 Leuven, Belgium
[4]European Bioinformatics Institute, EMBL-EBI, Hinxton, Cambridge CB10 1SD, UK
[5]Lead Contact
*Correspondence: silvia.santos@imperial.ac.uk
http://dx.doi.org/10.1016/j.molcel.2016.09.018

SUMMARY

Cell division is characterized by a sequence of events by which a cell gives rise to two daughter cells. Quantitative measurements of cell-cycle dynamics in single cells showed that despite variability in G1-, S-, and G2 phases, duration of mitosis is short and remarkably constant. Surprisingly, there is no correlation between cell-cycle length and mitotic duration, suggesting that mitosis is temporally insulated from variability in earlier cell-cycle phases. By combining live cell imaging and computational modeling, we showed that positive feedback is the molecular mechanism underlying the temporal insulation of mitosis. Perturbing positive feedback gave rise to a sluggish, variable entry and progression through mitosis and uncoupled duration of mitosis from variability in cell cycle length. We show that positive feedback is important to keep mitosis short, constant, and temporally insulated and anticipate it might be a commonly used regulatory strategy to create modularity in other biological systems.

INTRODUCTION

The cell cycle is characterized by a sequence of events by which a cell gives rise to two genetically identical daughter cells. In order to maintain the integrity of the genome, chromosome replication (S-phase) and chromosome segregation into the two daughter cells (M-phase) must be coordinated in a manner that ensures the faithful transmission of hereditary information from one generation of cells to the next. Indeed, the timely execution of each stage of the cell cycle is intimately linked to key developmental processes such as differentiation and organogenesis. On the other hand, failure to precisely regulate cell-cycle progression leads to various disease states such as cancer.

Transitions within the cell cycle have been thought to be regulated by activation and deactivation cycles of cyclin-dependent kinases (Cdks) (Solomon et al., 1990; and reviewed in Uhlmann et al., 2011) and of Cdk counteracting phosphatases (Bouchoux and Uhlmann, 2011), synthesis and degradation of regulatory cyclins (Murray et al., 1989; Murray and Kirschner, 1989), and activation and deactivation cycles of checkpoints (Hartwell and Weinert, 1989) at specific cell-cycle stages. These regulate proper ordering of cell-cycle phases and full completion of one phase before the onset of the next. The existence of such well conserved regulatory mechanisms and biochemical machinery that drives cell division in all animal cells would predict that cell division cycles might be similar in different cells. However, both within the same organism different cell types have different lengths of cell division cycles and within the same population cell-cycle length varies for individual cells (Minor and Smith, 1974).

Different models were devised to explain the temporal ordering of events during cell-cycle progression and, in particular, of mitosis: a threshold model (Lindqvist et al., 2007; Gavet and Pines, 2010) and a cascade model (Georgi et al., 2002). Whereas the former says that the various cell-cycle events require different threshold levels of Cdk activity, the latter would predict that early mitotic events promote the subsequent activation of the regulators of later mitotic events. Either model would predict that there should be a strong correlation between the duration of successive cell-cycle events. In other words, cells that are quick to complete one cell-cycle phase are more likely (than cells that did this phase slowly) to complete the next phase quickly. Here, we test whether this is true by combining quantitative measurements of cell-cycle dynamics using live cell imaging of cell-cycle biosensors and computational modeling. We find that, at the single cell level, the duration of G1-, S-, and G2-phases is highly variable and correlates well with cell-cycle length. However, the duration of mitosis is short, remarkably constant, and surprisingly uncoupled from variability in early cell-cycle phases (Figures 1 and 2). The question is thus, what controls proper duration of mitosis and ensures that it is a short fraction of the cell division cycle, uncoupled from timing of upstream events?

Entry and progression through mitosis depends on the activity of Cdk1 and its regulatory protein Cyclin B1. Work from many labs have described that Cdk1-cyclin B1 is embedded within

 © 2016 The Authors. Published by Elsevier Inc.
This is an open access article under the CC BY license (http://creativecommons.org/licenses/by/4.0/).

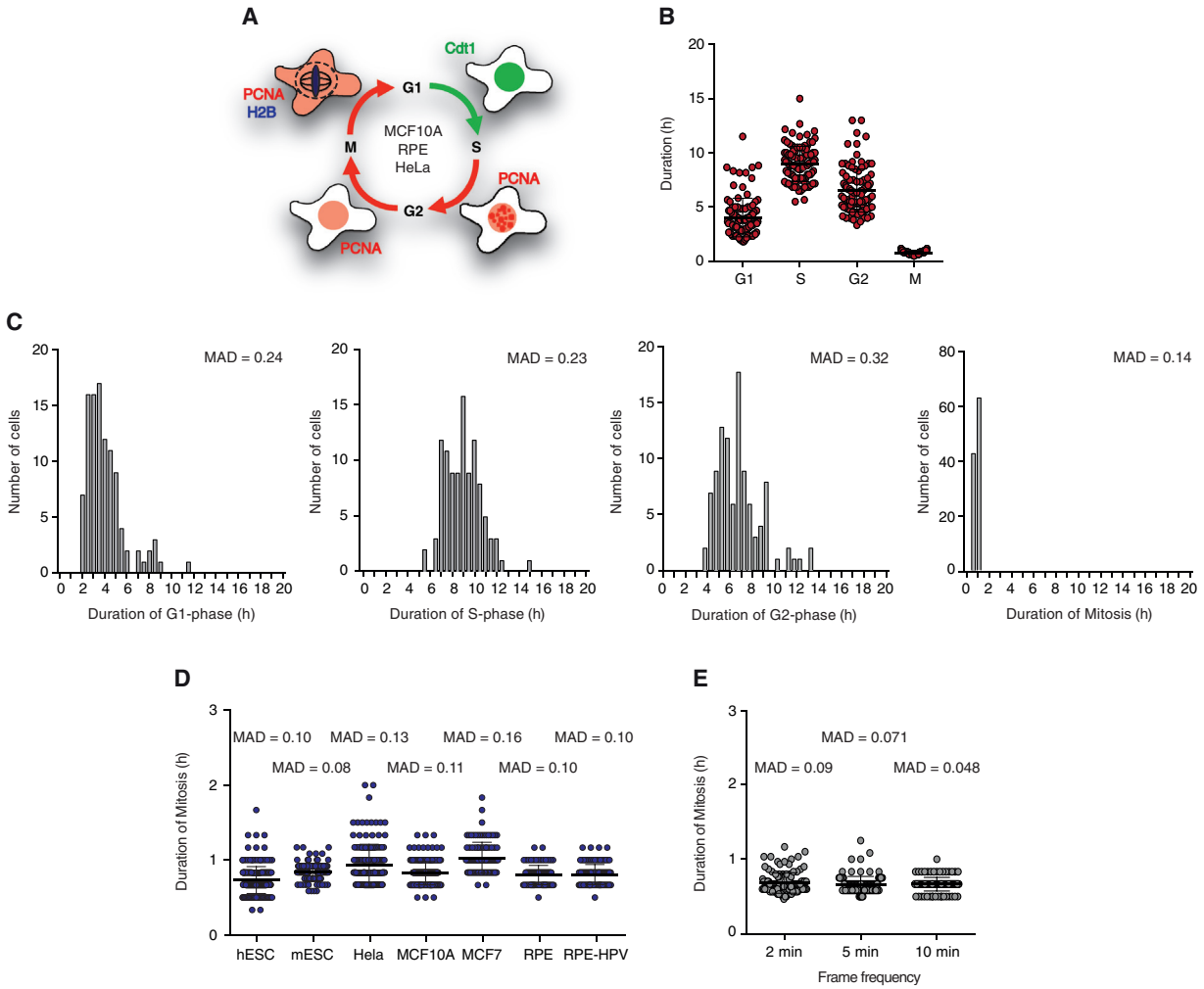


Figure 1. Duration of Mitosis Is Short and Constant

(A) Schematic of cell lines and biosensors used to measure cell-cycle dynamics in single cells.

(B) Duration of G1-, S-, G2-, and M-phases in single MCF10A cells. The error bars show mean ± SD (G1: 4.04 ± 1.78 hr, S: 8.97 ± 1.63 hr, G2: 6.52 ± 1.99 hr, and M: 48.0 ± 6.4 min).

(C) Histograms showing duration of G1-, S-, G2-, and M-phases. The normalized MAD/mean are shown. n > 200 cells for each experimental condition. This is representative of n = 3 experiments.

(D) Duration of mitosis in single cells as measured by live imaging for seven different human and mouse cell lines. H1 embryonic stem cells (hESC). R1 mouse embryonic cells (mESC). MAD is shown.

(E) Duration of mitosis in single cells as measured by live imaging at different frame frequencies (2, 5, and 10 min per imaging frame). Mean ± SD (41.6 ± 8 min, 39 ± 6.6 min, and 40.2 ± 6 min for 2, 5, and 10 min, respectively) and MADs are shown. n > 100 cells were analyzed for each experimental condition.

positive and negative feedback regulation. The former relies on the ability of Cdk1-cyclin B1 to inhibit the activity of its own inhibitor, the kinase Wee1 (McGowan and Russell, 1995; Mueller et al., 1995; Tang et al., 1993) and activate its own activator, the phosphatase Cdc25 (Kumagai and Dunphy, 1992; Izumi et al., 1992). On the other hand, active Cdk1-cyclin B1 complexes activate the anaphase promoting complex APC-cdC20, which stimulates Cyclin B1 degradation and thereby Cdk1 inactivation, forming a negative feedback loop. It has been shown that these feedback loops allow Cdk1-cyclin B1 to have a switch-like activation and the Cdk1-cyclin B1 network to collectively function as a bistable trigger that helps make transition from interphase into mitosis all-or-none and irreversible in nature (Novak and Tyson, 1993; Sha et al., 2003; Pomerening et al., 2003).

This led us to hypothesize that positive feedback and bistability in the protein networks that regulate entry and progression through mitosis may result in the duration of mitosis remaining short, constant, and temporally insulated from temporal variability in earlier cell-cycle phases. Here, we test this hypothesis and find that, at the single cell level, and contrary to G1-, S-, and G2-phases, duration of mitosis is short, remarkably constant, and uncoupled from variability in cell-cycle duration. We show that checkpoint control alone cannot explain these

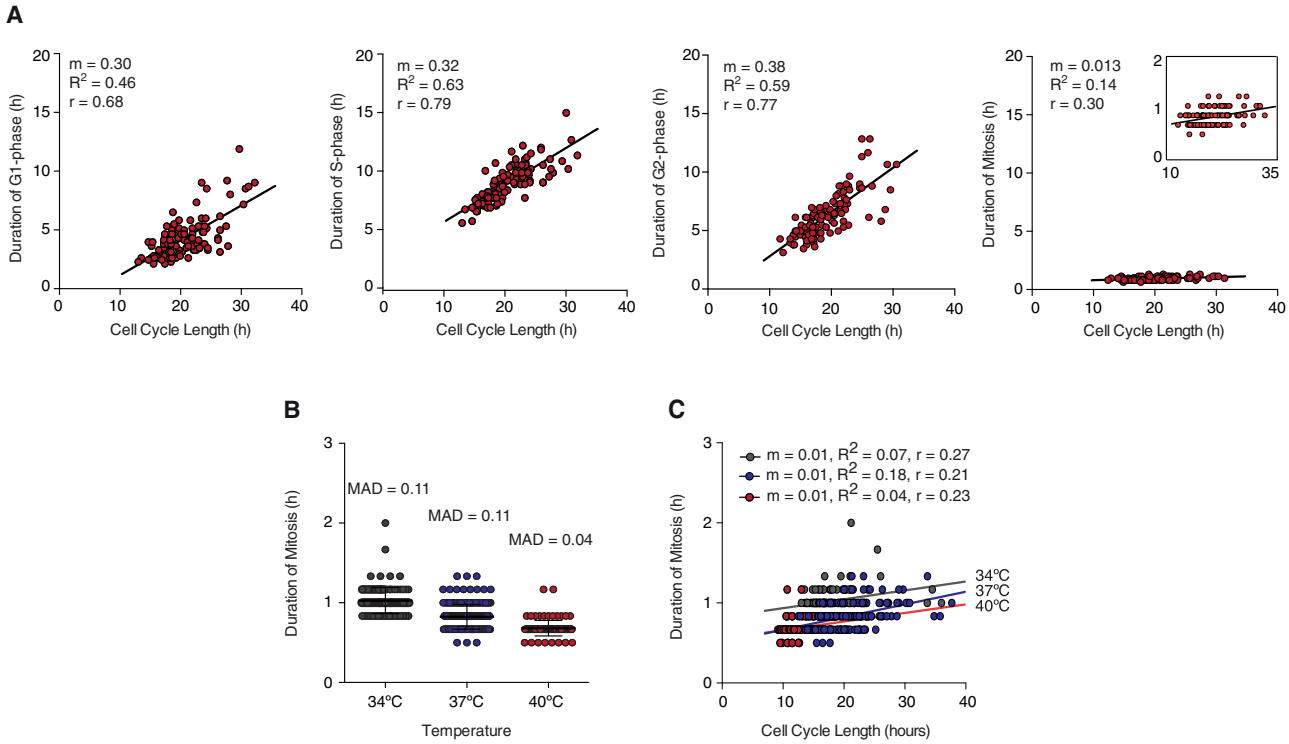


Figure 2. Duration of Mitosis Is Independent of Variability in Cell Cycle Length

(A) Duration of G1-, S-, G2-, and M-cell-cycle phases in single cells as a function of cell-cycle length measured by single cell live imaging. The inset shows same data on a 0–2 hr y axis scale.

(B) Duration of mitosis as measured by live cell imaging performed at 34°C, 37°C, and 40°C. The mean ± SD (61.6 ± 9.8 min, 49.4 ± 9.3 min, and 40.8 ± 5.8 min for 34°C, 37°C, and 40°C, respectively) and MAD are shown.

(C) Duration of mitosis in single cells as a function of cell-cycle length measured at 34°C, 37°C, and 40°C. The trend lines with respective slope (m), R-squared (R^2), and Pearson r are shown. n > 100 cells were analyzed for each experimental condition.

properties and find that positive feedback in Cdk1-cyclin B1 regulatory network can account for the temporal insulation of mitosis. We show that compromising feedback control (both in the presence or absence of checkpoint activation) resulted in a sluggish mitotic entry and a slower, more variable progression into mitosis. Importantly, compromising positive feedback resulted in the coupling of duration of mitosis with cell-cycle length. In other words, a longer time completing G1-, S-, and/or G2-phase results in longer duration of mitosis. We therefore show that positive feedback can give rise to temporal insulation of mitosis. Finally, we formulate a simple theoretical model for entry and progression through mitosis, which accounts for the observed role of positive feedback as a control strategy to create modularity in cell-cycle regulation.

RESULTS

Duration of Mitosis Is Short and Remarkably Constant

In order to measure cell-cycle dynamics in single cells, MCF10A (epithelial mammary) cells stably expressing Cdt1-YFP, PCNA-mCherry, and H2B-CFP fusions (Figures 1A and S1) were imaged for two consecutive divisions. G1 length was monitored by the appearance and disappearance of Cdt1 (Sakaue-Sawano et al., 2008). S-phase length was defined as the time between the appearance and disappearance of nuclear speckles (Sporbert et al., 2005). Duration of G2 was measured by monitoring time between disappearance of PCNA speckles and nuclear envelope breakdown (NEB). Duration of mitosis was defined by the time between NEB and nuclear envelope reformation (NER). Cell-cycle length was measured as the time between two consecutive NER events (Figures 1A and S1). The overall cell-cycle length of MCF10A cells is 21 hr long, on average (Figure 1B). Cells spend 95% of their cell division cycle in interphase (G1-, S-, and G2-phases) with average durations of 4 hr, 9 hr, and 5 hr to complete G1-, S-, and G2-phases, respectively. This results in cells spending only 5% of their cell-cycle time (less than 1 hr) in mitosis (Figures 1B–1D). Similar cell-cycle dynamics are seen for other human somatic cells such as RPE (epithelial, retina) and HeLa (epithelial, cervix) cells (Figure S1). In addition, measuring dynamics of individual cell-cycle phases revealed that mitosis is not only the shortest cell-cycle phase, but is also remarkably constant. Whereas timing of G1-, S-, and G2-phases gave rise to wide distributions with high (normalized) mean absolute deviations, MAD, and coefficients of variation, CV, (G1-phase: MAD = 0.24, CV = 0.44; S-phase: MAD = 0.23, CV = 0.28, and G2-phase: MAD = 0.32, CV = 0.30), the distribution of mitotic duration was tight, with little variability (normalized MAD = 0.14 and CV = 0.18) (Figure 1C). Similar results were seen

for RPE and HeLa cells (Figure S1) and across seven human (and mouse) cell lines (Figure 1D), where the measured mitotic duration was on average 45 min (with MAD values between 0.08 and 0.16). Increasing the temporal resolution of acquired images to 2, 5, and 10 min showed no effect on duration of mitosis (average duration 42 min, with MAD < 0.09) (Figure 1E).

Altogether, these data suggest that despite variability in cell-cycle dynamics duration of mitosis is short and kept fairly constant in mammalian cells.

Duration of Mitosis Is Temporally Insulated from Variability in Cell-Cycle Length

In addition, quantitative measurements of cell-cycle dynamics in MCF10A cells showed that in single cells, the relative cell-cycle length could be estimated by measuring duration of interphase. There is a good correlation between duration of individual cell-cycle phases and cell-cycle length (correlation coefficient, r, r = 0.68) (Figure 2A). In other words, if G1-, S-, or G2-phases are particularly long in a cell, the overall duration of the cell cycle for that cell is also long. Similar results were also seen for RPE and HeLa cells (Figure S2) and when correlating pairwise G1-, S-, and G2-phases (data not shown). However, this trend is not observed when duration of mitosis is analyzed in single cells. Regardless of the overall cell-cycle length for individual cells, there is very little correlation between duration of mitosis and cell-cycle length (r = 0.30) (Figure 2A). This was also observed for RPE and HeLa cells (Figure S2) and by monitoring cell-cycle dynamics in MCF10A, RPE, and HeLa cells with a different set of biosensors, DNA-ligase and Dnmt1 (Easwaran et al., 2005) and H2B (data not shown). This suggests that in single cells duration of mitosis is temporally uncoupled from variability in the duration of interphase.

To test this idea, we artificially slowed down and sped up the cell cycle by imaging MCF10A cells at low (34°C) and high (40°C) temperatures. Cells were monitored for two consecutive division cycles. Comparatively to control cells imaged at 37°C (where mitosis took on average 49.2 ± 5 min), duration of mitosis was longer (60 ± 9 min) at 34°C and shorter (40.8 ± 5.8 min) when cells were imaged at 40°C (Figure 2B). However, slowing or speeding up the cell cycle did not affect variability in mitotic duration, as measured by calculating CV (CV = 0.10 for 34°C, 37°C, and 40°C) and MAD values (MAD = 0.11 for 34°C; MAD = 0.11 for 37°C; and MAD = 0.04 for 40°C) (Figure 2B). This was also observed in RPE cells as shown in Figure S2. Notably, under these experimental conditions there was still very little correlation between duration of mitosis and overall cell-cycle length (Figures 2C and S2).

Altogether, these results suggest that duration of mitosis is temporally insulated (or uncoupled) from duration of upstream cell-cycle events.

Perturbing Spindle Assembly Checkpoint Does Not Affect Temporal Insulation of Mitosis

We then set out to investigate what is the molecular mechanism underlying the observed modularity of mitosis. Transitions during the somatic cell cycle are heavily controlled by checkpoint regulation. Checkpoints assure that one cell-cycle phase begins only when the previous finishes and can thereby regulate the duration of individual cell-cycle phases (Hartwell and Weinert, 1989). The spindle assembly checkpoint (SAC) regulates metaphase to anaphase transition during mitosis (Gardner and Burke, 2000; Wells, 1996). SAC assures that segregation of chromosomes, progression to anaphase, and mitotic exit only happens once all the chromosomes are properly aligned in a metaphase plane and bound to microtubules, forming the mitotic spindle (reviewed in Wells, 1996; Gardner and Burke, 2000). Due to its key role in regulating duration of mitosis, it was conceivable that SAC could play a role in keeping duration of mitosis short, constant, and uncoupled from previous cell-cycle events. We tested this by downregulating the expression of Mad2, a crucial SAC component (Li and Murray, 1991), by 20%–40% with short hairpin RNA (shRNA) (Figure S3). MCF10A cells stably expressing either shMad2 or shScramble as control were imaged for two division cycles. In line with the prediction that Mad2 and SAC play a role specifically during mitosis, Mad2 downregulation had no effect on duration of G1 (shControl 3.3 ± 1.6 hr and shMad2 3.3 ± 1.8 hr, p value > 0.7 by Mann-Whitney test) (Figure 3A), but resulted in a shorter duration of mitosis (shControl 43.8 ± 8 min and shMad2 31.2 ± 6 min, p < 0.0001 Mann-Whitney test) (Figure 3B). This was also observed in RPE and HeLa cells as shown in Figure S3. However, even in SAC perturbed cells, duration of mitosis is kept constant (with low variability) when compared to control cells (shControl MAD = 0.10 and shMad2 MAD = 0.073) in the three cell lines tested (Figures 3B and S3). As seen previously, even in the absence of SAC, there is a high correlation between duration of G1-phase and cell-cycle length (shControl, r = 0.70 and shMad2, r = 0.76) (Figure 3A). Remarkably, perturbing Mad2 expression and SAC had no effect in insulating duration of mitosis from cell-cycle length, as seen by the lack of correlation between duration of mitosis and cell-cycle duration (shControl, r = 0.36 and shMad2, r = 0.21) (Figure 3B). Experiments performed in RPE and HeLa cells showed similar results (Figure S3).

Taken together, these results suggest that while SAC plays a role in regulating duration of mitosis, it is not the molecular mechanism that keeps duration of mitosis short, constant, and temporally insulated from upstream cell-cycle events.

Positive Feedback Keeps Mitosis Temporally Insulated from Variability of Early Cell-Cycle Events

The question remained of what could the molecular mechanism be? Mitotic onset is initiated by a bistable trigger, which is thought to be the basis for a unidirectional, all-or-none and irreversible entry and progression through mitosis. (Novak and Tyson, 1993; Sha et al., 2003; Pomerening et al., 2003; Santos et al., 2012). A switch-like activation (Tyson and Novak, 2001; Thron, 1996; Sha et al., 2003; Pomerening et al., 2003) and spatial redistribution of Cdk1-cyclin B1 due to positive feedback control (Santos et al., 2012) at the onset of mitosis is at the heart of the observed bistability. Compromising the abruptness of Cdk1-cyclin B1 activation and nuclear import has been shown to affect progression through mitosis (Holt et al., 2008; Santos et al., 2012).

We hypothesized that positive feedback could be the molecular mechanism underlying the short, constant duration of mitosis and its modular character. How could this work? Cdk1 activation

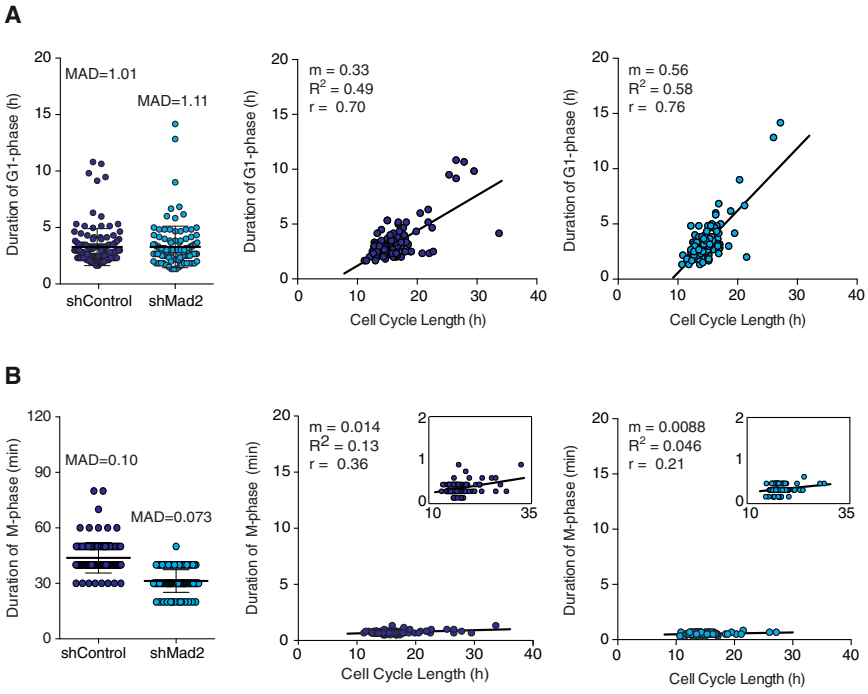


Figure 3. Perturbing the Spindle Assembly Does Not Make Mitotic Duration Variable nor Dependent on Cell Cycle Length

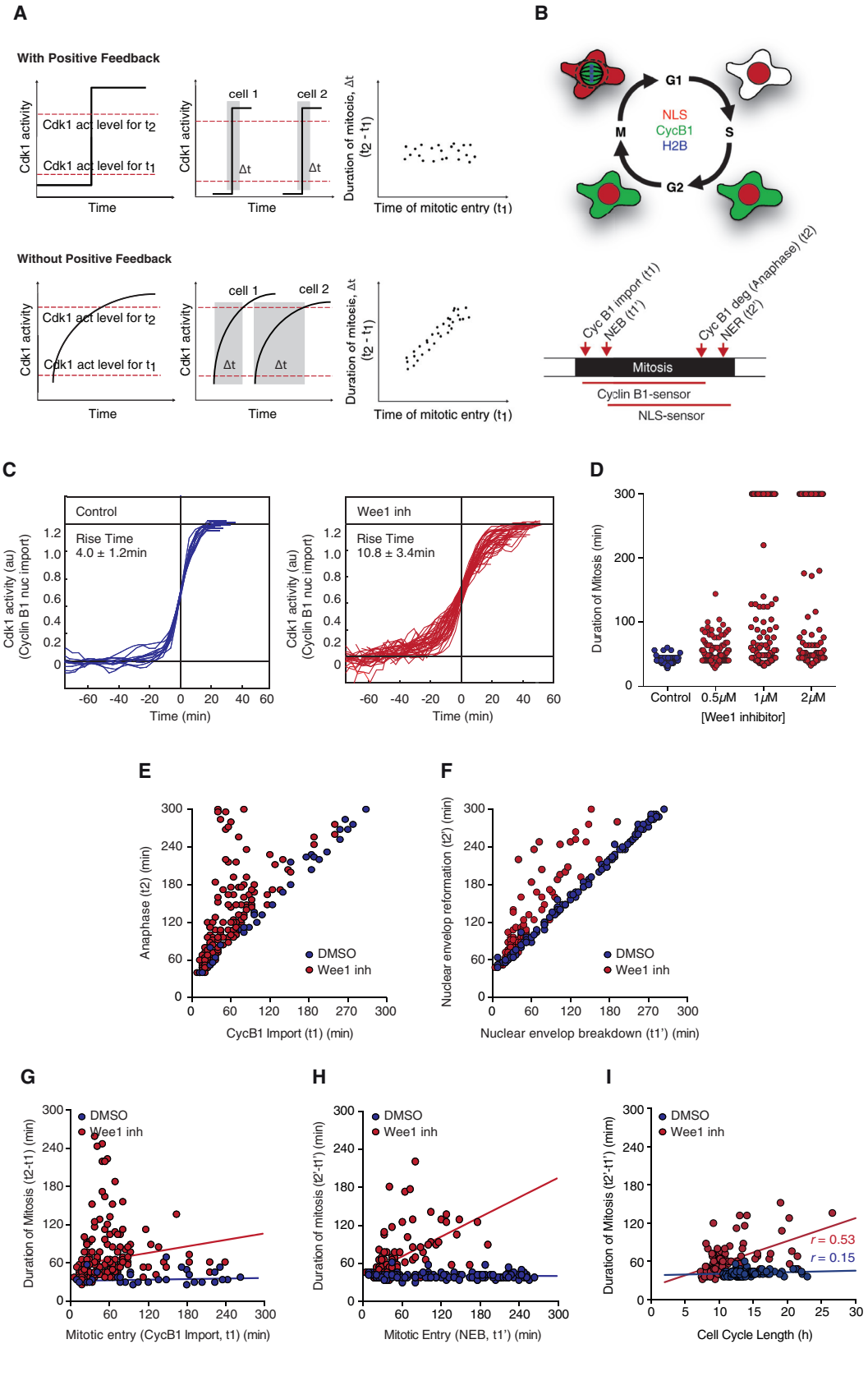
(A) Left: duration of G1-phase measured in single cells in the presence (shControl) and absence (shMad2) of SAC. shScramble vector was used as control (shControl). The mean ± SD (shControl 3.30 ± 1.6 min and shMad2 3.28 ± 1.84 min) and MAD are shown. The duration of G1-phase in control cells plotted as a function of cell-cycle length is shown (middle). The duration of G1-phase in SAC perturbed (shMad2) cells plotted as a function of cell-cycle length is shown (right). The trend lines with respective slope (m), R-squared (R^2), and Pearson r are shown. n > 110 cells were analyzed for each experimental condition.

(B) Left: duration of mitosis measured in single cells in the presence (shControl) and absence of SAC (shMad2). shScramble vector was used as control (shControl). The mean ± SD (shControl 43.8 ± 8.2 min and shMad2 31.2 ± 6.1 min) and MADs are shown. The duration of mitosis in control cells plotted as a function of cell-cycle length is shown (middle). The duration of mitosis in SAC perturbed (shMad2) cells plotted as a function of cell-cycle length is shown (right). The trend lines with corresponding m and R^2 are shown. Pearson r was calculated. The insets show same data on a 0–2 hr y axis scale. n > 115 cells were analyzed for each experimental condition.

is required for mitotic entry and progression into mitosis. As shown schematically in Figure 4A, it is plausible that early mitotic events (t1) require lower levels of Cdk1 activity, while late mitotic events (t2) require perhaps higher levels. The presence of positive feedback gives rise to a fast, sharp, sigmoidal activation of Cdk1. As a result, regardless of when individual cells enter mitosis, the time that it takes to go from an early to a late mitotic event (Δt) is likely to be short and relatively constant. Consequently, no correlation is expected between when individual cells initiate mitosis and duration of mitosis (Figure 4A). When positive feedback is compromised, however, Cdk1 switch-like activation is also compromised. We expect this to result in a more sluggish and more variable entry and progression through mitosis (Santos et al., 2012). Depending on how strongly positive feedback is compromised in individual cells, cells that initiate mitosis early might finish mitosis early as compared to cells that started mitosis later. This may result in a correlation (or coupling) between when individual cells entered mitosis and duration of mitosis (Figure 4A).

In order to test whether positive feedback could underlie temporal insulation in mitosis, Cdk1 activation dynamics as well as early and late mitotic events (i.e., duration of mitosis) were measured in the presence and absence of positive feedback in single cells. MCF10A cells stably expressing Cyclin B1-YFP, NLS-mCherry, and H2B-CFP biosensors were used (Figure 4B). Cyclin B1 nuclear translocation was used as a proxy for Cdk1 activation, since Cyclin B1 redistribution at the onset of mitosis is dependent on Cdk1 activity (Santos et al., 2012). Time of Cyclin B1 nuclear import, as well as time of NEB, were measured as early mitotic events (t1). Time of Cyclin B1 degradation, as well as time of NER, were measured as late mitotic events. Duration of mitosis was estimated as the time between Cyclin B1 import and its degradation and/or the time between NEB and NER (Figure 4B). Positive feedback was compromised by 75% by treating cells with the small molecule PD 166285, a specific Myt1/Wee1 inhibitor (Figure S4) (Hashimoto et al., 2006). Perturbing positive feedback resulted in a more graded Cdk1 activation, as seen by the increased rise time of Cdk1 activation curves (Figure 4C). Similar results were seen in RPE cells (Figure S4).

Notably, cells where positive feedback is compromised took longer to complete mitosis, presumably because it took longer for the cells to satisfy the spindle assembly checkpoint and/or activate APC-cdc20 (Figure 4D), and showed a more variable duration of mitosis (Figure 4D). In addition, breaking positive feedback resulted in loss of synchronicity between early (Cyclin B1 import and NEB) and late mitotic events (Cyclin B1 degradation and NER) (Figures 4E and 4F). Importantly, in control cells with intact feedback regulation, the length of mitosis is kept constant and there is no correlation (r = 0.047) between the time at which individual cells entered mitosis (t1 and t1′) and duration of mitosis (t2-t1 or t2′-t1′) (Figures 4G and 4H), emphasizing the independence of these events. Strikingly, when positive feedback is compromised, there is a correlation (r = 0.55) between the time at which cells entered mitosis and duration of mitosis (Figures 4G and 4H). Measuring early and late events with both Cyclin B1-YFP and NLS-mCherry biosensors provided similar results (Figures 4G and 4H). Similar results were also seen in both RPE and HeLa cells (Figure S4). Notably, measuring cell-cycle length between two consecutive divisions (time between NER of the first division and NEB of the second division) showed that perturbing positive feedback



(legend on next page)

couples variability in cell-cycle length to duration of mitosis (Figures 4H and S4I)

Similar results were also obtained when we perturbed feedback regulation that leads to both activation and spatial redistribution of Cdk1 in different ways: by expressing Cdk1-AF, a form of Cdk1 which cannot be phosphorylated by Wee1 (Figures 5A, 5B, and 5G); by expressing Cdc25C-C337S, a catalytic dead Cdc25C phosphatase (Figures 5C, 5D, and 5H); and by treating cells with leptomycin B, perturbing spatial positive feedback (as described in Santos et al., 2012) (Figures 5E, 5F, and 5I). As described previously, all these perturbations of feedback regulation render Cdk1 activation more graded (Figures 5A, 5C, and 5E), duration of mitosis longer and more variable (Figures 5B, 5D, and 5F), and couple duration of mitosis to cell-cycle length (Figures 5G–5I). Similar results were also seen in other cells (Figure S5).

Taken together, these results suggest that positive feedback is important to keep mitotic events synchronized and that duration of mitosis is insulated from duration of earlier cell-cycle phases. This strongly suggests that positive feedback regulation may underlie temporal modularity in mitosis.

SAC Does Not Contribute to Temporal Insulation of Mitosis

In order to rule out the contribution of SAC to the temporal insulation of mitosis, we next tested the effect of compromising positive feedback in the absence of checkpoint activation. We perturbed checkpoint activation either by using cell lines stably expressing shMad2, as described above, or by using a specific SAC inhibitor, Reversine, which targets the kinase Mps1 (Santaguida et al., 2010). Mitotic duration was measured in MCF10A cells either treated with DMSO or Myt1/Wee1 inhibitor PD 166285 in the absence (shMad2) or presence (shEmpty vector or shScramble) of checkpoint control. As seen previously, in control cells, mitosis is shorter when SAC is inhibited (shMad2 28.9 ± 4.6 min, shEmpty vector 37.5 ± 4.2 min, and shScramble 37.9 ± 5.1 min), but mitotic duration remains constant. By treating cells with Myt1/Wee1 inhibitor, positive feedback is perturbed and mitosis becomes longer and more variable in both control and SAC inhibited cells (Figure 6A). In addition, SAC inhibition alone does not interfere with synchronicity between early and late mitotic events (Figure 6B). Only when positive feedback is perturbed does the timing between early and late mitotic events become unsynchronized (Figure 6B). Importantly, SAC inhibition alone does not uncouple the timing of mitotic entry from duration of mitosis. In the presence or absence of SAC, timing of mitotic entry or overall cell-cycle length and duration of mitosis are only correlated when positive feedback is compromised (Figures 6C and 6D). Similar results were seen in RPE and HeLa cells (Figure S6). We further repeated these experiments in the presence of the SAC inhibitor reversine and obtained strikingly similar results (Figures 6E–6H). Moreover, measurements performed in RPE and HeLa cells showed similar outcomes (Figure S6).

These results suggest that positive feedback alone and not SAC activation ensures mitosis is short, constant, and temporally uncoupled from earlier cell-cycle events.

ODE Model Predicts Positive Feedback Brings about Temporal Modularity in Mitosis

We next set out to determine whether positive feedback could plausibly be expected to insulate mitosis from previous cell-cycle events and thereby generate modularity. To this end, we formulated a simple model of ordinary differential equations (ODEs) describing the basic regulatory network that drives cells in and out of mitosis (Figure 7A, see Supplemental Information for details). We implemented a set of deterministic ODEs with a noisy parameter variation from cell to cell rather than a stochastic Gillespie

Figure 4. Positive Feedback Keeps Mitosis Temporally Insulated from Upstream Cell Cycle Events

(A) Schematic of the thought experiment to test importance of positive feedback in keeping duration of mitosis constant and uncoupled from previous cell-cycle events. The presence of positive feedback results in a sharp, sigmoidal activation of Cdk1 and a short, constant time between an early (t1) and a late (t2) mitotic events (top). This may result in two cells entering mitosis at different times to keep a short and constant time between t1 and t2 (Δt). As a consequence, there might be no correlation between the time at which individual cells entered mitosis (t1) and duration of mitosis (t2-t1). The absence of positive feedback results in a graded, hyperbolic activation of Cdk1 and a long, variable time between an early (t1) and a late (t2) mitotic event (bottom). Consequently, there might be some degree of correlation between the time at which cells entered mitosis (t1) and duration of mitosis (t2-t1).

(B) Schematic of stable cell lines and biosensors used to measure Cdk1 activity and early (Cyclin B1 import and nuclear envelope breakdown [NEB]) and late (Anaphase and nuclear envelope reformation [NER]) mitotic events.

(C) Quantification of Cdk1 activation over time in single cells in the absence (blue) or presence (red) of 1 μM Wee1 inhibitor, PD166285. Time courses of individual cells were fitted to the logistic equation $y = a+b/1+e^{-(t-t0/\tau)}$ and were scaled to their fitted maximum and minimum values (b and a, respectively) and half-maximal times (t0). The rise times (τ) were calculated from the curve fits for all cells and are expressed as means ± SD. n > 20 cells in each condition.

(D) Duration of mitosis in single cells in the presence (red) and absence (blue) of Wee1 inhibitor at the shown concentrations. n > 100 cells were analyzed for each experimental condition.

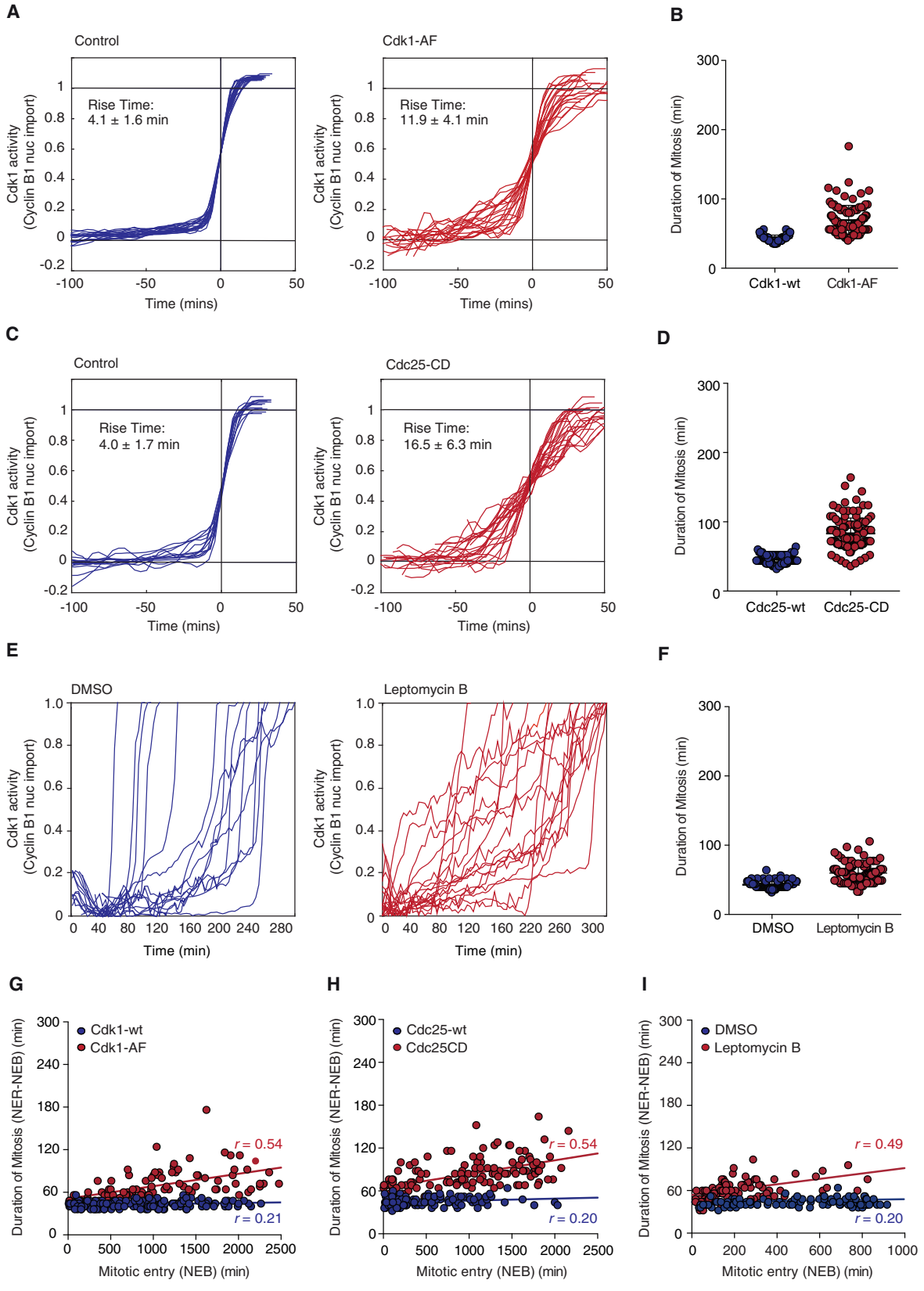
(E) Time of anaphase as a function of Cyclin B1 nuclear import in cells either treated with DMSO (blue) or with Wee1 inhibitor (red).

(F) Time of NER as a function of NEB in cells either treated with DMSO (blue) or with Wee1 inhibitor (red). n > 200 cells were analyzed for each experimental condition.

(G) Duration of mitosis (measured by the time between Cyclin B1 nuclear import and the onset of anaphase) as a function of Cyclin B1 import (t1) in the presence (red) or absence (blue) of 1 μM Wee1 inhibitor. The trend lines are shown (blue line: m = 0.015, R^2 = 0.012, r = 0.16 and red line: m = 0.17, R^2 = 0.025, r = 0.16).

(H) Duration of mitosis (measured by the time between NEB and NER) and the onset of NEB (t1') in the presence (red) or absence (blue) of Wee1 inhibitor. DMSO was used as control. n > 200 cells were analyzed for each experimental condition. The trend lines are shown. (blue line: m = 0.0029, R^2 = 0.0022, r = 0.047 and red line: m = 0.52, R^2 = 0.30, r = 0.55).

(I) Duration of mitosis (measured by the time between NEB and NER) as a function of cell-cycle length in the presence (red) or absence (blue) of 0.5 μM Wee1 inhibitor. The trend lines are shown (blue line: m = 0.004, R^2 = 0.021, r = 0.15 and red line: m = 0.060, R^2 = 0.28, r = 0.53). n > 100 cells were analyzed for each experimental condition.



(legend on next page)

model because the number of Cdk1-cyclin B1 complexes in a somatic cell is large ($\approx 1.6 \times 10^6$ (Sun et al., 2010). The final model used consists of three ODEs as follows:

$$\frac{d[Cdk1^*](t)}{dt} = k_s - a_{\deg}[Cdk1^*](t) - b_{\deg}\frac{[APC](t)^{n_{apc}}}{EC50_{apc}^{n_{apc}} + [APC](t)^{n_{apc}}}[Cdk1^*](t) + \left(a_{cdc} + b_{cdc}\frac{[Cdk1^*](t)^{n_{cdc}}}{EC50_{cdc}^{n_{cdc}} + [Cdk1^*](t)^{n_{cdc}}}\right)([cycB](t) - [Cdk1^*](t)) - \left(a_{wee} + b_{wee}\frac{EC50_{wee}^{n_{wee}}}{EC50_{wee}^{n_{wee}} + [Cdk1^*](t)^{n_{wee}}}\right)[Cdk1^*](t)$$

$$\frac{d[cycB](t)}{dt} = k_s - a_{\deg}[cycB](t) - b_{\deg}\frac{[APC](t)^{n_{apc}}}{EC50_{apc}^{n_{apc}} + [APC](t)^{n_{apc}}}[cycB](t)$$

$$\frac{d[APC](t)}{dt} = \left(a_K + b_K\frac{[CycB - Cdk1](t)^{n_K}}{[CycB - Cdk1](t)^{n_K} + EC50_K^{n_K}}\right)(1 - [APC](t)) - \left(a_P + b_P\frac{EC50_P^{n_P}}{[APC](t)^{n_P} + EC50_P^{n_P}}\right)[APC](t)$$

Where the following parameters were chosen: $\kappa_s = 0.1$ nM min^{-1}, $a_{deg} = 0.001$ min^1, $b_{deg} = 0.02$ min^{-1}, $a_{cdc} = 0.5$ min^{-1}, $b_{cdc} = 1.5$ min^{-1}, $EC_{50cdc} = 30$ nM, $n_{cdc} = 10$, $a_{wee} = 0.5$ min^{-1}, $b_{wee} = 1$ min^{-1}, $EC_{50wee} = 30$ nM, $n_{wee} = 10$, $EC_{50apc} = 0.5$, $n_{apc} = 10$, $a_K = 0$ min^{-1}, $b_K = 0.25$ min^{-1}, $EC_{50K} = 0.18$, nK = 5, $a_P = 0.025$ min^{-1}, $b_P = 0.5$ min^{-1}, $EC_{50P} = 0.18$, and $n_P = 5$.

We first used the model to simulate the time evolution of the concentrations of active Cdk1-cyclin B1 complexes, of Cyclin B1, and of active APC-cdc20 (Figure 7B). The corresponding steady-state response of active Cdk1-cyclin B1 as a function of Cyclin B1 accumulation is also shown in Figure 7C. For intermediate values of Cyclin B concentration, two stable solutions exist (represented as a solid green line): high Cdk1 activity (M-phase) and low Cdk1 activity (interphase). One unstable solution (represented as a dashed green line) serves as a critical threshold value of Cdk1 activity, below which the system will switch to interphase and above which the system will switch to mitosis (Figure 7C). The solid black line corresponds to the trajectory in the (Cyclin B, active Cdk1-cyclin B1) plane of the cell-cycle oscillations toggling between M-phase and interphase, as shown in Figure 7B. We also show the steady-state response of APC-cdc20 activation as a function of Cdk1-cyclin B1 concentration (Figure 7D). The double-negative feedback loop involving APC-cdc20 and MAD2-cdc20 can give rise to bistability. For intermediate values of active Cdk1-cyclin B1 concentration, two stable solutions exist: high APC activity (represented as a solid blue line) and low APC activity (represented as a solid red line). The dashed line again shows the threshold value between both solutions. The region of bistability is greatly extended when MAD2 activity is increased (normal versus high MAD2 activity) (Figure 7D). Such high Mad2 activity prevents APC-Cdc20 activation when Cdk1-cyclin B1 increases, similar to when SAC is active. The solid black line corresponds to the trajectory in the (active Cdk1-cyclin B1, APC-cdc20 activation) plane of the cell-cycle oscillations shown in Figure 7B. This shows that upon Cdk1-cyclin B1 (in)activation, APC-cdc20 is fairly quickly (in)activated, except when Mad2 activity is high. Next, after implementation of noise in the model (see Supplemental Experimental Procedures), we simulated the probability

Figure 5. Breaking Cdk1 Activation and Spatial Positive Feedbacks Couples Duration of Mitosis to Upstream Cell-Cycle Events

(A) Quantification of Cdk1 activation over time in cells expressing Cdk1-wt (blue) or Cdk1-AF (red). The time courses of individual cells were fitted as described in Figure 4C. Rise times (τ) were calculated from the curve fits for all cells and are expressed as means ± SD. n > 20 cells in each condition.

(B) Duration of mitosis in cells ectopically expressing Cdk1-wt (blue) or Cdk1-AF (red). n > 100 cells were analyzed for each experimental condition.

(C) Quantification of Cdk1 activation over time in cells expressing Cdc25C-wt (blue) or Cdc25C-CD (C377S) (red). The time courses of individual cells were fitted as described in Figure 4C. Rise times (τ) were calculated from the curve fits for all cells and are expressed as means ± SD. n > 20 cells in each condition.

(D) Duration of mitosis in cells ectopically expressing Cdc25C-wt (blue) or Cdc25C-CD (red). n > 100 cells were analyzed for each experimental condition.

(E) Quantification of Cdk1 activation over time in single cells in the absence (blue) or presence of leptomycin B (red).

(F) Duration of mitosis absence (blue) or presence of leptomycin B (red). n > 100 cells were analyzed for each experimental condition.

(G) Duration of mitosis as measured by the time between NEB and NER and the onset of NEB in cells expressing Cdk1-wt (blue) or Cdk1-AF (red). The trend lines are shown (blue line: m = 0.0016, $R^2 = 0.043$, r = 0.21 and red line: m = 0.017, $R^2 = 0.30$, r = 0.54). n > 100 cells were analyzed for each experimental condition.

(H) Duration of mitosis as measured by the time between NEB and NER and the onset of NEB in cells expressing Cdc25C-wt (blue) or Cdc25C-CD (C377S) (red). The trend lines are shown (blue line: m = 0.0027, $R^2 = 0.041$, r = 0.21 and red line: m = 0.019, $R^2 = 0.29$, r = 0.54). n > 100 cells were analyzed for each experimental condition.

(I) Duration of mitosis as measured by the time between NEB and NER and the onset of NEB in the absence (blue) or presence of leptomycin B (red). The trend lines are shown (blue line: m = 0.0039, $R^2 = 0.041$, r = 0.20 and red line: m = 0.038, $R^2 = 0.24$, r = 0.49). n > 100 cells were analyzed for each experimental condition.

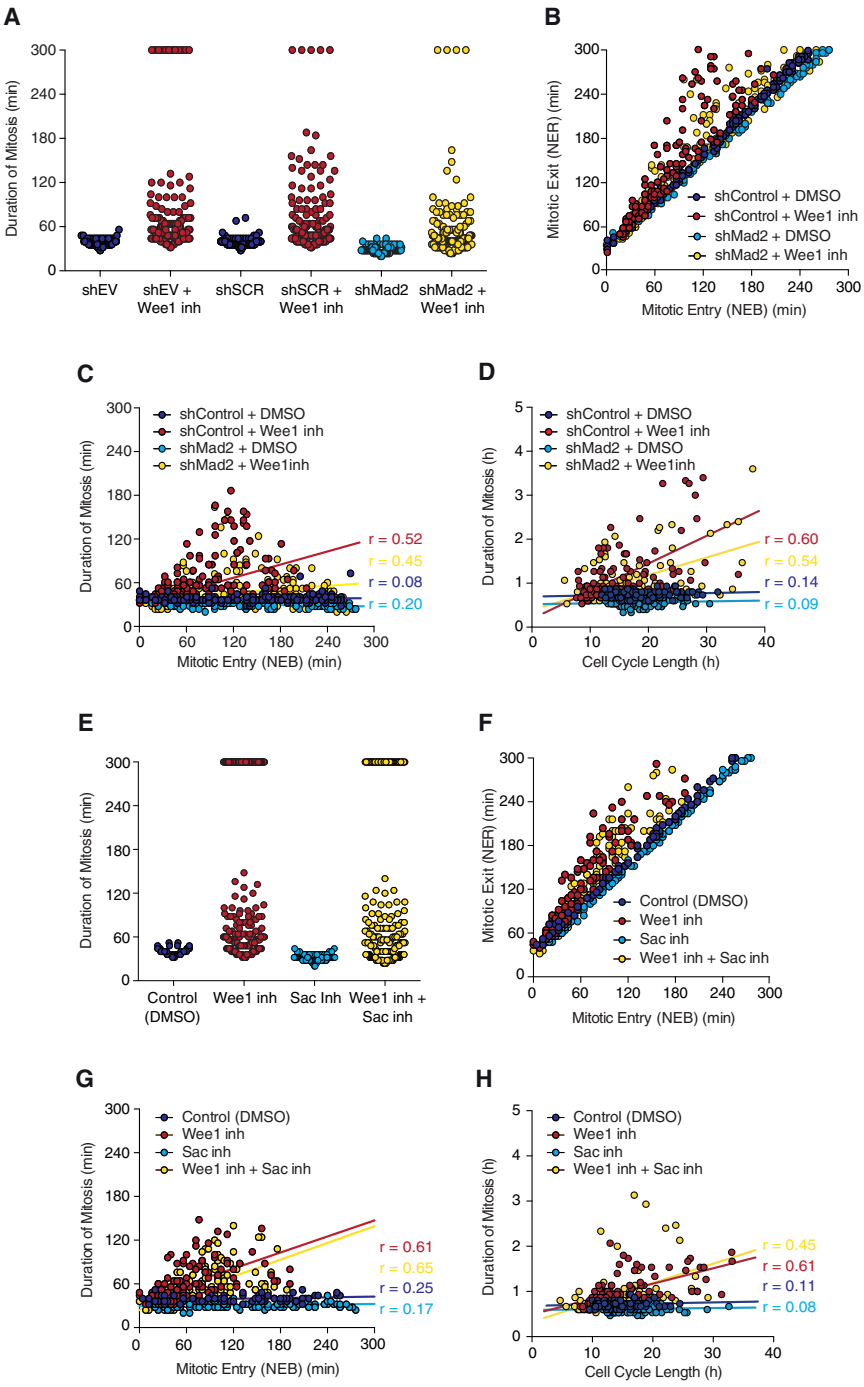


Figure 6. SAC Does Not Contribute to Duration of Mitosis Being Temporally Insulated from Duration of Upstream Cell-Cycle Events

(A) Duration of mitosis (measured by the time between NEB and NER) in the presence or absence of Wee1 inhibitor in single cells stably expressing shEmpty vector or shScramble as controls or shMad2 for SAC inhibition. n > 115 cells were analyzed for each experimental condition.

(B) Time of mitotic exit (NER) as a function of time of entry into mitosis (NEB) in control (shScramble) and SAC perturbed (shMad2) cells. The cells were either treated with DMSO or Wee1 inhibitor. n > 100 cells were analyzed for each experimental condition.

(C) Duration of mitosis as a function of mitotic entry (NEB) in control (shScramble) and SAC perturbed (shMad2) cells. The cells were either treated with DMSO or Wee1 inhibitor. n > 100 cells were analyzed for each experimental condition. The trend lines are shown. (dark blue line: m = 0.0054, R^2 = 0.0061, r = 0.078; light blue line: m = 0.014, R^2 = 0.054, r = 0.020; red line: m = 0.30, R^2 = 0.20, r = 0.52; and yellow line: m = 0.077, R^2 = 0.054, r = 0.45).

(D) Duration of mitosis as a function of cell-cycle length in control (shScramble) and SAC perturbed (shMad2) cells. The cells were either treated with DMSO or Wee1 inhibitor. n > 100 cells were analyzed for each experimental condition. The trend lines are shown. (dark blue line: m = 0.0027, R^2 = 0.0019, r = 0.14; light blue line: m = 0.0021, R^2 = 0.0076, r = 0.087; red line: m = 0.061, R^2 = 0.36, r = 0.60; and yellow line: m = 0.040, R^2 = 0.030, r = 0.54).

(E) Duration of mitosis in single cells treated with SAC inhibitor (Sac inh) in the presence or absence of Wee1 inhibitor. DMSO was used as a control. n > 100 cells were analyzed for each experimental condition.

(F) Time of mitotic exit (NER) as a function of time of entry into mitosis (NEB) in control (DMSO) and SAC inhibitor treated cells in the presence or absence of Wee1 inhibitor. n > 200 cells were analyzed for each experimental condition.

(G) Duration of mitosis as a function of mitotic entry (NEB) in control (DMSO) and SAC inhibited (Sac inh) cells. The cells were either treated with DMSO or Wee1 inhibitor. n > 100 cells were analyzed for each experimental condition. The trend lines are shown. (dark blue line: m = 0.016, R^2 = 0.062, r = 0.25; light blue line: m = 0.0098, R^2 = 0.03, r = 0.17; red line: m = 0.37, R^2 = 0.37, r = 0.61; and yellow line: m = 0.38, R^2 = 0.43, r = 0.65).

(H) Duration of mitosis as a function of cell-cycle length in control (DMSO) and SAC inhibited (Sac inh) cells. The cells were either treated with DMSO or Wee1 inhibitor. n > 100 cells were analyzed for each experimental condition. The trend lines are shown. (dark blue line: m = 0.0025, R^2 = 0.012, r = 0.11; light blue line: m = 0.0014, R^2 = 0.006, r = 0.077; red line: m = 0.034, R^2 = 0.37, r = 0.61; and yellow line: m = 0.043, R^2 = 0.21, r = 0.45).

distribution function of the duration of interphase and mitosis in control cells, in cells where SAC was inhibited and in the presence or absence of positive feedback (Figure 7E). We observed that the duration of interphase was unchanged both in control cells and when SAC was inhibited. On the contrary, cells where positive feedback was compromised showed shorter interphase duration, as expected by the premature entry into mitosis after Myt1/Wee1 inhibition. Importantly, duration of mitosis, while short and constant in both control and SAC inhibited cells, became longer and more variable when positive feedback was compromised (Figure 7E). Remarkably, these simulations are well in line with the measured experimental data for MCF10A,

RPE, and HeLa cells (Figures 4 and S4). In addition, simulating the duration of mitosis as a function of duration of interphase (an approximation of cell-cycle length) showed no correlation in control and SAC inhibited conditions (shControl, r = 0.155 and shMad2, r = 0.146, respectively), suggesting that duration of mitosis is uncoupled from duration of interphase (Figure 7G). However, when positive feedback is perturbed, in the presence or absence of SAC, duration of mitosis becomes coupled to duration of interphase, as seen by the resulting strong correlations (shControl+Wee1 inhibitor, r = 0.675 and shMad2+ Wee1 inhibitor, r = 0.589; Figure 7G). Thus, this simple model predicts that positive feedback accounts for the experimentally observed short, constant duration of mitosis in somatic cells and for temporally insulating mitotic duration from variability in duration of upstream cell-cycle events (Figure 1). The model therefore predicts that positive feedback endows mitotic regulatory networks with the potential to bring about modularity.

DISCUSSION

In summary, the evidence presented here argues that positive feedback, a recurrent motif in cell-cycle regulation, is a key mechanism to ensure that duration of mitosis is kept a short, constant fraction of a typically long and variable cell cycle (Figure 1). In the human somatic cell lines we tested, the length of the cell-cycle scales well with the number of chromosomes. In other words, there is some degree of correlation between chromosome number and cell-cycle duration (i.e., cells with higher number of chromosomes have longer cell-cycle lengths). This may potentially be a direct consequence of the time needed to replicate and segregate mammalian chromosomes, arguably the main function of a cell division cycle. However, at the single cell level, individual cells have highly variable cell-cycle length. We found that this was a consequence of a high variability in the dynamics of G1-, S-, and G2-phases (Figure 1). Surprisingly, this variability was not seen for mitotic duration. There was in fact no correlation between cell-cycle length and duration of mitosis in single cells (Figure 2). This suggests that it does not seem to matter how long it takes for previous cell-cycle phases to be completed, once a cell enters mitosis it decisively completes mitosis within a short, remarkably constant time. We therefore found that duration of mitosis is temporally insulated from any variability in upstream events. We suggest that these properties are unlikely to be due to checkpoint control mechanisms since compromising the activation of the spindle assembly checkpoint failed to couple duration of mitosis and cell-cycle length (Figure 3).

Our results are consistent with earlier studies in *Xenopus* extracts (Georgi et al., 2002), a system where checkpoint control is inactive. Here, the lag time between phosphorylation of Cdc25 and phosphorylation of Cdc27 (an early and a late mitotic event, respectively) was shown to be constant regardless of how long the extract stayed in interphase (Georgi et al., 2002). In other words, it did not matter how long interphase took, duration of mitosis was kept constant. In addition, the authors observed that once Cdk1 become active, the nuclear envelope broke down and chromatin condensed within the same (constant) lag time (Georgi et al., 2002). This strongly suggests that a short and constant duration of mitosis, which is uncoupled from the timing of early events, is unlikely to be specific to mammalian somatic cells, but rather a general design principle of cell-cycle regulation.

We propose that positive feedback in the networks that regulate mitosis is the molecular mechanism that insulates duration of mitosis from the measured variability in earlier cell-cycle events. Consistent with this, compromising the switch-like activation of Cdk1-cyclin B1, a master regulator of mitosis, compromised the ability of cells to complete mitosis in a timely, constant fashion and coupled duration of mitosis to duration of interphase (or overall cell-cycle length) (Figures 4 and 5). This was indeed the case regardless of spindle assembly checkpoint activation (Figure 6). Breaking positive feedback regulation causes mitosis to become considerably longer and variable in individual cells. We observe that under these circumstances cells die during mitosis or shortly after, never reaching a second round of division (Figure S5). This suggests that a short, constant mitosis, uncoupled from variability in upstream events, is a crucial property for fidelity of cell division and cell survival. Positive feedback may help and achieve proper Cdk1 activation thresholds underlying proper progression and exit from mitosis. This observation is consistent with the elegant work from Reijo-Pera and colleagues (Wong et al., 2010) on in vitro fertilized human embryos, which showed in early embryonic divisions, a constant (15 min) duration of cytokinesis was essential to ensure embryo viability and progression through development. This raises the hypothesis that a constant duration of mitosis might be advantageous for cells and that cells have actively kept a mechanism to temporally insulate mitosis and ensure cell survival.

Together with the described Cdk1 regulatory networks and the spindle assembly checkpoint, temporal control of mitosis is also regulated by mitotic phosphatases, namely members of the PP1 and PP2A families (Bollen et al., 2009). PP2A and PP1 have been implicated in both mitotic entry and exit from mitosis by reversing Cdk1 substrate phosphorylation (reviewed in Bollen et al., 2009). Due to the fact that PP1 and PP2A have been implicated in feedback regulation with Cdk1 (Burgess et al., 2010; Castilho et al., 2009; Dohadwala et al., 1994; Kwon et al., 1997), we anticipate that compromising specifically PP1 and PP2A activation will likely impact on the observed modularity of mitosis.

Computational modeling was used to test whether positive feedback could account for the observed temporal insulation of mitosis. Our model expanded previous ODE models describing the activation and deactivation cycles of Cdk1-cyclin B1 (Pomerening et al., 2003; Yang and Ferrell, 2013) by including feedback regulation between APC-cdc20 and Mad2, an important component of the spindle assembly checkpoint. Notably, the model predicted that positive feedback in the Cdk1-cyclin B1 regulatory network alone could give rise to short mitoses whose duration was uncoupled from the duration of interphase (Figure 7). As seen experimentally, compromising positive feedback compromised temporal insulation of mitosis.

One of the most important steps forward in our understanding of the systems biology of cellular decision making has been the appreciation that there are simple, ubiquitous motifs that define how genes and proteins regulate each others' activities (Alon,

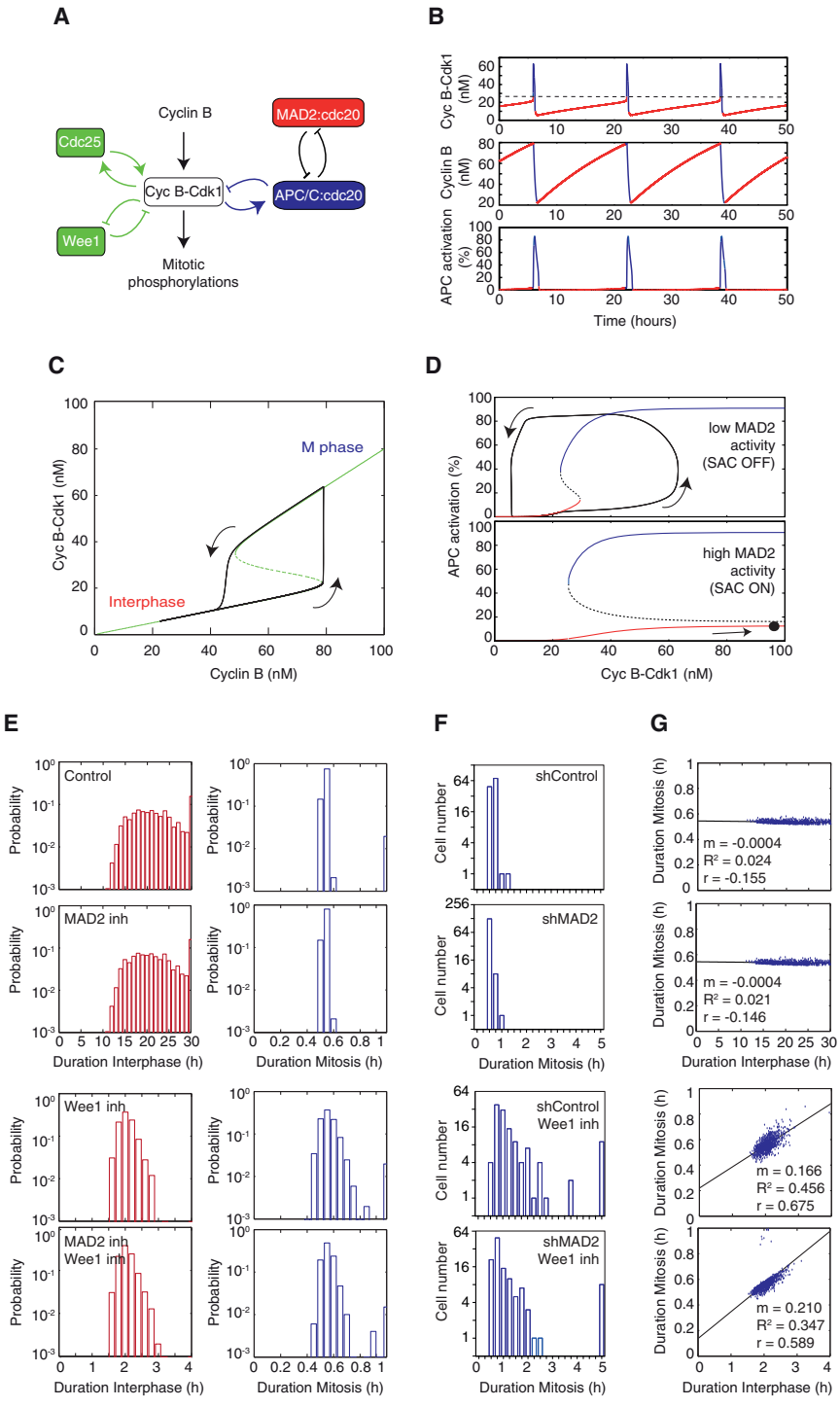


Figure 7. ODE Modeling Predicts that Positive Feedback Promotes Temporal Modularity in Mitosis

(A) Wiring diagram showing a simplified Cdk1 regulatory network, including positive and negative feedback loops.

(B) Simulation of the time evolution of the concentration of active Cdk1-cyclin B1 complexes (top), the concentration of Cyclin B (middle), and APC-cdc20 activation (bottom).

(C) Steady-state responses of Cdk1-cyclin B1 activation as a function of Cyclin B1 concentration. The positive and double-negative feedback loops involving Cdc25, Wee1, and Cdk1-cyclin B1 (A, green) can give rise to bistability.

(D) Steady-state responses of APC-cdc20 activation as a function of active Cdk1-cyclin B1 concentration. The double-negative feedback loop involving APC-cdc20 and MAD2-cdc20 (A, blue/red) can give rise to bistability.

(E) Simulated probability distribution function (in log scale) of the duration of interphase (left panel) and mitosis (right panel) in control cells (control), with inhibition of SAC (MAD2 inh), with inhibition of the positive feedback loops involving Wee1 (Wee1 inh), or with inhibition of both SAC and Wee1 positive feedback loops (MAD2 inh + Wee1 inh). n = 100 cells were simulated for each condition.

(F) Histograms (in log scale) showing experimentally measured duration of mitosis in control (shScramble), with inhibition of SAC (MAD2 inh), with inhibition of the positive feedback loops involving Wee1 (Wee1 inh), or with inhibition of both SAC and Wee1 positive feedback loops (MAD2 inh + Wee1 inh). n > 120 cells were analyzed for each experimental condition.

(G) Simulated duration of mitosis as a function of duration of interphase for control cells (control), with inhibition of SAC (MAD2 inh), with inhibition of the positive feedback loops involving Wee1 (Wee1 inh), or with inhibition of both SAC and Wee1 positive feedback loops (MAD2 inh + Wee1 inh). The trend lines and associated slopes, m, R^2 and Pearson r, are shown.

2007). Positive feedback loops are examples of such recurrent cellular strategies and have been shown to bring about amplification, maintenance, and rapid switching of activities in time and space (Ferrell, 2002; Santos et al., 2012; Chang and Ferrell, 2013, among others) and be the basis for unidirectional, coherent, and all-or-none cellular events (Ferrell and Machleder, 1998; Xiong and Ferrell, 2003; Novak et al., 2007; Holt et al., 2008; Skotheim et al., 2008; López-Avilés et al., 2009; He et al., 2011).

The work presented here shows that positive feedback regulation can generate temporal insulation and bring about modularity. In mammalian cells, coupling timing of G1-, S-, and G2-phases may endow cells with the potential to couple growth, DNA replication, and repair, all cell-cycle events that are likely to influence (and depend) on one another. A delay in cell growth during G1 might delay commitment to DNA replication. Delay in DNA replication might delay completion of DNA repair. However, when entering mitosis, cells will undergo dramatic morphological changes, stopping most metabolic and transcriptional activity in preparation for an even segregation of chromosomes. Uncoupling mitosis from earlier events might allow

individual cells to avoid noise and variability of the early phases and (truly) irreversibly commit to segregating chromosomes into daughter cells in a short, fast, and all-or-none manner. Given how modularity is emerging as an important and widespread feature of biological systems (Atay and Skotheim, 2014; Hartwell et al., 1999; Nachman et al., 2007), we anticipate that positive feedback may prove to be a recurrent cellular strategy to temporally uncouple events beyond the cell-cycle field.

EXPERIMENTAL PROCEDURES

Cell Lines

All the experiments in this study were performed in human MCF10A, RPE, and HeLa cell lines. Details on growth and maintenance of all the cell lines used can be found in Supplemental Experimental Procedures.

Biosensors, shRNAs, and Establishment of Stable Lines

cDNAs for Histone H2B fused to Cerulean, Cdt1 (amino acid [aa], 30–120) (Sakaue-Sawano et al., 2008) fused to YFP, PCNA fused with RFP (Sporbert et al., 2005), Cyclin B1 fused with YFP (Santos et al., 2012), Cdk1-AF, Cdk1-wt (Santos et al., 2012), Cdc25C-wt, and Cdc25C-Catalytic dead (C377S) (Santos et al., 2012), NLS (×3) fused to mCherry (Santos et al., 2012) were all cloned into the lentiviral vector CSII-EF-1-MCS-2 by restriction digestion and ligation reactions. The CSII-EF-1-MCS-2 plasmid is a modified CSII-EF-1-MCS backbone vector where a linker TCGAAGC TAGCCCTGCAGGTTAATTAAC has been added to the MCS to increase the number of unique restriction sites. Stable MCF10A, RPE, and HeLa cells lines were made with the following combination of cell-cycle biosensors: Cdt1-YFP, PCNA-mCherry, and H2B-Cerulean or Cyclin B1-YFP and NLS3-mCherry and H2B-CFP. Lentivirus production was carried out in 293T cells transfected with DNA of interest and lentivirus assembly vectors (PAX2 and VSV-G) using with Polyethylenimine (PEI). Cells were infected for 12 hr using polybrene (8 μg). 72 hr post-infection, transduced cells were sorted on a Becton Dickinson FACSAria III influx to obtain pure populations expressing the desired fluorescent reporters. For creation of shMad2 stable lines, a set of two shRNA (GIPZ lentiviral shRNA Pool, Dharmacon, Thermo Scientific) specific to Mad2 in lentiviral constructs were used (clone V3LHS_327851: TGCTGTTGACAGTGAGCGCCTGGTTGTAGTTATCTCAAATTAGTGAAGCCACAGATGTAATTTGAGATAACTACAACCAGTTGCCTACTGCCTCGGA and clone V3LHS_403761:TGCTGTTGACAGTGAGCGCATGGATATTTGTACTGTTTAATAGTGAAGCCACAGATGTATTAAACAGTACAAATATCCATTTGCCTACTGCCTCGGA). Stable lines expressing shEmpty (pGIPZ, Dharmacon, Thermo Scientific) vector and shScramble (GIPZ non-silencing shRNA control. Sequence: TGCTGTTGACAGTGAGCGATCTCGCTTGGGCGAGAGTAAGTAGTGAAGCCACAGATGTACTTACTCTCGCCCAAGCGAGAGTGCCTACTGCCTCGGA) were used as controls for experiments with shMad2. MCF10A, RPE, and HeLa cells were infected with the pool of two shRNAs. Transduced cells were selected with 2 μg/mL of puromycin.

Inhibitors

The inhibitors used in this study were: Wee1/Myt1 inhibitor, PD 166285, (at 0.5 μM, 1 μM, and 2 μM), SAC inhibitor, Reversine, (at 1 μM), and Leptomycin B (at 100 ng/mL).

Microscopy and Data Analysis

Live cell imaging was performed on either ScanR, a fully motorized and automated inverted epifluorescence microscope system IX83 (Olympus) combined with cellVivo (Olympus) or IncuCyte Zoom (Essen BioScience). Both equipped with temperature, humidity, and CO_2 levels control to keep the sample integrity and perfect focus. Details of objectives and lenses used and details on imaging procedures can be found in Supplemental Information.

Image analysis was done with scripts written in Matlab (Mathworks) and ImageJ (NIH). Mann-Whitney and Kolmogrov-Smirnov tests were used to estimate p values. Trend lines, R^2, person correlation coefficient, and mean absolute deviation were calculated using Prism6.

Mathematical Modeling

In brief, the model used consists of three ODEs to simulate the time evolution of the total amount of active Cdk1 ([Cdk1*](t)), the synthesis and destruction of the mitotic cyclins, Cyclin B ([cycB](t)), and active APC-cdc20 ([APC](t)). The detailed information on the model construction (equations and parameters used), noise implementation, and the setup of the numerical simulations can be found in the Supplemental Information.

SUPPLEMENTAL INFORMATION

Supplemental Information includes Supplemental Experimental Procedures and seven figures and can be found with this article online at http://dx.doi.org/10.1016/j.molcel.2016.09.018.

AUTHOR CONTRIBUTIONS

A.R.A. performed all the experiments. L.G. performed all the simulations and wrote the associated methods. A.R.A., R.S.M.S., and S.D.M.S. analyzed the data. A.R.A. and S.D.M.S. designed the experiments. S.D.M.S. conceived the study and wrote the paper.

ACKNOWLEDGMENTS

We thank James Elliott and Thomas Adejumo at the CSC FACS facility for excellent technical support. We also thank the Cardoso lab for the kind gift of the PCNA-RFP plasmid and Borzo Gharibi for help with mES cells. Pedro Beltrao, Roy Wollman, Tobias Warnecke, Borzo Gharibi, and Alexandra Gunne-Braden for critical reading of the manuscript. A.R.A. is supported by a PhD studentship (SFRH/BD/52193/2013) from Fundação para a Ciência e Tecnologia (FCT). This study was supported by the Medical Research Council (MRC) (MCA652-5PZ600).

Received: May 10, 2016
Revised: August 9, 2016
Accepted: September 14, 2016
Published: October 20, 2016

REFERENCES

Alon, U. (2007). Network motifs: theory and experimental approaches. Nat. Rev. Genet. *8*, 450–461.

Atay, O., and Skotheim, J.M. (2014). Modularity and predictability in cell signaling and decision making. Mol. Biol. Cell *25*, 3445–3450.

Bollen, M., Gerlich, D.W., and Lesage, B. (2009). Mitotic phosphatases: from entry guards to exit guides. Trends Cell Biol. *19*, 531–541.

Bouchoux, C., and Uhlmann, F. (2011). A quantitative model for ordered Cdk substrate dephosphorylation during mitotic exit. Cell *147*, 803–814.

Burgess, A., Vigneron, S., Brioudes, E., Labbé, J.C., Lorca, T., and Castro, A. (2010). Loss of human Greatwall results in G2 arrest and multiple mitotic defects due to deregulation of the cyclin B-Cdc2/PP2A balance. Proc. Natl. Acad. Sci. USA *107*, 12564–12569.

Castilho, P.V., Williams, B.C., Mochida, S., Zhao, Y., and Goldberg, M.L. (2009). The M phase kinase Greatwall (Gwl) promotes inactivation of PP2A/B55delta, a phosphatase directed against CDK phosphosites. Mol. Biol. Cell *20*, 4777–4789.

Chang, J.B., and Ferrell, J.E., Jr. (2013). Mitotic trigger waves and the spatial coordination of the Xenopus cell cycle. Nature *500*, 603–607.

Dohadwala, M., da Cruz e Silva, E.F., Hall, F.L., Williams, R.T., Carbonaro-Hall, D.A., Nairn, A.C., Greengard, P., and Berndt, N. (1994). Phosphorylation and inactivation of protein phosphatase 1 by cyclin-dependent kinases. Proc. Natl. Acad. Sci. USA *91*, 6408–6412.

Easwaran, H.P., Leonhardt, H., and Cardoso, M.C. (2005). Cell cycle markers for live cell analyses. Cell Cycle *4*, 453–455.

Ferrell, J.E., Jr. (2002). Self-perpetuating states in signal transduction: positive feedback, double-negative feedback and bistability. Curr. Opin. Cell Biol. *14*, 140–148.

Ferrell, J.E., Jr., and Machleder, E.M. (1998). The biochemical basis of an all-or-none cell fate switch in Xenopus oocytes. Science *280*, 895–898.

Gardner, R.D., and Burke, D.J. (2000). The spindle checkpoint: two transitions, two pathways. Trends Cell Biol. *10*, 154–158.

Gavet, O., and Pines, J. (2010). Progressive activation of CyclinB1-Cdk1 coordinates entry to mitosis. Dev. Cell *18*, 533–543.

Georgi, A.B., Stukenberg, P.T., and Kirschner, M.W. (2002). Timing of events in mitosis. Curr. Biol. *12*, 105–114.

Hartwell, L.H., and Weinert, T.A. (1989). Checkpoints: controls that ensure the order of cell cycle events. Science *246*, 629–634.

Hartwell, L.H., Hopfield, J.J., Leibler, S., and Murray, A.W. (1999). From molecular to modular cell biology. Nature *402* (6761, Suppl), C47–C52.

Hashimoto, O., Shinkawa, M., Torimura, T., Nakamura, T., Selvendiran, K., Sakamoto, M., Koga, H., Ueno, T., and Sata, M. (2006). Cell cycle regulation by the Wee1 inhibitor PD0166285, pyrido [2,3-d] pyimidine, in the B16 mouse melanoma cell line. BMC Cancer *6*, 292.

He, E., Kapuy, O., Oliveira, R.A., Uhlmann, F., Tyson, J.J., and Novák, B. (2011). System-level feedbacks make the anaphase switch irreversible. Proc. Natl. Acad. Sci. USA *108*, 10016–10021.

Holt, L.J., Krutchinsky, A.N., and Morgan, D.O. (2008). Positive feedback sharpens the anaphase switch. Nature *454*, 353–357.

Izumi, T., Walker, D.H., and Maller, J.L. (1992). Periodic changes in phosphorylation of the Xenopus cdc25 phosphatase regulate its activity. Mol. Biol. Cell *3*, 927–939.

Kumagai, A., and Dunphy, W.G. (1992). Regulation of the cdc25 protein during the cell cycle in Xenopus extracts. Cell *70*, 139–151.

Kwon, Y.G., Lee, S.Y., Choi, Y., Greengard, P., and Nairn, A.C. (1997). Cell cycle-dependent phosphorylation of mammalian protein phosphatase 1 by cdc2 kinase. Proc. Natl. Acad. Sci. USA *94*, 2168–2173.

Li, R., and Murray, A.W. (1991). Feedback control of mitosis in budding yeast. Cell *66*, 519–531.

Lindqvist, A., van Zon, W., Karlsson Rosenthal, C., and Wolthuis, R.M. (2007). Cyclin B1-Cdk1 activation continues after centrosome separation to control mitotic progression. PLoS Biol. *5*, e123.

López-Avilés, S., Kapuy, O., Novák, B., and Uhlmann, F. (2009). Irreversibility of mitotic exit is the consequence of systems-level feedback. Nature *459*, 592–595.

McGowan, C.H., and Russell, P. (1995). Cell cycle regulation of human WEE1. EMBO J. *14*, 2166–2175.

Minor, P.D., and Smith, J.A. (1974). Explanation of degree of correlation of sibling generation times in animal cells. Nature *248*, 241–243.

Mueller, P.R., Coleman, T.R., and Dunphy, W.G. (1995). Cell cycle regulation of a Xenopus Wee1-like kinase. Mol. Biol. Cell *6*, 119–134.

Murray, A.W., and Kirschner, M.W. (1989). Cyclin synthesis drives the early embryonic cell cycle. Nature *339*, 275–280.

Murray, A.W., Solomon, M.J., and Kirschner, M.W. (1989). The role of cyclin synthesis and degradation in the control of maturation promoting factor activity. Nature *339*, 280–286.

Nachman, I., Regev, A., and Ramanathan, S. (2007). Dissecting timing variability in yeast meiosis. Cell *131*, 544–556.

Novak, B., and Tyson, J.J. (1993). Numerical analysis of a comprehensive model of M-phase control in Xenopus oocyte extracts and intact embryos. J. Cell Sci. *106*, 1153–1168.

Novak, B., Tyson, J.J., Gyorffy, B., and Csikasz-Nagy, A. (2007). Irreversible cell-cycle transitions are due to systems-level feedback. Nat. Cell Biol. *9*, 724–728.

Pomerening, J.R., Sontag, E.D., and Ferrell, J.E., Jr. (2003). Building a cell cycle oscillator: hysteresis and bistability in the activation of Cdc2. Nat. Cell Biol. *5*, 346–351.

Sakaue-Sawano, A., Kurokawa, H., Morimura, T., Hanyu, A., Hama, H., Osawa, H., Kashiwagi, S., Fukami, K., Miyata, T., Miyoshi, H., et al. (2008). Visualizing spatiotemporal dynamics of multicellular cell-cycle progression. Cell *132*, 487–498.

Santaguida, S., Tighe, A., D'Alise, A.M., Taylor, S.S., and Musacchio, A. (2010). Dissecting the role of MPS1 in chromosome biorientation and the spindle checkpoint through the small molecule inhibitor reversine. J. Cell Biol. *190*, 73–87.

Santos, S.D., Wollman, R., Meyer, T., and Ferrell, J.E., Jr. (2012). Spatial positive feedback at the onset of mitosis. Cell *149*, 1500–1513.

Sha, W., Moore, J., Chen, K., Lassaletta, A.D., Yi, C.S., Tyson, J.J., and Sible, J.C. (2003). Hysteresis drives cell-cycle transitions in Xenopus laevis egg extracts. Proc. Natl. Acad. Sci. USA *100*, 975–980.

Skotheim, J.M., Di Talia, S., Siggia, E.D., and Cross, F.R. (2008). Positive feedback of G1 cyclins ensures coherent cell cycle entry. Nature *454*, 291–296.

Solomon, M.J., Glotzer, M., Lee, T.H., Philippe, M., and Kirschner, M.W. (1990). Cyclin activation of p34cdc2. Cell *63*, 1013–1024.

Sporbert, A., Domaing, P., Leonhardt, H., and Cardoso, M.C. (2005). PCNA acts as a stationary loading platform for transiently interacting Okazaki fragment maturation proteins. Nucleic Acids Res. *33*, 3521–3528.

Sun, T., Yang, X., Wang, W., Zhang, X., Xu, Q., Zhu, S., Kuchta, R., Chen, G., and Liu, X. (2010). Cellular abundance of Mps1 and the role of its carboxyl terminal tail in substrate recruitment. J. Biol. Chem. *285*, 38730–38739.

Tang, Z., Coleman, T.R., and Dunphy, W.G. (1993). Two distinct mechanisms for negative regulation of the Wee1 protein kinase. EMBO J. *12*, 3427–3436.

Thron, C.D. (1996). A model for a bistable biochemical trigger of mitosis. Biophys. Chem. *57*, 239–251.

Tyson, J.J., and Novak, B. (2001). Regulation of the eukaryotic cell cycle: molecular antagonism, hysteresis, and irreversible transitions. J. Theor. Biol. *210*, 249–263.

Uhlmann, F., Bouchoux, C., and López-Avilés, S. (2011). A quantitative model for cyclin-dependent kinase control of the cell cycle: revisited. Philos. Trans. R. Soc. Lond. B Biol. Sci. *366*, 3572–3583.

Wells, W.A. (1996). The spindle-assembly checkpoint: aiming for a perfect mitosis, every time. Trends Cell Biol. *6*, 228–234.

Wong, C.C., Loewke, K.E., Bossert, N.L., Behr, B., De Jonge, C.J., Baer, T.M., and Reijo Pera, R.A. (2010). Non-invasive imaging of human embryos before embryonic genome activation predicts development to the blastocyst stage. Nat Biotechnol. *28*, 1115–1121.

Xiong, W., and Ferrell, J.E., Jr. (2003). A positive-feedback-based bistable 'memory module' that governs a cell fate decision. Nature *426*, 460–465.

Yang, Q., and Ferrell, J.E., Jr. (2013). The Cdk1-APC/C cell cycle oscillator circuit functions as a time-delayed, ultrasensitive switch. Nat. Cell Biol. *15*, 519–525.